A genetic screen to identify novel regulators of Ikaros-mediated cell cycle arrest.

By

Lee Cooper

A thesis submitted to Imperial College London

for the degree of Doctor of Philosophy

MRC Clinical Science Centre

Imperial College School of Medicine

September 2015

I, Lee Cooper, declare that the work presented in this thesis is my own, and that any work carried out by others has been acknowledged and appropriately referenced in the text.

The Fall of Icarus – Henri Matisse 1869-1954

Abstract

Failure to regulate cellular proliferation is one of the hallmarks of cancer. The development of pre-B cells is demarcated by alternating stages of quiescence, in which immunoglobulin receptors are sequentially rearranged, and clonal expansion, in which signals from the assembled pre-B cell receptor lead to proliferation. Ikaros (encoded by *Ikzf1* in mice) is a transcription factor that regulates gene expression in cycling B cell progenitors to enforce proliferative arrest. In humans *IKZF1* mutations are prevalent in subsets of haematological malignancies and result in inappropriate proliferation, therefore the regulation of the cell cycle by Ikaros may be fundamental to its tumour suppressor function. The study of Ikaros-mediated cell cycle arrest in pre-B cells is complicated by the role of Ikaros in the regulation of genes involved in pre-B cell differentiation. I used 3T3 fibroblasts as a reductionist model to study the regulation of the cell cycle by Ikaros independently of pre-B cell receptor signalling. Using this model I performed an RNAi screen to discover novel regulators that cooperate with Ikaros to arrest the cell cycle. Amongst a number of candidates I identified the scaffolding protein SSeCKS (*Akap12*) as necessary for Ikaros-mediated proliferative arrest. Overexpression of Ikaros and SSeCKS synergistically arrested the cell cycle and silenced the expression of the proto-oncogene *Myc*. Utilising fibroblasts in which Ikaros and SSeCKS could be inducibly expressed I performed RNAseq to profile the global gene expression of cells that had undergone Ikaros and SSeCKS-mediated cell cycle arrest. Ikaros and SSeCKS together regulated the expression of hundreds of genes to coordinate proliferative arrest. The insights gained from these analyses may be applied to pre-B cells to deepen our understanding of the role of Ikaros in the regulation of proliferation in normal development and in the leukaemic state.

Acknowledgements

First and foremost I would like to thank my supervisor Matthias for all the help and support over these years, and having faith in me when my own was lacking. I would like to thank Gopu for all the (occasionally begrudging) bioinformatics help. Without that analysis my project would not have progressed. I would also like to thank James for tirelessly sorting my cells and lending a sympathetic ear (and cup of tea) for when experiments didn't work out quite the way I wanted to.

I would like to thank my family for all the love and support they have given me. Without them I would not be here today. I would particularly like to thank my mum for fuelling my late night writing sessions with delicious gin and tonics.

I would like to thank all the members of lymphocyte development for making the lab a productive, and deep down, enjoyable place to work. Thanks go to Isa and Ziwei for teaching me the techniques required for successful lab work. Special shout out to Anne, for stocking the 'secret' stash of sugary sweets that sustained me through many of my experiments. Many thanks to Grainne for her two rather large contributions at my birthday party. Thanks to Hakan for opening my eyes to the academic resource 'urban dictionary'. Thanks to Leopard for being the object of my derision for four years. Thanks to Liz for all the cat pictures. Thanks to Preksha for her unintentionally hilarious jokes. Thanks to Allifia for giving me fantastic career guidance. Thanks to Sergi, who taught me that you are never too old to party. Thanks to Ludovica for coining the term 'cucumberons'. Thanks to Stefan for the buffers I stole. Thanks to Feng for opening my eyes to the wonders of Tian Fu. Thanks to Lesly for making me cultured by taking me to the ballet. Thanks to Toby for never understanding a word I say. Thanks to Kotryna for so efficiently aliquoting the FCS. Thanks to Aljer, who is always a pleasant distraction from work at any hour of the day (mostly because he doesn't seem to sleep). I'd like to thank Raj – we made it! Finally I would like to thank my cute kitty Tofu, who did his darndest to prevent me writing by sleeping on my laptop.

Table of contents

Figures and Tables

List of Figures

List of tables

Abbreviations

µ Micro
4-OHT 4-hydroxytamoxifen
ATP Adenosyl triphosphate
ALL Acute lymphoblastic leukaemia
BCR B cell receptor
BFP Blue fluorescent protein
bp base pair
Cas CRISPR-associated
cDNA Complementary DNA
ChIP Chromatin immunoprecipitation
ChIP ChIP followed by high-throughput sequencing
C(t) Threshold Cycle
CRISPR clustered regularly interspaced short palindromic repeats
DAPI 4,6-diaminido-2-phenylindole
DMEM Dulbecco's Modified Eagle
DMSO Dimethyl sulfoxide
DNA Deoxyribonucleic acid
dNTP Deoxyribonucleotide triphosphate
Dox Doxycycline
DN Dominant negative
DN double negative thymocyte
DP double positive thymocyte
DSB Double strand break
DTT Dithiothreitol
EDTA Ethylene diamine tetraacetic acid
EGTA Ethylene diamine tetraacetic acid
EdU 5-ethynyl-2-deoxyuridine
ERt2 Eostrogen receptor
ERK Extracellular signal regulated kinase
EtOH Ethanol
FACS Fluorescence activated cell sorting
FCS Fetal Calf Serum
FDR False discovery rate
FrC' Fraction C' large cycling pre-B cells
FrD Fraction D small resting pre-B cells
G1,G2 Gap phases
gDNA Genomic DNA
GFP Green Fluorescent Protein
GO term Gene Ontology term
HDAC Histone deacetylase
HIF Hypoxia-inducible factor
HRP horseradish peroxidase
IF Immunofluorescence
IgH Immunoglobulin heavy chain
Igk Immunoglobulin kappa chain
IL-7 Interleukin 7
IMDM Iscove's Modified Dulbecco's medium
Indel Insertion / Deletion
IP Immunoprecipitation
kb Kilo base
ml Millilitre
M mitosis
M Molar
MEF Mouse embryonic fibroblast

mRNA messenger RNA
MSCV Murine stem cell virus
Multiplicity of infection
n Nano
NGS Next generation sequencing
NHEJ Non-homologous end joining
NURD Nucleosome Remodelling Deacetylase
PAGE Polyacrylamide gel elctrophoresis
PBS Phosphate Buffered Saline
PCA Principle Component Analysis
PCR Polymerase Chain Reaction
PI Propidium iodide
qPCR Quantitative PCR
RFP Red fluorescent protein
RNA Ribonucleic acid
RNAi RNA interference
RNA PolII RNA Polymerase II
RMP Reads per million
RT Reverse Transcription
S phase DNA synthesis
sgRNA single guide RNA
shRNA short hairpin RNA
siRNA short interfering RNA
SNP Single nuclear Polymorphism
SWI/SNF SWItch/Sucrose NonFermentable
SDS Sodium Dodecylsulfate
t Time
Tet Tetracycline
TSS Transcription start site
U Unit
WT Wild type

Chapter 1

Introduction

1.1 Ikaros family members in haematopoiesis, cell cycle regulation and leukaemia

Ikaros proteins are essential for multiple stages of haematopoietic development. Gain and loss of function studies have elucidated the role of Ikaros in processes pertinent to lymphocyte development, cell cycle regulation and the suppression of carcinogenesis. Here I give an account of Ikaros function in the development of B cell progenitors, in which the regulation of the cell cycle is inextricably linked to differentiation and the suppression of malignancy. Understanding the necessary function of Ikaros in such fundamental processes may deepen our understanding of the role of these proteins in the suppression of the leukaemic state.

1.1.1 The function of Ikaros in early lymphocyte progenitors

Haematopoiesis is a hierarchical process involving a gradual restriction of developmental potential in the production of the lineage-committed cells of the haematopoietic system (figure 1.1) (Busslinger, 2004; Cedar and Bergman, 2011). All the cells of the blood system are generated from a multipotent and self-renewing population of haematopoietic stem cells (HSC) in the bone marrow of adults, and the fetal liver of developing embryos (Busslinger, 2004). HSCs give rise to multipotent precursors (MPP) that retain broad developmental potential but lack self-renewing properties (Morrison and Weissman, 1994). Commitment to the B cell lineage begins as MPPs differentiate into lymphoid-primed multipotent progenitors (LMPP) that possess a combined myeloid and lymphoid potential, but are unable to commit to the erythroid or megakaryocyte lineages (Adolfsson *et al.,* 2005). LMPPs

differentiate into common lymphoid progenitors (CLPs) that can further commit to the B cell lineage, or give rise to T lymphocytes and natural killer cells (NK) (Busslinger, 2004). Each stage of development is characterised by a series of gene regulatory networks governed by transcription factors that function in a hierarchical and combinatorial manner to specify cell fate (Singh *et al.,* 2005). These transcription factors promote lineage-specific gene expression programs and repress lineage inappropriate expression to generate the mature cells of the haematopoietic system.

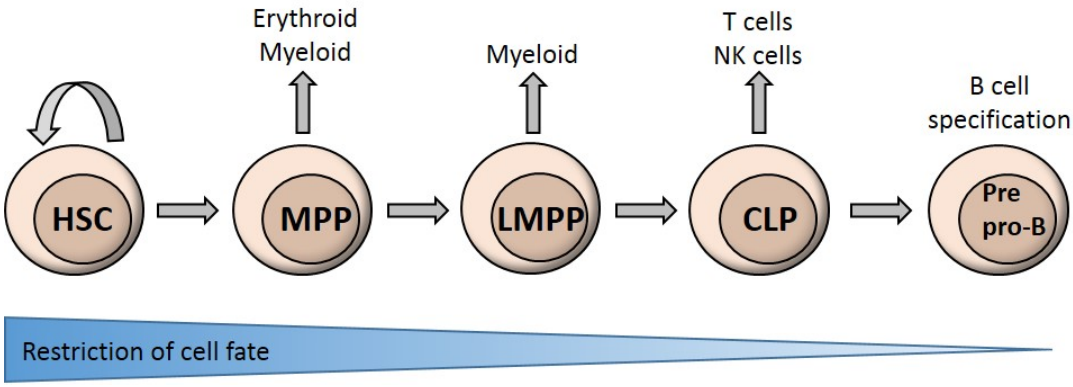

Figure 1.1 – Haematopoietic lineage restriction. Schematic outlining the orderly restriction in cell fate from a self-renewing haematopoietic stem cell to the earliest specified B cell precursor. HSC = Haematopoietic stem cell, MPP = Multipotent precursor, LMPP = Lymphoid-primed multipotent progenitor, CLP = Common lymphoid progenitor.

Genetic ablation studies have elucidated the transcriptional networks that direct the progression of lymphoid progenitors to the B cell lineage. These include the transcription factors PU.1, E2A, EBF1, Pax5 and Ikaros (Busslinger, 2004; Mandel and Grosschedl, 2010, Singh *et al.,* 2005). Ikaros (encoded by *Ikzf1*) is the founding member of a family of zinc finger transcription factors that are required for lymphocyte development. Other members of the family include Aiolos (*Ikzf3*) and Helios (*Ikzf2*), two proteins that exhibit high sequence homology to Ikaros. The expression of these related factors is primarily restricted to lymphoid lineages, and

they are believed to directly associate and interact with Ikaros (Morgan *et al.,* 1997; Hahm *et al.,* 1998). Two additional family members, Eos (*Ikzf4*) and Pegasus (*Ikzf5*), were subsequently discovered. These are more broadly expressed and can be detected in non-haematopoietic tissues such as brain, heart and skeletal muscle (Honma *et al.,* 1999; Perdomo *et al.,* 2000).

Full length Ikaros protein (Ik-1) contains two separate domains of zinc fingers that mediate its transcriptional function (figure 1.2). The N-terminal domain consists of 4 zinc fingers that are required for DNA binding at target genes (Hahm *et al.,* 1994). The C-terminal domain contains 2 zinc fingers that can form homodimers, as well as heterodimers with other Ikaros family members (Sun *et al.,* 1996). Dimerisation of Ikaros proteins is required for high affinity interactions with DNA (Sun *et al.,* 1996). Alternative splicing can generate multiple Ikaros isoforms that differ in the composition of zinc fingers, cellular localisation and transcriptional activity (Molnar and Georgopoulos, 1994; Hahm *et al.,* 1994; Molnar *et al.,* 1996). Isoforms that lack the N-terminal zinc fingers are unable to bind to DNA but can still dimerise with other family members, thereby exerting a dominant negative effect by preventing the transcriptional function of full length isoforms (Sun *et al.,* 1996). DNA binding-deficient dominant negative isoforms are overexpressed in B cell acute lymphoblastic leukaemia (B-ALL), illustrating the requirement for appropriate Ikaros function in B cell development (Nakase *et al.,* 2000).

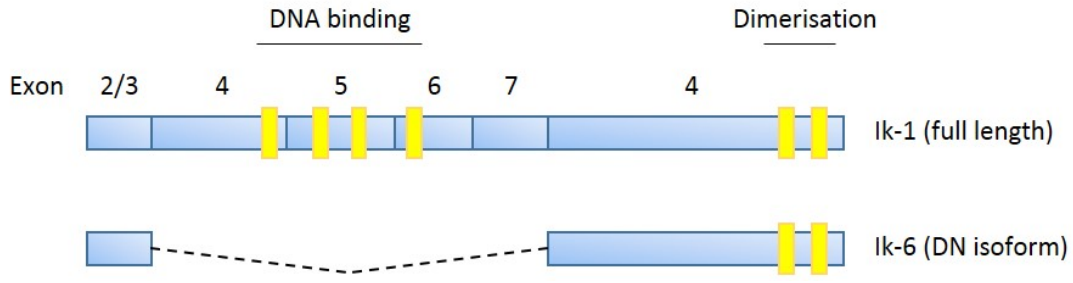

Figure 1.2 – Ikaros zinc finger isoforms. Diagram showing the full length (519 amino acid) Ikaros protein (Ik-1) that contains 4 N-terminal zinc fingers that mediate DNA binding and 2 C-terminal zinc fingers required for dimerisation. Multiple isoforms differ in the composition of zinc finger domains. The dominant negative (DN) Ik-6 isoform lacks the zinc fingers required for DNA binding but retains the C-terminal zinc fingers.

The role of Ikaros in the regulation of transcription was first uncovered by DNAse I footprinting and gel shift analysis of the promoter of the lymphocyte specific gene *Dntt*. Ikaros bound to an element in the promoter of *Dntt* and negatively regulated its transcription (Lo *et al.,* 1991; Trinh *et al.,* 2001). A further role for Ikaros in lymphocyte development was highlighted by the activation of the T cell differentiation antigen CD3 delta (Georgopoulos *et al.,* 1992). The essential requirement for Ikaros function in developing lymphocytes was illustrated by Ikaros-deficient mouse models, in which the zinc finger domains were selectively deleted. Deletion of the exon encoding the C-terminal zinc fingers resulted in an Ikaros-null mouse (Wang *et al.,* 1996). These mutant proteins are destabilised and are deficient in dimerisation and transcriptional activity (Wang *et al.,* 1996). Ikaros-null mice displayed a complete absence of foetal and adult derived B and NK cells, and a lack of foetally derived T cells. Adult T cells developed postnatally, but were skewed towards the $CD4^+$ lineage. These cells underwent clonal expansion and hyperproliferated in response to TCR engagement, indicating a role for Ikaros in the regulation of proliferation (Wang *et al.,* 1996). A more severe phenotype was observed in mice that contained a mutation in the DNA binding domain of Ikaros (Georgopoulos *et al.,* 1994). Mice homozygous for this dominant negative mutation exhibited a complete block in lymphocyte development and their earliest precursors, suggesting a function for Ikaros prior to lymphocyte specification (Georgopoulos *et al.,* 1994). The more severe effect of the dominant negative mutation highlighted the requirement for dimerisation with other isoforms or family members for appropriate Ikaros function in lymphocyte development. T cells from mice heterozygous for the dominant negative mutation displayed augmented proliferation and developed leukaemia and lymphoma with high penetrance, coinciding with the loss of the wild type Ikaros allele (Winandy *et al.,* 1995). The hyperproliferative T cell phenotype in Ikaros deficient mice was analysed further. These cells proliferated as a result of lower TCR activation thresholds (Avitahl *et al.,* 1999). The reduced expression of Ikaros protein in *Ikzf1*$^{+/-}$ null and dominant negative T cells correlated with the progression to S phase in these cells (Avitahl *et al.,* 1999). Ikaros was found to colocalise with sites of active DNA replication and

was important in the fidelity of chromosome propagation as Ikaros-deficient T cells displayed increased chromosomal aberrations compared to wild type (Avitahl *et al.,* 1999). These studies provided the first evidence that Ikaros was required for the attenuation of proliferation and suppression of malignancy in developing lymphocytes.

Studies in Ikaros-null mice have revealed a requirement for Ikaros function at the very earliest stages of haematopoietic development. These mice showed decreased numbers of HSCs and did not express the receptor tyrosine kinase Flt3 (Nichogiannopoulou *et al.,* 1999). Flt3 is required for the formation of common lymphocyte progenitors (CLP) and subsequent lymphocyte development (Mackarehtschian *et al.,* 1995; Sitnicka *et al.,* 2002). A detailed study further investigated Ikaros function in early haematopoiesis through the use of a GFP reporter under control of the *Ikzf1* regulatory elements (Yoshida *et al.,* 2006). GFP expression could be detected in early lineage restricted precursors corresponding to lymphoid-primed multipotent progenitors (LMPP). Ikaros-null GFP^+ LMPPs were defective in the formation of CLPs and subsequent B cell development (Yoshida *et al.,* 2006). This study was extended by transcriptional analysis of GFP^+ Ikaros-null LMPPs. Ikaros was required to downregulate stem cell gene expression signatures in these cells and promote the priming and maintenance of lymphoid specific gene expression (Ng *et al*., 2009). These genes included the B cell heavy chain *Igh-6* and the interleukin 7 receptor *Il-7r*. Signalling through the IL-7 cytokine receptor is essential for the commitment to the pre-pro-B cell stage and subsequent proliferation and survival of B cell progenitors (Miller *et al.,* 2002; Clark *et al.,* 2014). This illustrates the requirement for Ikaros in the commitment to the B and T cell lineages and helps explain the absence of B cells observed in Ikaros-null mice.

1.1.2 The regulation of the cell cycle by Ikaros in B cell precursors

Specification and commitment to the B cell lineage begins in IL-7R expressing progenitors and involves the expression of key transcription factors (Busslinger, 2004). PU.1 and E2A are required to regulate the expression of EBF in B cell restricted progenitors (Busslinger, 2004; Singh *et al.,* 2005). EBF expression is also dependent on activation by STAT5, a signalling molecule downstream of the IL-7 receptor (Kikuchi *et al.,* 2005). EBF and E2A in turn regulate the expression of Pax5, a gene essential for B cell lineage commitment (Busslinger, 2004). Pax5 suppresses lineage inappropriate gene expression and upregulates genes encoding the antigen receptor and its downstream signalling molecules (Busslinger, 2004; Singh *et al.,* 2005).

B cell development is characterised by distinct stages of proliferation and quiescence, in which antigen receptor loci are sequentially rearranged and expressed (Reth *et al.,* 1987). Genomic rearrangements are mediated by the synergistic activity of the recombination-activating genes *Rag1* and *Rag2* (Oettinger *et al.,* 1990). The expression and activity of Rag1 and Rag2 is strictly controlled and limited to G0 and G1 phases of the cell cycle. Enforced Rag2 activity in other cell cycle stages results in aberrant recombination and increased genomic instability (Zhang *et al.,* 2011). This is presumably because DNA repair by non-homologous end joining (NHEJ) is preferentially used to repair Rag-mediated double strand breaks in G0/G1 stage. In later cell cycle stages repair by homologous recombination (HR) is more active. Enforced Rag2 activity in later cell cycle stages may increase the risk of translocations due to the abarrent activation of the HR repair pathway (Zhang *et al.,* 2011). For these reasons, sequential rounds of rearrangements and proliferation in B cell progenitors must be highly orchestrated to prevent genomic instability and leukaemogenesis (figure 1.3).

Pre-pro-B cells (Hardy fraction A, FrA) display germline configuration of the

immunoglobulin loci and are the earliest committed cells to the B lineage (Hardy *et al*., 1991; Herzog *et al*., 2009). Somatic recombination of the diversity (D_H) and joining (J_H) segments of the immunoglobulin heavy chain (IgH) occurs as cells transition into the pro-B cell stage (FrB/C). Further recombination of the variable (V_H) segments to DJ_H occurs at the late pro-B cell stage. Productive IgH rearrangement results in the expression of the pre-B cell receptor (pre-BCR) that consists of IgH and the surrogate light chain components λ5 (*Igll1*) and Vpre-BI (*Vpre-b1*), associated with the signalling subunits Igα and Igβ (Nishimoto *et al.,* 1991; Herzog *et al*., 2009). Signalling through this receptor results in a burst of proliferation to clonally expand cells with successful rearrangements in the large cycling pre-B cell stage (FrC') (Hess *et al.,* 2001). Signalling through the pre-BCR acts as a cell autonomous proliferation switch that limits its own replication (Hendricks and Middendorp, 2004). Thus pre-BCR signalling is terminated by the downregulation of the surrogate light chain components in a feedback loop (Thompson *et al.,* 2007). The cells drop out of cycle and begin rearrangement of the immunoglobulin light chain (IgL) genes in the small resting pre-B cell stage (FrD) (Busslinger, 2004). The rearranged light chains associate with IgH to form the B cell receptor that is expressed on immature B cells (FrE) (Hardy *et al*., 1991; Herzog *et al*., 2009).

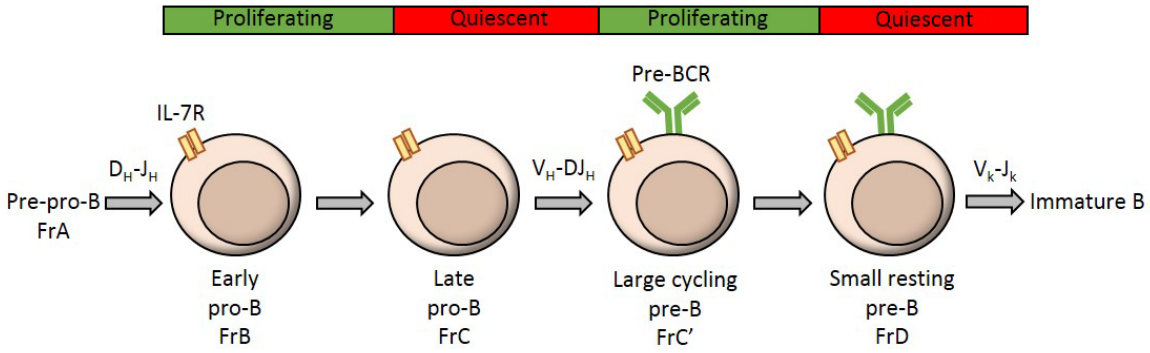

Figure 1.3 – Pre-B cell development. Schematic displaying the discrete stages of pre-B cell development from the earliest specified progenitor (pre-pro-B) to the immature B cell. Recombination of the heavy chain ($_H$) and light chain ($_k$) occurs in sequential stages of quiescence, punctuated by proliferative bursts. Ikaros contributes to cell cycle exit at the transition to the resting pre-B cell stage (FrD). This stage is characterised by proliferative arrest, quiescent metabolic reprogramming and rearrangement of the immunoglobulin $_k$ loci. The production of a functional B cell receptor marks the transition to the immature B cell stage and exit from the bone marrow.

Aiolos-null mice illustrated the requirement for Ikaros family members in B cell development. These mice had an increased population of pre-B cells, indicating a partial block in the differentiation of pre-B precursors (Wang *et al.,* 1998). Peripheral B cells displayed augmented proliferation in response to BCR engagement, reminiscent of the hyperproliferative phenotype observed in Ikaros-null T cells (Wang *et al.,* 1998; Avitahl *et al.,* 1999). Aiolos-null mice eventually developed B cell lymphomas, illustrating the essential requirement for Ikaros family members to suppress inappropriate proliferation and malignancy (Wang *et al.,* 1998). The requirement for Ikaros function in B cell development was illustrated by a mouse model that contained a β-galactosidase reporter inserted into the *Ikzf1* coding sequence. Low levels of Ikaros protein expression persisted, enabling some B cells to develop postnatally (Kirstetter *et al.,* 2002). These mice displayed a partial block in development at the pro-B or large cycling pre-B cell stage and peripheral B cells proliferated in response to lower thresholds of BCR signalling (Kirstetter *et al.,* 2002). These observations suggest that Ikaros and Aiolos are required for appropriate B cell development and negatively regulate proliferation in response to B cell receptor signalling.

Studies investigating the rearrangement and expression of IgH in pro-B cells uncovered a direct role for Ikaros in B cell differentiation. Complementing EBF expression in *Ikzf1*$^{-/-}$ haematopoietic progenitors was sufficient to partially rescue the complete block in B cell development in Ikaros-null mice (Reynauld *et al.,* 2008). Small numbers of B cells were discovered that were developmentally blocked at the pro-B cell stage (FrB/C) and defective in IgH recombination. Reconstitution of Ikaros into these cells directly upregulated the expression of *Rag1* and *Rag2* and induced the rearrangement of V_H-DJ_H genes (Reynauld *et al.,* 2008). Foxo1 is required for appropriate V_H-DJ_H recombination by ensuring the correct splicing of *Ikzf1* mRNA, as aberrant transcripts were detected in *Foxo1*-deficient cells (Alkhatib, 2012). Foxo1 activity is repressed by pro-proliferative IL-7 signalling through the phosphatidylinositol-3-OH kinase (PI3K) and protein kinase B (PKB/AKT) pathway

(Ochiai *et al.,* 2012). Thus there is balance between proliferation and cell cycle withdrawal in B cell development that Ikaros can influence to promote differentiation.

Signalling through the assembled pre-BCR and IL-7 receptors results in a burst of proliferation in the large cycling pre-B cell stage (FrC') (Clark *et al.,* 2014). IL-7 promotes the survival and proliferation of pre-B cells through the activation of AKT and upregulation of the proto-oncogene *Myc* (Corfe and Paige*,* 2012; Morrow *et al.,* 1992). IL-7 can also promote G1/S progression by upregulating the expression of *Ccnd2* through the downstream transcription factor STAT5 (Goetz *et al.,* 2004). Upon pre-BCR activation, the immunoreceptor tyrosine-based activation motifs (ITAMS) of the intracellular portion of Igα and Igβ are phosphorylated and recruit the Src kinase Syk (Herzog *et al.,* 2009). Syk can phosphorylate the mitogen-activated protein kinase (Mapk) ERK, which upregulates the expression of *Myc* through the downstream activator Elk1 (Yasuda *et al.,* 2008). Myc is required for the proliferation of large cycling pre-B cells (FrC') as *Myc* reconstitution restored proliferation in ERK1/2 deficient cells (Yasuda *et al.,* 2008).

Proliferating FrC' cells must drop out of cycle and rearrange the light chain loci at the small resting pre-B cell stage (FrD). This depends on the termination of pre-BCR and IL-7 signalling (Clark *et al.,* 2004). Activated Syk phosphorylates multiple residues on the scaffolding protein SLP65 (Herzog *et al.,* 2009). SLP65 (Blnk) is a molecular scaffold that exerts a tumour suppressor effect by binding and facilitating interactions between downstream signalling molecules. Scaffolding proteins are believed to be important for the regulation of immune cell signalling cascades by integrating multiple inputs to influence complex downstream effects. These include setting thresholds for proliferation, setting graded and oscillatory signalling responses, and regulating the spatiotemporal localisation of signalling (Shaw and Filbert, 2009; Thomlinson *et al.,* 2000). Pre-B cells in *Slp65*$^{-/-}$ mice display enhanced proliferation and a high incidence of pre-B cell lymphoma (Flemming *et al.,* 2003). Signalling downstream of SLP65 via the transcriptional activators IRF4 and IRF8

sharply upregulates the expression of Aiolos (*Ikzf3*) at the transition to the small resting pre-B cell stage (FrD) (Ma *et al.,* 2008; Thompson *et al.,* 2007). Ikaros and Aiolos bind directly to the promoter of the surrogate light chain *Igll1* (Lo *et al.,* 1991; Sabbattini *et al.,* 2001) and downregulate its expression in competition with the transcriptional activator EBF (Thompson *et al.,* 2007). This feedback loop terminates pre-BCR signalling at the small resting pre-B cell stage.

The cessation of pre-BCR signalling alone is not sufficient for light chain recombination as cell cycle arrest is required for Rag activity (Zhang *et al.,* 2011). The upregulation of *Ikzf3* by IRF4/8 contributes to cell cycle arrest, as reconstitution of Ikaros or Aiolos in IRF4/8 null pre-B cells was sufficient to induce G1 arrest (Ma *et al.,* 2008). Gene expression analysis was performed on IRF4/8 null pre-B cells reconstituted with Ikaros or Aiolos. Ikaros and Aiolos repressed the expression of *Myc* by directly binding to its promoter and arrested the cells in G1 (Ma *et al.,* 2010). *Myc* downregulation was essential for cell cycle withdrawal, as enforced *Myc* expression prevented Aiolos-mediated cell cycle arrest (Ma *et al.,* 2010). Following *Myc* depletion, the cells downregulated cyclin D3 and upregulated the cell cycle inhibitor *Cdkn1b* (hereon referred to as p27 protein or *Cdkn1b* gene). The induction of p27 was also necessary for G1 arrest as the growth antagonising function of Ikaros and Aiolos was attenuated slightly in p27 deficient pre-B cells (Ma *et al.,* 2010).

The regulation of gene expression by Ikaros was further explored by microarray analysis of *Ikzf1* overexpression in an IL-7 transgenic lymphoma cell line developmentally blocked at the FrC' stage (B3 cells, Ferreiros-Vidal *et al.,* 2013). In these experiments Ikaros activity was conditionally induced and gene expression analysis was performed at time points prior to, and after Ikaros-mediated cell cycle arrest. This was combined with ChIP-Seq analysis to correlate differential gene expression with direct regulation by Ikaros binding. Ikaros overexpression induced gene expression changes resembling the differentiation of cycling (FrC') to resting (FrD) pre-B cells in vivo (Ferreiros-Vidal *et al.,* 2013). Ikaros downregulated the expression of *Myc*, *Cdk6, Ccnd2/3* and *E2F* amongst others, and upregulated the cell

cycle inhibitors *Cdkn1a* (p21), *Cdkn1b* (p27) and *Cdkn2a* (p16). In addition to cell cycle genes, Ikaros regulated the expression of developmentally restricted genes involved in pre-BCR signalling such as *Blnk* (*Slp65*) *Rag1/2, Syk, Igll1, Foxo1* and components of the PI3K pathway including *Akt* (Ferreiros-Vidal *et al.,* 2013). Thus Ikaros can directly control the expression of cell cycle genes (based on ChIP-seq and microarray data) to enforce proliferative arrest and regulate the expression of key genes downstream of the pre-BCR to promote differentiation. Other genes involved in DNA replication, ribosome biogenesis and metabolism were also downregulated, illustrating the ability of Ikaros to regulate many essential pathways to enforce quiescence at the small resting pre-B cell stage (FrD) (Ferreiros-Vidal *et al.,* 2013).

Cell cycle arrest and differentiation depend on the attenuation of pro-proliferative signals from the IL-7 receptor (Ochiai *et al.,* 2012). Conditional inactivation of *Ikzf1* in early B cell progenitors resulted in a complete block at the large cycling pre-B cell stage, illustrating the requirement for Ikaros function in the transition to the small resting pre-B cell stage (Heizmann *et al.,* 2013). Reconstitution of Ikaros into these cells overcame the differentiation block and rescued B cell development. Ikaros synergistically cooperated with IL-7 withdrawal to repress *Myc* mRNA expression, enforce cell cycle arrest, downregulate the pre-BCR and recombine immunoglobulin light chain loci (Heizmann *et al.,* 2013). Microarray analysis demonstrated that Ikaros antagonised the expression of genes reliant on IL-7 signalling and introduced a more differentiated gene expression profile. Thus Ikaros enhanced pre-B cell differentiation by attenuating IL-7 signalling (Heizmann *et al.,* 2013). An additional mouse model was created in which the DNA binding zinc fingers of Ikaros were conditionally deleted in pro-B cells, creating a dominant negative protein (Joshi *et al.,* 2014). The cells were developmentally blocked at the large cycling pre-B cell stage and exhibited increased integrin-dependent binding to stromal cells, which supported survival and proliferation through the secretion of growth factors such as IL-7 and SCF. These hyperproliferative cells subsequently displayed high leukaemic potential (Joshi *et al.,* 2014). This study indicates that Ikaros is not only required to antagonise IL-7 dependent gene expression, but is also required to downregulate the

expression of integrins, allowing the cells to physically dissociate from IL-7 secreting stroma (Joshi *et al.,* 2014). Ikaros can regulate the proliferation and differentiation of pre-B cells by integrating and regulating multiple signalling pathways downstream of IL-7, integrin and focal adhesion receptors, growth factor receptors and the pre-B cell receptor. This delicate balance between growth and differentiation is lost upon Ikaros deletion, tipping the balance towards proliferation and leukaemogenesis.

1.1.3 Mechanisms of transcriptional regulation by Ikaros

Ikaros was identified as a transcription factor that could bind and negatively regulate the expression of the lymphocyte specific genes *Dntt* and *Igll1* (Lo *et al.,* 1991; Trinh *et al.,* 2001; Sabbattini *et al.,* 2001). Ikaros can also activate the lymphocyte specific gene CD3 delta (Georgopoulos *et al.,* 1992) and transactivate or repress reporter plasmids (Molnar and Georgopoulos, 1994; Koipally *et al.,* 1999; Trinh *et al.,* 2001). Subsequent genome wide expression profiling studies have identified many hundreds of target genes involved in pre-B cell development, adhesion, metabolism, signal transduction, cell cycle and DNA replication (Ferreiros-Vidal *et al.,* 2013; Heizmann *et al.,* 2013; Joshi *et al.,* 2014; Schwickert *et al.,* 2014). Therefore Ikaros regulates many diverse pathways that are widely expressed outside of the haematopoietic system. The combined effect of this regulation is to reconfigure the phenotype of proliferating B cell progenitors towards quiescence.

To gain an insight in the mechanisms of transcriptional regulation by Ikaros, the *Dntt* locus was studied further (Trinh *et al.,* 2001). The binding site for Ikaros overlapped with the transcriptional activator Elf-1. Gel shift assays suggested that Ikaros and Elf-1 bound competitively at the promoter of *Dntt*, and reporter constructs confirmed that Ikaros was required to downregulate the expression of *Dntt* by excluding Elf-1 (Trinh *et al.,* 2001). Downregulation of *Dntt* coincided with increased chromatin compaction at this locus, suggesting epigenetic mechanisms of repression (Trinh *et al.,* 2001). A similar competitive binding mechanism was observed at the promoter

of *Igll1*, where Ikaros competes with EBF to downregulate this gene at the transition from large cycling (FrC') to small resting (FrD) pre-B cells (Thompson *et al* 2007).
In addition to competitive binding, Ikaros can regulate transcription through associations with chromatin modifying complexes. A major fraction of Ikaros and Aiolos proteins localise with the Mi-2β nucleosome remodelling and deacetylase complex (Mi-2β/NuRD) in the nucleus of T cells (Kim *et al.,* 1999). This complex contains dual ATPase-dependent chromatin remodelling and histone deacetylation activity, and can activate or repress the transcription of target genes (Dege and Hagman, 2014). In double negative thymocytes Ikaros represses the transcription of CD4 by binding to a silencer element (Naito *et al.,* 2007). In double positive thymocytes CD4 is expressed by the combined binding of Mi-2β and Ikaros, suggesting an antagonistic regulation in the expression of lineage appropriate genes (Naito *et al.,* 2007). A genome wide study of Ikaros and Mi-2β DNA binding in double positive thymocytes indicated that Ikaros recruited this complex to active genes involved in thymocyte development (Zhang *et al.,* 2012). Though Mi-2β/NuRD is primarily a repressive complex, Ikaros prevented its histone deacetylation activity at sites of permissive chromatin. Loss of Ikaros DNA binding reduced the expression of these lymphoid specific target genes due to increased deacetylation and chromatin remodelling at these loci. The Mi-2β/NuRD complex was subsequently redistributed to transcriptionally poised non-Ikaros target genes involved in proliferation and metabolism, activating their expression (Zhang *et al.,* 2012). This provides a potential mechanism for leukaemogenesis in the absence of Ikaros function. Ikaros can also bind to the transcriptional corepressors Sin3 and CtBP (Koipally *et al.,* 1999; Koipally and Georgopoulos, 2000) and the Brg1-SWI/SNF chromatin remodelling complex (Kim *et al.,* 1999). Ikaros exists in a complex consisting of Mi-2β/NuRD and SWI/SNF (PYR complex) that regulates the β-globin locus in erythroid cells (O'Neill *et al.,* 2000). Thus Ikaros is believed to activate and repress transcription based on its association with these chromatin-modifying complexes.

Interestingly, experiments combining immunofluorescence and fluorescence *in situ* hybridisation (Immuno-FISH) showed that Ikaros complexes form foci at

pericentromeric heterochromatin that are rich in gamma-satellite sequences and heterochromatin-1 (HP1) binding (Brown *et al.,* 1997). Ikaros clusters colocalised with genes that are developmentally silenced in lymphocytes (Brown *et al.,* 1997). In resting lymphocytes these silent genes are not associated with centromeric foci, but upon stimulation they are dynamically repositioned towards Ikaros clusters (Brown *et al.,* 1999). Both *Igll1* and *Dntt* displayed this dynamic repositioning in B and T cells respectively. This led to the hypothesis that Ikaros associates with developmentally silenced genes at heterochromatin regions to ensure hereditary silencing following cell division (Brown *et al.,* 1999). Ikaros is targeted to pericentromeric regions through direct DNA binding, as dominant negative isoforms that are compromised in DNA binding do not form these clusters (Cobb *et al.,* 2000). Ikaros proteins form dimers and higher order multimers through contacts mediated by the C-terminal zinc fingers. This facilitates DNA binding to centromeric heterochromatin and the recruitment of target genes to these silencing regions (Cobb *et al.,* 2000; Trinh *et al.,* 2001).

It is of great interest that Ikaros is able to form clusters when ectopically expressed in 3T3 fibroblasts, indicating that binding to centromeric heterochromatin is not a lymphocyte specific phenomenon (Cobb *et al.,* 2000). Ectopic expression of Ikaros in these cells is sufficient to induce G1 arrest (Gomez Del-Arco *et al.,* 2004). Ikaros is hypophosphorylated and active in G1 phase, but is subsequently phosphorylated at the G1/S transition by casein kinase 2 (CK2) (Gomez Del-Arco *et al.,* 2004). This phosphorylation restricts the ability of Ikaros to form centromeric clusters, bind target genes and regulate the cell cycle (Gomez Del-Arco *et al.,* 2004; Gurel *et al.,* 2008). Conversely, dephosphorylation by protein phosphatase 1 (PP1) restores Ikaros activity (Popescu *et al.,* 2009). Syk colocalises with Ikaros in the nucleus of B cells and phosphorylates Ikaros on serine residues (Uckun *et al.,* 2012). In contrast to CK2, Syk phosphorylation augments sequence specific binding of Ikaros. Analysis by immunofluorescence demonstrated that IKAROS is unable to form centromeric foci in $Syk^{-/-}$ primary B cell ALL samples (Uckun *et al.,* 2012). Thus, in addition to upregulating the expression of Aiolos via the Slp65 scaffold, Syk can

postranslationally modify Ikaros to enhance its function. IKAROS can negatively regulate the expression of cell cycle genes in a human pre-B leukaemic cell line to arrest proliferation (Song *et al.,* 2015). Pharmacological inhibition of CK2 promoted IKAROS mediated gene regulation in these cells. Remarkably, CK2 inhibition could restore IKAROS binding and the repression of IKAROS target genes involved in cell cycle progression in primary B-ALL leukaemia cells, and reduce the leukaemic potential of these cells in human-mouse xenograft models (Song *et al.,* 2015). The phosphorylation of IKAROS by CK2 in human ALL cells is cell cycle specific, as observed in mice (Li *et al.,* 2012). Phosphorylation occurs at the transition into S phase, thereby linking the inactivation of IKAROS to cell cycle progression (Li *et al.,* 2012). Thus the regulation of the cell cycle is inextricably linked to IKAROS function and is essential to suppress leukaemia. Together these studies indicate that in addition to the regulation of the cell cycle by Ikaros, the cell cycle can also dynamically regulate the localisation and function of Ikaros. The complex interplay underlining these interactions remains to be fully elucidated and has implications for developmental processes and malignancy.

1.1.4 Ikaros as a tumour suppressor

Ikaros is a transcription factor that is involved in diverse cellular processes such as proliferation, metabolism, adhesion and epigenetic regulation of developmental gene expression. It is therefore not surprising that it is a tumour suppressor and perturbations to Ikaros function can result in leukaemia. The first evidence of its tumour suppressor function was that mice homozygous for a dominant negative Ikaros mutation develop T cell leukaemia and lymphoma (Winandy *et al.,* 1995). Evidence of a bona-fide tumour suppressive function in mice came from the observation that the reintroduction of *Ikzf1* into an Ikaros-null T leukaemia cell line arrested its proliferation (Kathrein *et al.,* 2005). Ikaros upregulated the cell cycle inhibitor p27, initiated a T cell differentiation program and enforced G1/G0 arrest in these cells (Kathrein *et al.,* 2005). Ikaros-null mice fail to produce any cells belonging

to the B cell lineage (Georgopoulos *et al.,* 1994), but conditional mutagenesis generates highly proliferative cells that are developmentally blocked at the large cycling pre-B cell stage (Joshi *et al.,* 2014). Recipient mice that are transplanted with these cells develop aggressive leukaemias with 100% mortality (Joshi *et al.,* 2014).

In a landmark paper IKAROS was identified as the defining oncogenic lesion in Philadelphia positive B-progenitor acute lymphoblastic leukaemia (ALL) (Mullighan *et al.,* 2008). Philadelphia chromosome is a reciprocal translocation between chromosome 9 and 22 that generates the *BCR-ABL* fusion gene. This encodes a constitutively active tyrosine kinase that activates a number of signalling pathways that promote survival and proliferation including RAS/ERK, PI3K, JAK/STAT and SRC (Salesse and Verfaillie *et al*., 2002). Remarkably, *IKZF1* is deleted in over 80% of BCR-ABL positive ALL due to aberrant Rag-induced recombination (Mullighan *et al.,* 2008). These deletions generate haploinsufficiency, dominant negative isoforms and IKAROS-null mutations (Mullighan *et al.,* 2008). *IKZF1* copy number alterations are prevalent in high risk B cell progenitor ALL and correlate with poor outcome with increased risk of relapse (Mullighan *et al.,* 2009). Transcriptional profiling of these cells revealed an upregulation in the HSC gene expression signature and downregulation of B lineage genes (Mullighan *et al.,* 2009). BCR-ABL induces aberrant splicing of *IKZF1* mRNA resulting in an overexpression of the dominant negative IK6 isoform in ALL patients (Nakase *et al.,* 2000; Klein *et al.,* 2006). Treatment with a BCR-ABL inhibitor reduced the expression of the truncated IK6 isoform and knockdown of IK6 by RNA interference (RNAi) partially restored lineage commitment to these cells (Klein *et al.,* 2006). Interestingly, different DNA binding zinc fingers in the N-terminal domain of Ikaros are involved in the regulation of different subsets of genes. Zinc fingers 2 and 3 bind to the canonical GGGAA Ikaros consensus sequence, whilst zinc fingers 1 and 4 confer sequence specificity and mediate binding to distinct genomic sites (Schjerven *et al.,* 2013). Selective deletion of zinc finger 4 in mice ($Ikzf1^{\Delta F4/\Delta F4}$) upregulated genes involved in adhesion, cell communication and signal transduction in double positive thymocytes and resulted in the development of aggressive lymphomas (Schjerven *et al.,* 2013). $Ikzf1^{\Delta F4/\Delta F4}$ B

cell progenitors cooperated with BCR-ABL to induce proliferation and malignancy in recipient mice. This suggested that zinc finger 4 was selectively required for the tumour suppressor function of Ikaros (Schjerven *et al.,* 2013).

The molecular interactions between IKAROS and BCR-ABL were investigated in Philadelphia positive B-ALL cells (Trageser *et al.,* 2009). A majority of BCR-ABL positive ALL cells lack productive IgH V_H-DJ_H rearrangements and are dysfunctional in pre-BCR signalling, indicating that the pre-BCR is a tumour suppressor that promotes B cell differentiation (Trageser *et al.,* 2009). Reconstitution of pre-BCR signalling attenuated proliferation, but expression of the dominant negative *IKZF1* isoform IK6 prevented G1 arrest. Reconstitution of *IKZF1* reduced growth and redirected the oncogenic kinase activity of BCR-ABL away from pro-proliferative SRC kinases towards the SLP65 tumour suppressor (Trageser *et al.,* 2009). Tyrosine phosphorylated SLP65 is able to scaffold and inactivate aberrant JAK3 signalling, resulting in the induction of *Cdkn1b* (p27) and cell cycle arrest (Nakayama *et al.,* 2009). Thus IKAROS functions as a tumour suppressor downstream of the pre-BCR by promoting cell cycle arrest and differentiation. Understanding the role of Ikaros in the regulation of the cell cycle may therefore be key to understanding its role in the prevention of malignancy.

1.2 Regulation of the cell cycle

The cell cycle is a highly orchestrated series of events involving sequential duplication and segregation of the genome (figure 1.4). It can be broadly characterised into the stages of mitosis, in which the chromosomes are segregated into two daughter cells, and interphase, in which the cells grow in size and replicate their DNA (Schafer, 1998). Interphase can be further divided into gap phases and DNA synthesis (S phase). Quiescent cells remain in the non-proliferative G0 phase until stimulated by mitogenic signals (Coller, 2007). Entry into the cell cycle through the first gap phase (G1) is marked by an increase in cell growth and protein synthesis in preparation for DNA replication (Lee and Finkel, 2013). For the cell to progress to S phase it must pass through the G1/S checkpoint (Schafer, 1998). Failure to pass this checkpoint due to nutrient withdrawal or DNA damage results in G1 arrest. Removal of serum or nutrients in early G1 phase was demonstrated to induce a quiescent state in certain cell lines (Pardee, 1974). Blocking DNA synthesis with hydroxyurea and then plating cells in low serum did not affect subsequent DNA replication. This indicated an all or nothing restriction point in G1 phase that marks the transition to mitogen independence and commitment to cell cycle progression (Pardee, 1974). Following DNA replication the cells enter G2 phase and prepare for cell division. Progression into mitosis depends on passage though the G2/M checkpoint (Schafer, 1998). Mitosis gives rise to two daughter cells that can permanently exit the cell cycle through terminal differentiation, enter into the quiescent G0 phase or continue to proliferate by entering again into G1 phase (Schafer, 1998).

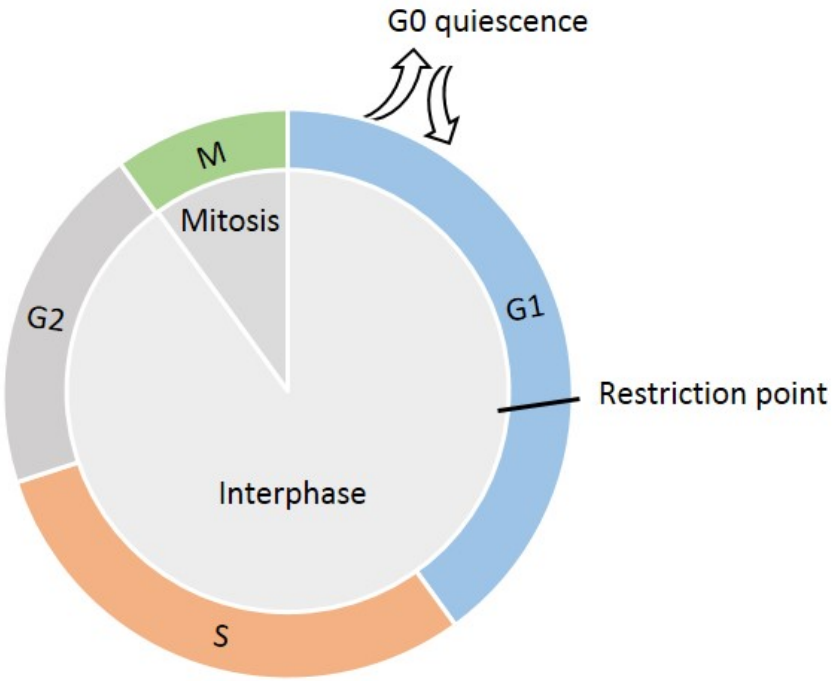

Figure 1.4 – The cell cycle. Following mitotic division the daughter cells enter into G1. Signals such as the availability of nutrients can influence the decision to continue to proliferate through the cell cycle or exit to a quiescent G0 state. Passage through the restriction point marks the serum-independent progression into S phase. The newly replicated chromosomes are subsequently segregated into two daughter cells in mitosis.

Progression through the cell cycle is controlled by successive waves of cyclin-dependent kinase (Cdk) activity, which are dependent on binding to their cyclin partners (Schafer, 1998). Cyclins display a tightly regulated oscillatory expression profile that is determined by transcriptional regulation and degradation (Evans *et al.,* 1983; Schafer, 1998). Progression through G1 phase is primarily driven by the action of Cdk4/6 bound to D type cyclins and cyclin E-Cdk2 complexes. G2/M progression is driven by cyclins A and B bound to Cdk2 and Cdk1 respectively (Schafer, 1998). The activity of cyclin-Cdk complexes can in turn be negatively regulated through the action of cell cycle inhibitors of the Cip/Kip and Ink4a/Arf families (Sherr and Roberts, 1999). The decision to proliferate or remain quiescent depends on a balance of competing inputs including mitogenic signals, energy sensing, metabolic competence and cytoskeletal remodelling (Coller, 2007; Lee and Finkel, 2013). As cancer is manifested through a misregulation of growth and proliferation, the

regulation of the cell cycle is intimately linked to the suppression of malignancy (Hanahan and Weinberg, 2000). The oncogenic activities of proteins such as Myc promote aberrant proliferation and pose a risk to genomic integrity (Bretones *et al.,* 2015). Tumour suppressors such as Ikaros oppose this activity and promote quiescence and differentiation (Ma *et al.,* 2010; Kathrein *et al.,* 2005). These competing interests must be finely balanced to ensure normal development. Here I give an overview of the regulation of the mammalian cell cycle. As the activity of Ikaros primarily arrests cells in G1 phase, I will focus on the regulatory mechanisms that govern progression past the G1/S checkpoint.

1.2.1 The G1/S checkpoint

Pioneering studies in yeast identified the cell cycle as a sequence of highly orchestrated events requiring the temporal expression of genes involved in the progression through checkpoints (Hartwell *et al.,* 1974). Progression through the G1/S checkpoint depends on the activity of Cdc28 (Cdc2), a protein kinase that is activated by its association with cyclin binding partners (Hartwell *et al.,* 1974; Nurse and Bisset, 1981; Reed *et al.,* 1985; Evans *et al.,* 1983; Sudbery *et al.,* 1980). An analogous system of regulation is conserved in mammals, in which specialised Cdks control progression through different cell cycle checkpoints. Progression through the G1/S checkpoint in mammals depends on the activity of the interphase cyclin-dependent kinases Cdk4, Cdk6 and Cdk2 (Schafer, 1998). Mitogenic stimulation in early G1 phase induces the expression of D-type cyclins that bind to and activate the activity of Cdk4 and Cdk6 complexes (Matsushime *et al.,* 1992; Meyerson and Harlow, 1994). The D-type cyclins were originally identified in macrophages stimulated with colony-stimulation factor CSF1 (Matsushime *et al.,* 1991). CSF1 induces an acute and transient activation of immediate-early genes such as *c-Fos* and *c-Myc* (Orlofsky and Stanley, 1987). This is followed by the cyclical upregulation of the three D-type isoforms cyclin D1, D2 and D3 in early/mid G1, before their degradation at the onset of S phase (Matsushime *et al.,* 1991). In this capacity D-

type cyclins act as growth factor sensors whose transcription depends on mitogenic stimuli. Removal of mitogenic stimuli quickly results in their nuclear export and proteasomal degradation (Sherr and Roberts, 1999).

The importance of D-type cyclins in G1 progression was illustrated by experiments in rodent fibroblasts. Overexpression of cyclin D1 and cyclin D2 shortened the G1 interval and rendered the cells less dependent on serum stimulation for proliferation (Quelle *et al.,* 1993). Inhibition of cyclin D1 by injecting the cells with an anti-cyclin D1 monoclonal antibody shortly after serum stimulation prevented entry into S phase, suggesting that D-type cyclins perform a rate limiting function during G1/S progression (Quelle *et al.,* 1993). Inhibition of cyclin D1 near the S phase boundary had no anti-proliferative effect, placing D-type cyclins early in the temporal sequence of events, at the boundary of the serum-dependent restriction point (Quelle *et al.,* 1993). Genetic ablation studies have highlighted potential tissue-specific functions for D-type cyclins and Cdks. Cyclin D triple knockout mice are embryonic lethal and show marked haematopoietic defects, suggesting D-type cyclins are required for the proliferation and expansion of HSCs (Kozar *et al.,* 2004). Surprisingly, mouse embryonic fibroblasts derived from cyclin D deficient mice were able to proliferate, but required increased mitogenic stimulation to enter the cell cycle (Kozar *et al.,* 2004). Similar phenotypes were observed in Cdk4/6 knockout mice, suggesting that cyclin D-Cdk complexes are required for haematopoiesis (Malumbres *et al.,* 2004). A unique role for cyclin D3 was identified in the development of pre-B cells. In these cells cyclin D1 is not detectable, but there is a substantial reduction in both cyclin D2 and D3 as the cells enter the resting pre-B cell stage (Cooper *et al.,* 2006). Cyclin $D3^{-/-}$ cells were blocked at the pro-B cell stage and were unable to enter into the large cycling pre-B cell stage (FrC') (Cooper *et al.,* 2006). Cyclin D3 protein expression is stabilised downstream of pre-BCR and cytokine signalling pathways, which need to be terminated to proceed to the small resting pre-B cell stage (FrD) (Cooper *et al.,* 2006).

Binding of cyclin D to Cdk4/6 forms a catalytic complex that can phosphorylate the

retinoblastoma tumour suppressor RB. This is contingent upon phosphorylation of the cyclin-Cdk complex by the Cdk-activating kinase (CAK), which increases the catalytic activity of the complex (Desai *et al.,* 1992). Catalytically active cyclin D-Cdk4/6 complexes can subsequently phosphorylate RB, partially facilitated by the ability of cyclin D to bind to pRB directly (Kato *et al.,* 1993; Matsushime *et al.,* 1994). RB undergoes cell cycle-dependent phosphorylation and dephosphorylation, controlling the decision to proliferate or remain quiescent. RB is hypophosphorylated in G1 but is hyperphosphorylated and inactivated as the cells transition into S phase (Ludlow *et al.,* 1990). Only the hypophosphorylated form of RB is able to associate with the E2F1 transcription factor to inhibit its activity (Chellappan *et al.,* 1991; Hiebert *et al.,* 1992). Phosphorylation of RB by cyclin-Cdk complexes allows the dissociation of E2F1 from RB inhibition and activation of its transcriptional program (Dyson, 1998). E2F1 overexpression is sufficient to induce early entry into S phase and overcome proliferative arrest as a result of serum starvation (Johnson *et al.,* 1993; Shan and Lee, 1994). E2F activates the transcription of Cdk2 and cyclin E, which form a complex in late G1 phase before the onset of DNA synthesis (Koff *et al.,* 1992; Botz *et al.,* 1996). The phosphatase cdc25A removes an inhibitory phosphate group on Cdk2, shortening G1/S transition by activating the cyclin E-Cdk2 complex (Blomberg and Hoffman, 1999). The cyclin E-Cdk2 complex can in turn fully phosphorylate RB to further facilitate E2F-dependent transcription of genes required for DNA replication (Dyson, 1998).

Two families of cyclin-dependent kinase inhibitors regulate the sequence of events governing G1/S transition. The INK4 family consists of p15, p16, p18 and p19 that specifically bind and inhibit the G1 Cdks. INK4 proteins bind to uncomplexed Cdks and allosterically inhibit the binding of cyclins, thereby preventing complex formation (Pavletich, 1999). As cells reach replicative senescence defined by the Hayflick limit, the expression of p16 dramatically increases. This in turn inhibits Cdk4 and Cdk6 and prevents cell cycle progression (Alcorta *et al.,* 1996). INK4 proteins form stable complexes with Cdks that are unaffected by the expression level of cyclins (Schafer, 1998). The Cip/Kip family of inhibitors include p21, p27 and p53.

This family displays a broader specificity than INK4 and can bind to most Cdks that are already in complex with cyclins (Sherr and Roberts, 1999). Unlike INK4, the inhibitory action of Cip/Kip can be outcompeted by increasing the concentration of cyclins in the cell (Schafer, 1998). DNA damage blocks cell cycle progression and must be repaired before DNA replication and mitosis. DNA damage is sensed by p53, which induces the expression of p21 to inhibit cyclin-Cdk complexes (Pavletich, 1999). P27 was first identified as a cyclin E-Cdk2 inhibitor that is active in growth arrested cells (Polyak *et al.,* 1994). P27 overexpression was sufficient to arrest cells by binding to cyclin E-Cdk2 complexes, which inhibited the activation of E2F (Polyak *et al.,* 1994). Cyclin D-Cdk4 complexes sequester p27 protein in proliferating cells, thereby preventing its inhibition of cyclin E-Cdk2 (Polyak *et al.,* 1994). Binding of p21 and p27 helps to stabilise cyclin D-Cdk4 complexes, resulting in enhanced sequestration (Sherr and Roberts, 1999). The loss of proliferative signalling depletes the levels of cyclin D in the cell, facilitating the redistribution of p21 and p27 to cyclin E-Cdk2 complexes (Sherr and Roberts, 1999). This results in the termination of proliferation and an accumulation of cells in G0/G1 phase.

1.2.2 Myc and the regulation of the cell cycle

Myc is an proto-oncogenic transcription factor that controls many cellular processes relevant to malignancy including metabolism, DNA replication, cell cycle, angiogenesis, apoptosis, transcription and translation (Dang, 2012). *c-Myc* was first discovered as the cellular homologue of the avian myelocytomatosis virus oncogene *v-Myc* (Vennstrom *et al.,* 1982). Aberrant expression of *MYC* by gene amplification, overexpression, chromosomal translocation or retroviral insertion can lead to inappropriate proliferation and cooperate with other oncogenic lesions to promote the development of cancer (Meyer and Penn, 2008). The oncogenic activity of MYC was confirmed by the discovery of a balanced chromosomal translocation that places *Myc* expression under the control of the *IgH* locus in Burkitts lymphoma (Dalla-Favera *et al.,* 1982). Transgenic mice that bear the *Myc* gene coupled to the IgH

enhancer (Eμ) exhibit a partial block in pre-B cell development at the large cycling pre-B cell stage (Langdon *et al.,* 1986). These highly proliferative cells inevitably form leukaemias and lymphomas, suggesting that *Myc* downregulation is essential for the differentiation of B cells and the prevention of malignancy (Langdon *et al.,* 1986). The transforming property of Myc in other cell types was demonstrated by its ability to cooperate with *Ras* to promote the tumourigenic conversion of primary rat fibroblasts (Land *et al.,* 1983). This work was further explored using an inducible Myc protein fused to the oestrogen hormone binding domain (Myc-ER). Induction of Myc-ER caused a reversible transformation of rat fibroblasts, contingent on the presence of the ER ligand oestradiol (Eilers *et al.,* 1989).

The expression of *Myc* is tightly controlled downstream of growth factor receptors, and its expression is correlated with proliferation (Shichiri *et al.,* 1993). *Myc* expression is low in quiescent cells, but is sharply upregulated in response to growth factors. Mitogenic signalling through the Ras/Raf/Mek/Erk cascade elevates the expression of *Myc* (Kerkhoff *et al.,* 1998). *Myc* is also upregulated downstream of other signalling pathways including Wnt, Jak/Stat, Bcr-Abl, Src, Akt and integrins (Bretones *et al.,* 2015; Benaud and Dickson, 2001). Antiproliferative signalling due to conditions such as serum starvation or contact inhibition results in a sharp reduction in *Myc* mRNA levels, which exhibit a short half-life of around 20 minutes (Dean *et al.,* 1986). The half-life of Myc protein is similarly short, and Myc is subject to post-translational modifications that influence its stability. Phosphorylation of serine 62 by ERK in the N-terminal domain of Myc stabilises the protein in early G1 phase, but subsequent phosphorylation at threonine 62 by GSK-3 promotes its ubiquitination and proteasomal degradation (Sears *et al.,* 2000). Thus the level of Myc expression is tightly controlled to facilitate growth and proliferation, and must be attenuated to promote quiescence.

Myc transcriptional activity rests on its C-terminal basic helix-loop-helix-leucine zipper (bHLHZip) DNA interaction domain (Baudino and Cleveland, 2001). Myc alone is unable to transactivate or repress transcription, and must dimerise with other

bHLHZip family members. Myc heterodimerises with Max, and this association is required for Myc transcriptional activity and its ability to promote cellular transformation (Blackwood and Eisenman, 1991; Baudino and Cleveland, 2001). In contrast to Myc, the expression of Max is maintained at a constant level throughout the cell cycle and is unaffected by serum or confluence (Berberich *et al.,* 1992). Max can also bind to Mad, which promotes an opposing transcriptional profile to Myc-Max heterodimers (Ayer *et al.,* 1993; Blackwood and Eisenman, 1991). Thus a model was proposed that Myc competes with other repressive proteins to bind to Max (Blackwood and Eisenman, 1991). As *Myc* expression is serum responsive, the increase in Myc protein in preparation for cell cycle progression would result in the preferential formation of Myc-Max heterodimers and a proliferative transcriptional program (Blackwood and Eisenman, 1991).

Myc-Max heterodimers bind to the E box sequence, a frequently occurring motif in the genome (Meyer and Penn, 2008). Indeed Myc can bind to thousands of genes, occupying up to 15% of all promoters (Dang, 2012; Zeller *et al.,* 2006). There are multiple ways in which can regulate transcription. Myc can activate transcription through its association with TRRAP, a coactivator that recruits histone acetyltransferase complexes to chromatin (Meyer and Penn, 2008). Myc also associates with INI1, a component of the SWI/SNF chromatin remodelling complex (Meyer and Penn, 2008). Loss of Myc results in a global change in chromatin status towards an inactive state, characterised by hypoacetylation (Knoepfler *et al.,* 2006). Furthermore, Myc is also able to recruit pTEFb to promoter-proximal paused RNA polymerase II (Pol II), which phosphorylates Pol II and facilitates transcriptional elongation (Rahl *et al.,* 2010). Through these actions Myc was proposed to act as a universal amplifier of active genes (Nie *et al.,* 2012). In addition to activation, Myc can transcriptionally repress genes, particularly cell cycle regulators (Yang *et al.,* 2001; Coller *et al.,* 2000). For example Myc is able to bind to the transcriptional activator Miz-1 and prevent the recruitment of p300 to the p15 locus (Gartel and Shchors, 2003). Myc can also repress gene expression by activating the microRNA cluster miRNA 17-92, which negatively regulates the expression of cell cycle

inhibitors (Dang, 2012; Bretones *et al.,* 2015).

The importance of Myc in cell cycle progression was illustrated by experiments in which conditional Myc-ER activation was able to facilitate re-entry into the cell cycle in serum starved, confluent fibroblasts (Eilers *et al.,* 1991). Myc is also able to regulate genes independently of serum, which are primarily involved in metabolic processes necessary for cell growth in anticipation of DNA synthesis and mitosis (Schlosser *et al.,* 2005; Perna *et al.,* 2012). Knockdown of *MYC* using RNA interference results in a strong arrest at the G1/S checkpoint in normal cells and arrests tumour cell proliferation in multiple cell cycle stages (Wang *et al.,* 2008). Myc is able to directly activate the transcription of genes required for the progression through the G1 checkpoint including cyclin D2, cyclin D3, cyclin E, Cdk4, Cdk6 and multiple members of the E2F family (Bretones *et al.,* 2015). In addition to directly upregulating the expression of cyclin E, Myc can indirectly regulate its expression through the upregulation of E2F (Bretones *et al.,* 2015). Myc can also promote the activity of Cdks by increasing the activity of CAK phosphorylation required for Cdk activation. This is achieved through enhanced protein translation of the CAK subunits (Cowling and Cole, 2007). Furthermore, Myc can recruit CAK to transcription start sites, where it phosphorylates Pol II to promote transcriptional initiation (Cowling and Cole, 2007).

Myc is able to regulate the expression of p21 through association with Miz-1, turning Miz-1 into a repressive complex (Peukert *et al.,* 1997). Myc also upregulates the expression of AP4, a transcription factor that directly represses p21 expression (Jung *et al.,* 2008). Myc regulates the expression and activity of p27 through a number of mechanisms including transcriptional repression, microRNA regulation, protein sequestration and protein degradation (Bretones *et al.,* 2015). Myc can upregulate the expression of G1 cyclins, facilitating the sequestration of p27 in cyclin D-Cdk4/6 complexes and enabling free cyclin E-Cdk2 complexes to phosphorylate RB and promote S phase progression (Perez-Roger *et al.,* 1999). Myc also upregulates the expression of members of the SCF^{SKP2} complex that ubiquitinate p27, resulting in

proteasomal degradation (Bretones *et al.,* 2015). As a result of this regulation, the growth antagonising effects of p27 are overridden by elevated Myc expression (Vlach *et al.,* 1996). In conclusion, Myc is able to promote cell cycle progression through positive and negative regulation of key cell cycle components. Deregulated *MYC* expression is involved in the genesis of many cancers, highlighting the importance of regulating this proto-oncogene to maintain normal development.

1.2.3 Scaffolding proteins in the regulation of the cell cycle

Scaffolding proteins play integral roles in the regulation of signalling cascades by organising the vast array of intracellular signalling molecules into discrete subsets of proteins, promoting an efficient flow of information through intracellular networks at the correct point in space and time (Good *et al.,* 2011). Scaffolding proteins form hubs downstream of kinase, GTPase, immune receptor, and cell-cell signalling cascades (Good *et al.,* 2011; Shaw and Filbert, 2009). They facilitate protein-protein interactions by physically tethering interacting components of a network together and ensure the correct compartmentalisation of signalling molecules. The molecular circuits formed by these interactions can be simple and linear, but can also promote branching signals to multiple outputs and create feedback loops, forming positive and negative gradations of signalling (Shaw and Filbert, 2009). In addition to regulating components of a pathway, scaffold proteins themselves are subject to regulation, and this influences downstream signalling. An example of this can be observed by the phosphorylation of Blnk/Slp65 in response to pre-BCR signalling. Slp65 is phosphorylated by Syk, and this recruits SH2 domain containing effector molecules that mediate pre-BCR signalling and proliferative arrest (Fu *et al.,* 1998). A similar mechanism of regulation is observed for LAT and SLP76, scaffolding proteins that lie downstream of the T cell receptor (TCR) (Zhang *et al.,* 1998).

A-kinase anchoring proteins (AKAPs) are scaffolding proteins that contain a short peptide motif that can bind to the regulatory subunit of protein kinase A (PKA).

Outside of this domain the proteins are highly variable and are able to bind to a range of receptors, ion channels, phosphatases and GTPases (Han *et al.,* 2015). This diversity in family members ensures specificity in response to signalling inputs. Akap12 (SSeCKS) negatively regulates the G1/S transition by ERK-dependent downregulation of *Ccnd1* (cyclin D1) (Lin *et al.,* 2000). SSeCKS likely inhibits ERK activation by scaffolding Src in lipid rafts away from focal adhesion kinase (FAK) complexes (Su *et al.,* 2013). In addition to transcriptional repression of *Ccnd1*, SSeCKS can directly bind cyclin D1 protein and sequester it in the cytoplasm (Lin *et al.,* 2000). Posttranslational modifications can additionally regulate the activity of SSeCKS. Phosphorylation by protein kinase C (PKC) has been shown to negatively regulate the ability of SSeCKS to interact with cyclin D (Lin and Gelman, 2002). This example shows how extracellular signals can be relayed through integrin clusters to the nucleus to influence cell cycle progression. The decision to proliferate depends on multiple signals that must be integrated to regulate the expression and activity of the cell cycle machinery. Scaffolding proteins form nodes in these networks by bringing together and influencing these signals, altering the balancing between proliferation and quiescence.

1.3 RNA interference

High throughput technologies can provide a wealth of data concerning the normal functioning of the cell and the mutations that give rise to cancer. Whole genome sequencing of tumours using techniques such as RNA-seq offer a deep insight into the differential expression of genes involved in the development of cancer (Lizardi *et al.,* 2011). It can be somewhat difficult to detect the causal drivers of the progression to cancer, and important candidates can be overlooked in the data. RNA interference (RNAi) offers the ability to perform unbiased genome wide loss of function screens to identify genes with a direct casual role in the phenotype studied. RNAi screens have been deployed to identify tumour suppressors that prevent the aberrant proliferation and survival of transformed cells, and genes that are required for the maintenance of cancer viability (Schlabach *et al.,* 2008; Silva *et al.,* 2008; Berns *et al.,* 2004; Westbrook *et al.,* 2005). RNAi is therefore an important technology that can deepen our understanding of cellular processes to aid in the prevention and treatment of cancer (Bernards *et al.,* 2006; Lizardi *et al.,* 2011).

RNAi is a regulatory mechanism present in most eukaryotic cells that utilises double stranded RNA (dsRNA) molecules to direct homology dependent degradation of target mRNA. The first reported discovery of the RNAi phenomenon was in plants, in which an enzyme involved in violet colouration was overexpressed (Napoli *et al.,* 1990). Overexpression of a transgene encoding the chalcone synthase (CHS) enzyme resulted in white colouration and a drastic reduction in the mRNA level of the endogenous and introduced CHS gene. This was termed 'co-suppression' and was an early example of post-transcriptional regulation involving dsRNA (Napoli *et al.,* 1990). Similar results were observed in fungi, in which the introduction of exogenous sequences silenced or 'quelled' the expression of endogenous genes (Romano and Macino, 1992). The effect of double stranded RNA interference was conclusively shown in *C. elegans* by injecting sense and antisense transcripts against a variety of target genes (Fire *et al.,* 1998). The researchers found that dsRNA

transcripts were orders of magnitude more efficient at gene silencing than single stranded templates alone. They found that just a few dsRNA molecules per cell were sufficient to elicit a null phenotype, arguing against a stoichiometric silencing and hinting at a possible catalytic mechanism. Targeting promoter regions or introns did not result in efficient silencing, suggesting a post-transcriptional degradation of mRNA (Fire *et al.,* 1998).

A potential catalytic mechanism was further explored by introducing long dsRNA molecules targeting cyclin E mRNA in cultured *Drosophila* cells (Hammond *et al.,* 2000). Introduction of these molecules degraded endogenous cyclin E transcripts and arrested the cell cycle. They discovered that transcripts were degraded by a sequence specific nuclease termed the RNA-induced silencing complex (RISC). Fractionation of the RISC complex co-purified with 25 nucleotide (nt) fragments with homology to the dsRNA molecule. This suggested that the original dsRNA was converted into small intermediates that acted as guides to facilitate cleavage of the target transcript (Hammond *et al.,* 2000). The cleavage of longer dsRNA molecules into small interfering RNA (siRNA) is carried out by the RNase III ribonuclease Dicer. RNAi knockdown of Dicer itself prevented silencing of other genes, proving that this enzyme was essential in the production of siRNA that mediate mRNA silencing (Bernstein *et al.,* 2001). Dicer is a component of the RISC complex alongside TRBP and Argonaute 2 (Sen and Blau, 2006). Dicer-cleaved siRNA duplexes are loaded into the RISC complex and Argonaute 2 cleaves the 'passenger strand' (Matranga *et al.,* 2005). The remaining antisense guide strand subsequently directs Argonaute cleavage of complementary mRNA transcripts (Liu *et al.,* 2004). Thus dsRNA can direct sequence-specific catalytic cleavage of mRNA (Figure 1.5). Transfection of siRNA into an array of mammalian cells was shown to elicit gene silencing, demonstrating that the RNAi pathway is conserved across species (Elbashir *et al.,* 2001). This opened up new avenues of loss-of-function research.

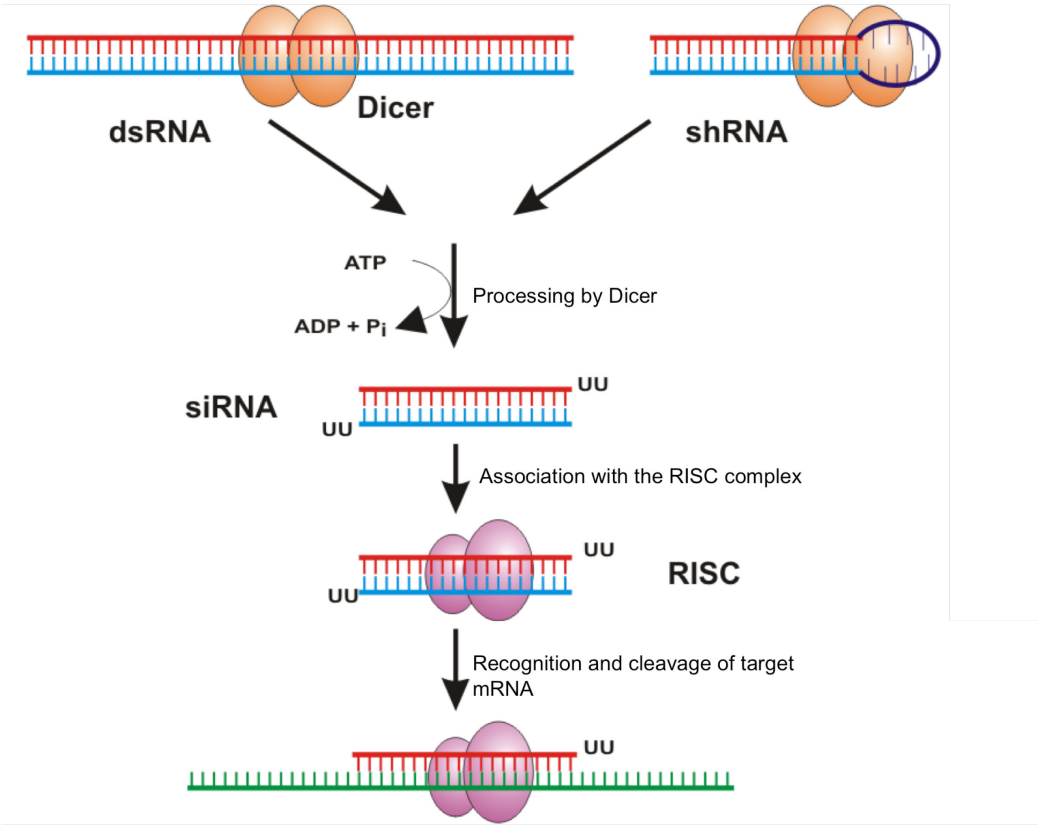

Figure 1.5 – The RNAi pathway. Figure outlining the mechanism of RNA interference. Long dsRNA templates and shRNA hairpins are processed by dicer into siRNA. siRNA are integrated into the RISC complex and mediate homology-dependent cleavage of target mRNA by Argonaute. Figure modified from Rutz and Scheffold, 2004.

Whilst providing potent knockdown of gene targets, transient transfection with small chemically synthesised siRNA is ineffectual at studying the long term effects of gene depletion. RNAi was advanced by modelling interfering dsRNA on the endogenous microRNA system of post-transcriptional regulation (Paddison *et al.,* 2002). Such short hairpin (sh)RNA molecules consist of a stem-loop-stem structure that potently target mRNA knockdown in a similar manner to siRNA (Figure 1.6). shRNA constructs can be virally inserted into the genome and transcribed from a RNA III polymerase promoter, facilitating stable and heritable gene silencing (Paddison *et al.,* 2002). Following transcription the shRNA duplexes are exported out of the nucleus by exportin 5 and the loop is cleaved by Dicer (Rao *et al.,* 2009). The siRNA is then incorporated into the RISC complex for target specific degradation.

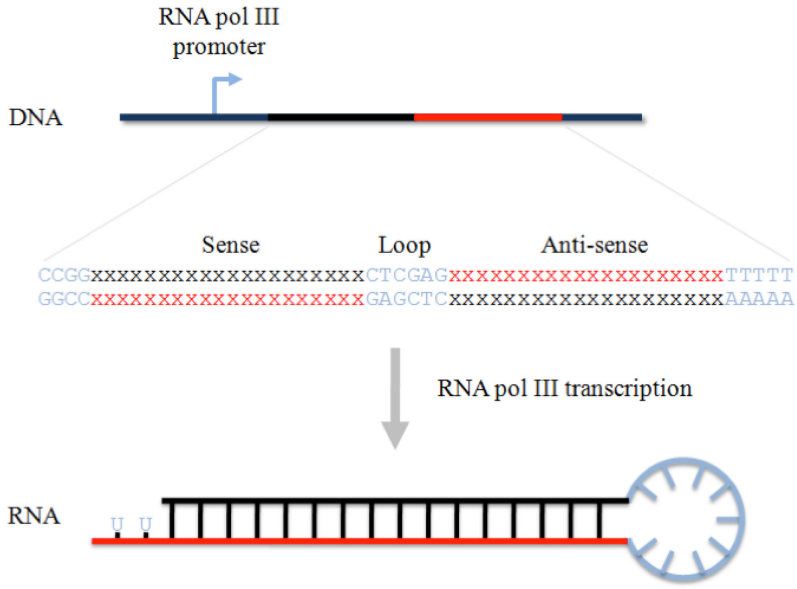

Figure 1.6 – shRNA hairpin design. The integrated shRNA cassette is transcribed from an RNApol III promoter. Sense and antisense sequences are separated by a loop region which facilitates folding into a stem-loop hairpin structure. Taken from O'Keefe, 2013.

Synthetic siRNAs are cost effective and efficient at gene silencing and are generally used in single well assays. When coupled with live cell imaging, they are effective at studying complex cell phenotypes in a high content manner. In one such experiment, Hela cells were plated on top of arrays spotted with siRNA molecules and screened for mitotic defects (Neumann *et al.,* 2006). Stably integrated viral vector based shRNA libraries are preferred when the phenotype of interest is optimally observed over a long time period, and when the target cells are hard to transfect. Pools of cells can be transduced with the viral packaged shRNA library, reducing the time and complexity of single well-based assays (Bernard *et al.,* 2006; Mohr *et al.,* 2014). Each shRNA in the library contains a unique molecular identifier known as a barcode. This means that cells containing different shRNA can be grown in the same plate in a competitive barcode screen. A selective pressure is applied for the duration of the experiment (growth arrest in response to drug treatment or overexpression of a gene for example) and the enrichment of shRNA in the experimental samples is compared to a control treatment (Bernard *et al.,* 2006; Sims *et al.,* 2011). Potential candidates are then identified by their barcodes and subjected to validation experiments. A positive selection screen aims to identify

candidates that can overcome a negative selection pressure to become enriched within a population. This is particularly useful for discovering tumour suppressors that suppress inappropriate growth (Berns *et al.,* 2004; Westbrook *et al.,* 2005). Negative selection screens aim to identify depleted candidates that are depleted from the population due to a loss of viability (Schlabach *et al.,* 2008; Silva *et al.,* 2008). Both approaches are useful for asking different questions relating to cancer cell biology.

As technology has evolved, so has the design and output of shRNA screens. An early example of a positive selection screen was performed in human fibroblasts, with the aim to identify shRNA that bypass p53-induced proliferation arrest (Berns *et al.,* 2004). The experimenters isolated colonies of cells that proliferated over the time course and PCR amplified the barcodes. The barcodes were cloned into intermediate vectors and transformed into bacteria, before colonies were harvested for sequencing. Several interesting candidates were detected that contributed to the upregulation of p21 in response to p53 induction. Nonetheless the experimental procedure was long and laborious, and difficult to perform on a large scale. To scale up the experiment, the PCR amplified barcodes were labelled with fluorescent dyes and hybridised to microarrays (Berns *et al.,* 2004). Similar approaches were undertaken to study genes involved in anchorage-independent growth in cellular transformation (Westbrook *et al.,* 2005; Kolfschoten *et al.,* 2005). Since the advent of next generation sequencing methods, the ease and scale of genome-wide RNAi screening has greatly increased. In these screens the entire transduced pool of cells is harvested for genomic DNA and the barcodes are PCR amplified before deep sequencing (Bassik *et al.,* 2009). The sequencing data is then bioinformatically analysed to identify significantly enriched or depleted candidates relative to a control treatment (Sims *et al.,* 2011). Such protocols offer a feasible method for the investigator to probe the phenotypic consequences of the loss of function of thousands of genes simultaneously, without the requirement for high-throughput technologies.

1.3.1 Aims of the thesis

Ikaros is able to regulate the cell cycle, and may exert its tumour suppressor function by antagonising aberrant proliferation. It is therefore important to understand the mechanisms of this regulation. Although much light has been shone on this area by genome wide transcriptional studies, RNAi offers a direct way to antagonise the function of thousands of genes in an unbiased, systematic fashion to identify genes that are directly required for the cessation of proliferation in response to Ikaros activity. I therefore planned to perform a pooled, positive selection shRNA screen to identify novel regulators that contribute to Ikaros-mediated cell cycle arrest. In this screen a population of cells were transduced with an shRNA library and selected for one week in the presence or absence of Ikaros-enforced arrest, prior to next generation sequencing. shRNA that facilitated escape from cell cycle arrest were able to proliferate over the time course and become enriched within the population. These shRNA were therefore enriched within the sequencing data, allowing us to identify the genes that are required to cooperate with Ikaros to enforce proliferative arrest. In this manner I am able to identify genes that directly contribute to the regulation of the cell cycle by Ikaros.

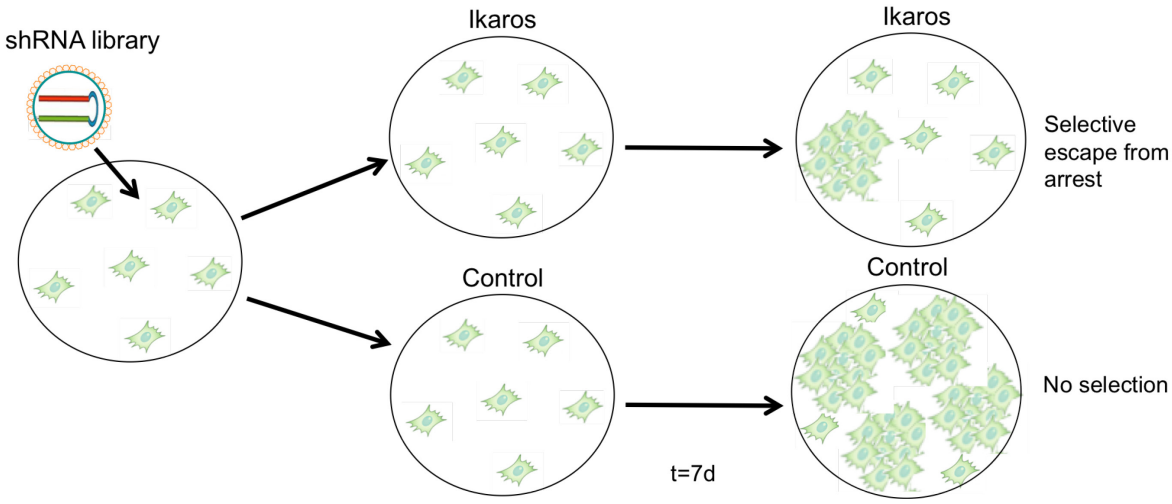

Figure 1.7 – Experimental outline. A pool of fibroblasts were transduced with an shRNA library and split into 'Ikaros arrested' and 'control' conditions. Control cells proliferated normally and should contain an equal distribution of shRNA in the population. *Ikzf1* expressing cells were arrested for the duration of the experiment. Certain shRNA will override Ikaros-mediated arrest and selectively proliferate over the time course, becoming enriched within the population. This enrichment can be detected after deep sequencing. T=time.

Chapter 2

Materials and Methods

2.1 Materials

2.1.1 Antibodies

Ikaros Rabbit polyclonal to Ikaros obtained from the laboratory of Professor Stephen Smale. Used for western blot at 1:20,000 dilution, 15µl used per IP for ChIP. Used for immunofluorescence (IF) at 1:1000 dilution.

H3 Rabbit polyclonal to histone 3 (ab1791, Abcam). Used for western blot at 1:20,000 dilution.

Tubulin Mouse monoclonal to tubulin (T9026, Sigma). Used for western blot at 1:10,000 dilution.

Myc Rabbit polyclonal to c-Myc (sc-764, Santa Cruz). Used for western blot at 1:1000 dilution.

SSeCKS Mouse monoclonal to Akap12/SSeCKS (ab49849, Abcam). Used for western blot at 1:20,000 dilution, 5µg used per IP for pulldown.

Cyclin D1 Rabbit monoclonal to cyclin D1 (ab40754, Abcam). Used for western blot at 1:5000 dilution. Used for IF at 1:200 dilution.

Cyclin D2 Mouse monoclonal to cyclin D2 (ab3085, Abcam). Used for western blot at 1:200 dilution.

Cyclin D3 Rabbit monoclonal to cyclin D3 (ab52598, Abcam). Used for western blot at 1:5000 dilution.

IgG Normal rabbit IgG (sc-2027, Santa Cruz). Used as a negative control in ChIP, 2µg per IP.

IgG Normal mouse IgG (sc-2025, Santa Cruz). Used as a negative control for pulldowns, 2.5µg used per IP.

2.1.2 Cell lines

NIH 3T3 Commercially available mouse embryonic fibroblast (MEF) cell line.

B3 Pre-B cell line resembling cells at the large cycling pre-BI (FrC') stage. Originally derived in our laboratory from an IL-7 transgenic mouse lymphoma (Fisher *et al.,* 1995).

HEK293t Commercially available human endothelial kidney cell line. Used for viral packagaing.

S24 Tetracycline regulated *SSeCKS* overexpressing NIH 3T3 cells (Lin *et al.,* 1997). A kind gift from Professor Irwin Gelman.

2.1.3 Primer and adaptor sequences

Table 1 Primers for gene expression

Primer		Sequence 5'-3'
SSeCKS mature transcript	Forward	ACGGACCAAAGCTAACCGAG
	Reverse	CAATGAGCAACTCACGTCTTAGG
SSeCKS primary transcript	Forward	CGTGTAGCGCCTTTGAAGAG
	Reverse	TCAACAACTGTGGAACTGGC
Myc mature transcript	Forward	GCCCAAATCCTGTACCTCGTCC
	Reverse	CTCTTCTCCACAGACACCACATCA
Myc primary transcript	Forward	GCTGCTGTCCTCCGAGTCCT
	Reverse	CGCTTCCTACCCTGCTGTGA
Ubc	Forward	AGGAGGCTGATGAAGGAGCTTGA
	Reverse	TGGTTTGAATGGATACTCTGCTGGA
Itga5	Forward	TCCCACATCTATTGGAGCCC
	Reverse	GTAGGGGAGGGAACGTTTGA
Itgb1	Forward	TCAGAGCTGGCCTTCTCAC

	Reverse	CAGTTGTCACGGCACTCTTG
Ccnd2	Forward	GATCCGAACGAGACCAAGAA
	Reverse	CCCTCTGGCTCACTTCTCAG
Cdk6	Forward	GCCCAAGTTCAGTTCTCAGC
	Reverse	CGTCTCTGTGTGTGGGAATG
Cdkn1a	Forward	CCTGGTGATGTCCGACCTG
	Reverse	CCATGAGCGCATCGCAATC
Cdkn1b	Forward	GCAGTGTCCAGGGATGAGGAA
	Reverse	AGTGCCAGCGTTCGGGGAAC
Igll1	Forward	GGACTTGAGGGTCAATGAAGCTC
	Reverse	GTGGGATGATCTGGAACAGGAG
Hk2	Forward	TGATCGCCTGCTTATTCACGG
	Reverse	AACCGCCTAGAAATCTCCAGA
Ldha	Forward	CATTGTCAAGTACAGTCCACACT
	Reverse	TTCCAATTACTCGGTTTTTGGGA
Hoxa1	Forward	AGAAACCCTCCCAAAACAGG
	Reverse	TTGTTGAAGTGGAACTCCTTCTC

Table 2 Primers for ChIP analysis

Primer		Sequence 5'-3'
SSeCKS	Forward	AGTGGCTTTCCTACTCTCGC
	Reverse	ATTCTCAGTCCGGGTGTGTT
Igll1-12	Forward	AGTCCGAGAACAGCCTGGGT
	Reverse	AGTTGTGCTGCCCACAGAGG
Igll1-18	Forward	CTGGGATCCTTCTGCATCTACTTCAG
	Reverse	GAGGATGTGAAGAGTCTGGCCAT
Myc-1	Forward	GCCCAAATCCTGTACCTCGTCC
	Reverse	CTCTTCTCCACAGACACCACATCA
Myc-4	Forward	AAGCTTTTCGGGCGTTTTT
	Reverse	CACTCCAGAGCTGCCTTCTT

Table 3 Primers for shRNA amplification and sequencing

Primer		Sequence 5’-3’
HTS	Forward	TTCTCTGGCAAGCAAAAGACGGCATA
	Reverse	TGCCATTTGTCTCGAGGTCGAGAA
Gex	Forward	CAAGCAGAAGACGGCATACGAGA
	Reverse	AATGATACGGCGACCACCGAGA
GexSeqN	Forward	ACAGTCCGAAACCCCAAACGCACGAA

Table 4 Primers for barcode PCR

Primer	Sequence 5'-3'
shIkzf1-B	ATCAGTACTGCATGTGACTG
shIkzf1-D	ATGTGTTGTGACACGTGTGT
shRag1	ATGTGTTGACGTTGGTTGGT

Table 5 Primers for cloning

Primer		Sequence 5'-3'
Tag-BFP	Forward	TGCTCTAGACGCCACCATGAGCGAGCTG
	Reverse	CGCGGATCCATTAAGCTTGTGCCCCAG
SSeCKS	Forward	AATCTCGAGCGCCACCATGGGTGCAGGCAGTTCCAC
	Reverse	CCGGAATTCTTAGGATTCTGTCAGGTCTC

Table 6 shRNA design

Primer		Sequence 5'-3' (target sequence in red)
shIkzf1-A	Forward	TAGAAGACGCACCGGCGGCCTTATCTATCTAACTAAGTTAATATTCATAGC TTGGTTAGGTAGATAAGGCCGTTTTTTTTCGCCGTCTTCGT
	Reverse	ACGAAGACGGCGAAAAAAAAACGGCCTTATCTACCTAACCAAGCTATGAAT ATTAACTTAGTTAGATAGATAAGGCCGCCGGTGCGTCTTCTA
shIkzf1-B	Forward	TAGAAGACGCACCGGCCGTTGGTAAGTCTCATAAATGTTAATATTCATAGC ATTTGTGAGGCTTACCAACGGTTTTTTTTCGCCGTCTTCGT
	Reverse	ACGAAGACGGCGAAAAAAAAACCGTTGGTAAGCCTCACAAATGCTATGAAT ATTAACATTTATGAGACTTACCAACGGCCGGTGCGTCTTCTA
shIkzf1-C	Forward	TAGAAGACGCACCGGGCCCTATGATAGTGCCAATTAGTTAATATTCATAGC TAGTTGGCACTGTCATAGGGCTTTTTTTTCGCCGTCTTCGT
	Reverse	ACGAAGACGGCGAAAAAAAAAGCCCTATGACAGTGCCAACTAGCTATGAAT ATTAACTAATTGGCACTATCATAGGGCCCGGTGCGTCTTCTA
shIkzf1-D	Forward	TAGAAGACGCACCGGCGCCAAATGTAAGAGCTTTATGTTAATATTCATAGC ATAGAGCTCTTACGTTTGGCGTTTTTTTTCGCCGTCTTCGT
	Reverse	ACGAAGACGGCGAAAAAAAAACGCCAAACGTAAGAGCTCTATGCTATGAAT ATTAACATAAAGCTCTTACATTTGGCGCCGGTGCGTCTTCTA
shSSeCKS-B	Forward	TAGAAGACGCACCGGGCCAGTGTTAAAGAAAGTGTTGTTAATATTCATAG CAACACTTTCTTTGACACTGGCTTTTTTTTCGCCGTCTTCGT
	Reverse	ACGAAGACGGCGAAAAAAAAAGCCAGTGTCAAAGAAAGTGTTGCTATGAA TATTAACAACACTTTCTTTAACACTGGCCCGGTGCGTCTTCTA
shSSeCKS-C	Forward	TAGAAGACGCACCGGGCAGAGTCCATCCTAATAATAGTTAATATTCATAGC TATTATTGGGATGGACTCTGCTTTTTTTTCGCCGTCTTCGT
	Reverse	ACGAAGACGGCGAAAAAAAAAGCAGAGTCCATCCCAATAATAGCTATGAAT ATTAACTATTATTAGGATGGACTCTGCCCGGTGCGTCTTCTA

Table 7 Illumina adaptor sequences

Adapter	Sequence 5'-3'
AR002	CGATGT
AR004	TGACCA
AR005	ACAGTG
AR006	GCCAAT
AR007	CAGATC
AR012	CTTGTA
AR013	AGTCAA
AR014	AGTTCC
AR001	ATCACG
AR003	TTAGGC
AR008	ACTTGA
AR009	GATCAG

2.2 Methods

2.2.1 Cell culture

NIH3T3, S24 and HEK293t cells were cultured in Dulbecco's Modified Eagle Medium (DMEM, Invitrogen) supplemented with 10% (v/v) foetal calf serum (FCS) (Biosera), 2mM L-glutamine, antibiotics (100U/ml Penicillin and 100µg/ml Streptomycin) and 50µM β-mercaptoethanol (Gibco, Invitrogen). The media of S24 cells was additionally supplemented with 1µg/ml doxycycline (Sigma-Aldrich) to suppress the transactivation of the *SSeCKS* transgene. Cells were passaged every two days to maintain the population at less than 80% confluence. NIH3T3 and S24 cells were detached using 0.05% trypsin-EDTA (Invitrogen).

B3 cells were cultured in suspension with Iscove's Modified Dulbecco's Medium (IMDM, Invitrogen) supplemented with 10% (v/v) foetal calf serum (FCS) and antibiotics (100U/ml Penicillin and 100µg/ml Streptomycin). The cells were passaged every two days to maintain the culture concentration between 0.5-3x10^6

cells/ml. Primary pre-B cells were cultured in IMDM supplemented with 10% (v/v) foetal calf serum (FCS), 2mM L-glutamine, antibiotics (100U/ml Penicillin and 100µg/ml Streptomycin), 50µM β-mercaptoethanol and 5ng/ml IL-7 (R&D systems). The cells were cultured in 6 well plates coated with irradiated ST2 fibroblasts as feeder cells. The cells were passaged every two days to maintain the culture concentration between 0.5-2x10^6 cells/ml.

All cells were maintained at 37°C in a humidified chamber with 5% (v/v) O_2. Frozen stocks were generated by resuspending 1x10^6 cells in 1ml of FCS containing 10% (v/v) DMSO (Sigma) followed by cooling in a Mr Frosty freezing container (Thermo Scientific) at -80°C. After 24 hours, the cells were transferred to liquid nitrogen containers for long term storage.

2.2.2 Viral packaging and transduction

2.2.2.1 Retroviral packaging and transduction

To generate fibroblast and pre-B cell lines expressing the inducible Ikaros-ERt2-GFP construct, or MSCV-*Ikzf1*-GFP construct, retrovirus was generated by transfecting HEK293t cells using the calcium phosphate method. 4µg of the Ikaros expression vectors were suspended with 4µg of the pCL-Eco ecotropic packaging vector (Addgene) in 500µl of a 0.4M $CaCL_2$ solution. DNA precipitates were formed by the dropwise addition of 500µl 2X HEBS buffer (280nM NaCl, 10mM KCl, 1.5mM $Na_2HPO_4.H_2O$, 12mM glucose, 50mM HEPES free acid, pH 7.05 in distilled water). 1ml of the DNA precipitate was added to 50% confluent HEK293t cells grown in 10cm^3 culture dishes with 9ml of medium and the cells were incubated at 37°C. Fresh medium was fed to the cells 12 and 24 hours post-transfection. 3.5ml of viral supernatant was collected at 36, 48 and 60 hours post-transfection, pooled and purified through a 0.22µM filter.

Fibroblasts were transduced by plating $0.5x10^6$ cells per $10cm^2$ dish in 5ml of viral supernatant supplemented with 4µg polybrene and 10mM HEPES pH 7.6 (Sigma) per ml, and incubated for 8-12 hours at 37°C, then replaced by fresh media. Pre-B cells were transduced by suspending $2x10^6$ cells in 4ml of viral supernatant supplemented with 4µg polybrene and 10mM HEPES pH 7.6, in a single well of a 6-well plate. The plates were centrifuged at 37°C for 90 minutes at 900g, then incubated for 3 hours at 37°C. The viral supernatant was then replaced by fresh media.

2.2.2.2 Lentiviral packaging and titration

I used lentiviral particles to introduce shRNA vectors into my cells. Lentivirus was generated by transfecting HEK293t cells using the lipofectamine2000 reagent (Invitrogen). 23µl of an amphotropic packaging plasmid mix (0.5µg/µl psPax2 and pCMV-VSV-G in a 4:1 ratio v/v) (Addgene) was mixed with 2.3µl (1µg/µl) of the pRSI9-shRNA expression vector (Cellecta) in 1ml of Opti-MEM media (Invitrogen). This 1ml suspension was mixed with 1ml of Opti-MEM media containing 35µl lipofectamine 2000, and incubated at room temperature for 15 minutes. 2ml of DNA/lipofectamine complexes were added to 90% confluent HEK293t cells grown in $10cm^3$ culture dishes with 10ml of DMEM medium without antibiotics, and incubated at 37°C. Fresh medium was fed to the cells 12 and 24 hours post-transfection, and lentiviral supernatant was collected 48 hours post-transfection and purified through a 0.22µM filter. Stocks of the M1 lentiviral library (Cellecta, decipherproject.org) were aliquoted into 1ml screw cap tubes (Starlab), snap frozen in liquid nitrogen and stored at -80°C.

Viral stocks were titrated by plating $0.1x10^6$ NIH3t3 cells in 6 well dishes with 4ml media supplemented with 4µg polybrene and 10mM HEPES pH 7.6. Individual wells were infected with 100µl, 33µl, 10µl, 3µl and 0µl of viral stocks and incubated for 8-12 hours at 37°C before changing to fresh medium. 72 hours post-infection, the percentage of transduced cells expressing red or blue fluorescent protein (RFP or

BFP) was observed by flow cytometry. The multiplicity of infection (MOI) was calculated from the percentage of transduced cells using the graph in figure 2.1 (taken from the Decipher project user manual, Cellecta).

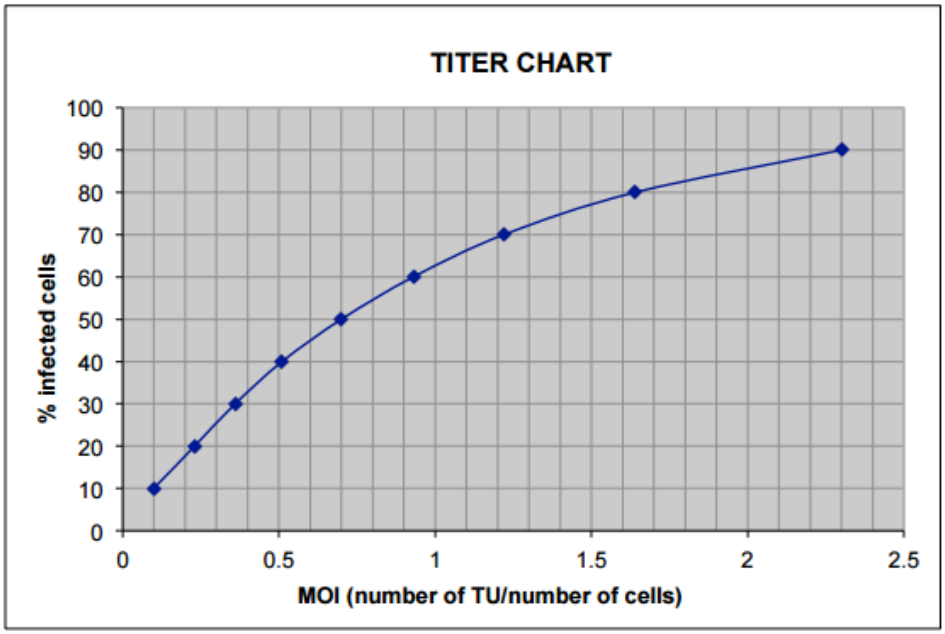

Figure 2.1 – Lentiviral titer chart. The multiplicity of infection can be determined by interpolating the % infected cells to the standard curve. Taken from the Decipher project user manual (decipherproject.net).

The lentiviral titre, expressed as transduction units per ml (TU/ml), was calculated using the following formula:

TU= (number of transduced cells ($0.1x10^6$)) * (MOI)/(ml of viral stock used for transduction)

Once the titre is known, the amount of virus stock required to infect target cells at a particular MOI can be calculated by using the following rearranged formula:

Volume of viral stock required = total number of cells * (MOI/(TU/ml))

2.2.2.3 Cell sorting

Once infected with retroviral or lentiviral constructs, the cells were incubated for 72 hours for the maximal expression of fluorescence. $10x10^6$ cells were pelleted and suspended in 1ml phosphate buffered saline ($PBS^{-/-}$) supplemented with 5% (v/v) FCS, and passed through a cell strainer cap into 12x75mm polypropylene tubes. Samples were submitted on ice to the medical research council (MRC) flow cytometry facility, and the cells were sorted on the BD FACSAriaIII based on the expression of green, blue or red fluorescence.

2.2.3 Cloning

2.2.3.1 Generating *shIkzf1* and *shSSeCKS* lentiviral vectors

To generate shRNA constructs targeting *Ikzf1* or *SSeCKS*, I cloned shRNA templates into the pRS-I9-RFP lentiviral expression vector. The full hairpin structure containing the targeting sequence of each shRNA (table 6) was obtained from an open access database (Cellecta, decipherproject.org). 2.5µM of the forward and reverse shRNA oligos were diluted in H_2O and annealed by heating to 95°C for 30 seconds, before being cooled to room temperature. The pRS-I9-RFP vector was digested with BpiI (Thermo Scientific) and purified using the QIAquick gel extraction kit (Qiagen). 0.2µM of each annealed shRNA oligo pair was ligated into 10ng of the BpiI digested gel purified pRS-I9-RFP vector using 1µl (40U) of T4 DNA ligase (NEB) for 2 hours at room temperature.

2.2.3.2 Generating blue fluorescent protein (BFP) expressing lentiviral vectors

To generate shRNA vectors that express blue fluorescent protein (BFP) instead of red fluorescent protein (RFP), I amplified the coding sequence of BFP from the tagBFP vector (Evrogen) using high fidelity phusion polymerase (Thermo scientific). The

tagBFP forward primer (table 5) used for amplification contained sequences complementary to the 5' end of the BFP coding sequence and included the start codon, a kozac consensus sequence and a XbaI restriction site. The reverse primer contained a BamHI cut site. The amplified BFP sequence was ligated into the gel purified pRS-I9-shIkaros and pRS-I9-empty lentiviral vectors cut with XbaI-BamHI.

2.2.3.3 Cloning an *SSeCKS* overexpression vector

A full length cDNA clone of *SSeCKS* was purchased from Source BioScience and PCR amplified using high fidelity phusion polymerase. The *SSeCKS* forward primer (table 5) contained sequences complementary to the 5' end of the cDNA clone, a kozac consensus sequence and an XhoI restriction site. The reverse primer contained an EcoRI restriction site. The amplified sequence was ligated into the gel purified MSCV-IRES-GFP retroviral vector cut with XhoI-EcoRI.

2.2.3.4 Bacteria transformation and plasmid DNA isolation

Following ligation, 5µl of the ligation construct was mixed with 20µl of 5x KCM buffer (0.5M KCL, 0.15M $CaCl_2$, 0.25M $MgCl_2$) and made to a total of 100µl with H_2O. This was mixed with 100µl DH5α competent bacteria and incubated on ice for 20 minutes, followed by 10 minutes at room temperature. 500µl lysogeny broth (LB) was added and the mixture was incubated for 1 hour at 37°C before plating on LB plates supplemented with 100µg/ml ampicillin (Sigma) overnight at 37°C. Individual colonies were picked and grown in 2ml of LB supplemented with ampicillin and plasmid isolation was performed using the QIAprep spin miniprep kit (Qiagen), or the LB cultures were expanded into 200ml and plasmid isolation was performed using the maxiprep kit (Qiagen). Successful cloning was determined by appropriate restriction digestion and DNA sequencing at the MRC genomics facility.

2.2.4 Cellular proliferation assays

2.2.4.1 Propidium iodide (PI) staining

$0.5x10^6$ cells were washed once with PBS and resuspended in 300ul PBS supplemented with 50µg/ml propidium iodide (Sigma), 10µg/ml RNase A (Life technologies) and 0.05% v/v NP40 (Calbiochem, Merck Millipore) for 30 minutes on ice. The cell cycle profile was obtained using the BD LSRII flow cytometer. Live cells were gated based on forward scatter (FSC) and side scatter (SSC) profiles, and doublets were discriminated using FSC-W/FSC-A gating. PI fluorescence was obtained by excitation with the yellow green laser, and emission was detected at 610/20nm. Cell cycle histograms and analysis was performed using FlowJo software.

2.2.4.2 Multicolour enrichment assay

Ikaros-ERt2-GFP expressing fibroblasts were infected with lentiviral particles containing the M1 (RFP^+) shRNA library and an empty pRSI9 shRNA vector expressing BFP (shEmpty-BFP) or a BFP^+ shRNA vector targeting Ikaros (sh*Ikzf1*-BFP). The cells were infected at a MOI of 0.5 so that each cell would contain on average a single shRNA. Cells successfully transduced with lentivirus were selected for by maintaining the cells in 2µg/ml puromycin for 3 days. Cells containing the shRNA library-RFP were plated at a density of $0.5x10^6$ in a $10cm^2$ dish along with $0.05x10^6$ cells containing either the shEmpty-BFP or sh*Ikzf1*-BFP vector (10:1 ratio) in media supplemented with 0.5µM 4-hydroxytamoxifen (4-OHT, Sigma-Aldrich) and 1.5µg/ml puromycin. Flow cytometric analysis was performed at day 0, day 3 and day 5. Alive, GFP positive cells were gated (Emission 525/50nm), and the percentage of cells that were RFP^+ (610/20nm) or BFP^+ (450/50nm) was recorded and plotted.

2.2.4.3 Crystal violet staining

$0.1x10^6$ Ikaros-ERt2 expressing fibroblasts were plated in single wells of a 6 well plate and grown for up to 7 days in media supplemented with 0.5µM 4-OHT. At each time point the media was aspirated and the cells washed once with PBS. The cells were fixed by incubating with 1ml of 0.5% glutaraldehyde (Sigma-Aldrich) for 15 minutes. The glutaraldehyde was removed and the cells were stained by the addition of 1ml 0.2% crystal violet solution (Sigma-Aldrich) for 20 minutes. The solution was subsequently removed and the plates were washed with distilled water to remove excess dye and left to dry. The plates were then scanned using the EPSON 2400 photo scanner. To quantify the intensity of the staining, 1ml of 1% SDS was added to each well and the plates were incubated on a rocker (Stuart, Bibby Scientific) until the dye was fully resuspended. 50µl of this SDS-crystal violet solution was aliquoted in duplicate into a round bottomed 96 well plate (Thermo Scientific) and the intensity of the staining was analysed using a plate reader (Spectra max) by measuring the absorbance at 570nm.

2.2.5 Positive selection shRNA screen

2.2.5.1 shRNA screening

The M1 shRNA library (Cellecta) was packaged into lentiviral particles and titrated as outlined in **2.2.2.** Retroviral particles containing MSCV-*Ikzf1*-GFP or MSCV-Empty-GFP constructs were generated by the calcium phosphate method. Wild type 3T3 fibroblasts were co-infected with the RFP positive lentiviral library and GFP positive retroviral constructs. The lentivirus was infected at a multiplicity of infection of 0.5 to ensure a low probability of multiple integrations per cell. At least 200 cells were infected on average with each shRNA to maintain the diversity of the library. As there are 27,500 hairpins in the population, this meant that at least $5.5x10^6$ cells were infected with the shRNA library. This ≥200 fold representation was maintained throughout the experimental period.

72 hours post infection, GFP/RFP double positive cells were sorted on the BD FACSAriaIII flow cytometer and plated at a density of $1x10^6$ cells per $15cm^2$ gelatinised dish in a 50/50 mix of fresh and conditioned fibroblast media. The day 0 control population was snap frozen by dipping the pelleted cells in a 15ml falcon tube in liquid nitrogen immediately after sorting, followed by storage at -80°C. The remaining cells were grown for 7 days at 37°C in a humidified chamber with 5% O_2. Control cells were kept in a logarithmic growth phase throughout the experiment to maintain the shRNA library diversity. At least $27x10^6$ cells were kept in culture after splitting to maintain 1000 fold representation of each shRNA in the control population. At day 7, control and *Ikzf1* expressing cell populations were pelleted and snap frozen before DNA extraction. All screens were performed in three independent biological replicates.

2.2.5.2 shRNA Library preparation

Genomic DNA was obtained from each sample by phenol chloroform extraction. The pelleted samples were thawed and suspended in 1ml lysis buffer per $5\text{-}10x10^6$ cells (10mM NaCl, 10mM Tris pH7.5, 10mM EDTA, 0.5% (v/v) Sarcosyl) supplemented with 200µg/ml proteinase K and incubated at 55°C overnight with agitation. One volume of phenol (Sigma-Aldrich) was added to each sample and vortexed, before spinning at 15,000RCF for 5 minutes. The aqueous phase was transferred to new 1.5ml tubes before the addition of an equal volume of phenol/chloroform/isoamyl alcohol (25:24:1), followed by vortex and spin. The aqueous phase was transferred and mixed with an equal volume of chloroform, vortexed and spun for 5 minutes. 2 volumes of ice cold 100% EtOH were added to each sample with 0.1 volume of 3M NaOAc and the samples were incubated at -80°C for 30 minutes to precipitate DNA. The samples were spun at 15,000 RCF for 20 minutes at 4°C to pellet DNA. The pelleted DNA samples were washed once with 70% EtOH and resuspended in H_2O to an optimal concentration of 5µg/µl.

Amplification of the shRNA barcodes was performed by nested PCR in 4 parallel reactions per condition (Control and Ikaros), each using 50µg genomic DNA as a template (200µg gDNA in total per sample). This meant that on average each shRNA was represented 1000 fold at the start of the amplification stage. A sample containing no gDNA was included as a negative control. The PCRs were performed in 2 stages using a nested set of primers (table 3). In the first stage, 50µg of gDNA was mixed with 3µl of the forward and reverse HTS primers (10µM), 2µl of dNTP mix (10mM each), 10µl of 10x Titanium Taq buffer and 1µl of 50x Titanium Taq polymerase (Takara) and topped up to a volume of 100µl with H_2O. This was run with the following program: an initial denaturation step of 94°C for 3 minutes, and 16 cycles of 94°C for 30 seconds, annealing at 55°C for 10 seconds and elongation at 72°C for 20 seconds, followed by one cycle of 68°C for 2 minutes. All 4 parallel reactions were pooled into one tube and 2µl of each amplified first round product were used as the template in 3 parallel second round PCR reactions with 5µl of forward and reverse Gex primers (10µM each), 10µl of 10x Titanium Taq buffer and 1µl of 50x Titanium Taq polymerase (Takara) and topped up to a volume of 100µl with H_2O. This was run with the same program as before with 14 cycles of amplification, and all 3 parallel reactions were pooled for each sample. The Gex primers contained sequences complementary to the immobilised primers on the Illumina flow cell, negating the requirement for adaptor ligation. The expected amplification band size of 106bp was checked by running on a 3% agarose gel followed by purification using the QIAquick gel purification kit (Qiagen).

2.2.5.3 shRNA library validation and sequencing

A validation was performed on the amplified barcode libraries prior to sequencing to test if the screen was successful. 10ng of each sample was run in a qPCR reaction (according to **2.2.10.2**) using the forward Gex primer and reverse primers specific to positive and negative control barcode sequences (table 4). The relative enrichment of barcodes was determined by comparing the ΔC(t) of Ikaros samples to control

samples for the positive and negative control barcodes.

The samples were quantified using the Qubit high sensitivity dsDNA assay (Life Technologies) and loaded in separate lanes of the Illumina HiSeq platform in a single read run using the custom GexSeqN primer (table 3). Following sequencing, the samples were aligned to the reference shRNA barcode library and assigned gene ID's. The differential expression of each shRNA was calculated using the DeSeq method.

2.2.6 Immunofluorescence (IF)

$0.25x10^6$ Ikaros-ERt2 expressing fibroblasts were cultured in 6 well dishes on top of sterile coverslips and induced with 0.5µM 4-OHT, or an equal volume of EtOH for 24 hours. The media was subsequently aspirated and the wells washed with 3ml PBS, then incubated with 1ml 4% paraformaldehyde (PFA, Sigma-Aldrich) in PBS for 10 minutes at room temperature before aspiration. Fixed samples were permeabilised with 1ml 0.1% Triton X-100 solution for 10 minutes at room temperature. Samples were subsequently incubated in blocking solution (5% bovine serum albumin (BSA), 0.05% Triton (Sigma-Aldrich)) for 1 hour at room temperature, followed by incubation with primary antibody in blocking solution at the appropriate dilution (displayed in **2.1.1**) in a humidified chamber for 2 hours at room temperature. Coverslips were washed 3 times with PBS and incubated with the secondary antibodies coupled with appropriate fluorophores (Molecular Probes) diluted in blocking buffer for 1 hour at room temperature in a dark humidified chamber. Slides were subsequently washed 3 times with PBS and mounted in Vectorshield (Vector Laboratories) with DAPI (0.1µg/ml). Samples were visualised using a TCS SP5 Leica laser scanning confocal microscope. Microscope settings and laser power were kept constant among samples. Images were processed using Leica confocal software and ImageJ.

2.2.7 Western blot

2.2.7.1 Sample preparation

Whole cell extracts were obtained by pelleting $1x10^6$ cells and resuspending in 50µl PBS supplemented with 1x protease inhibitor cocktail (Roche) and 50µl of 2x sample buffer (100mM Tris (pH 6.8), 20% glycerol, 2% SDS). Samples were denatured by incubating at 95°C for 5 minutes. Protein concentration was measured using the Pierce BCA protein assay kit (Thermo Scientific) according to the manufacturer's instructions. Following quantification, 10% v/v β–mercaptoethanol and 0.002% bromophenol blue were added to protein samples and stored at -20°C.

2.2.7.2 SDS-PAGE

Depending on the protein of interest, between 5-20µg of protein were loaded alongside 10µl of Benchmark pre-stained protein ladder (Invitrogen) on a SDS-polyacrylamide gel (4% stacking gel [4% acrylamide, 125mM Tris-HCL (pH 6.8), 0.1% SDS, 0.067% ammonium persulphate (APS) and 0.12% N,N,N',N'-tetramethylethylenediamine (TEMED)] 10% resolving gel [10% acrylamide, 390mM Tris-HCL (pH8.8), 0.1%SDS, 0.05% APS, 0.1% TEMED]). For large proteins such as SSeCKS, 4-15% precast polyacrylamide gels (Bio-Rad) were used. Proteins were separated by running the gel in running buffer (25mM Tris base, 192mM glycine, 0.1% SDS) for 60-90 minutes at 25mA per gel, using the Bio-Rad minigel system.

2.2.7.3 Transfer and detection

Resolved gels were blotted onto a Protan nitrocellulose transfer membrane (Schleicher & Schuell Bioscience) using the trans-blot semi-dry transfer apparatus (BioRad) in transfer buffer (48mM Tris base, 39mM glycine, 0.037% SDS and 20% methanol) for 90 minutes at 140mA/gel. Alternatively for large proteins, a wet

transfer was performed for 1 hour at 350mA/250V in wet transfer buffer (25mM Tris, 192mM glycine, 0.037% SDS and 5% methanol). For fluorescent western blot, immobilon-FL PVDF membranes (Merck Millipore) were pre-soaked in methanol prior to transfer. Following transfer, the membrane was incubated for 30 minutes in blocking buffer (5% fat free milk powder (Marvel) in 1x TBS supplemented with 0.1% tween-20 (TBST)) followed by incubation with the primary antibody diluted in blocking buffer at the appropriate dilution (outlined in **2.1.1**) for 1 hour at room temperature or overnight at 4°C with agitation. The membranes were then washed three times for 10 minutes in 1x TBST at room temperature before incubation with horseradish peroxidase coupled secondary antibodies (anti-mouse and anti-rabbit purchased from Amersham and used at 1:5000 dilution in blocking buffer) for 45 minutes at room temperature. Following washes of the secondary antibody, detection was performed using the Luminata Crescendo Western HRP substrate (Millipore) following the manufacturer's instructions with Kodak X-Omat photographic films. Alternatively, secondary fluorescent antibodies (Invitrogen) were diluted at 1:10,000 in blocking buffer and incubated with the membranes for 45 minutes at room temperature away from light. The appropriate fluorophores were detected using the LI-COR Odyssey CLx imaging system.

2.2.8 Ikaros chromatin immunoprecipitation (ChIP)

2.2.8.1 Chromatin sample preparation

All buffers were supplemented with freshly prepared 1x protease inhibitor cocktail. $1x10^8$ Ikaros-ERt2 expressing fibroblasts were harvested after treatment for 24 hours with 0.5µM 4-OHT, resuspended in 35ml PBS-/- containing 1mM Disuccinimidyl glutarate (DSG, Thermo Scientific) and incubated for 30 minutes at room temperature on a rotating platform. The cells were washed with PBS and resuspended in 35ml PBS containing 1% fix solution (50mM Tris-HCL pH 8.0, 0.5mM EGTA pH 8.0, 100mM NaCL, 1% formaldehyde final) and incubated for 10 minutes at room temperature on a rotating platform. The fixation was quenched by the

addition of glycine (Sigma-Aldrich) to a final concentration of 140mM, followed by a 5 minute incubation at room temperature. The cells were pelleted at 1800RCF for 5 minutes at 4°C, washed twice with ice-cold PBS and lysed by the addition of 1ml Lysis buffer (5mM PIPES pH 8.0, 85mM KCL, 0.5% NP-40) for 20 minutes on ice. The cell lysis solution was spun at 900RCF for 10 minutes at 4°C and the supernatant aspirated before the addition of 500µl nuclear lysis buffer (50mM Tris-HCL pH8.1, 10mM EDTA pH8.0, 0.5% SDS) for 10 minutes on ice. The samples were sonicated for 20 minutes at 4°C with 30 seconds on, 30 seconds off using a Bioruptor sonicator (Diagenode). Debris was removed by spinning the samples at 2500RCF for 20 minutes at 4°C, and the supernatant was ran on a 1% agarose gel to check the size of the chromatin fragments (optimal between 500-1000bp). The chromatin was quantified by nanodrop measurement and the samples were diluted in standard RIPA buffer (10mM Tris-HCL pH7.5, 1mM EDTA pH8.0, 0.5mM EGTA pH8.0, 1% Triton X-100, 0.1% SDS, 0.1% Na Deoxycholate, 140mM NaCl) to 200ng/µl and stored at -20°C.

2.2.8.2 Chromatin immunoprecipitation

50µl of A Dynabeads (Life Technologies) per IP were washed twice with cold standard RIPA buffer on a magnetic stand and incubated with 15µl of the Ikaros antibody or 2µg normal rabbit IgG (santa Cruz) for 3 hours at 4°C on a rotating platform. The beads were washed twice with cold RIPA buffer and 100µg of chromatin was added, topped up to a final volume of 500µl in RIPA buffer, and incubated overnight at 4°C on an orbital shaker. Unbound chromatin and non-specific binding were washed away sequentially with standard RIPA buffer, high salt RIPA buffer (10mM Tris-HCL pH7.5, 1mM EDTA pH8.0, 0.5mM EGTA pH8.0, 1% Triton X-100, 0.1% SDS, 0.1% Na Deoxycholate, 500mM NaCl), LiCL RIPA buffer (10mM Tris-HCL pH7.5, 1mM EDTA pH8.0, 0.5mM EGTA pH8.0, 1% Triton X-100, 0.1% SDS, 0.1% Na Deoxycholate, 250mM LiCL) and TE buffer (10mM Tris-HCL, 1mM EDTA, pH7.5). The samples were reverse crosslinked by incubating in 300µl elution buffer (20mM

Tris-HCL pH7.5, 5mM EDTA pH 8.0, 50mM NaCL, 1%SDS, 50µg/ml proteinase K, 100µg/ml RNase A) at 68°C overnight with agitation. DNA was extracted by the phenol chloroform method and suspended in 100µl h_2O. 2µl of ChIP DNA was used per qPCR reaction using primers outlined in 4.

2.2.9 Protein pulldown

2.2.9.1 Preparation of lysates

Ikaros-ERt2 expressing B3 cells were plated and treated with 0.5µM 4-OHT or an equivalent volume of EtOH for 24 hours. Around $100x10^6$ cells were pelleted for each condition and washed with ice cold PBS supplemented with 1x complete EDTA-free protease inhibitor (CEF) before suspension in 5ml of lysis buffer (150mM NaCl, 2mM $MgCl_2$, 25mM Tris pH7.5, 10% glycerol, 1% Triton X-100, 0.5mM DTT, 1X CEF protease inhibitor). The samples were homogenised with 15 strokes of the large clearance Dounce homogeniser (Sigma-Aldrich) and incubated in a 15ml falcon tube on a roller for 30 minutes at 4°C. The samples were transferred to Lo-bind microcentrifuge tubes (Sigma-Aldrich) and spun at 15,000RCF for 20 minutes at 4°C before transferring the supernatant to fresh tubes for storage at -80°C.

2.2.9.2 Immunoprecipitation

For each IP, 40µl of protein G Dynabeads were washed with 1ml PBS supplemented with 0.1% Triton X-100 on a magnetic rack. The beads were blocked by the addition of 800µl PBS + 0.1% Triton and 200µl of non animal protein (NAP) block (G Biosciences) and incubated for 5 minutes on a rotating wheel at room temperature. The supernatant was discarded and antibody coupling was accomplished by resuspending the beads in 28µl PBS (+0.1% Triton +1x protease inhibitor) with 3µl NAP and 5µg of anti-SSeCKS antibody, followed by 3 hours of incubation on a rotating wheel at 4°C. 2.5µg of normal mouse IgG was used as a negative control.

The beads were washed on ice three times with 1ml cold PBS (+0.1% Triton +1x protease inhibitor) and incubated with 500µl of pre-prepared cell lysates plus 1x protease inhibitor for 4 hours at 4°C on a rotating platform. The beads were then washed three times on ice with cold lysis buffer before elution by the addition of 50µl 0.2M glycine pH2.3 for 10 minutes with agitation in two sequential elution steps (100µl total eluate). The eluted samples were then mixed with two volumes of 2x western sample buffer and boiled at 95°C for 5 minutes, subjected to SDS-PAGE then blotted for cyclin D.

2.2.10 Real-time Quantitative PCR (RT-qPCR)

2.2.10.1 RNA extraction and reverse transcription

RNA extraction was performed using the QIAshredder and RNeasy mini kits (Qiagen), residual DNA was eliminated using 2U turboDNase (Ambion) according to the manufacturer's instructions and RNA was quantified by nanodrop. Reverse transcription was performed using the Superscript III first strand synthesis mix (Invitrogen). 500ng of total RNA was combined with 1µl of 10mM dNTP mix, 1µl of 250ng/µl random primers and topped up to 13µl with sterile RNase free H_2O before incubation in a thermal cycler at 65°C for 5 minutes. Following incubation, 4µl of 5x first strand buffer, 1 µl of 0.1M DTT, 1µl RNaseOUT and 1µl of 200U/µl Superscript III reverse transcriptase was added to the mixture to a final volume of 20µl. The reaction mixture was incubated at 25°C for 5 minutes, 50°C for 60 minutes and 70°C for 15 minutes. The cDNA was diluted 1:5 with sterile H_2O to a final concentration of 5ng/µl and stored at -20°C.

2.2.10.2 RT-qPCR

Primers were designed using the primer3 design tool (http://primer3.ut.ee) using sequences obtained from the UCSC genome browser. The primers were tested using

2 fold serial dilutions of genomic DNA and those that displayed linear fits of the C(t) versus logarithm of the genomic DNA concentration (R2>0.99), and amplification efficiencies in the range of 1.8-2 were selected.

PCR reactions were made by mixing 2µl of cDNA (10ng total) with 2X SYBR Green qPCR master mix (Qiagen) and 0.3mM primers to a total volume of 12µl. This reaction was carried out using an Opticon or CFX96 real time qPCR machine using the following program: an initial denaturation step at 95°C for 15 minutes, 40 cycles of denaturation at 94°C for 15 seconds, annealing at 60°C for 30 seconds, elongation at 72°C for 30 seconds at which point the fluorescence was read at 72°C, 75°C, 78°C and 83°C. The melting curve was determined from 70°C to 90°C at 0.2°C intervals. A reaction without DNA was included as a control and each measurement was performed in triplicate. The quantification of amplified sequences was determined using the ΔC(t) method. ΔC(t) corresponds to the number of amplification cycles after which fluorescence of PCR products can be detected above background. Assuming an amplification efficiency close to 2, the relative abundance of a gene of interest (C(t)1) compared to a control (C(t)2) can be calculated at $2^{-\Delta C(t)1}/2^{-\Delta C(t)2}$. *Ubc* was generally used as an internal housekeeping control for data normalisation.

2.2.11 RNA-seq

2.2.11.1 Library preparation

$0.5x10^6$ S24 fibroblasts expressing the Ikaros-ERt2 construct were plated in $10cm^2$ dishes and induced for 24 hours with a combination of 1µg/ml doxycycline and 0.5µM 4-OHT, or an equal volume of EtOH as the vehicle control. Total RNA was extracted using the QIAshredder and RNeasy mini kits (Qiagen), residual DNA was eliminated using 2U turboDNase (Ambion) according to the manufacturer's instructions and RNA was quantified by nanodrop. RNA quality was assessed by Bioanalyser (Agilent) using the total RNA nano chip. All samples displayed RNA integrity numbers (RIN) of over 9.5, indicating good quality RNA with low

degradation. qPCR analysis was performed on each sample prior to library preparation looking at target gene expression (i.e *Myc*) to check that the induction worked as expected. Intronic primers designed against non expressed genes in fibroblasts (i.e *Igll1*) were used as a negative control to ensure there was no genomic DNA contamination in the samples.

RNA libraries were prepared using the Truseq stranded total RNA prep kit (Illumina), using ribozero ribosomal RNA (rRNA) depletion. 500ng of total RNA was loaded for each sample in a hardshell 96 well plate (Biorad) and incubated with biotinylated rRNA oligos at 68°C for 5 minutes. Depletion of rRNA was achieved by the addition of rRNA binding magnetic beads followed by incubation on a magnetic stand and transfer of the ribosomal depleted RNA supernatant to a new plate. The ribosomal depleted RNA was cleaned by binding to RNAclean XP beads (Agencourt) and washed with 70% EtOH on a magnetic stand, following elution of purified RNA.

The purified RNA was fragmented and primed for first strand cDNA synthesis by the addition of the Elute, Prime, Fragment Mix and incubated at 94°C for 8 minutes. First strand cDNA synthesis was carried out using random primers and SuperScript II reverse transcriptase using the following program: 25°C for 10 minutes, 42°C for 15 minutes, 70°C for 15 minutes. Immediately following first strand synthesis, the RNA strand was degraded with RNA H and the second cDNA strand was synthesised by the addition of the Second Strand Marking Master Mix followed by incubation for 1 hour at 16°C. The subsequent double stranded cDNA was cleaned by binding to RNAclean XP beads and sequentially washed with two rounds of 80% EtOH on a magnetic stand, followed by elution.

The blunt double stranded cDNA was adenylated with the addition of a single 'A' nucleotide that is complementary to the single 'T' nucleotide on the adaptor sequences. A-tailing mix was added to each cDNA sample and incubated at 37°C for 30 minutes, followed by 70°C for 5 minutes. Adaptors specific for the Illumina

sequencing platform (table 7) were subsequently ligated to the cDNA fragments by mixing the ligation mix and adaptor indexes from RNA adaptor tubes with the cDNA samples and incubating at 30°C for 10 minutes. The adapted cDNA fragments were cleaned by binding to RNAclean XP beads followed by 2 sequential rounds of 2X 80% EtOH washes before elution. The adapted sequences were then enriched by PCR amplification using the following program: initial denaturation at 98°C for 30 seconds followed by 15 cycles of 98°C for 10 seconds, 60°C for 30 seconds, 72°C for 30 seconds and 72°C for 5 minutes. This was followed by a final round of cleaning using RNAclean XP beads with 80% EtOH washes.

2.2.11.2 Library validation and sequencing

The purity of the cDNA libraries was assessed by Bioanalyser, using a high sensitivity DNA chip. All samples were fragmented in approximately 300bp fragments. The concentration of the samples was measured using the Qubit high sensitivity dsDNA assay (Life Technologies) and each sample was diluted to 15ng/µl. qPCR analysis was performed on each sample prior to sequencing looking at target gene expression to ensure correct library preparation. 5µl of each sample was pooled into a single well and delivered to the MRC genomics facility for cluster generation and paired end 100bp sequencing in 2 lanes of the Hi-Seq sequencing platform. Following sequencing, each sample was demultiplexed and aligned to the reference mouse genome, and the differential expression of each gene was calculated using the EdgeR package.

Chapter 3

A model system to study the regulation of the cell cycle by Ikaros

3.1 Introduction

IKZF1 is the defining oncogenic lesion in Philadelphia chromosome positive B-progenitor acute lymphoblastic leukaemia (ALL) (Mullighan *et al.,* 2008). In mice the expression of dominant negative Ikaros isoforms result in lymphoproliferation and the development of leukaemias and lymphoma (Winandy *et al.,* 1995). Evidence linking Ikaros to the regulation of proliferation was observed in studies that showed cell cycle withdrawal in murine thymocytes and pre-B cells in response to *Ikzf1* overexpression (Kathrein *et al.,* 2005; Ma et al., 2008). Ikaros can directly antagonise the regulation of genes involved in proliferation, exemplified by its direct repression of the oncogene *Myc* and induction of the cell cycle inhibitor *Cdkn1b* (Ma *et al.,* 2010). These reports of Ikaros-induced cell cycle arrest in lymphocytes have been complemented with genome-wide expression profiling studies utilising models of *Ikzf1* overexpression (Ferreiros-Vidal *et al.,* 2013) and conditional inactivation (Schjerven *et al.,* 2013, Joshi *et al.,* 2014), further elucidating the gene expression program induced by Ikaros. In pre-B cells proliferative arrest is required to allow Rag-dependent rearrangement of immunoglobulin light chain loci to proceed (Zhang *et al.,* 2011), thereby linking B cell differentiation with cell cycle dynamics.

Interestingly the ectopic expression of *Ikzf1* results in G1 arrest in fibroblasts, as well as in lymphocytes (Gomez Del-Arco *et al.,* 2004). This provides an opportunity to investigate Ikaros function in a reductionist model system. The rationale for this approach is as follows. Fibroblasts do not endogenously express *Ikzf1*, so the regulation of the cell cycle can be studied upon the introduction of Ikaros into these cells. Furthermore, fibroblasts do not express components of the pre-B cell receptor

or its downstream signalling molecules, allowing the investigation of Ikaros function in the regulation of the cell cycle independently of its role in B cell differentiation. RNAi can be used to systematically screen thousands of genes in a parallel fashion to identify factors that are directly required for cell cycle arrest. I therefore planned to perform a positive selection RNAi screen to identify shRNA that override Ikaros-induced proliferative arrest in the fibroblast model system. Before embarking on the screen I wished to characterise this model system by comparing and contrasting the Ikaros-induced gene expression changes and cell cycle profiles in pre-B cells and fibroblasts.

3.2 An inducible system of Ikaros activity

To interrogate Ikaros function I took advantage of a fusion construct that consists of HA-tagged Ikaros fused with a modified form of the oestrogen receptor hormone binding domain, driven by MSCV long terminal repeats (Ikaros-ERt2) (Figure 3.1A). This construct contains an internal ribosome entry site (IRES) that allows for translation of green fluorescent protein (GFP) and Ikaros-ERt2 from the same transcript. This enables me to sort cells with different levels of Ikaros expression by flow cytometry based on GFP fluorescence. Cells expressing this construct grow normally, as the Ikaros-ERt2 protein is sequestered in the cytoplasm with heat shock proteins until the addition of the ERt2 ligand 4-hydroxytamoxifen (4-OHT). Binding of 4-OHT to the ERt2 domain releases the Ikaros-ERt2 protein from cytoplasmic heat shock proteins. This allows the Ikaros nuclear localisation signal (NLS) to direct the translocation of Ikaros-ERt2 into the nucleus, where it can bind to DNA and regulate the expression of Ikaros target genes (Figure 3.1B).

I demonstrated this sytem visually by performing immunofluorescence staining and confocal microscopy using an anti-Ikaros antibody in Ikaros-ERt2 expressing fibroblasts. Figure 3.1C shows that 4-OHT treatment induced Ikaros translocation into the nucleus to overlap DAPI staining, whereas Ikaros was excluded from the nucelus in cells treated with the vehicle control ethanol (EtOH) and exhibited predominantly cytoplasmic staining. The advantage of using this construct is that cells expressing Ikaros-ERt2 continue to proliferate until Ikaros translocation is induced by the addition of 4-OHT. This allows precise temporal control over the timing of Ikaros induction.

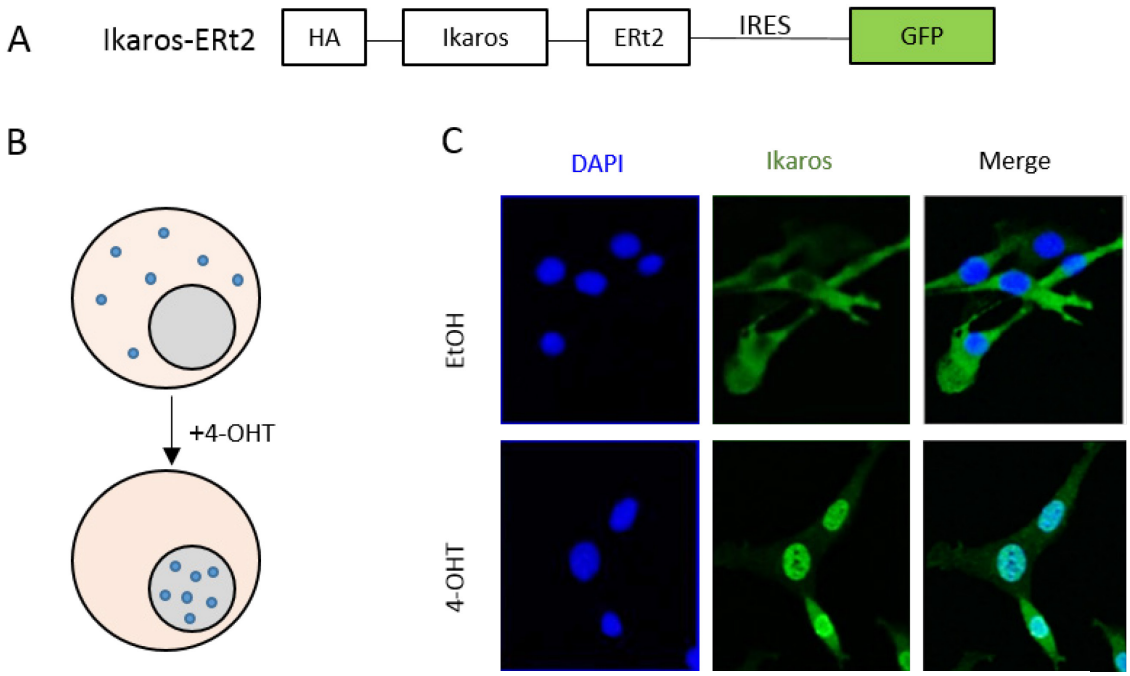

Figure 3.1 – An inducible system of Ikaros activity. (**A**) Schematic depicting the Ikaros-ERt2 construct. (**B**) Addition of the ligand 4-OHT directs nuclear translocation of the Ikaros-ERt2 protein. (Blue dots) (**C**) Immunofluorescence (IF) images obtained by confocal microscopy depicting Ikaros-ERt2 expressing fibroblasts treated with EtOH (top panels) or 4-OHT (bottom panels) for 24 hours. Treatment with 4-OHT resulted in a predominantly nuclear staining as Ikaros (green) colocalised with DAPI staining (blue).

3.3 Ikaros regulates the cell cycle in pre-B cells and fibroblasts

I proceeded to use the inducible Ikaros-ERt2 construct to characterise the regulation of the cell cycle by Ikaros in pre-B cells and fibroblasts. For this purpose I used the pre-B cell line B3, which is derived from an IL-7 transgenic lymphoma and is developmentally blocked at a stage resembling large cycling pre-B cells (FrC') (Fisher *et al.,* 1995). I transduced B3 cells with the Ikaros-ERt2 construct, or a dominant negative form of Ikaros (DN-Ikaros-ERt2) that contains a substitution of an asparagine to alanine at amino acid position 159 in one of the N-terminal zinc fingers critical for DNA binding (Cobb *et al.,* 2000). This mutant is unable to bind DNA but can still dimerise with members of the Ikaros family through its C-terminal zinc fingers. This prevents DNA binding of its dimerisation partner in a dominant negative fashion.

It has previously been shown that B3 cells withdraw from the cell cycle after 16 hours of 4-OHT treatment, and are arrested in G1 after 24 hours of treatment (Ferreiros-Vidal *et al.,* 2013). I used staining with the DNA intercalating dye propidium iodide (PI) coupled with flow cytometry to analyse the DNA content of B3 cells after 24 hours treatment with EtOH or 4-OHT (figure 3.2). The induction of Ikaros nuclear translocation by 4-OHT treatment resulted in a reduction in the fraction of cells in S and G2/M phase of the cell cycle and an accumulation of >80% of cells in G1 phase, compared to <50% of cells in G1 phase in the EtOH treated control cells (figure 3.2A, top panel). Induction of the Ikaros 159A mutant isoform had no discernible impact on the cell cycle profile, indicating that DNA binding by Ikaros is required to impose cell cycle arrest (figure 3.2A, bottom panel).

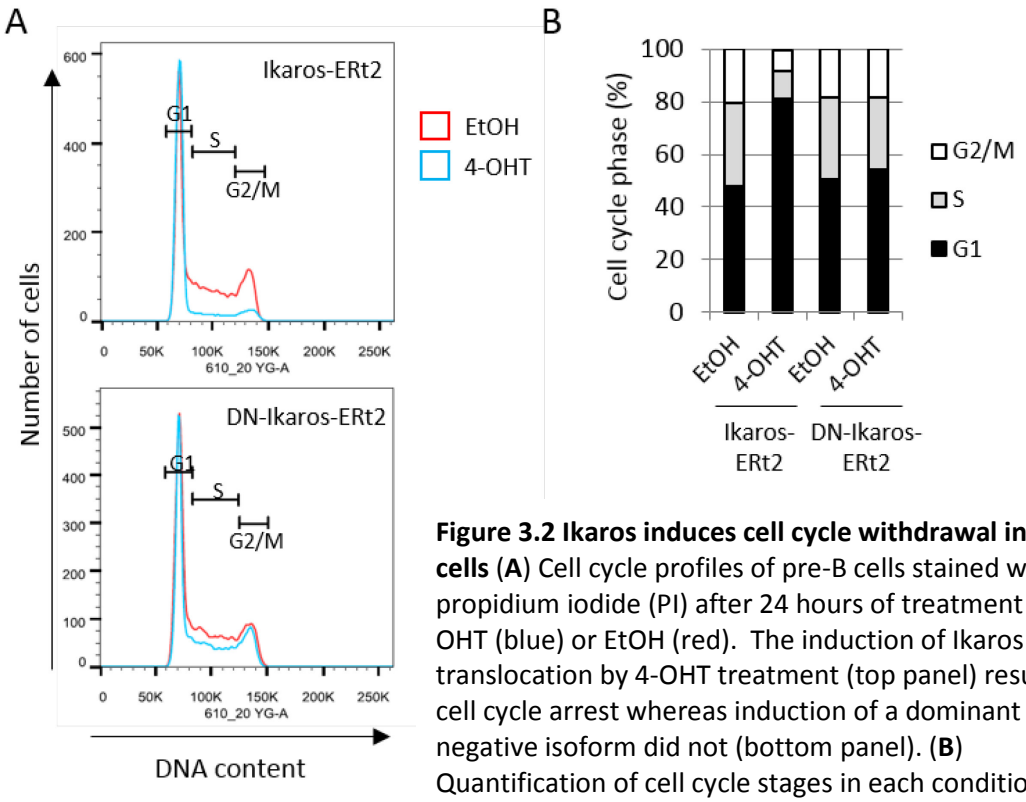

Figure 3.2 Ikaros induces cell cycle withdrawal in pre-B cells (**A**) Cell cycle profiles of pre-B cells stained with propidium iodide (PI) after 24 hours of treatment with 4-OHT (blue) or EtOH (red). The induction of Ikaros nuclear translocation by 4-OHT treatment (top panel) resulted in cell cycle arrest whereas induction of a dominant negative isoform did not (bottom panel). (**B**) Quantification of cell cycle stages in each condition; black for G1, grey for S, white for G2/M.

I performed quantitative polymerase chain reaction (qPCR) analysis to investigate Ikaros-induced gene expression changes using RNA extracted from cells treated for 6 hours, 16 hours and 24 hours with EtOH or 4-OHT (figure 3.3). These represent time points that are prior to cell cycle arrest, undergoing arrest, and stably arrested. In accordance with previous reports (Ferreiros-Vidal *et al.,* 2013, Ma *et al*., 2010, Kathrein *et al*., 2005) and the cell cycle profiles shown in figure 3.2, Ikaros instigated an anti-proliferative gene expression program.

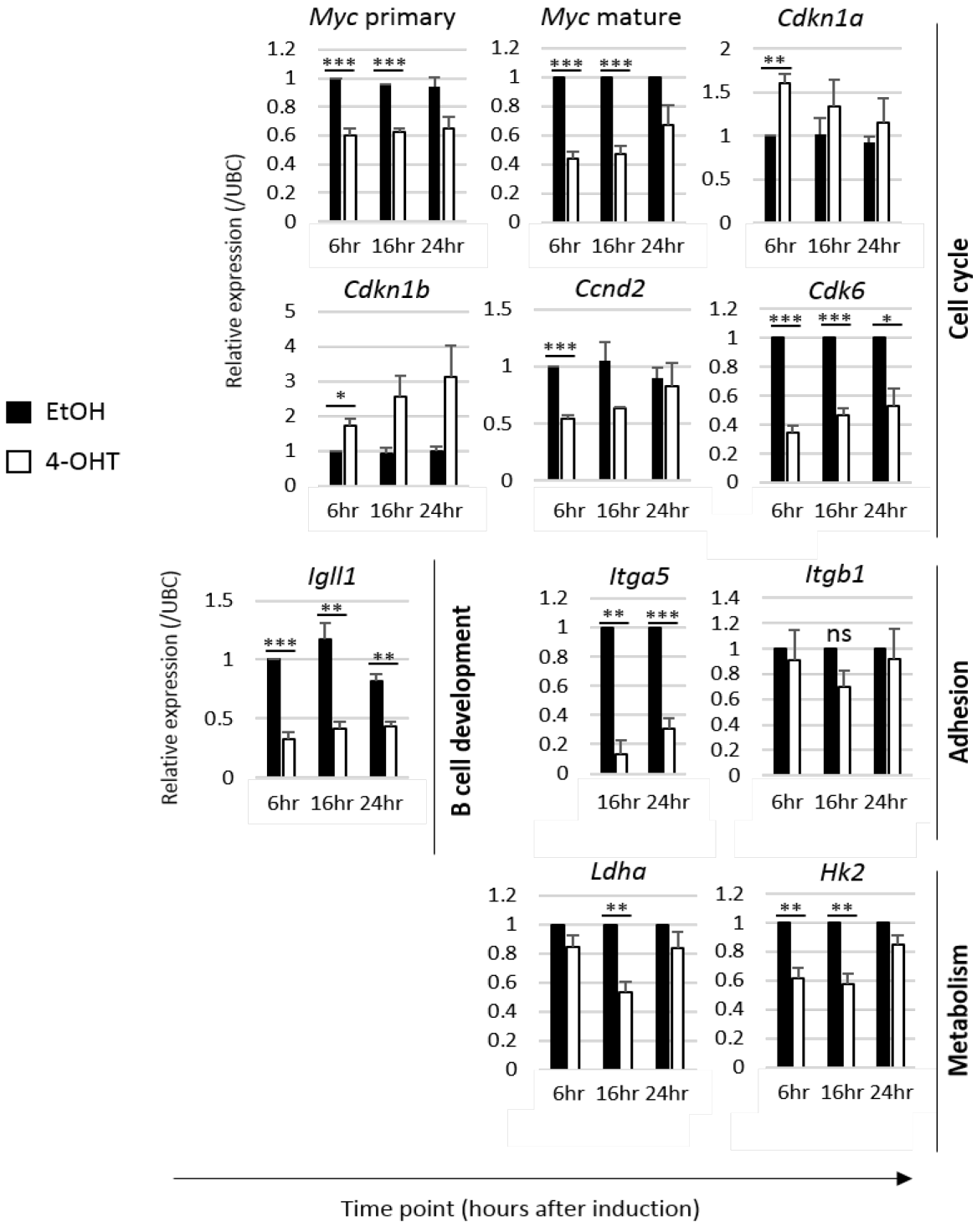

Figure 3.3 Ikaros induction directs B3 cell gene expression towards a quiescence-like state. qPCR analysis was performed on RNA extracted from B3 cells collected at 6, 16 and 24 hours after treatment with 4-OHT (white bars) or EtOH (black bars). Ikaros target genes are grouped in order of their function encompassing the cell cycle, B cell development, adhesion and metabolism. The graphs display mean gene expression changes induced by Ikaros (Mean+SE; N=3, student T test: * p<0.05 **p<0.01 *** p<0.001)

Figure 3.3 displays the expression of Ikaros target genes grouped in the distinct yet interlinked processes of cell cycle, adhesion and metabolism. The downregulation of the surrogate light chain component *Igll1* was included as the prototypic positive control for successful Ikaros induction (Thompson *et al.,* 2007). Focusing on the genes involved in G1-S progression, the induction of Ikaros nuclear translocation resulted in the repression of pro-proliferative genes such as *Myc*, *Ccnd2* (cyclin D2) and *Cdk6* and the upregulation of the cell cycle inhibitors *Cdkn1a/b* (p21/p27). These gene expression changes occurred early on as significant changes could be detected after 6 hours of 4-OHT treatment, preceding cell cycle arrest. The data observed in figure 3.3 does not seem to correlate with the cell cycle profiles shown in figure 3.2, as the gene expression changes appear to lessen at 24 hours, when cell cycle arrest is strongest. These target genes have previously been shown to be strongly differentially expressed up to 48 hours after Ikaros induction (Ferreiros-Vidal *et al.,* 2013). One explanation for this discrepancy is that the two analyses were performed on different batches of cells. It is likely that the weak gene expression changes are the result of low Ikaros expression in these cells due to poor transduction efficiency.

It has recently been shown that Ikaros is required to downregulate components of the integrin signalling pathway (Joshi *et al.,* 2014). Conditional inactivation of Ikaros in pre-B cells resulted in augmented stromal-dependent proliferation and survival (Joshi *et al.,* 2014). I investigated the expression of two previously identified Ikaros regulated genes, *Itga5* and *Itgb1,* which encode the $\alpha_5\beta_1$ integrin receptor (Joshi *et al.,* 2014). The induction of Ikaros translocation resulted in a sharp reduction in transcript of one half of this receptor (*Itga5*). As metabolic output is important in sustaining cellular growth and proliferation (Dang *et al.,* 2009), I investigated the expression of two metabolic genes that encode enzymes involved in the glycolysis and fermentation pathways. *Ldha* converts pyruvate to lactate, and *Hk2* phosphorylates glucose in a rate-limiting step committing glucose to the glycolytic pathway. Work performed by my colleague Dr. Ferreiros-Vidal indicates that Ikaros

directs a metabolic reprogramming of B3 cells away from a 'cancer like' state exhibiting aerobic glycolysis and lactate production to a 'resting like' oxidative metabolism (a reversal of the Warburg effect). As shown in figure 3.3, both *Hk2* and *Ldha* were repressed after Ikaros induction.

I went on to investigate the effect of introducing the Ikaros-ERt2 construct into fibroblasts. The cell cycle profile of Ikaros-ERt2 expressing 3T3 fibroblasts was similar to that of B3 cells, as >80% of cells accumulated in G1 phase after 24 hours of 4-OHT treatment (figure 3.4 A,B). A system of persistent cell cycle arrest over long time periods (>24 hours) is required to perform a positive selection RNAi screen in fibroblasts. This will maximise the signal-to-noise ratio and enrich for shRNA that allow cells to escape from Ikaros-enforced cell cycle arrest. To test the effect of Ikaros induction over long time periods, I plated Ikaros-ERt2 expressing fibroblasts at equal density and supplemented the media with EtOH or 4-OHT for up to one week. I then stained with crystal violet to visualise colony density by the intensity of the staining. There was a stark contrast in the intensity of staining between 4-OHT and EtOH treated cells after 7 days of treatment, illustrating the antiproliferative effect of Ikaros in these cells (figure 3.4C). At later time points however (day 6 and over) Ikaros-mediated cell cycle repression began to lift as colonies could be detected in the 4-OHT treated samples (figure 3.4C). If Ikaros-arrested cells stochastically re-enter the cell cycle at late time points the background noise in the shRNA screen will increase. Subsequent experiments were performed within a 7 day time window to minimise this confounding effect.

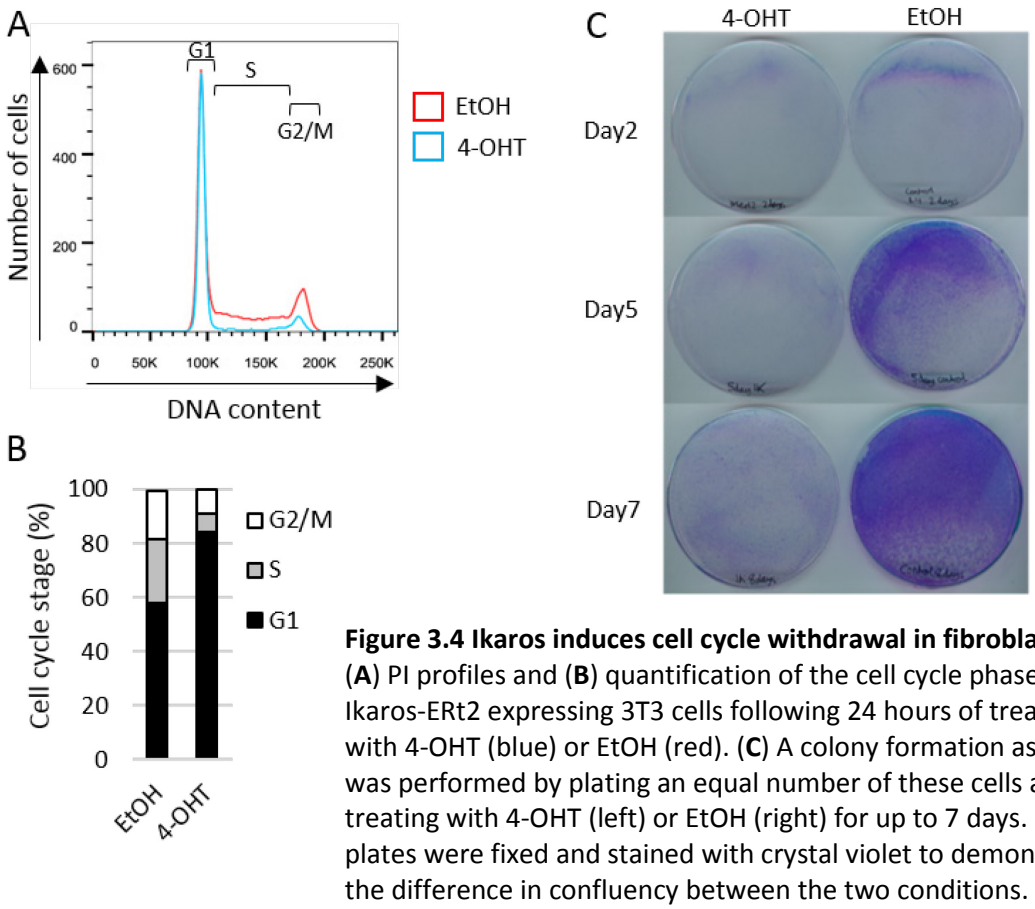

Figure 3.4 Ikaros induces cell cycle withdrawal in fibroblasts. (**A**) PI profiles and (**B**) quantification of the cell cycle phase of Ikaros-ERt2 expressing 3T3 cells following 24 hours of treatment with 4-OHT (blue) or EtOH (red). (**C**) A colony formation assay was performed by plating an equal number of these cells and treating with 4-OHT (left) or EtOH (right) for up to 7 days. The plates were fixed and stained with crystal violet to demonstrate the difference in confluency between the two conditions.

I investigated the gene expression changes induced by Ikaros in 3T3 fibroblasts before (6 hours) and after (24 hours) cell cycle arrest (figure 3.5A). The patterns of gene expression were broadly consistent with those observed in pre-B cells. *Myc* appears to be a central target of Ikaros in the regulation of the cell cycle, exemplified here by the notably sharp and persistent depletion of *Myc* transcript following the induction of Ikaros nuclear translocation. Consistent with this observation, the repression of *Ldha* and *Hk2* was particularly strong following Ikaros induction. Myc promotes many components of the glycolytic pathway, and directly upregulates the expression of these two genes (reviewed in Dang *et al.,* 2009). The observed repression of *Myc* expression in fibroblasts appears to be stronger than that observed in B3 cells (figure 3.3). This likely reflects a higher 'dosage' of the Ikaros transgene in fibroblasts than in B3 cells, due to higher transduction efficiency.

One observation that ran contrary to expectation was the apparent downregulation of the cell cycle inhibitor *Cdkn1a* upon the induction of Ikaros translocation and G1 arrest in fibroblasts (figure 3.5A). This is at odds with the regulation of this gene in pre-B cells (figure 3.3), but was consistently observed using different primer sets and in different fibroblast lines.

To corroborate the gene expression data I investigated the Ikaros-induced changes in protein expression of Myc, and the two predominant isoforms of cyclin D expressed in fibroblasts. Western blot analysis confirmed that both Myc and cyclin D2 were downregulated at the protein level (figure 3.5B), and confocal images of IF stained fibroblasts demonstrated that cyclin D1 protein was undetectable in the nucleus after 24 hours of 4-OHT treatment (figure 3.5C). In conclusion, my results demonstrate that Ikaros induces some key gene expression changes relating to the cell cycle in pre-B cells and fibroblasts. This translates into an arrest of the cell cycle in G1/G0 phase.

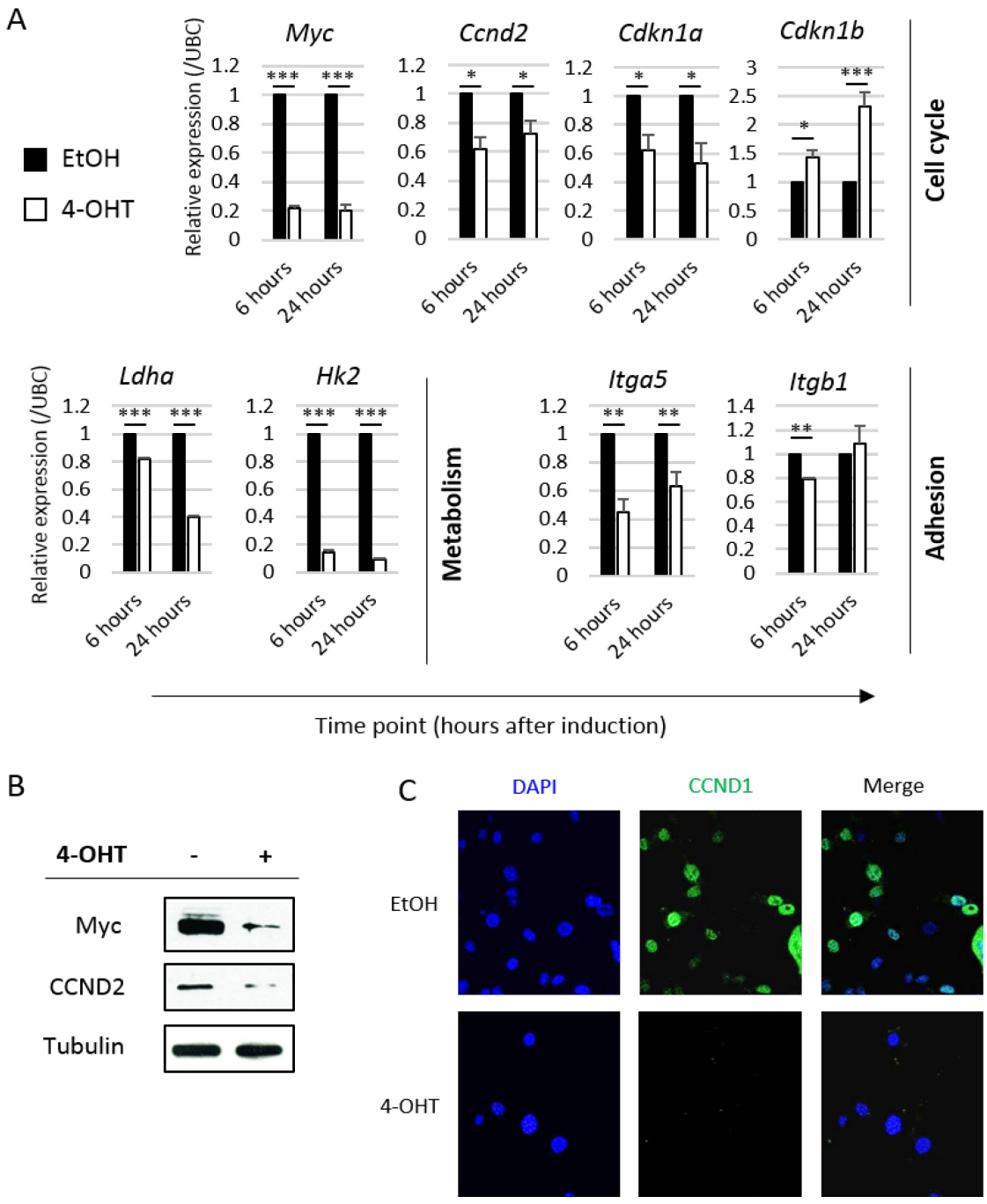

Figure 3.5 Ikaros-induced gene expression and protein changes in fibroblasts. (**A**) qPCR analysis was performed on RNA extracted from Ikaros-ERt2 expressing 3T3 cells collected at 6 and 24 hours after treatment with 4-OHT (white bars) or EtOH (black bars). Gene expression changes were normalised to *Ubc* expression. (Mean+SE; N=3, student T test: * p<0.05 **p<0.01 *** p<0.001). (**B**) Protein extracts from Ikaros-ERt2 expressing fibroblasts treated for 24 hours with EtOH (left column (**-**)) or 4-OHT (right column (**+**)) were analysed for Myc (top panel) and cyclin D2 expression (Middle panel). An anti-tubulin antibody was included as a loading control (bottom panel). (**C**) Confocal images of IF stained fibroblasts treated with EtOH (top) or 4-OHT (bottom) for 24 hours. Nuclear staining by DAPI is shown in blue and cyclin D1 was visualised by incubating with an anti-cyclin D1 primary antibody and a fluorescent secondary antibody (green).

3.4 Enforced *Myc* expression overrides Ikaros-induced cell cycle arrest

Myc appears to be a focal point in the regulation of the cell cycle by Ikaros. As Myc downregulation appeared to precede cell cycle arrest, I wanted to test if this arrest could still occur in the presence of sustained Myc expression. Ikaros directly represses the transcription of *Myc* (Ma *et al*., 2010), so I made use of an inducible form of Myc (Myc-ERt2) encoded from a MSCV vector. Ikaros is unable to repress this construct, ensuring that *Myc* expression is maintained in Ikaros expressing cells. 3T3 cells expressing Ikaros-ERt2, Myc-ERt2 or both were treated for 24 hours with EtOH or 4-OHT and the cell cycle profiles were analysed by PI staining and flow cytometry. Ikaros induction by 4-OHT treatment resulted in an accumulation of cells in G1 phase as expected. The induction of Myc nuclear translocation stimulated cells to proliferate, as an increased proportion of cells were in S and G2/M compared to EtOH treated control cells (figure 3.6A,B). When Ikaros and Myc were induced together the cells were unable to arrest and there was a slight increase in cells in S phase. This is in accordance with similar results in pre-B cells showing that Myc overexpression antagonised the growth inhibitory effect of the Ikaros family member Aiolos (Ma *et al.,* 2010). Thus *Myc* downregulation appears to be a prerequisite for Ikaros-induced cell cycle withdrawal.

I performed qPCR analysis on these cells to investigate Ikaros-Myc antagonism at the level of gene expression. As expected from the cell cycle profile, Myc induction increased the expression of *Ccnd2* at 24 hours and decreased the expression of the cell cycle inhibitor *Cdkn1b* (p27) (figure 3.6C). The latter gene is particularly interesting as Ikaros and Myc appear to have direct and opposing effects on p27 expression. Ikaros upregulated the expression of *Cdkn1b* and Myc repressed its transcription. There was no mean change in the expression of *Cdkn1b* when Ikaros and Myc were induced together. The converse situation to *Cdkn1b* can be observed in *Hk2* expression, which is repressed by Ikaros and upregulated by Myc. The induction of Ikaros and Myc together resulted in an intermediate gene expression

profile in between that of Ikaros or Myc induction alone. These cells displayed a higher expression of *Hk2* than when Ikaros was induced alone and a lower expression than when Myc was induced alone. Interestingly there appeared to be a synergistic regulation of *Itga5* expression. The induction of Ikaros and Myc together resulted in a more enhanced repression of this gene than either condition alone. Hence there appears to be a more nuanced system of gene regulation than a simple dichotomy of Ikaros-Myc antagonism.

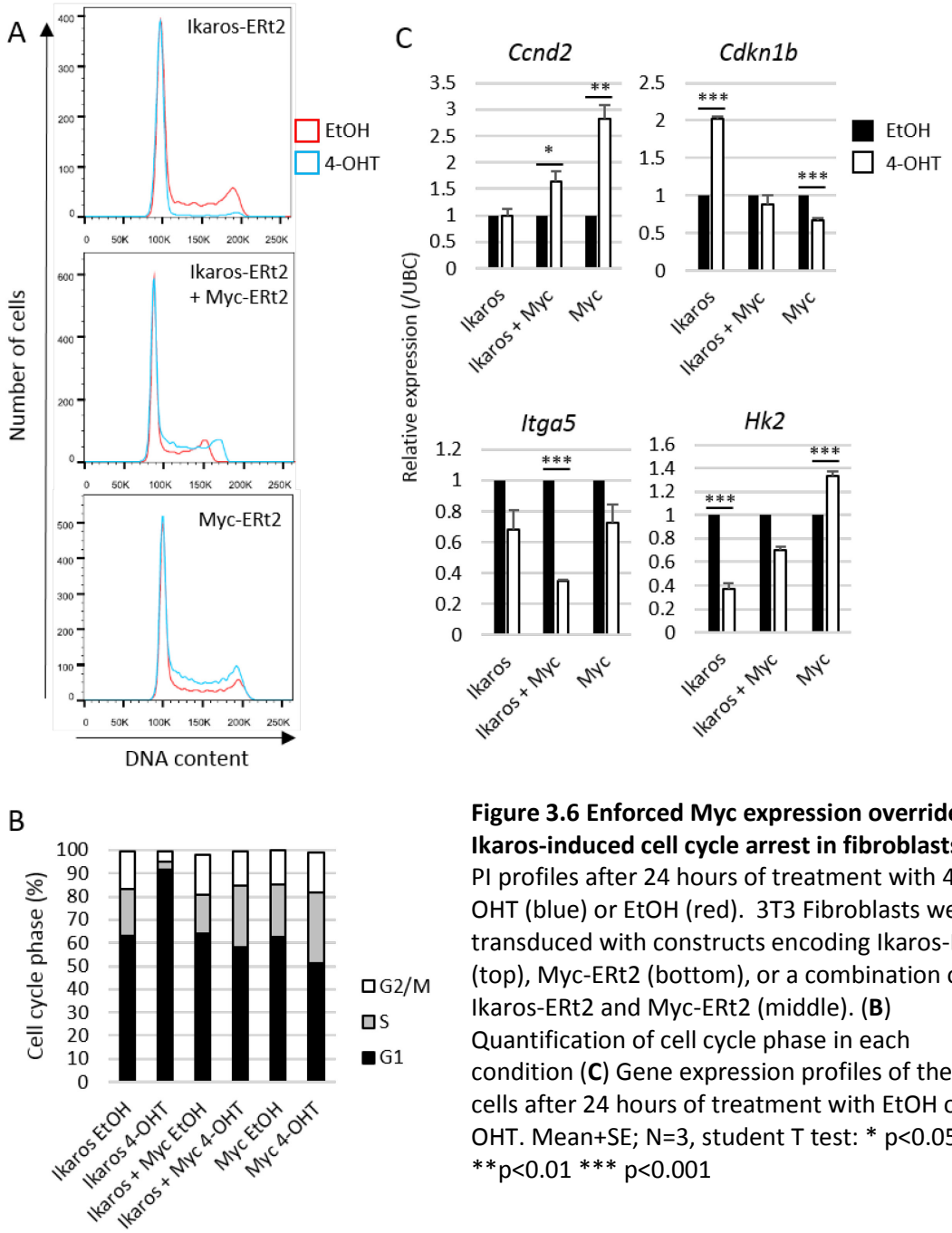

Figure 3.6 Enforced Myc expression overrides Ikaros-induced cell cycle arrest in fibroblasts (**A**) PI profiles after 24 hours of treatment with 4-OHT (blue) or EtOH (red). 3T3 Fibroblasts were transduced with constructs encoding Ikaros-ERt2 (top), Myc-ERt2 (bottom), or a combination of Ikaros-ERt2 and Myc-ERt2 (middle). (**B**) Quantification of cell cycle phase in each condition (**C**) Gene expression profiles of these cells after 24 hours of treatment with EtOH or 4-OHT. Mean+SE; N=3, student T test: * p<0.05 **p<0.01 *** p<0.001

3.5 Knockdown of *Ikzf1* expression restored proliferation

As Ikaros is able to induce cell cycle arrest in fibroblasts, it stood to reason that knockdown of *Ikzf1* would restore proliferation to Ikaros-arrested cells. Following this logic, shRNA targeting *Ikzf1* would serve as an ideal positive control readout of

cellular proliferation in the planned shRNA screen. This is because cells containing this shRNA should escape growth arrest and become enriched within the population. To test this hypothesis I cloned 4 individual shRNA targeting different regions of the *Ikzf1* coding sequence into lentiviral vectors (referred to as sh*Ikzf1* A,B,C and D respectively), and transduced these into Ikaros-ERt2 expressing 3T3 cells. I then assessed the level of knockdown by conventional (figure 3.7A) and fluorescent (figure 3.7B) western blot using an anti-Ikaros antibody. All four shRNA depleted Ikaros protein to some extent relative to control non-shRNA transfected (Ikaros-ERt2) or empty shRNA vector transfected cells. In accordance with the reduction in Ikaros protein, *Ikzf1* knockdown (by sh*Ikzf1*-D) reversed the repression of *Myc* and restored its mRNA expression to a level comparable to the EtOH treated control (figure 3.7C). This was reflected in a partial restoration of Myc and cyclin D2 protein expression in these cells (figure 3.7D).

I visualised the effect of *Ikzf1* knockdown on proliferation by plating the cells at equal density and cultured them for up to one week in media supplemented with 4-OHT, before staining with crystal violet (figure 3.7E). As expected, cells that expressed the Ikaros-ERt2 construct showed a marked disparity in the intensity of staining compared with cells that expressed an empty MSCV vector. Cells that expressed Ikaros-ERt2 and an empty shRNA vector did not proliferate over the time course. Knockdown of *Ikzf1* by two independent shRNA (sh*Ikzf1*-B and –D) restored proliferation, as observed by the increased intensity of crystal violet staining that was comparable to the empty MSCV vector control. In conclusion, *Ikzf1* knockdown restored proliferation to Ikaros-arrested fibroblasts. This shows that shRNA targeting *Ikzf1* are a valid positive control for use in the shRNA screen.

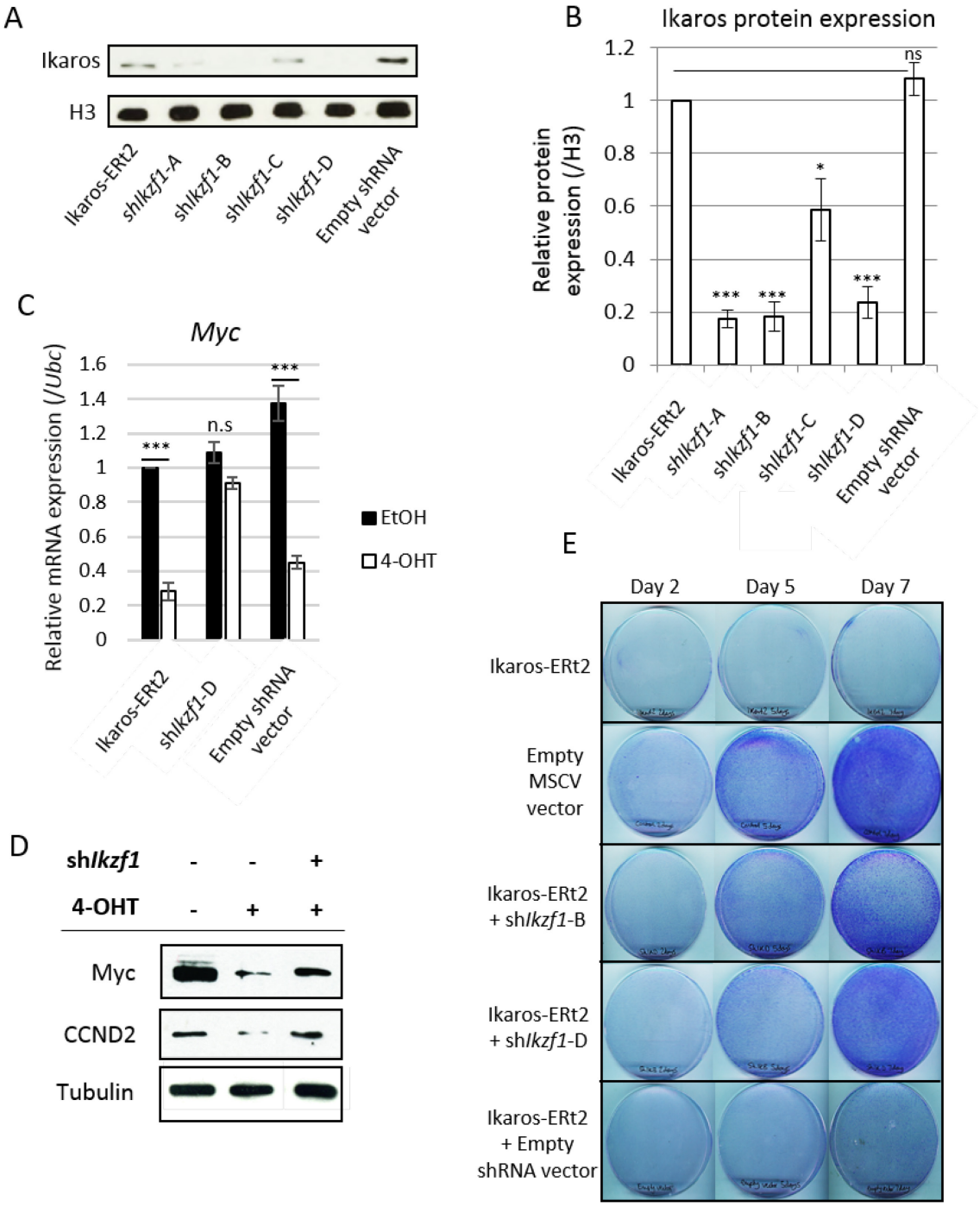

Figure 3.7 Ikaros knockdown restored proliferation. (**A**) Western blot from 3T3 whole cell lysates showing Ikaros protein expression. An anti-histone H3 antibody was included as a loading control (bottom panel). (**B**) Relative protein expression after *Ikzf1* knockdown using a fluorescent secondary antibody. Fluorescent values were normalised to H3 then plotted relative to non-shRNA transfected Ikaros-ERt2 samples. (**C**) Relative *Myc* mRNA expression before and after *Ikzf1* knockdown with sh*Ikzf1*-D, normalised to the housekeeping gene *Ubc*. (**D**) Western blot showing Myc and cyclin D2 protein expression with and without Ikaros induction (**4-OHT +/-**) or knockdown of *Ikzf1* (**sh*Ikzf1* +/-**). Tubulin was included as a loading control. (**E**) Colony formation assay of 3T3 cells that were plated at equal density and treated for up to 7 days with 4-OHT, before staining with crystal violet. Mean+SE; N=3, student T test: * p<0.05 **p<0.01 *** p<0.001

3.6 A proof of principle positive enrichment shRNA screen

To test the effects of *Ikzf1* knockdown in a situation more analogous to the shRNA screen, I carried out a proof of principle experiment by enriching shRNA targeting *Ikzf1* in a pooled population of mixed shRNA. In this experiment Ikaros-ERt2 expressing 3T3 cells were infected with an shRNA targeting *Ikzf1* (sh*Ikzf1*-D), or a control empty shRNA vector (shControl). These were plated alongside Ikaros-ERt2 expressing 3T3 cells infected with a mixed library of shRNA targeting approximately 5000 genes (library obtained from decipherproject.net, discussed further in chapter 4.2). To make sh*Ikzf1* and shControl transduced cells detectable in this pooled population, I cloned blue fluorescent protein (BFP) into these vectors, replacing the red fluorescent protein (RFP) that was present originally. Thus cells that contained shControl or sh*Ikzf1* expressing vectors could be easily distinguished from cells that contained the shRNA library by the detection of blue or red fluorescence in the flow cytometer. Such multicolour enrichment assays have been demonstrated before to be effective in characterising the effect of shRNA on cellular proliferation (Zuber *et al.,* 2011).

A pure population of cells that displayed red fluorescence were plated at a 9:1 ratio alongside blue fluorescent cells that either expressed sh*Ikzf1*-D or the shControl vector. The enrichment of blue fluorescence relative to red fluorescence was monitored over a 5 day time course, in which the nuclear translocation of the Ikaros-ERt2 construct was induced with 4-OHT treatment (figure 3.8A). As knockdown of *Ikzf1* provides a proliferative advantage (figure 3.7E) it was expected that cells expressing the sh*Ikzf1*-D vector could outcompete other cells and become enriched within the population over time. Indeed it was observed in figure 3.8B (right panel) that sh*Ikzf1*-D expressing cells were enriched, as BFP fluorescent cells increased from 10% of the total population to >40% by day 5. In contrast, the empty shControl vector did not confer a competitive advantage, as the proportion of these BFP fluorescent cells remained at <10% of the total population throughout the time

course (left panel). It might be possible to repeat this experiment using lower ratios than 9:1 to better reflect the shRNA library diversity, however it is unclear at this stage if an enrichment could be detected if the positive control shRNA was diluted to a final proportion of less than 10%. Based on the data presented in figure 3.8 however, *Ikzf1* knockdown provides a competitive advantage that can be detected by an enrichment of this shRNA in a mixed population. This validated the theory that we can enrich for shRNA that override Ikaros-induced cell cycle arrest, and provided a proof of principle demonstration that the shRNA screen is feasible.

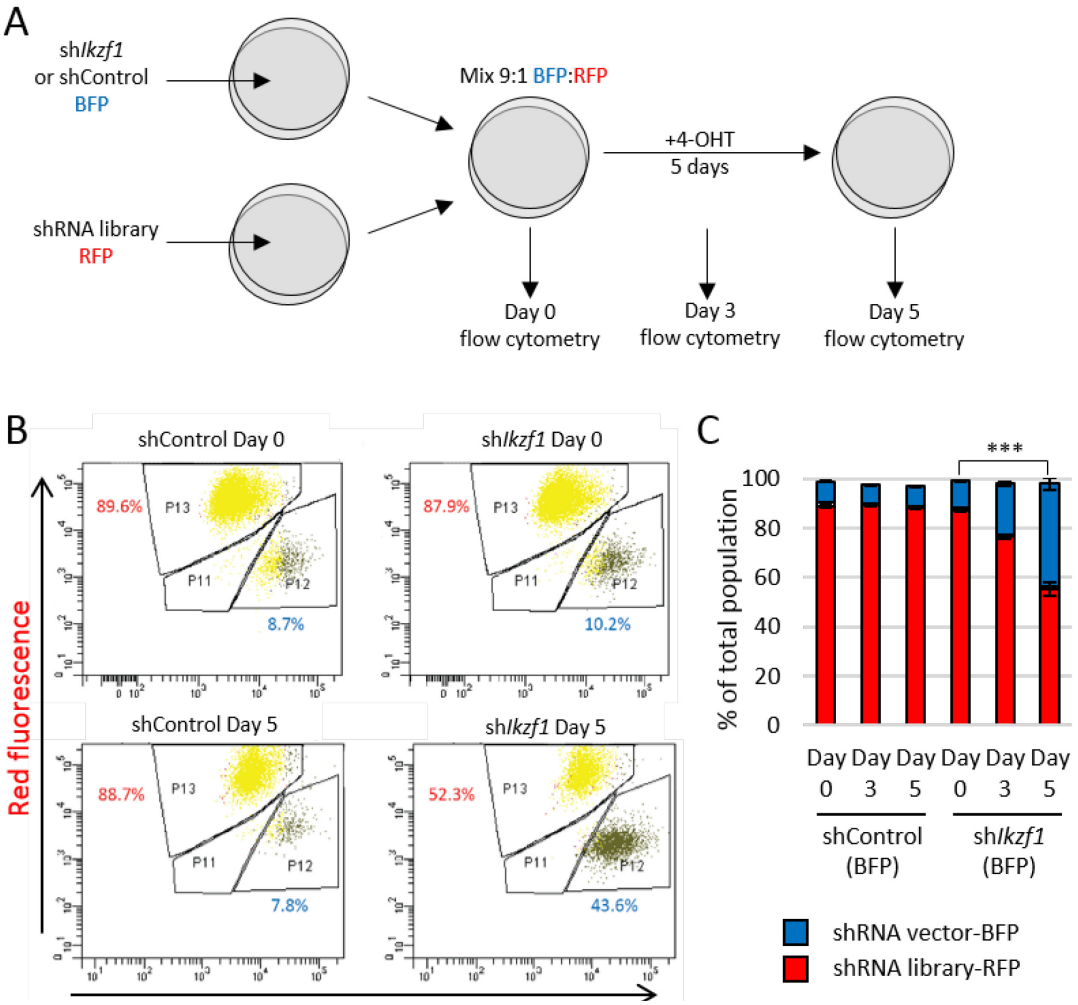

Figure 3.8 Ikaros knockdown in fibroblasts provides a competitive advantage in a mixed shRNA background. (**A**) Schematic depicting the experimental outline of the competition assay. (**B**) Flow cytometry plots displaying blue fluorescence on the x axis versus red fluorescence on the y axis. Alive, single GFP (Ikaros-ERt2) positive cells were gated and the proportion of cells displaying red (shRNA library) or blue (sh*Ikzf1*) fluorescence was recorded at day 0, day 3 and day 5 after 4-OHT treatment. An empty shRNA vector that expressed BFP was included as a negative control (shControl). (**C**) The percentage of red versus blue fluorescent cells was plotted for shControl and sh*Ikzf1* samples. Knockdown of *Ikzf1*, but not the control, provided a competitive growth advantage over the time course. (Mean+SE; N=3, student T test: *** p<0.001)

3.7 Discussion

3.7.1 Ikaros directs cells towards a quiescence-like state

Ikaros contributes to the transition of large cycling pre-B cells (FrC') to small resting pre-B cells (FrD) (Ferreiros-Vidal *et al.,* 2013). This not only involves directing the appropriate expression of B cell lineage genes such as the recombinases *Rag1/2* (required for VDJ recombination of immunoglobulin loci), but also a wholescale rewiring of gene expression towards a quiescent state that encompasses metabolism, cell cycle and adhesion (Ferreiros-Vidal *et al.,* 2013; Ma *et al.,* 2010; Reynaud *et al.,* 2008; Joshi *et al.,* 2014). Here I demonstrated that some of the key gene expression changes observed in pre-B cells related to cell cycle regulation also occur in fibroblasts, a cell type that does not endogenously express Ikaros proteins. Ectopic introduction of an inducible Ikaros-ERt2 construct into fibroblasts resulted in an accumulation of cells in G1 and a sustained withdrawal from the cell cycle (figure 3.4). Consistent with this observation, previously identified Ikaros target genes relevant to the cell cycle such as *Myc* and *Ccnd2* were repressed at the mRNA and protein level following Ikaros induction. I chose the 6-hour time point to investigate mRNA expression as this precedes cell cycle arrest, yet shows many significant changes in gene expression (Ferreiros-Vidal *et al.,* 2013). One observation that was difficult to reconcile was the apparent downregulation of *Cdkn1a* mRNA expression in fibroblasts. *Cdkn1a* encodes the cell cycle inhibitor p21, and I would expect its expression to increase in G1 arrested cells. Indeed, its expression is increased as a result of Ikaros induction in B3 cells (figure 3.3). The most likely explanation is that this downregulation is not reflected in the protein concentration within these cells. For example, p21 protein could be stabilised by post-translational modifications. Phosphorylation by protein kinase C (PKC) and PKB can regulate the stability of p21 to promote or decrease the half-life of this protein (reviewed in Jung *et al*., 2010). If the observation is true however and p21 is decreased in these cells then it is possible that Ikaros can regulate the cell cycle independently of p21. Evidence supporting

this can be seen in the literature, as reports show that Ikaros does not significantly regulate *Cdkn1a* expression in *IRF4/8* deficient pre-B cells (Ma *et al.,* 2010) or thymocytes (Kathrein *et al.,* 2005). This is in contrast to B3 cells in which *Cdkn1a* is regulated by Ikaros (Ferreiros-Vidal *et al.,* 2013). This highlights possible cell type specificity in the regulation of gene expression by Ikaros, though more work needs to be done to fully elucidate this picture.

As cells withdraw from proliferation in response to Ikaros induction, there is decreased anabolic demand and fewer requirements for cellular ATP levels to be replenished at high rates. Therefore the cells switch from reliance on aerobic glycolysis towards oxidative phosphorylation. The reliance on glycolysis to meet the metabolic demand of highly proliferative cells has particular relevance to cancer (reviewed in Vander Heiden *et al.,* 2009). Work performed by my colleague has demonstrated that Ikaros rewires the metabolism of B3 cells towards a resting, quiescent state. This is demonstrated by a decrease in the extracellular acidification rate, a readout of lactate secretion (Ferreiros-Vidal, manuscript in preparation). I have demonstrated here that Ikaros induction results in the repression of two key enzymes in the glycolytic and fermentation pathways in fibroblasts, *Hk2* and *Ldha*. It would be interesting to see if this results in a shift away from utilisation of the glycolysis pathway in fibroblasts, as observed in B3 cells.

It has been previously demonstrated that Ikaros is required to downregulate the expression of adhesion related molecules in pre-B cells (Joshi *et al.,* 2014). Conditional inactivation of Ikaros DNA binding activity arrests pre-B cell differentiation at the large cycling stage (FrC'), in which cells are dependent on stromal contact for survival and proliferation. Cells that express DNA binding-deficient Ikaros exhibit increased expression of integrins and enhanced integrin and focal adhesion kinase (FAK) signaling and remodelling of the actin cytoskeleton (Joshi *et al.,* 2014). Integrins link spatial signals from the extracellular environment to signalling pathways involved in G1-S progression (reviewed in Moreno-Layseca and

Streuli, 2014). During pre-B cell differentiation, downregulation of adhesion to the stromal niche may allow migration away from IL-7 secreting cells. Cessation of IL-7 signalling is required for cell cycle withdrawal, light chain rearrangement and quiescent metabolic reprogramming, and Ikaros can directly antagonise IL-7 regulation of many genes involved in these pathways (Heizmann *et al.,* 2013). Thus Ikaros appears to function at a nexus linking cell cycle, adhesion and metabolism to B cell development. As shown in figure 3.5, the regulation of *Itga5* is also preserved in fibroblasts. The consequences of this downregulation are at this point unclear. It is likely that a complex network of growth factors and adhesion molecules link the context of the extracellular environment to intracellular cytoskeletal and signalling dynamics, influencing the decision to spread and proliferate. Ikaros may be able to exert some influence onto these decisions.

Whilst it is premature to draw broad conclusions based on gene expression data from a handful of target genes, there are hints that Ikaros can promote a quiescence-like gene expression program in pre-B cells and fibroblasts. It would be useful to investigate these changes at a genome-wide level using an approach such as RNAseq, to definitively compare and contrast the effects of Ikaros in diverse cell types.

3.7.2 Ikaros and Myc – an antagonistic relationship?

In the results presented here I have provided a brief glimpse into the complex interplay underlying the relationship between Myc and Ikaros. *Myc* transcription is repressed early after Ikaros induction, and many genes are overlapping targets of regulation by Ikaros and Myc. It is therefore important to understand which genes are direct Ikaros targets and which genes are differentially expressed as a consequence of *Myc* downregulation. I attempted to address this question by co-expressing Ikaros and Myc in the same cells (figure 3.6). When *Myc* expression was maintained, Ikaros was no longer able to arrest the cell cycle, and parts of the gene

expression program instilled by Ikaros was reversed. Ikaros and Myc appear to have direct antagonistic functions in relationship to cell cycle progression and metabolism, as Myc promotes a proliferative and anabolic state. The downregulation of *Myc* may be an obligate function of Ikaros in its role as a tumour suppressor. At first glance these results may appear discouraging, given that I aim to identify novel regulators of Ikaros-induced cell cycle arrest. However this does not preclude other mechanisms that Ikaros may exploit to bring about cell cycle arrest. Ikaros may induce a factor that transcriptionally co-represses Myc for example, or induce a factor that functions after Myc depletion to maintain a stable arrest. Or Ikaros may alter the balance of post translational modifications towards Myc protein, such as the phosphorylation of Ser 62 and Thr 58 residues that regulate Myc stability and degradation (Sears *et al*., 2000).

Overexpression of Ikaros and Myc may appear to be a somewhat crude approach, as it does not take into account the relative expression of each protein for example, which may impact on the regulation of target gene expression. It is still informative however, and provides interesting glimpses into the relationship between Ikaros and Myc. One interesting example was the apparent synergy involved in the repression of *Itga5*, demonstrating that the relationship is not entirely mutually antagonistic. Myc has been shown to repress a variety of adhesion molecules, and it is believed that this enables anchorage independent growth (Dang *et al.,* 1999). It is perhaps surprising that Ikaros and Myc should share a common function in this area. This repression is most likely context specific, as in the pre-B cell niche, and adhesion pathways may be co-opted in different contexts to achieve disparate goals (differentiation versus malignancy).

To shine more light on the relationship between Ikaros and Myc, Dr Ferreiros-Vidal has undertaken a genome-wide approach, comparing nascent RNAseq profiles of B3 cells expressing inducible Ikaros and Myc constructs. Early results segregated genes according to Ikaros or Myc regulation; Ikaros regulated genes tended to be involved

in B cell differentiation, whilst Myc regulated genes were involved in anabolic processes such as ribosome biogenesis. This approach will be useful to dissect the role that Ikaros and Myc play in the balance between differentiation and proliferation and facilitate the identification of overlapping gene targets that are synergistically or antagonistically regulated by these two factors.

3.7.3 A proof of principle shRNA screen

It was important to demonstrate the robustness of my experimental system and its suitability to perform an RNAi screen. Pooled shRNA screening protocols are lengthy and require considerable optimisation to produce robust, replicable results (Sims *et al.,* 2011). In a system such as mine, that compares two different treatments (4-OHT vs EtOH) on a pool of transfected cells, it is of particular importance that control treated cells grow logarithmically throughout the experiment and 'experimentally' treated cells show little or no growth. This helps reduce the background noise that will inevitably introduce stochasticity into the sequencing data. Here I demonstrated that 4-OHT treated cells displayed a growth defect compared to control, and knockdown of *Ikzf1* restored proliferation to these cells (figure 3.7). Importantly, cells in which *Ikzf1* was knocked down (demarcated by blue fluorescence) could outcompete cells transduced with a pooled shRNA library plated in the same dish (figure 3.8). This demonstrated the efficacy of this approach, and showed that shRNA targeting *Ikzf1* are a good positive readout for the shRNA screen.

Several caveats to this system must be borne in mind. Whilst it is true that shRNA targeting *Ikzf1* could be enriched in a pooled competitive screen, it stands to question whether the degree of this enrichment is sufficient to be significantly detected above background noise. Whilst having many positive features, the inducible system may not provide a robust arrest over the length of the whole experiment. At long times points (>6 days) Ikaros-ERt2 induced cells began to lose growth arrest (figure 3.4C). It is unlikely that these cells have lost the Ikaros-ERt2

transgene, as GFP expression persists even after several weeks of culture (data not shown). It may be possible that the Ikaros protein is degraded, or is no longer binding appropriately in the nucleus. This could be tested by observing Ikaros binding at pericentromeric foci by immunofluorescence and confocal microscopy (Brown *et al.,* 1997). Another potential problem with the inducible system is the negative effect on cell viability that may arise due to extended treatment with 4-OHT. There are potential alternatives to the inducible system that may be used, such as direct overexpression of Ikaros protein lacking the ERt2 domain. Despite these caveats, the successful enrichment of positive control shRNA observed in figure 3.8 encouraged us to proceed with a trial run of the screen using the inducible system.

Chapter 4

A genetic screen identifies *SSeCKS* as a positive regulator of Ikaros-induced cell cycle arrest

4.1 Introduction

Advances in gene silencing technology and next generation sequencing (NGS) have made large-scale loss of function screenings feasible and cost effective. Pooled screening methods have been developed for high throughput RNA interference (RNAi) assays that hugely scale up the power of the experiment whilst avoiding the time consuming aspects of single well screens. Coupled with massively parallel NGS, these technologies offer a quick and cost effective method of generating large quantities of data required to interrogate genome-wide screens (Sims *et al.,* 2011; Mohr *et al*., 2014).

Pooled RNAi can be used in positive or negative selection assays to study diverse biological processes. Negative selection assays screen for depleted hits and are ideal for discovering essential genes required for cell viability (Zuber *et al.,* 2011). Positive selection assays screen for enriched hits and are well suited for discovering knockdown targets that are able to bypass proliferative arrest. For example, positive selection screens have been applied to discover genes that are essential for p53-induced arrest in response to DNA damage and replicative senescence (Berns *et al.,* 2004; Burrows *et al.,* 2010). In general, stably transfected short hairpin RNAs (shRNAs) are preferred over transiently transfected small interfering RNA (siRNA) molecules as the former facilitate knockdown over longer time periods, extending the window for the enrichment of positive hits over background noise (Sharma and Rao, 2009).

To investigate the mechanisms by which Ikaros negatively regulates cell cycle progression I performed a pooled shRNA positive selection screen in the fibroblast model system outlined in chapter 3. In this screen, 3T3 cells were transduced with an shRNA library and split into control and Ikaros-arrested groups, and the relative distribution of shRNA within these populations after one week of selection was assessed by NGS. I was interested in enriching for shRNA that bypass Ikaros-induced proliferative arrest to identify novel targets that cooperate with Ikaros to regulate the cell cycle. Here I report the first preliminary screens performed in fibroblasts using the inducible Ikaros-ERt2 system. An unfavourable signal-to-noise ratio was observed in positive control shRNA, emphasising the requirement for experimental optimisation. An improved experimental protocol was implemented that utilised an *Ikzf1* overexpression vector lacking the ERt2 domain. In the following chapter, the delivery and outcome of these screens is discussed.

The bioinformatic analyses in this chapter were performed by *Gopu Dharmalingam.*

4.2 A positive selection RNAi screen in fibroblasts

I used a pooled shRNA library obtained from the open source decipher project to screen for regulators of Ikaros-induced cell cycle arrest in fibroblasts (Decipherproject.net). This library consisted of 27,500 hairpins targeting approximately 5000 genes. The library was chosen because many of the target genes encoded intracellular signalling molecules relevant to proliferation and cancer. For the screen I used 3T3 fibroblasts expressing an inducible Ikaros-ERt2 construct, heterogeneously transduced at a population level using retrovirus. This approach does not take into account the integration site of individual transgenes, unlike a clonal population. However, equal levels of Ikaros expression can be obtained by sorting the cells by flow cytometry, as measured by GFP fluorescence. A pool of Ikaros-ERt2 expressing fibroblasts were transduced with the lentivirally packaged shRNA library at a multiplicity of infection (MOI) of 0.5 (Figure 4.1A). The low MOI ensured that there were ≤1 shRNA integrations per cell, reducing the likelihood of combinatorial phenotypes. Library

diversity was maintained by infecting 5.5x10^6 cells, which ensures that each shRNA was represented by at least 200 clones in the population. As the shRNA plasmid expresses red fluorescent protein (RFP), successful transduction could be observed by the presence of a GFP/RFP double positive population by flow cytometric analysis. A pure double positive population was obtained through puromycin selection, and the population was split into EtOH (control), and 4-OHT (Ikaros) treated samples. A time point of 7 days growth selection was chosen based on the preliminary results observed in figure 3.7. Following one week of treatment with EtOH or 4-OHT the cells were harvested for genomic DNA (gDNA) before PCR amplification. Each shRNA in the library contained a unique 20nt barcode region downstream of the shRNA hairpin sequence that acted as a molecular identifier (figure 4.1B). This barcode region was PCR amplified in a nested reaction with primer sets that contained complementary regions to the immobilised primers of the Illumina HiSeq flow cell (figure 4.1B, primer sets f1-r1 and f2r2).

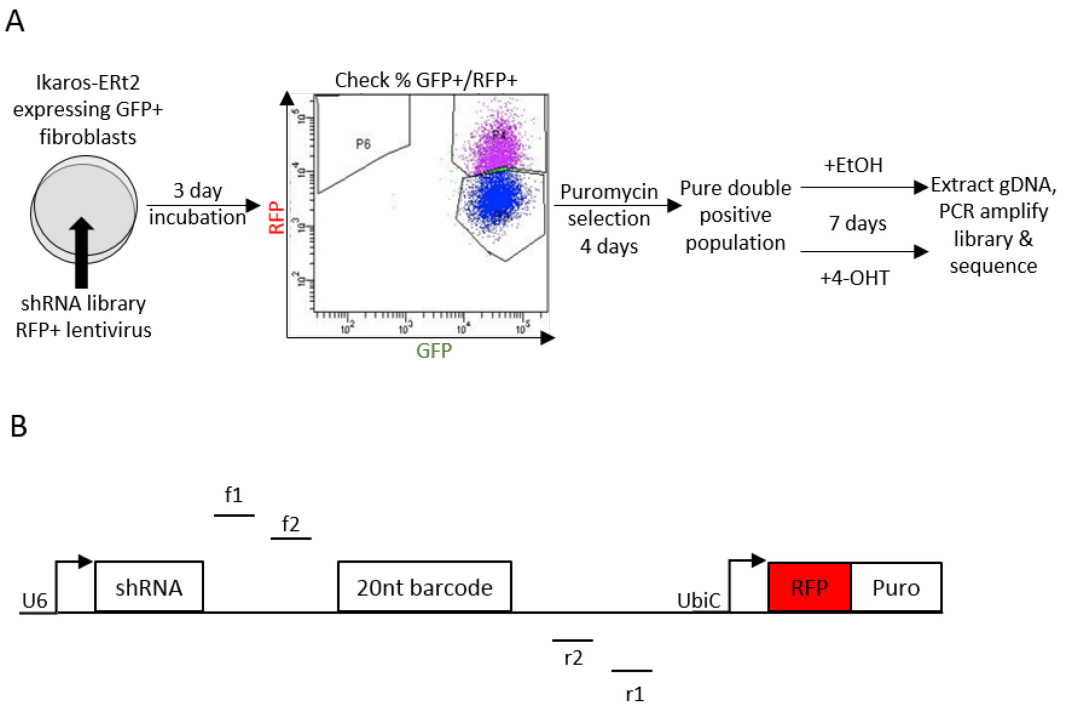

Figure 4.1 – shRNA screen using the inducible Ikaros construct. (**A**) Diagram displaying the experimental system. (**B**) Schematic outlining the amplification of the unique 20nt barcode region of each shRNA. The backbone of the PRS-I9 plasmid is displayed which contained the shRNA hairpin driven from a U6 promoter, a downstream barcode region and a RFP cassette driven by the UbiC promoter. The nested primer pairs used to amplify the barcode region are shown. F1-R1 refer to the forward and reverse HTS primers and F2-R2 correspond to the Gex primers outlined in table 3.

To test if the screen was successful, qPCR analysis was performed on the PCR amplified barcode library prior to NGS. As I showed previously, *Ikzf1* knockdown reversed the cell cycle arrest observed after 4-OHT treatment of Ikaros-ERt2 expressing fibroblasts (figure 3.7 and figure 3.8). These cells escaped Ikaros-mediated growth arrest and proliferated. Therefore I expected that barcodes corresponding to shRNA targeting *Ikzf1* would be highly enriched within the 4-OHT treated PCR amplified barcode library. *Ikzf1* barcodes in the EtOH treated samples should not be enriched, as there was no growth arrest in these cells. To detect this enrichment I performed qPCR analysis on EtOH and 4-OHT treated barcode libraries with primers that specifically amplified the barcode corresponding to sh*Ikzf1*-D. A negative control primer was included that amplified the barcode corresponding to an shRNA targeting *Rag1*. This gene is not expressed in fibroblasts so this shRNA was expected to be neutral. Figure 4.2A shows the log2 fold enrichment of barcodes corresponding to shRNA targeting *Ikzf1* and *Rag1* in 4-OHT treated samples relative to EtOH treated controls. As expected, the barcode corresponding to the negative control shRNA targeting *Rag1* was not enriched. The positive control barcode corresponding to the shRNA targeting *Ikzf1* showed an average log2 fold enrichment of around 2.7 over the two biological replicates, confirming that this knockdown conferred a proliferative advantage that bypassed Ikaros-mediated growth arrest.

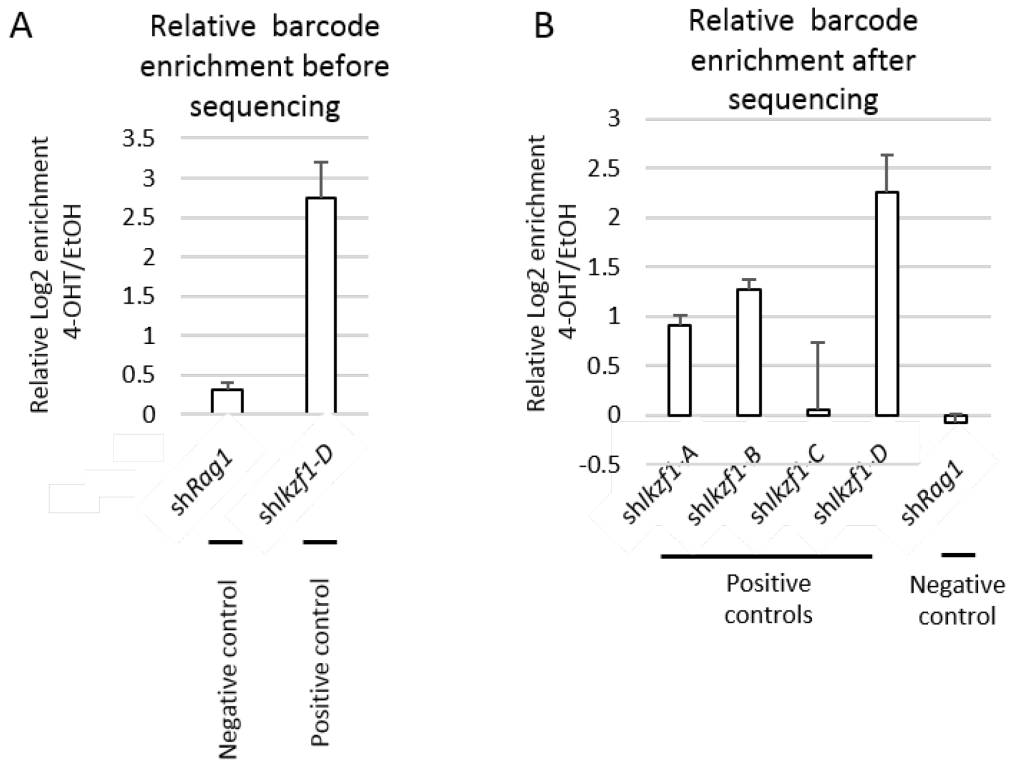

Figure 4.2 – Ikaros barcode enrichment in the amplified shRNA libraries. (**A**) qPCR analysis displaying the log2 fold enrichment of barcodes corresponding to shRNA targeting *Rag1* (left) and *Ikzf1* (right) in 4-OHT treated cells relative to EtOH treated cells, prior to NGS. (**B**) qPCR analysis displaying the log2 fold enrichment of barcodes corresponding to 4 independent shRNA targeting *Ikzf1* in 4-OHT treated cells relative to EtOH treated controls after NGS.

Having confirmed that one of the shRNA targeting *Ikzf1* was enriched, the amplified libraries of EtOH and 4-OHT treated samples were run in separate lanes of the Illumina Hi-Seq flow cell. After NGS the sequenced barcode reads were assigned gene identifications by alignment to the annotated shRNA library using shAlign. shAlign is a script specifically designed for aligning short barcode reads to a reference library, reducing the likelihood of misalignment that can occur when a whole genome reference is used (Sims *et al*., 2011). Following alignment, the number of reads for each barcode was normalised to the total number of sequencing reads to generate Reads Per Million (RPM), and the enrichment of 4-OHT treated samples relative to EtOH treated control samples was calculated to yield the Log2 fold change for each shRNA. I checked the enrichment of the four shRNA targeting *Ikzf1* contained in the library to verify that the screen worked as expected over the two replicates (figure 4.2B). The most highly enriched barcode corresponded to sh*Ikzf1*-D, which displayed an average log2 fold enrichment of 2.3. Two other shRNA targeting *Ikzf1* (sh*Ikzf1*-

A & sh*Ikzf1*-B) were less enriched, and displayed an average log2 fold enrichment of 0.9 and 1.3 respectively. The remaining shRNA (sh*Ikzf1*-C) was not enriched over the two experiments. The lack of enrichment of sh*Ikzf1*-C correlates with the poor knockdown of Ikaros protein by this shRNA observed in figure 3.7A. Only one of the positive control shRNA targeting *Ikzf1* (sh*Ikzf1*-D) was featured in the top 100 genes ranked according to log2 fold change between EtOH and 4-OHT treated samples. The relatively low enrichment of positive control shRNA was a concern, as it decreases the signal-to-noise ratio and makes it harder to detect true positive hits over background variation.

In order to conduct a successful screen I tried to maximise the enrichment of positive controls over background noise and to eliminate as much experimental variation as possible. Cellular stress may increase experimental error as it could inhibit proliferation and skew the representation of the shRNA library. The use of 4-OHT and puromycin may contribute to stress as some cells did not appear healthy after extended use of these drugs. Cellular stress was confirmed by gene ontology (GO) term analysis with the DAVID functional annotation tool (Huang *et al.,* 2009) (https://david.ncifcrf.gov/) using the list of enriched shRNA (defined as displaying a log2 fold enrichment of ≥1 in 4-OHT treated samples relative to EtOH treated samples). This analysis enriched for terms such as 'Regulation of programmed cell death' and 'Regulation of apoptosis' (supplementary figure S.1). To circumvent the use of 4-OHT and puromycin we redesigned the experimental system, taking advantage of a MSCV-*Ikzf1* overexpression construct that does not encode the ERt2 domain. This construct expresses full length Ikaros protein (Ikaros-1) that does not rely on 4-OHT treatment for nuclear translocation. The advantage of using this construct is that it provides a stronger and more persistent arrest of the cell cycle compared to the ERt2 system, with less background caused by cells escaping Ikaros-mediated arrest over the 7 day time course (data not shown). I decided to use flow cytometry to sort for Ikaros-GFP/shRNA-RFP double positive cells to eliminate the requirement for puromycin selection. I found that sorted cells attached more quickly and displayed a healthier morphology when plated on dishes coated in 0.1% gelatin. The use of medium conditioned by logarithmically growing fibroblasts also seemed to enhance the healthy morphology of Ikaros transfected

3T3 cells. I therefore investigated whether these changes to the experimental system would enhance the quality of the screen by increasing the signal-to-noise ratio and decrease variability.

Figure 4.3A outlines the new experimental system. Wild type 3T3 cells were co-infected with the MSCV-*Ikzf1*-GFP construct and the shRNA library that expresses RFP. Cells were infected with an empty MSCV-GFP plasmid as a control. The cells were sorted by flow cytometry upon detection of a GFP/RFP double positive population 72 hours later. Figure 4.3B shows that roughly 40% of the cells in the Ikaros and control conditions were GFP/RFP positive, corresponding to a MOI of 0.5. Control and *Ikzf1* expressing cells were separately plated on gelatinised dishes and cultured in conditioned media for 7 days before barcode library preparation. A day 0 time point was collected from control cells infected with the shRNA library and sorted by flow cytometry as an additional control. This was included because it gave a snapshot of the diversity of the shRNA library before the cells were cultured over the 7 day time course. Control cells were expected to grow logarithmically over the time course, but certain shRNA targeting genes essential for survival or cell cycle progression would be detrimental, resulting in a depletion of these shRNA from the control population. Such shRNA are likely be less detrimental to growth arrested cells so would not be depleted from the *Ikzf1* expressing population. These shRNA would therefore appear to be significantly enriched in *Ikzf1* expressing cells relative to control cells. By including this control we can normalise the diversity of the shRNA library in day 7 samples to day 0 and rule out such false positives. All 3 conditions (day 0 control, day 7 control and day 7 Ikaros) were carried out in 3 separate biological replicates.

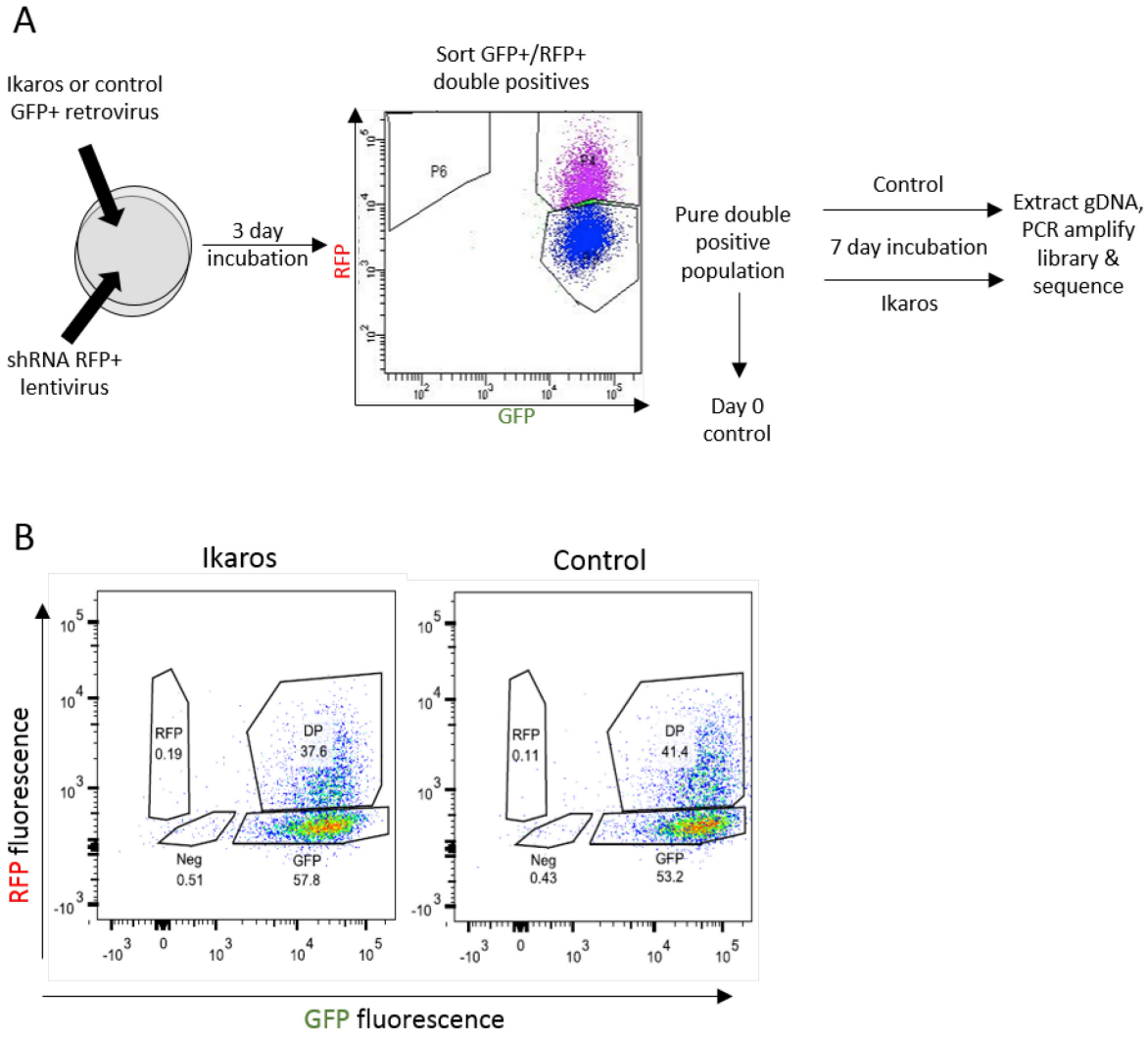

Figure 4.3 – A new experimental scheme using an *Ikzf1* overexpression construct. (**A**) Schematic outlining the changes made to the experimental system, designed to obtain higher enrichment of positive control shRNA. (**B**) Flow cytometry plots showing the proportion of cells infected with the shRNA library (RFP, y axis) and the *Ikzf1* (left) or empty control (right) expressing MSCV vectors (GFP, x axis). A double positive population comprising around 40% of the total was subsequently sorted.

Following barcode library preparation the enrichment of two positive control shRNA (sh*Ikzf1*-B and -D) was checked by performing qPCR with primers that amplify these barcodes (figure 4.4A). The negative control barcode corresponding to sh*Rag1* was not enriched in *Ikzf1* versus control expressing cells, but the two barcodes corresponding to shRNA targeting *Ikzf1* were highly enriched. The barcode corresponding to sh*Ikzf1*-D

displayed a mean log2 fold change of 4 over the three replicates, more than double the enrichment that was observed using the ERt2 system (figure 4.2A). After NGS the enrichment of the 4 positive control shRNA in *Ikzf1* expressing samples relative to control was observed (figure 4.4B). All barcodes targeting *Ikzf1,* besides sh*Ikzf1*-C, were highly enriched in the three replicates and displayed log2 fold change values that were more than double those observed using the ERt2 system (figure 4.2B). The reproducibility of the screens was investigated by comparing the log RPM of each barcode between replicates in a pairwise comparison (figure 4.4C). All replicates displayed high pearson correlation values of >0.7 indicating that the screen was robust across replicates (Sims *et al*., 2011). Taken together, these results indicate that the MSCV-*Ikzf1* overexpression system generated a favourable signal-to-noise ratio and improved the quality of the screen.

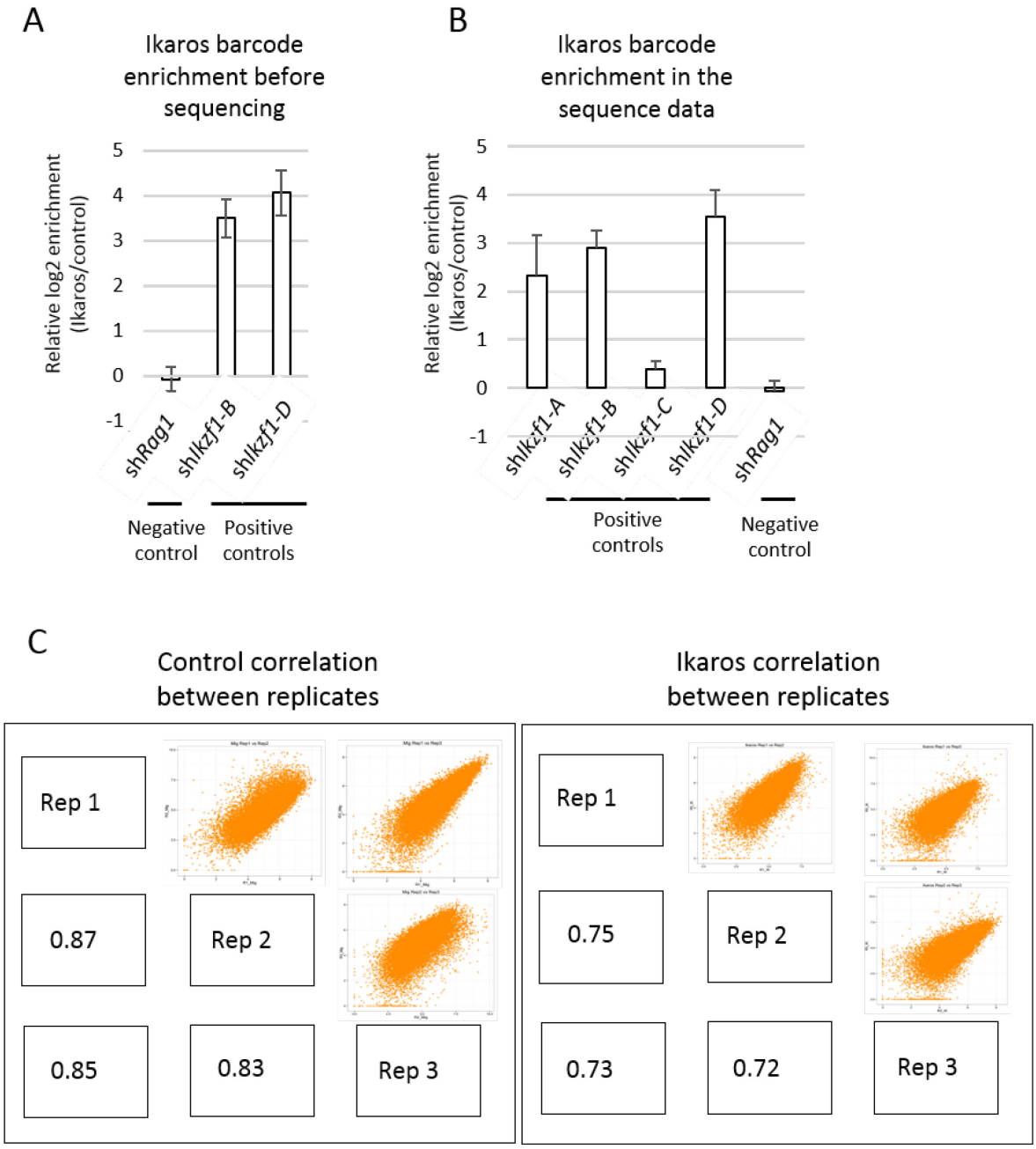

Figure 4.4 – Ikaros barcodes are highly enriched in the new experimental scheme. (**A**) qPCR analysis displaying the log2 fold enrichment of barcodes corresponding to shRNA targeting *Rag1* (left) and 2 independent shRNA targeting *Ikzf1* (right) in *Ikzf1* expressing cells relative to control. (**B**) qPCR analysis showing the log2 fold enrichment of barcodes corresponding to 4 independent shRNA targeting *Ikzf1* in *Ikzf1* expressing cells relative to control. (**C**) (top right) Plots showing the pairwise comparison of the log RPM of barcode reads in each replicate from control (left) and *Ikzf1* (right) expressing samples. (Bottom left) Boxes displaying the Pearson correlation values associated with each replicate comparison.

4.3 Identification of significantly enriched hits

A multi-step analysis pipeline was implemented to identify significantly enriched hits from the pool of aligned sequences (figure 4.5). Each shRNA was assigned a value based on its differential expression between day 7 *Ikzf1* and control expressing pools using Deseq, a statistical package optimised for differential expression analysis for RNA-seq, ChIP-Seq and barcode counts (Anders and Huber, 2010). This method has previously been applied to an *in vivo* pooled shRNA screen in mice to identify regulators of oncogenic growth (Beronja *et al*., 2013). Following Deseq analysis the enriched and depleted hits were ranked by significance according to their adjusted p values and non-significant hits (p=>0.05) were eliminated from downstream analysis. I was primarily interested in enriched hits that escaped Ikaros-mediated growth arrest. I therefore segregated significantly depleted hits (shRNA displaying ≤0 log2 fold change) from enriched hits (shRNA displaying ≥0 log2 fold change). These steps yielded 875 enriched hits from a starting total of 27,000 indicating that around 3% of shRNAs were enriched.

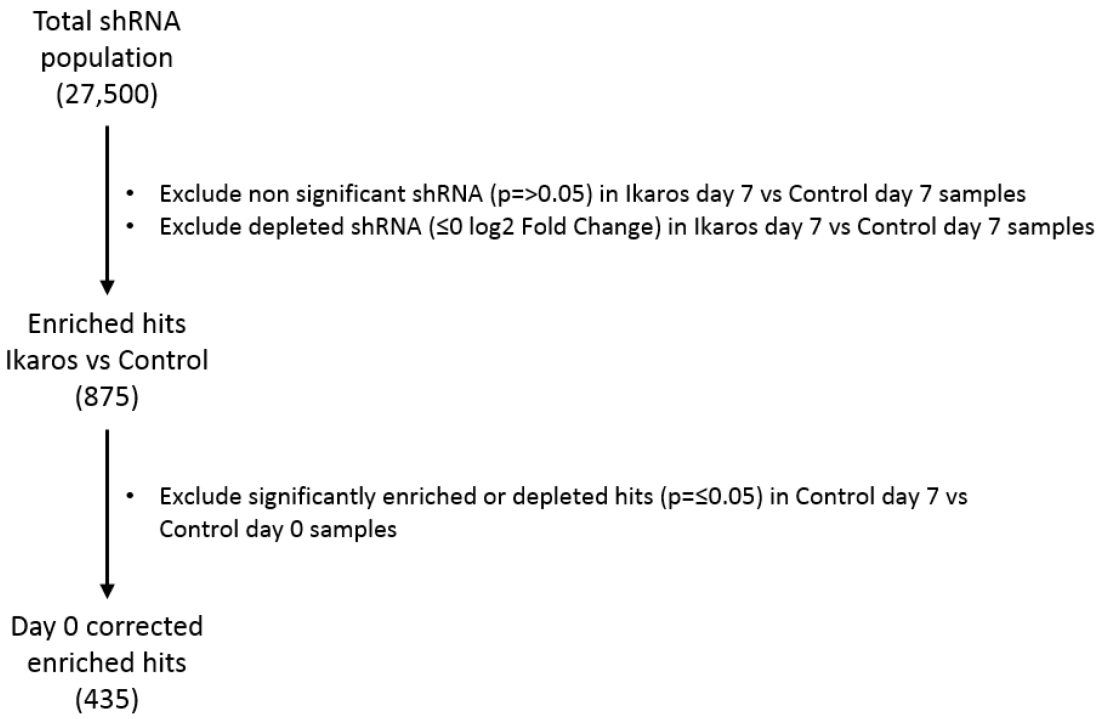

Figure 4.5 – An analysis pipeline to identify significantly enriched hits. Schematic showing the process used to obtain day 0 corrected enriched hits.

Next, day 7 control samples were normalised to day 0 control samples to eliminate false positive hits. Those shRNA that showed significant enrichment or depletion between day 7 control and day 0 control samples were excluded. This resulted in a final total of 435 'day 0 corrected' enriched hits (around 1.6% of total). The importance of the day 0 control is illustrated by looking at the example of shRNA targeting the genes *Ikzf1, SSeCKS* and *Gnb2l1.* These 3 hits were identified as significantly enriched in *Ikzf1* expressing samples relative to control samples at day 7 (figure 4.6A). When control day 7 samples were normalised to control day 0, shRNA targeting *Ikzf1* and *SSeCKS* were not significantly enriched or depleted (figure 4.6B, grey dots). *Gnb2l1* however was significantly depleted from control day 7 samples, indicating that this hit was a false positive. Another example is the large enrichment of hits targeting proteasome subunits. As protein degradation is an essential and ubiquitous process the proteasome is a 'frequent hitter' in RNAi screens, largely due to indirect effects on the phenotypic readout studied (Mohr *et al*., 2014; Schmidt *et al.,* 2013). A total of 35 enriched hits were identified that targeted different subunits of the proteasome in Ikaros day 7 versus control day 7 samples. This was reduced to 6 hits in the day 0 control corrected results. Although it is very difficult to eliminate all false positive results, these steps should increase the robustness of the screen and make it easier to identify truly enriched hits.

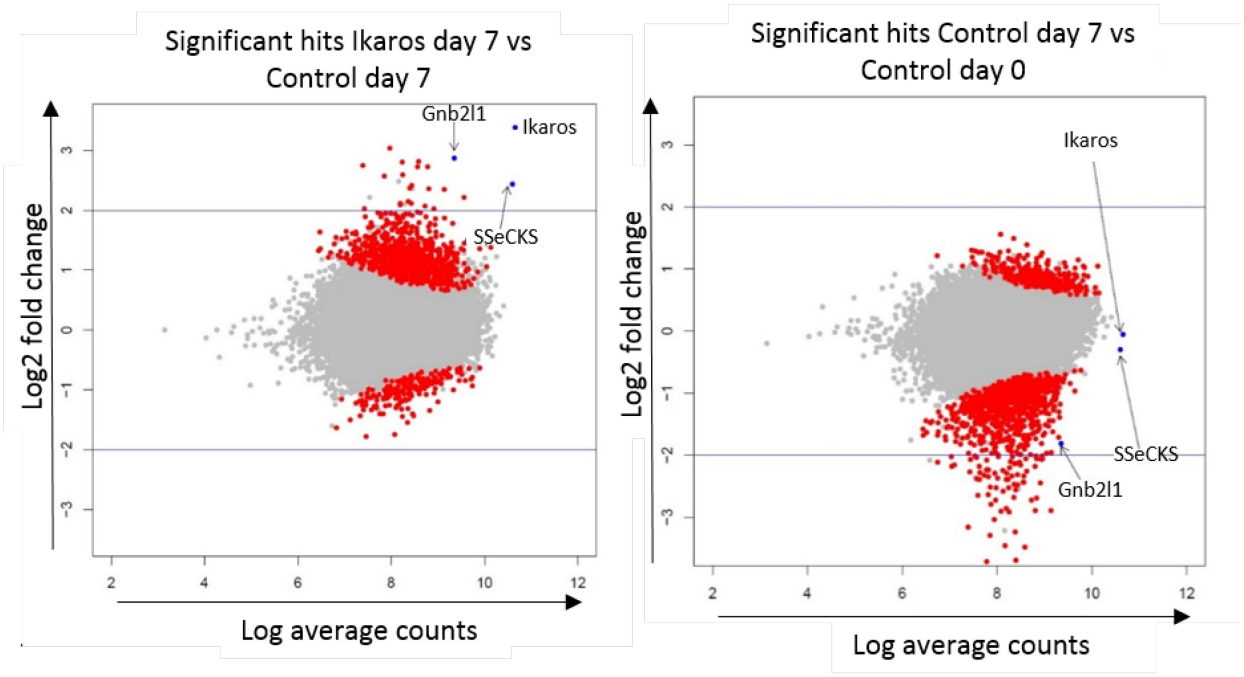

Figure 4.6 – Differentially expressed hits. Plots displaying the log average counts of each shRNA (x axis) versus the log2 fold change of each hit (y axis) in Ikaros day 7 versus control day 7 (left) and control day 7 versus control day 0 (right) samples. Red dots signify significantly enriched or depleted hits (p= ≤0.05). Three shRNA targeting *Ikzf1*, *SSeCKS* and *Gnb2l1* are illustrated.

4.4 Analysis of the day 0 corrected hits

The top 10 day 0 corrected hits are displayed in figure 4.7, ranked in significance according to their adjusted p values. Three separate shRNA targeting *Ikzf1* appear in the top 4 most highly enriched hits (figure 4.7, red font), validating the experimental approach. The 3rd most enriched target, *SSeCKS,* was extremely significant and displayed a large log2 fold change in *Ikzf1* expressing samples relative to control (log2 fold change of 2.4). This gene was particularly interesting as it has been characterised as a negative regulator of G1/S progression in fibroblasts (Lin *et al.,* 2000) and its expression is downregulated in an array of human cancers (Gelman, 2010). Additionally, *SSeCKS* was identified as an Ikaros bound target gene in B3 cells that was upregulated in response to *Ikzf1* overexpression (Ferreiros-Vidal *et al.,* 2013). The 5th most enriched target, *Gli2,* is a transcription factor that mediates Sonic hedgehog (Shh) signalling. Hits against the related protein Gli1 appear in both the significantly enriched and depleted datasets, hinting that shRNA targeting this pathway may

be false positives. The proteasome subunit *Psmd4* appears in the top 10 enriched hits, but is likely to be a false positive hit as discussed previously. *Zbtb32*, a member of the bric-a-brac zinc finger family of transcription factors, is essential for thymocyte development and promotes T cell proliferation by negatively regulating the expression of *Cdkn1a* (p21) (Iguchi *et al.,* 2015). *Smarce1* encodes a component of the SWI/SNF ATP-dependent chromatin remodelling complex that utilises ATP hydrolysis to restructure nucleosome octamers at target loci, facilitating gene activation or repression (Muchardt and Yaniv, 2001). Another component of the SWI/SNF complex, *Smarca4* (BRG1), also appears in the list of enriched shRNA hits. SWI/SNF complexes have been shown to negatively regulate proliferation by controlling the expression of genes required for progression past the G1 checkpoint (Muchardt and Yaniv, 2001; Ruijtenberg and van den Heuvel, 2015). Interestingly, Ikaros associates with BRG1 and they colocalise in the nucleus of resting T cells (Kim *et al.,* 1999). This raises the possibility that epigenetic regulation directed by Ikaros is required for the attenuation of proliferation.

Rank	Gene symbol	Log2 fold change (Ikaros day 7 vs Control day 7)	Adjusted p value	Ikaros bound in B3 cells?
1	*Ikzf1*	3.383259604	6.04E-43	
2	*Ikzf1*	2.729368303	2.03E-20	
3	*SSeCKS*	2.435507843	1.07E-18	
4	*Ikzf1*	2.218751357	9.40E-11	
5	*Gli2*	1.349663417	2.10E-07	
6	*B4galnt1*	1.383578536	8.90E-07	
7	*Zbtb32*	1.458810347	5.28E-06	
8	*Psmd4*	1.44113792	6.53E-06	
9	*Smarce1*	1.425878921	1.11E-05	
10	*Cfh*	1.187717679	2.98E-05	

Figure 4.7 – Top 10 significantly enriched candidates. The ranked list of the most significantly enriched shRNA alongside the associated log2 fold change (Ikaros day 7 relative to control day 7) and adjusted p values. The Ikaros binding status of each gene in B3 cells is displayed as bound (green), or not bound (red), based on ChIP-Seq data from Ferreiros-Vidal *et al.,* 2013.

It is interesting to note that the majority of the top 10 hits were found to be bound by Ikaros based on ChIP-seq analysis in the pre-B cell line B3 (Ferreiros-Vidal *et al.,* 2013). We cannot

extrapolate binding data from pre-B cells to fibroblasts directly without performing ChIP experiments in fibroblasts. We may however use this data as a rough guide to characterise the nature of these hits regarding the regulation of these genes by Ikaros. I therefore curated the list of significantly enriched and depleted hits with the Ikaros binding data obtained from B3 cells (figure 4.8). The first trend I observed was that there were many more hits that were enriched (435) than depleted (166). This was as expected because I performed a positive selection screen that should enrich for shRNA that enable proliferation over the time course of the experiment. The second trend I observed is that enriched hits were more likely to be targets of Ikaros binding in B3 cells than depleted hits. Figure 4.8B shows that around 45% of the total enriched hits corresponded to genes that were bound by Ikaros in B3 cells (green segment). The proportion of Ikaros-bound hits dropped to 32% in the depleted dataset (figure 4.8B). This trend was exacerbated when I focused on the top 10% of hits from the enriched and depleted datasets. From these highly significant candidates, 60% of the enriched hits corresponded to Ikaros-bound genes in B3 cells compared to only 19% of depleted hits. This suggests that the enriched hits were more likely to correspond to genuine targets of regulation by Ikaros in B3 cells, with the caveat that I am comparing hits observed in fibroblasts with binding data obtained from pre-B cells. It would have been informative to conduct a ChIP-seq experiment in fibroblasts to confirm this binding, given more time.

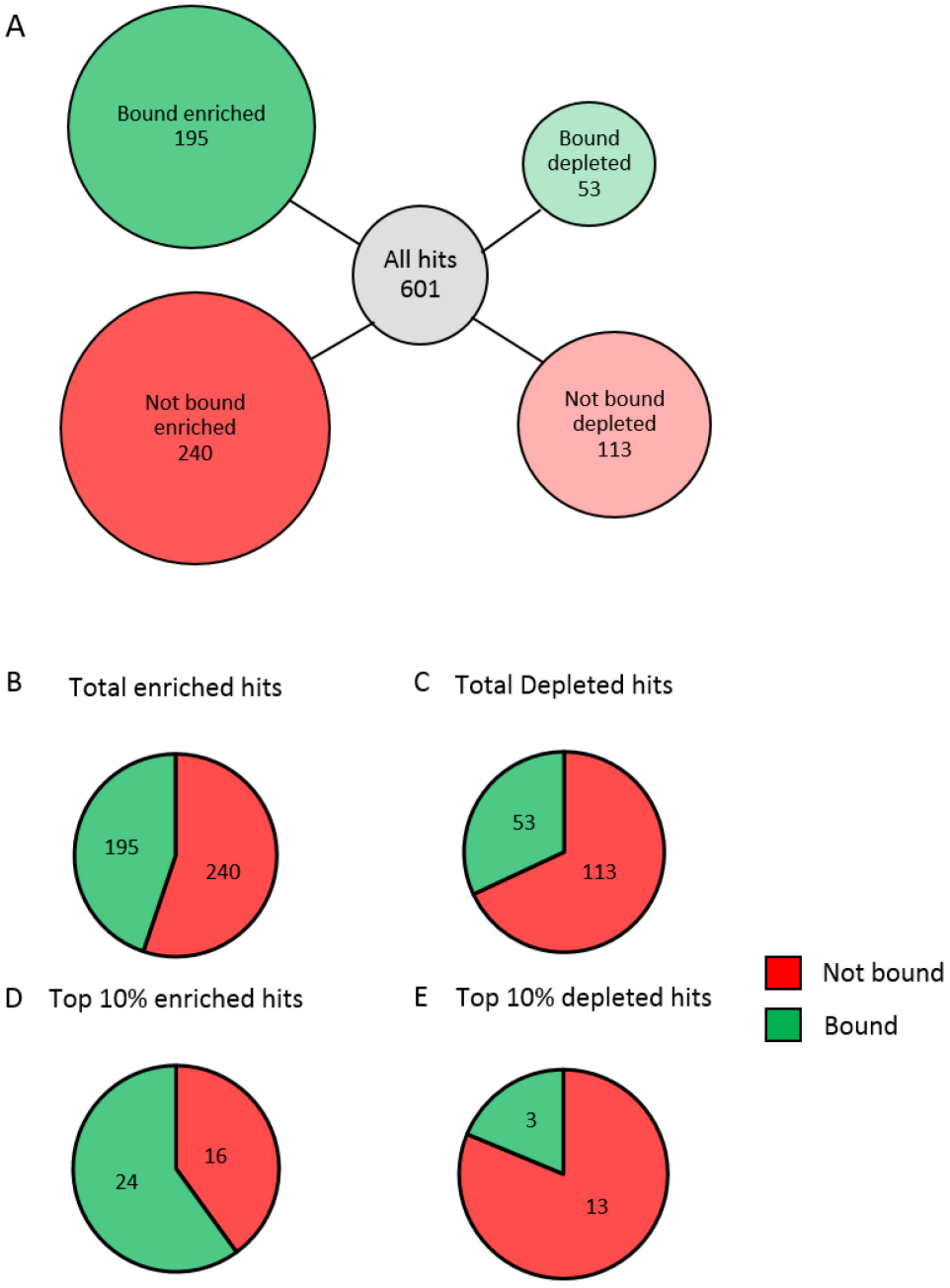

Figure 4.8 – Ikaros binding status of significant hits. (**A**) Diagram displaying the number of enriched hits that are bound (green) or not bound (red) by Ikaros in B3 cells and the number of depleted hits that are bound (pale green) and not bound (pale red) by Ikaros (not to scale). (**B**,**C**) The proportion of the total enriched and depleted hits that are bound (green) and not bound (red) by Ikaros. (**D**,**E**) The proportion of the top 10% of enriched and depleted hits that are bound (green) and not bound (red) by Ikaros.

I performed GO term analysis to understand the nature of the enriched hits. I began searching with the gene symbols of all enriched hits that I defined as bound by Ikaros in B3 cells. The most significant term returned from this analysis was 'Regulation of the cell cycle', which is expected from a proliferation screen (supplementary figure S.2A). The next most significant terms related to cell death and apoptosis, returning terms such as 'regulation of apoptosis', 'regulation of programmed cell death' and 'regulation of cell death'. Thus it appears that cellular stress still had an influence on the outcome of the screening process, despite the adjustments to the experimental protocol outlined in 4.2. It is likely that *Ikzf1* overexpression itself is a cause of this stress, as Ikaros has been implicated in the regulation of apoptosis (Pulte *et al*., 2006; Rebollo *et al.,* 2001). Therefore Ikaros-induced cell death in my screen may be an inescapable side effect of its tumour suppressive function.

I next looked at the enriched hits that were not bound by Ikaros in B3 cells (supplementary figure S.2B). The most significant term returned was 'cell-cell signalling' which raises the interesting possibility of intercellular signalling in the regulation of proliferation by Ikaros. No significant terms were returned when queried with the list of depleted hits from the screen (supplementary figure S.3).

To determine which pathways were enriched in the screen, I performed Kegg analysis on all the enriched hits using DAVID. The most significant term returned was 'pathways in cancer' (supplementary figure S.4A). When queried with hits that were Ikaros bound in B3 cells, the top term returned was 'cell cycle', though this did not reach the significance threshold (supplementary figure S.4B).

4.5 SSeCKS knockdown overrides Ikaros-induced cell cycle arrest

In lieu of a high throughput secondary screen (discussed further in 4.6.2), I decided to embark on a candidate based approach to detect positive hits. I focused on *SSeCKS*, due to its high significance and large log2 fold enrichment that was comparable to the positive

control shRNA targeting *Ikzf1* (figure 4.7). SSeCKS is a scaffolding protein that has been shown to negatively regulate progression past the G1/S checkpoint in fibroblasts by directly sequestering cyclin D1 in the cytoplasm (Lin *et al.,* 2000). As mentioned previously, Ikaros binds to the promoter of *SSeCKS* in B3 cells to upregulate its transcription as the cells transition from the cycling (FrC') to resting (FrD) pre-B stage (Ferreiros-Vidal *et al.,* 2013). This raises the possibility that SSeCKS may be required for Ikaros-induced growth arrest at this key stage in pre-B cell development.

To understand more about the regulation of this gene in lymphocyte development I decided to mine the public collection of microarray datasets made available by the immunological genome project (Heng *et al.,* 2008) (Immgen.org). Figure 4.9 shows the expression of *SSeCKS* in a number of key immune cell populations obtained from this database. The expression of *SSeCKS* is greatly increased in B cell precursors compared to other cell types. Furthermore the expression of *SSeCKS* is increased 3-fold as the cells transition from the cycling to resting pre-B cell stage (FrC' to FrD, labelled with arrows). In addition to pre-B cells, the expression of *SSeCKS* also appeared to be relatively high in the resting population of small double positive (DP) thymocytes. Based on this overview, I focused on the expression of *SSeCKS* in developing pre-B cell and thymocyte populations (figure 4.9B). In general the expression of *SSeCKS* gradually increased throughout differentiation in both populations and spiked as the cells entered the small resting pre-B and DP thymocyte stages, coinciding with withdrawal from the cell cycle.

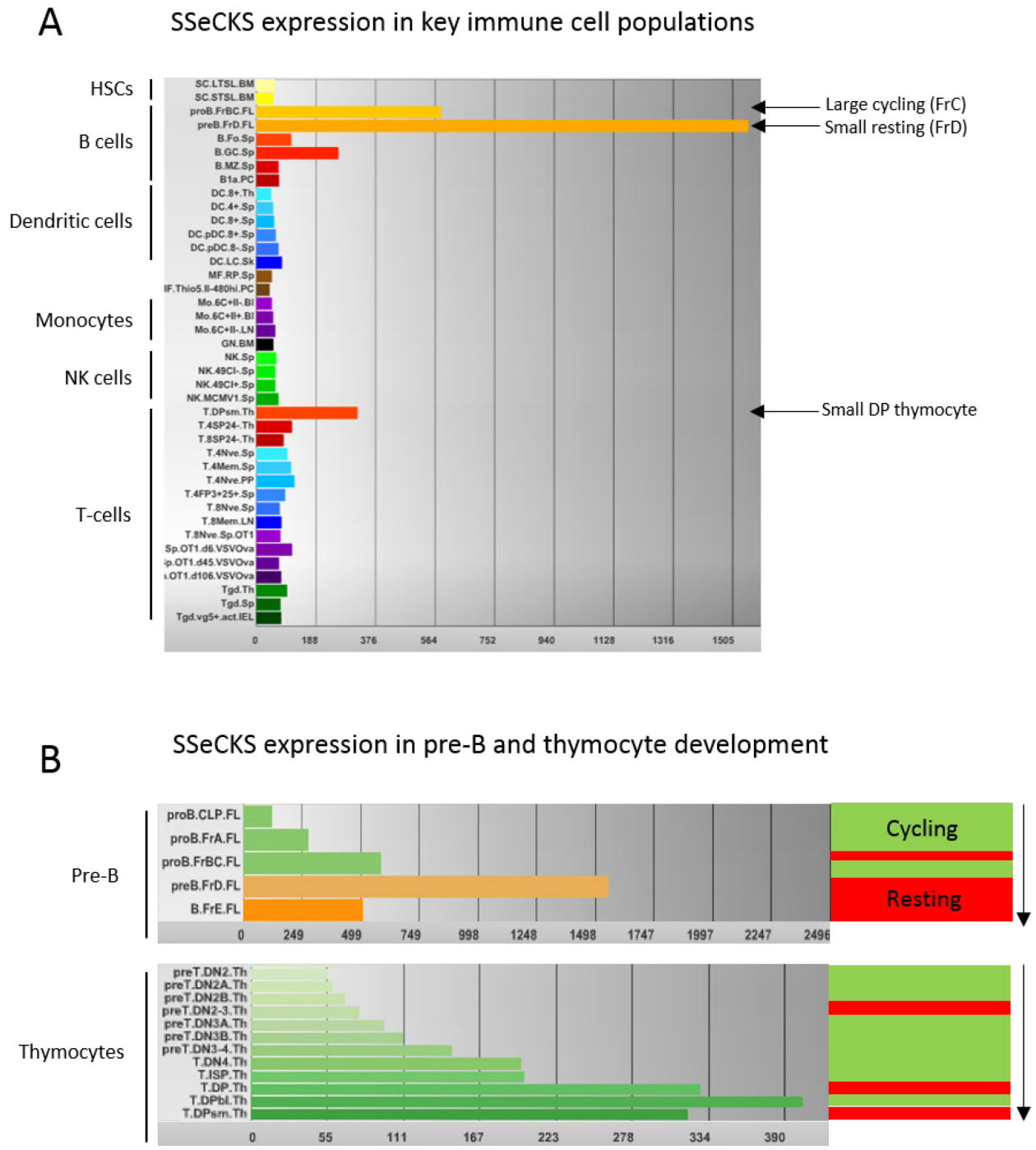

Figure 4.9 – SSeCKS expression in haematopoietic cells. (**A**) The expression of *SSeCKS* (horizontal bars) displayed in an array of immune cells. (**B**) *SSeCKS* expression in developing pre-B and thymocyte populations. The proliferative state of each developmental stage is illustrated by green (cycling) and red (resting) bars. The arrow indicates the orderly progression of cellular differentiation. The x axis displays microarray expression values obtained from Immgen.org.

As *SSeCKS* is an Ikaros target gene, I overlaid the expression of *SSeCKS* throughout different stages of pre-B cell development with that of *Ikzf1* and the Ikaros family member Aiolos (*Ikzf3*) (figure 4.10). In general the expression of *SSeCKS* (green) correlated with the upregulation of *Ikzf1* (orange) and *Ikzf3* transcripts (yellow) in these cells. The expression of *SSeCKS* peaked at the pro-B and resting pre-B cell stages which are characterised by cell cycle withdrawal required for antigen receptor rearrangement (Clark *et al*., 2014). Conversely the expression of *SSeCKS* was suppressed in the highly proliferative cycling pre-B cell stage (FrC'). This is expected, as the expression of SSeCKS is suppressed in highly proliferative cells that overexpress *Src* or *Myc* (Lin *et al.,* 1995). Thus it appears that the expression of *SSeCKS* is anticorrelated with cell cycle progression in B cell precursors. It is interesting to note that the expression of Ikaros and Aiolos alone is insufficient for cell cycle withdrawal, as high expression of both transcripts can be observed at the cycling pre-B cell stage. Signalling through the pre-BCR and IL-7 receptors at this stage strongly induces the expression of positive regulators of the cell cycle such as *Myc*. As I demonstrated in figure 3.6, the enforced expression of *Myc* is sufficient to override Ikaros-mediated cell cycle arrest. It is possible that a threshold of Ikaros and Aiolos expression is required to terminate pre-BCR signaling and antagonise the proliferation promoting properties of IL-7 signalling. Once this threshold is passed the cells can downregulate *Myc*, begin to arrest proliferation and differentiate into the resting pre-B cell stage.

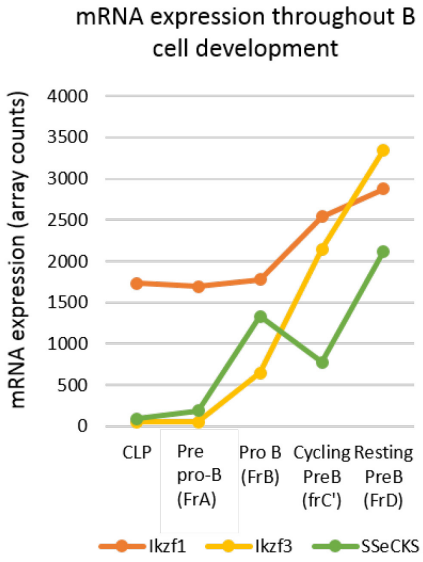

Figure 4.10 – Ikaros and SSeCKS mRNA expression in pre-B cell development. Graph showing the expression of *SSeCKS* (green), *Ikzf1* (red) and *Ikzf3* (yellow) in sequential stages of pre-B cell development. Expression data was obtained from immgen.org. CLP = Common lymphoid progenitor.

From this preliminary data it seemed that *SSeCKS* was a promising candidate to pursue. Before going further I wanted to show that SSeCKS was necessary for Ikaros-mediated cell cycle arrest. To this end, I cloned two shRNA targeting different exons of *SSeCKS* (sh*SSeCKS*-B and –C) and introduced them into 3T3 fibroblasts expressing the inducible Ikaros-ERt2 construct. Both shRNAs resulted in a reduction in SSeCKS protein expression compared to the empty vector control, with sh*SSeCKS*-B displaying the strongest knockdown (figure 4.11A). I tested the effect of this knockdown on cellular proliferation by growing the cells for up to one week in the presence of 4-OHT before staining with crystal violet (figure 4.11B). Knockdown of *SSeCKS* using either shRNA resulted in enhanced proliferation over the time course as measured by the increased intensity of staining. Importantly, the extent of the knockdown appeared to have an effect on the proliferation rate as cells transfected with sh*SSeCKS*-B displayed more intense staining at day 7. From this we can conclude that SSeCKS is required for Ikaros-mediated cell cycle arrest in fibroblasts.

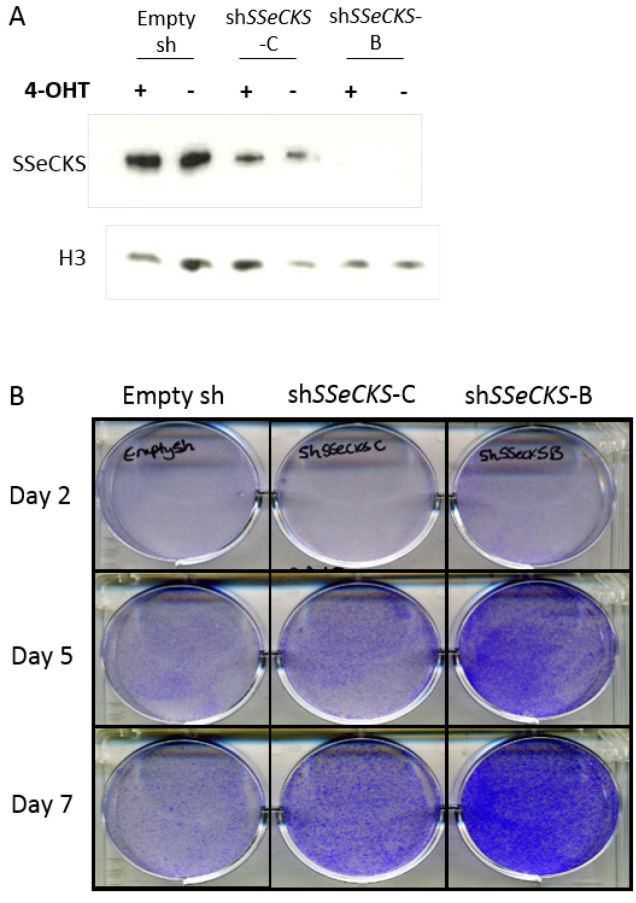

Figure 4.11 – *SSeCKS* knockdown overrides Ikaros-induced cell cycle arrest. (**A**) Western blot analysis of SSeCKS protein expression in 3T3 cells expressing Ikaros-ERt2 treated with 4-OHT (+) or EtOH (-) for 48 hours. (**B**) Colony formation assay of Ikaros-ERt2 expressing 3T3 cells treated with 4-OHT for up to 7 days before staining with crystal violet. The cells contain an empty shRNA vector (left column) or one of two shRNA targeting *SSeCKS* (sh*SSeCKS*-C and sh*SSeCKS*-B, right columns).

4.6 Discussion

4.6.1 Strategies for positive selection RNAi screening

In this study I outlined a positive selection shRNA screen designed to discover novel regulators of Ikaros-mediated cell cycle arrest. I opted for a pooled screening approach (barcode screening) in a fibroblast system in which cell cycle withdrawal was enforced by ectopic *Ikzf1* expression. Pooled screening offers the advantage of scale, allowing the interrogation of thousands of genes that may contribute towards a phenotype of interest at a relatively low cost. This is in contrast to array based screening that would require high throughput equipment to acquire the same depth of coverage (Campeau and Gobeil, 2011). One major consideration with pool based screening is the requirement to isolate or select the phenotype of interest above background noise. Therefore it is essential to maximise the signal-to-noise ratio to ensure the detection of robust and reproducible results.

Here I described a preliminary screen in fibroblasts using the inducible Ikaros-ERt2 system. The Ikaros-ERt2 system has been employed previously to characterise the Ikaros-regulated gene expression program in B3 cells (Ferreiros-Vidal *et al.,* 2013). The advantage of using this system is that Ikaros activity can be precisely timed by the addition of the ERt2 ligand 4-OHT, allowing the interrogation of Ikaros regulated genes at early time points after induction (Ferreiros-Vidal *et al.,* 2013). At later time points this system is not ideal as cells begin to escape Ikaros-mediated repression after 5-6 days in culture (figure 3.4). Furthermore this system requires extensive 4-OHT treatment over the time course of the experiment, potentially stressing the cells and biasing the results of the screen. One example of this is the enrichment of multiple shRNA targeting ATP binding cassette (ABC) transporters, which are known to bind and transport 4-OHT (Iusuf *et al.,* 2011). The resultant background noise of the experiment prevented robust detection of positive control shRNA targeting *Ikzf1* (figure 4.2B). I therefore implemented a new optimised protocol using an *Ikzf1* overexpression vector that lacked the ERt2 domain. The disadvantage of using this construct is that I lose precise control over the timing of Ikaros

nuclear translocation. This does not impact my screen because I am selecting for shRNA escapees over a long time period that are unaffected by the precise timing of Ikaros induction. This potential disadvantage is also outweighed by the stronger and more persistent arrest in response to the introduction of the MSCV-*Ikzf1* construct into the cells. The change in experimental approach was vindicated by the greatly improved enrichment of positive control shRNA targeting *Ikzf1*, with 3 out of 4 appearing in the top 4 most highly enriched hits (figure 4.7).

I implemented an analysis pipeline designed to detect significantly enriched hits and eliminate false positives. Following this analysis I identified a total of 435 'day 0 corrected' hits, of which *SSeCKS* was the most highly enriched. SSeCKS has previously been shown to arrest fibroblasts at the G1/S transition and is involved in the suppression of malignancy in an array of cell types (Gelman, 2010). It is also a direct transcriptional target of Ikaros in pre-B cells and is upregulated in response to *Ikzf1* overexpression (Ferreiros-Vidal *et al.,* 2013). Mining of microarray data in B cell precursors revealed that the gene expression pattern of *SSeCKS* correlated with *Ikzf1* and *Ikzf3* expression, culminating in a large upregulation in expression at the transition into the resting pre-B cell stage (FrD) and exit the cell cycle (figure 4.9&4.10). Knockdown of *SSeCKS* resulted in an increase in proliferation of Ikaros-arrested fibroblasts. Thus it appears that SSeCKS may be a novel regulator of Ikaros growth arrest.

In order to roughly characterise the nature of the remaining hits I assigned each hit as 'bound by Ikaros' or 'not bound by Ikaros' based on Chip-seq data obtained from B3 cells (Ferreiros-Vidal *et al.,* 2013). My rational was that genes bound by Ikaros in B3 cells were likely to be potential targets of regulation by Ikaros in fibroblasts, and thus likely to be involved in Ikaros-induced cell cycle arrest. Evidence for this idea comes from the observation that the most enriched hits were more likely to be bound by Ikaros in B3 cells than not bound (figure 4.8D). However the majority of hits are not bound by Ikaros in B3 cells (figure 4.8A) meaning that this strategy is not sufficient on its own to identify hits involved in the regulation of Ikaros-induced cell cycle arrest. It is possible that many of the

hits that escape Ikaros-mediated cell cycle arrest may not be regulated by Ikaros directly. It is likely that many layers of regulation converge to enforce the quiescent phenotype, with many of these regulators acting downstream of Ikaros in a knock on effect. Therefore it is too simplistic and restrictive to focus on direct targets of Ikaros regulation only. In addition to transcriptional regulation, other ways to identify hits would be to look at differential expression during pre-B cell development, mine the literature for relevant functions pertaining to proliferation, cell cycle and malignancy, and to look for possible co-localisation and interactions between Ikaros and the potential hits. Some potentially promising candidates have been identified in this fashion. As discussed earlier, components of the SWI/SNF chromatin remodelling complex have been identified in this screen. This complex has previously been linked to G1 progression and physically associates with Ikaros in lymphocytes (Kim *et al.,* 1999; Ruijtenberg and van den Heuvel, 2015). Another enriched hit, Tob2, is part of a family of anti-proliferative proteins that regulate G1/S progression. Overexpression of Tob2 in 3T3 cells results in withdrawal from the cell cycle at the G1/S checkpoint (Ikematsu *et al.,* 1999). Ikaros can bind to the promoter of *Tob2* in B3 cells (Ferreiros-Vidal *et al.,* 2013) and its expression is slightly increased at the transition into the resting pre-B cell stage (FrD) (Immgen.org). Despite ruling out many hits targeting the proteasome through the day 0 normalisation, 6 significantly enriched hits still remain. It is possible that the proteasome is indirectly required for Ikaros-mediated arrest by degrading positive regulators of the cell cycle. Ubiquitin-mediated proteasomal degradation by ubiquitin ligase complexes such as SCF can control the level of cell cycle regulators, ensuring unidirectionality of the cell cycle (Basserman *et al.,* 2014). Cul1, a member of the SCF ubiquitin ligase complex alongside SKP, is also enriched in my screen. There are potentially many more candidates that may be revealed with a detailed secondary screen.

4.6.2 Secondary screening

It is important to conduct a rigorous secondary screening process to verify potentially promising hits. There are several potential ways in which these screens can be performed (Mohr *et al*., 2014). One approach is to repeat the positive selection screen in another cell

type, preferably in cells in which Ikaros is endogenously expressed such as B3 cells. This approach is hampered by the apparent resistance of the B3 cell line to lentiviral infection, making it difficult to transduce the lentiviral library at an appropriate MOI (data not shown). A potential alternative to the B3 cell line would be to repeat the screen in wild type or Abelson virus-transformed primary pre-B cells that overexpress the MSCV-*Ikzf1* construct. The main advantage of this type of screen is that it would be conducted in a physiologically relevant context related to pre-B cell development. Hits that overlap between these different cell types would be promising targets for further investigation.

A candidate-based approach may be employed to validate the results in fibroblasts by individually targeting potential hits based on the published literature. The disadvantage to this approach is that it is time consuming and requires the extensive design and cloning of individual shRNA against many potential targets. Potential candidates may also be missed if they have not been characterised as cell cycle regulators. Alternatively an unbiased pooled shRNA screen may be employed with a custom library targeting the 435 previously identified hits. Another approach is to conduct a single well array-based screen utilising siRNA targeting these hits. This could be coupled with live cell imaging throughout the time course to visualise cellular proliferation in a high-throughput manner (Flaberg *et al.,* 2011). For the sake of simplicity and to reduce off target 'passenger' hits, I conducted the RNAi screen at a low MOI to ensure that on average each cell contained a single shRNA. This approach may miss potential redundancies or synergistic effects between two or more genes that contribute to the proliferative phenotype (Mohr *et al.,* 2014). To investigate this possibility, I could repeat the screen again in fibroblasts with a higher MOI to ensure that each cell contains two or more shRNA.

Chapter 5

Ikaros and SSeCKS regulate the cell cycle

5.1 Introduction

As described in chapter 4, an shRNA screen identified the scaffolding protein SSeCKS as a factor that contributes to the regulation of the cell cycle by Ikaros. The expression of *AKAP12*/*GRAVIN*, the human homologue of *SSeCKS*, is downregulated in an array of solid and haematological tumours (reviewed in Gelman, 2010). In myeloid malignancies *AKAP12* is epigenetically silenced by promoter methylation (Flotho *et al.,* 2007). SSeCKS is believed to act as a tumour suppressor by attenuating proliferation and metastasis (Gelman, 2012). In murine fibroblasts SSeCKS is able to scaffold cyclin D1 and sequester it in the cytoplasm, thereby preventing cyclin D1 nuclear translocation and G1/S progression (Lin *et al.,* 2000; Lin and Gelman, 2002). SSeCKS can also downregulate *Ccnd1* expression through the attenuation of serum-induced ERK2 activation (Lin *et al.,* 2000). *SSeCKS* null MEFs exhibit elevated basal and serum-induced ERK activation, serum-induced proliferation rates and demonstrate an enhanced susceptibility to transformation by *Ras* and *Src* oncogenes (Akakura *et al.,* 2010). In addition to cyclins, SSeCKS can interact with a number of signalling molecules such as protein kinase (PK) A, PKC, Calmodulin, Actin and Src (Gelman, 2012; Akakura and Gelman, 2012). SSeCKS is thought to regulate the activity and spatiotemporal localisation of these molecules to influence the cell cycle, cytoskeleton, adhesion and migration (Gelman, 2010). Though SSeCKS localisation is predominantly cytoplasmic, it is able to regulate downstream gene expression changes through its interaction with these signalling molecules to promote cell cycle withdrawal (Liu *et al.,* 2006).

The expression of *SSeCKS* is regulated by Ikaros in pre-B cells (Ferreiros-Vidal *et al.,* 2013) and correlates with cell cycle withdrawal at the small resting pre-B cell stage (frD) (Immgen.org, figure 4.9). This suggests a potential role for SSeCKS in the regulation of B cell development by cooperating with Ikaros to enforce G1 arrest at the resting pre-B cell stage.

I therefore wanted to further explore the regulation of the cell cycle by SSeCKS. This chapter investigates the transcriptional regulation of *SSeCKS* by Ikaros in pre-B cells and fibroblasts, and begins to explore the potential mechanisms of Ikaros and SSeCKS-mediated cell cycle arrest. I utilised a fibroblast cell line that contained a doxycycline-inducible *SSeCKS* construct to study the regulation of the cell cycle by SSeCKS. I performed RNAseq on cells that were induced to arrest by Ikaros or SSeCKS. This enabled me to characterise genes that were specifically regulated by Ikaros, SSeCKS, or both. The insights gained from this analysis may be applied to pre-B cells to deepen our understanding of the role of Ikaros and SSeCKS in the regulation of the cell cycle and B cell development.

The bioinformatic analyses in this chapter were performed by Gopu Dharmalingam.

5.2 SSeCKs is transcriptionally regulated by Ikaros in pre-B cells and fibroblasts

Having demonstrated that knockdown of *SSeCKS* can override Ikaros-induced cell cycle arrest in fibroblasts, I began to explore whether *SSeCKS* is a transcriptional target of Ikaros. My hypothesis was that Ikaros induces the upregulation of *SSeCKS* expression, and that SSeCKS cooperates with Ikaros to enforce cell cycle arrest. Knockdown of *SSeCKS* would prevent this upregulation, thereby permitting the cells to proliferate.

I began by confirming that Ikaros can transcriptionally regulate *SSeCKS* expression in B3 cells. Microarray analysis in B3 cells has shown that there is a small upregulation in *SSeCKS* mRNA expression following 6 hours of Ikaros induction, with a larger increase seen at 48 hours post induction (Ferreiros-Vidal *et al.,* 2013). I performed qPCR analysis using cDNA prepared from B3 cells in which Ikaros-ERt2 was induced for 6, 16 and 24 hours (figure 5.1A). In agreement with the microarray analysis both primary and mature *SSeCKS* transcripts were upregulated after 6 hours of Ikaros-ERt2 induction. This upregulation persisted at later time points and the largest increase was observed at 24 hours post-

induction, suggesting that *SSeCKS* mRNA expression correlated with cell cycle withdrawal in these cells. Next I looked at SSeCKS protein expression in these cells. The induction of Ikaros-ERt2 by 4-OHT treatment resulted in a noticeable increase in SSeCKS protein expression by 16 hours and a further increase at the 24 hour time point (figure 5.1B). SSeCKS protein has been shown previously to migrate as a doublet in western blots (Streb *et al.,* 2004). The top band corresponds to the alpha protein isoform and the bottom band corresponds to the beta and gamma isoforms. The alpha and beta isoforms of SSeCKS are ubiquitously expressed, but the gamma isoform is restricted to the testes (Camus *et al.,* 2001). Figure 5.1B shows that both the upper and lower bands increased in intensity, meaning that there was an elevated expression of the alpha and beta isoforms of SSeCKS following Ikaros induction.

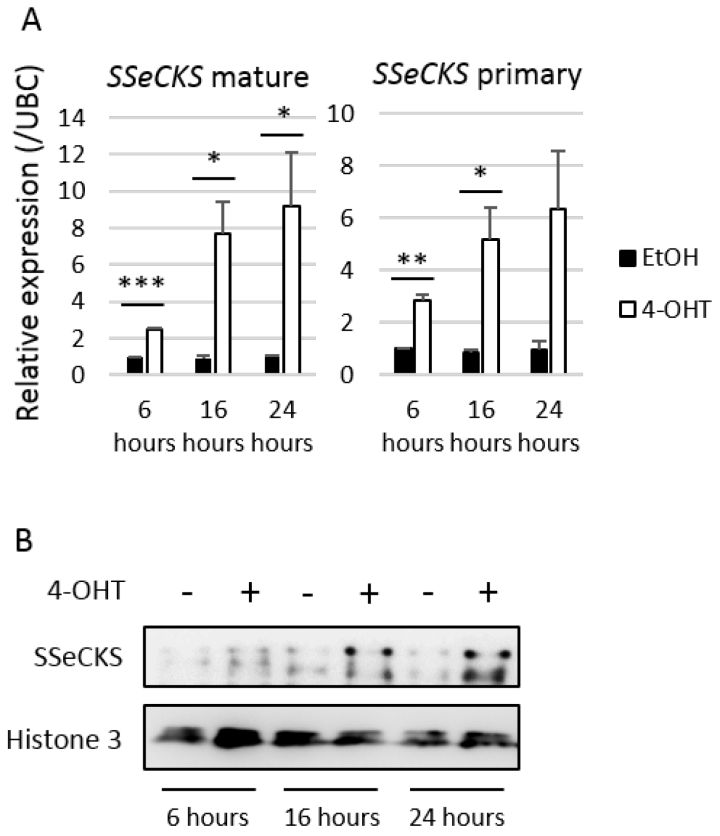

Figure 5.1 – Ikaros upregulates *SSeCKS* expression in pre-B cells. (A) qPCR analysis of *SSeCKS* expression in Ikaros-ERt2 expressing B3 cells treated with EtOH (Black bars) or 4-OHT (White bars) for 6, 16 and 24 hours (Mean+SE; N=3, student T test: * p<0.05 **p<0.01 *** p<0.001). (B) Western blot showing SSeCKS protein expression in B3 cells treated with EtOH (-) or 4-OHT (+). An anti-histone 3 antibody was included as a loading control.

Having confirmed that Ikaros transcriptionally regulated the expression of *SSeCKS* in B3 cells, I went on to investigate if this regulation was preserved in fibroblasts. Figure 5.2A confirms that *SSeCKS* mRNA expression was significantly upregulated after 24 hours of Ikaros-ERt2 induction in 3T3 cells, though the extent of this upregulation was less than in B3 cells (figure 5.1A). This upregulation was Ikaros dependent, as shRNA knockdown of *Ikzf1* abrogated the increase in *SSeCKS* mRNA expression (figure 5.2B). In accordance with the upregulated transcript, SSeCKS protein expression was increased after 24 hours of Ikaros induction (figure 5.2C). In contrast to B3 cells there was no discernible increase in *SSeCKS* transcript at the 6 hour time point, suggesting slower kinetics of induction in fibroblasts. There was also no increase in SSeCKS protein at this time point (data not shown). It would be useful to investigate a series of time points to more thoroughly track the kinetics of SSeCKS mRNA and protein induction in fibroblasts.

As discussed in chapter 3, Ikaros and Myc often display mutual antagonism in the regulation of gene expression. I therefore decided to investigate the regulation of *SSeCKS* transcription by these two factors. Figure 5.2D shows that *SSeCKS* transcription in fibroblasts was repressed after 24 hours of Myc-ERt2 induction by 4-OHT treatment. Induction of Ikaros and Myc together resulted in no significant changes in *SSeCKS* expression suggesting that Myc is able to override Ikaros-induced *SSeCKS* upregulation. This is consistent with the repression of *SSeCKS* transcription reported in *Myc*-transformed 3T3 fibroblasts (Lin *et al.,* 1995).

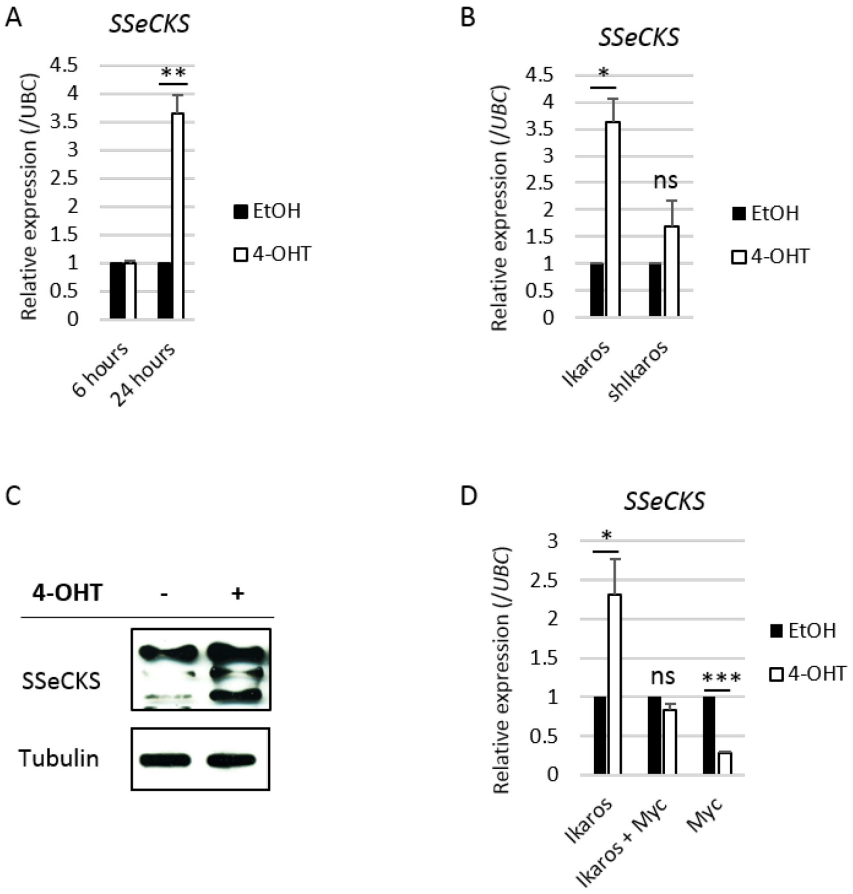

Figure 5.2 – Ikaros regulates the expression of *SSeCKS* in fibroblasts. (A) qPCR analysis of the expression of the mature transcript of *SSeCKS* in 3T3 cells expressing Ikaros-ERt2, treated with EtOH (black bars) or 4-OHT (white bars) for 6 and 24 hours. (B) qPCR analysis of *SSeCKS* expression in 3T3 cells after 24 hours of EtOH or 4-OHT treatment in the presence of an shRNA targeting *Ikzf1* (sh*Ikzf1*-D). (C) Western blot analysis of SSeCKS protein expression in 3T3 cells after treatment with EtOH (-) or 4-OHT (+) for 24 hours. Tubulin was used as a loading control. (D) qPCR analysis of *SSeCKS* expression after 24 hours of EtOH or 4-OHT treatment, in 3T3 cells expressing Ikaros-ERt2, Myc-ERt2, or a combination of the two. (Mean+SE; N=3, student T test: * p<0.05 **p<0.01 *** p<0.001)

It is unclear at this time if Ikaros and Myc are directly competing at the promoter of *SSeCKS* to control its expression. Genome wide mapping of Myc binding in mouse 3T9 fibroblasts by ChIP-seq failed to identify peaks around the *SSeCKS* promoter (defined as +/- 1000bp from the TSS) (Perna *et al.,* 2012). Similarly, supershift electrophoretic mobility assays (EMSA) performed with a c-Myc antibody failed to detect Myc binding at the alpha promoter of *SSeCKS* (Bu and Gelman, 2007). This suggests that *SSeCKS* repression may be a downstream effect of Myc activity.

Genome wide mapping of Ikaros binding in B3 cells by ChIP-seq revealed several peaks in around the promoter of *SSeCKS* (figure 5.3A) implying that *SSeCKS* is a direct transcriptional target of Ikaros (figure 5.3A) (Ferreiros-Vidal *et al.,* 2013). This binding occurs upstream of exon1a, corresponding to the promoter of the alpha isoform of SSeCKS (Bu and Gelman, 2007). To verify that Ikaros binds directly to the *SSeCKS* promoter in fibroblasts, I performed chromatin immunoprecipitation followed by qPCR (ChIP-qPCR) using Ikaros-ERt2 expressing 3T3 cells treated for 24 hours with 4-OHT. I enriched for Ikaros-bound chromatin fragments by immunoprecipitating with an Ikaros specific antibody, or an anti-IgG antibody as a control. For the qPCR I used forward and reverse primers that amplified a previously identified Ikaros peak at the promoter of *SSeCKS* in B3 cells (figure 5.3A – marked F1 and R1). Figure 5.3B shows the relative enrichment of Ikaros-bound chromatin fragments over 1% of input. There was a significant increase in chromatin enrichment at the *SSeCKS* promoter when the pulldown was performed using the Ikaros antibody versus IgG control. This enrichment was comparable to several positive control regions around the promoters of the Ikaros regulated genes, *Myc* and *Igll1.* A negative control was included at a region downstream of *Igll1*, which is not bound by Ikaros in B3 cells. In conclusion, Ikaros binds directly to the promoter of *SSeCKS* to regulate its expression in pre-B cells and fibroblasts.

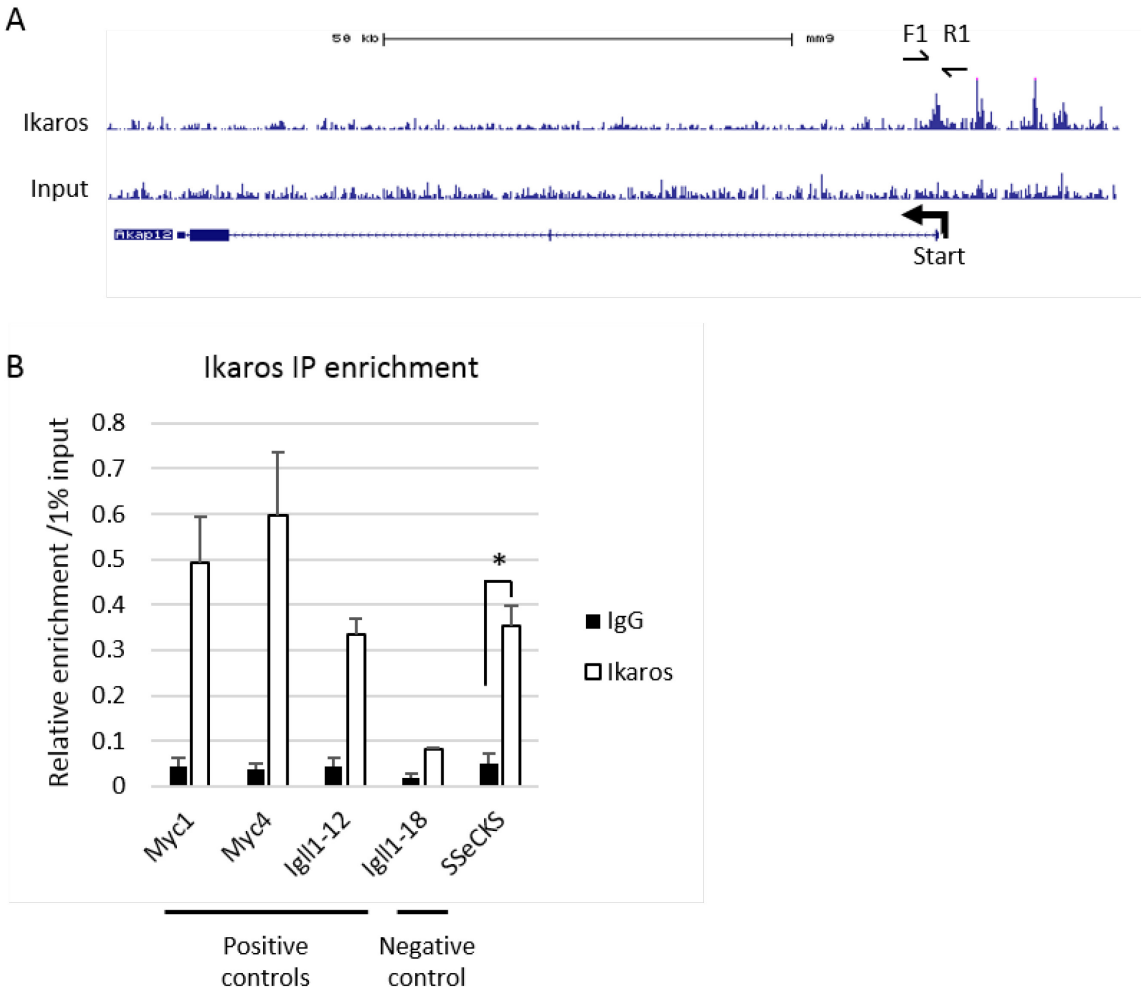

Figure 5.3 – Ikaros binds to the promoter of *SSeCKS* in pre-B cells and fibroblasts. (A) Ikaros chip-seq tracks in B3 cells around the promoter of *SSeCKS* (*Akap12*). Ikaros peaks were detected at the promoter of *SSeCKS* when Ikaros-ERt2 expressing cells were treated with 4-OHT (top track), but not in empty vector transfected cells (Input, bottom track). The scales for each track were set to the same value for comparison. F1 and R1 refer to the approximate primer positions (not to scale) used to verify Ikaros binding in fibroblasts. (B) qPCR analysis on chromatin immunoprecipitated using a control (black) or anti-Ikaros antibody (white) in Ikaros-ERt2 expressing 3T3 cells treated for 24 hours with 4-OHT. The relative enrichment of these fragments over 1% of input chromatin was plotted. Primers used to amplify positive and negative control regions are labelled accordingly. Standard deviation around the mean; N=2, student T test: * $p<0.05$

5.3 No observed binding between SSeCKS and cyclin D

In the previous analyses I demonstrated that *SSeCKS* is an Ikaros-regulated gene in pre-B cells and fibroblasts. The expression of *SSeCKS* appeared to correlate with cell cycle withdrawal, suggesting a role for SSeCKS in the regulation of the cell cycle by Ikaros. I therefore began to explore the potential mechanisms of cell cycle regulation by SSeCKS. *SSeCKS* overexpression in fibroblasts results in the transcriptional repression of *Ccnd1* and sequestration of cyclin D1 protein in the cytoplasm (Lin *et al.,* 2000). Direct binding of cyclin D1 to SSeCKS in these cells was shown by pulldown assay (Lin and Gelman, 2002). I hypothesised that the Ikaros-induced upregulation of SSeCKS protein would facilitate the sequestration of cyclin D in the cytoplasm. This may prevent cyclin D-Cdk4/6 complex formation and account for cell cycle arrest in G1/G0. As *Ikzf1* expression is primarily restricted to haematopoietic lineages, I wished to investigate this hypothesis in pre-B cells. To this end I treated B3 cells that expressed the Ikaros-ERt2 construct for 24 hours with EtOH or 4-OHT. I prepared lysates from these cells and immunoprecipitated (IP) with an anti-SSeCKS antibody or control IgG antibody. To detect SSeCKS pulldown I performed a western blot on the immunoprecipitated protein (figure 5.4A). SSeCKS protein was enriched after pulldown with an anti-SSeCKS antibody compared with input and was absent from the IP using the control antibody. Cyclin D1 is not expressed at an appreciable level in B3 cells (as confirmed by western blot, supplementary figure S.5), so I checked the presence of the two other cyclin D isoforms. Both cyclin D2 and cyclin D3 were detected in the input samples (figure 5.4A) but neither protein was detected after immunoprecipitation. It is unclear at this time if this negative result means that SSeCKS does not associate with cyclin D2/3 in pre-B cells, or if there were technical issues with the immunoprecipitation.

Given the previous result, I tried to observe possible SSeCKS-cyclin D association in an indirect way. In collaboration with Dr. Ziwei Liang, we investigated the cellular localisation of cyclin D3 by fractionation followed by western blot. B3 cells expressing Ikaros-ERt2 were treated for 6 hours with EtOH or 4-OHT and separated into cytoplasmic and nuclear fractions. If SSeCKS sequesters cyclins, we would expect to observe cyclin D protein in the

cytoplasmic fraction. Figure 5.4B shows that cyclin D3 protein was exclusively localised in the nucleus and was not detectable in the cytoplasmic fractions. This localisation was unaffected by Ikaros induction by 4-OHT treatment. Similar results were obtained using an anti-cyclin D2 antibody (data not shown). These results do not exclude a possible association between SSeCKS and cyclin D in pre-B cells, but at this time I do not observe any direct binding between SSeCKS and cyclin D proteins.

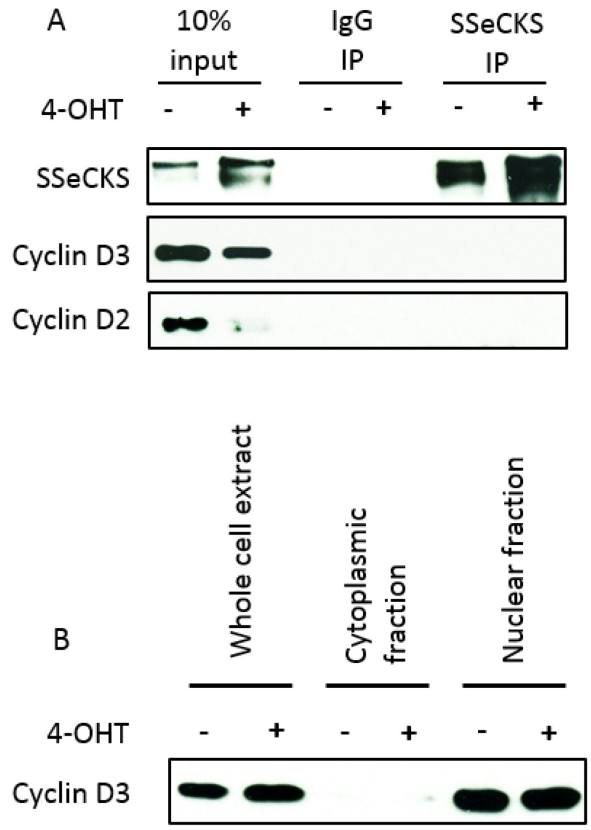

Figure 5.4 – No observed binding between cyclin D and SSeCKS. (A) Western blot analysis on lysates acquired from B3 cells expressing Ikaros-ERt2 treated for 24 hours with EtOH (-) or 4-OHT (+). The lysates were immunoprecipitated with an anti-SSeCKS antibody, or anti-IgG as a negative control. Input samples were loaded at 10% of the IP volume as a positive control. Antibodies for SSeCKS, cyclin D3 and cyclin D2 were used to detect the presence of these proteins after IP. (B) B3 cells expressing Ikaros-ERt2 were treated for 6 hours with EtOH or 4-OHT and fractionated into cytoplasmic or nuclear fractions. An anti-cyclin D3 antibody was used to detect its cellular localisation. Successful fractionation was tested by control experiments performed by Dr. Ziwei Liang. Tubulin was used as a cytoplasmic control and histone H3 was included as a nuclear control (data not shown).

5.4 *SSeCKS* overexpression in fibroblasts results in G1 arrest

As the expression of *SSeCKS* appeared to correlate with cell cycle withdrawal (figure 5.1 and 5.2) I wanted to test whether *SSeCKS* was sufficient to induce cell cycle arrest independently of Ikaros. To this end I attempted to overexpress *SSeCKS* in fibroblasts and pre-B cells. I

cloned *SSeCKS* cDNA into an MSCV-GFP vector and generated retrovirus to infect the target cells. No GFP expression was detected by flow cytometry in B3 cells or 3T3 fibroblasts (data not shown). The open reading frame of *SSeCKS* is over 5kb long, and this relatively large insert may be approaching the upper packaging limit of retroviral particles (Coffin *et al.,* 1997). Direct transfection of the MSCV plasmid by electroporation and chemical methods also failed to overexpress *SSeCKS* in these cells.

Having failed at directly overexpressing *SSeCKS*, I attempted to induce its expression by indirect means. The promoter of the beta isoform of *SSeCKS* contains a retinoic acid response element (RARE), and treatment of vascular smooth muscle cells with the retinoid all-trans retinoic acid (atRA) results in a moderate induction of *SSeCKS* mRNA and protein (Streb *et al.,* 2011). Interestingly atRA treatment has been shown to accelerate pre-B cell differentiation and progression to the resting pre-B cell stage (Chen *et al.,* 2008). I therefore treated pre-B cells with atRA or the vehicle control DMSO, and investigated *SSeCKS* induction by qPCR and the atRA-induced cell cycle profiles by PI staining and flow cytometry. B3 cells appeared unresponsive to atRA treatment (data not shown), so I used primary pre-B cells for the analysis. Treatment of primary pre-B cells with atRA for 24 hours resulted in a small but significant increase in primary *SSeCKS* transcript (figure 5.5A). The atRA target genes *Myc* and *Hoxa1* were included as positive controls for successful atRA induction. PI staining showed an accumulation of cells in G1 phase after 48 hours of atRA treatment that was comparable to Ikaros-ERt2 induction by 4-OHT (supplementary figure S.6). Thus retinoic acid treatment appeared to upregulate *SSeCKS* expression and promote cell cycle withdrawal in pre-B cells, though it was difficult to disentangle SSeCKS-specific effects from the pleiotropic effects of atRA treatment.

I required a stronger system of overexpression to investigate SSeCKS-specific regulation of the cell cycle. I obtained a 3T3 fibroblast cell line that expresses a tetracycline-regulated *SSeCKS* overexpression construct ('S24' cells, a kind gift from Professor Irwin Gelman) (Lin *et al.,* 2000). In this system *SSeCKS* cDNA lies downstream of the tetracycline response element (TRE). These cells were generated by transgene insertion and clonal selection, and

the expression cassette does not replace the endogenous *SSeCKS* gene. In the presence of the tetracycline analogue doxycycline (+Dox) the tetracycline transactivator protein (tTA) is unable to bind to the TRE, thereby preventing *SSeCKS* transactivation. Removal of doxycycline (-Dox) facilitates tTA binding to the TRE and transcription of *SSeCKS* cDNA (figure 5.5B). The removal of doxycycline results in the overexpression of *SSeCKS* and arrests fibroblasts in G1 phase (Lin *et al.,* 2000).

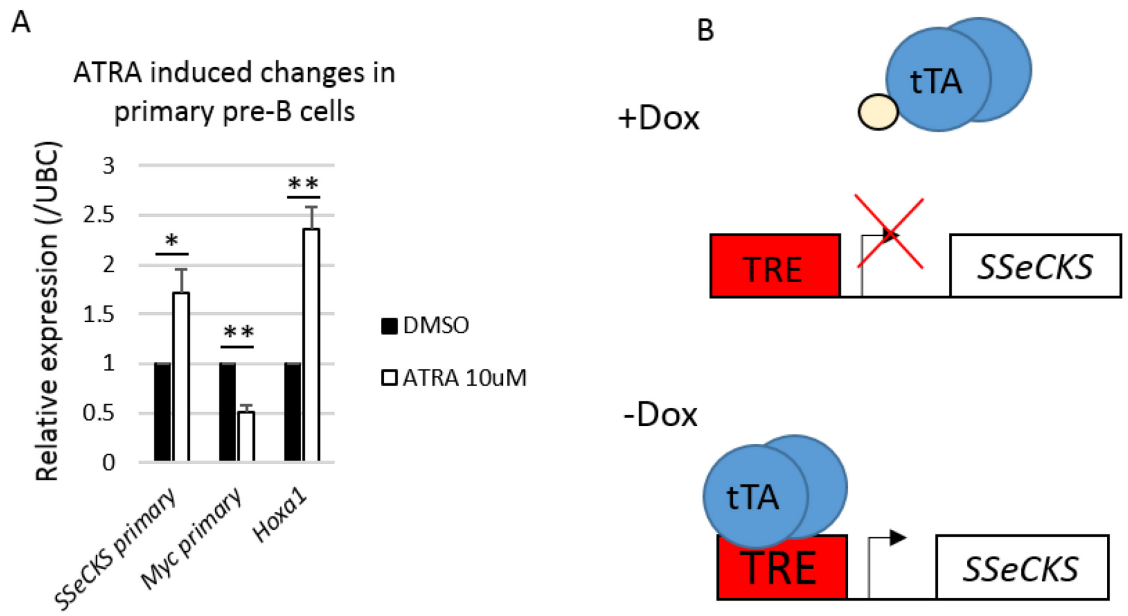

Figure 5.5 – Alternative methods of inducing *SSeCKS* overexpression. (A) qPCR analysis of primary pre-B cells treated for 24 hours with atRA (white bars) or the vehicle control DMSO (black bars). The primary transcripts of *SSeCKS* and *Myc* were measured along with the mature transcript of the positive control gene *Hoxa1* (Mean+SE; N=3, student T test: * p<0.05 **p<0.01). (B) Schematic outline of the TET-off system of *SSeCKS* overexpression in S24 fibroblasts. In the presence of doxycycline (top) tTA is unable to transactivate *SSeCKS* transcription. Removal of doxycycline (bottom) results in tTA dependent SSeCKS transcription. tTA = tetracycline transactivator protein. TRE = tetracycline response element.

I investigated the effect of *SSeCKS* overexpression on the cell cycle by plating S24 cells in the presence or absence of doxycycline for 24 and 48 hours. Removal of doxycycline for 48 hours resulted in a large upregulation of SSeCKS protein (figure 5.6A). At 24 hours post-doxycycline removal there was a noticeable withdrawal from proliferation, as >70% of cells

accumulated in G1 phase (figure 5.6B,C). By 48 hours >80% of cells had accumulated in G1 phase. I visualised the arrest over longer time periods by plating S24 cells in the presence or absence of doxycycline for up to 6 days before staining with crystal violet (figure 5.6D top panel). There was a marked difference in the intensity of the staining between the two conditions, indicating that *SSeCKS* overexpression enforced a sustained withdrawal from the cell cycle. I next attempted to reverse this arrest by shRNA mediated knockdown of *SSeCKS*. shRNA knockdown depleted SSeCKS protein in the presence and absence of doxycycline (figure 5.6E, lanes 2 and 4). However the knockdown failed to completely reverse the proliferative defect observed upon doxycycline withdrawal, as there was still a difference in the intensity of crystal violet staining between the +Dox and –Dox conditions (figure 5.6D, bottom panel). The failure to fully rescue the cell cycle arrest may be because the knockdown was not efficient enough to fully deplete SSeCKS protein. An argument against this is that protein levels were comparable between control ($S24^{+/+}$ +Dox) and knockdown ($S24^{shSSeCKS}$ –Dox) conditions (figure 5.E, lanes 1 and 4 respectively). There was a difference in confluence between these two conditions despite each displaying a similar level of SSeCKS protein (figure 5.6D). An alternative explanation is that post-translational modifications of the SSeCKS protein in conjunction with an elevation in SSeCKS protein expression may play an important role in the regulation of the cell cycle.

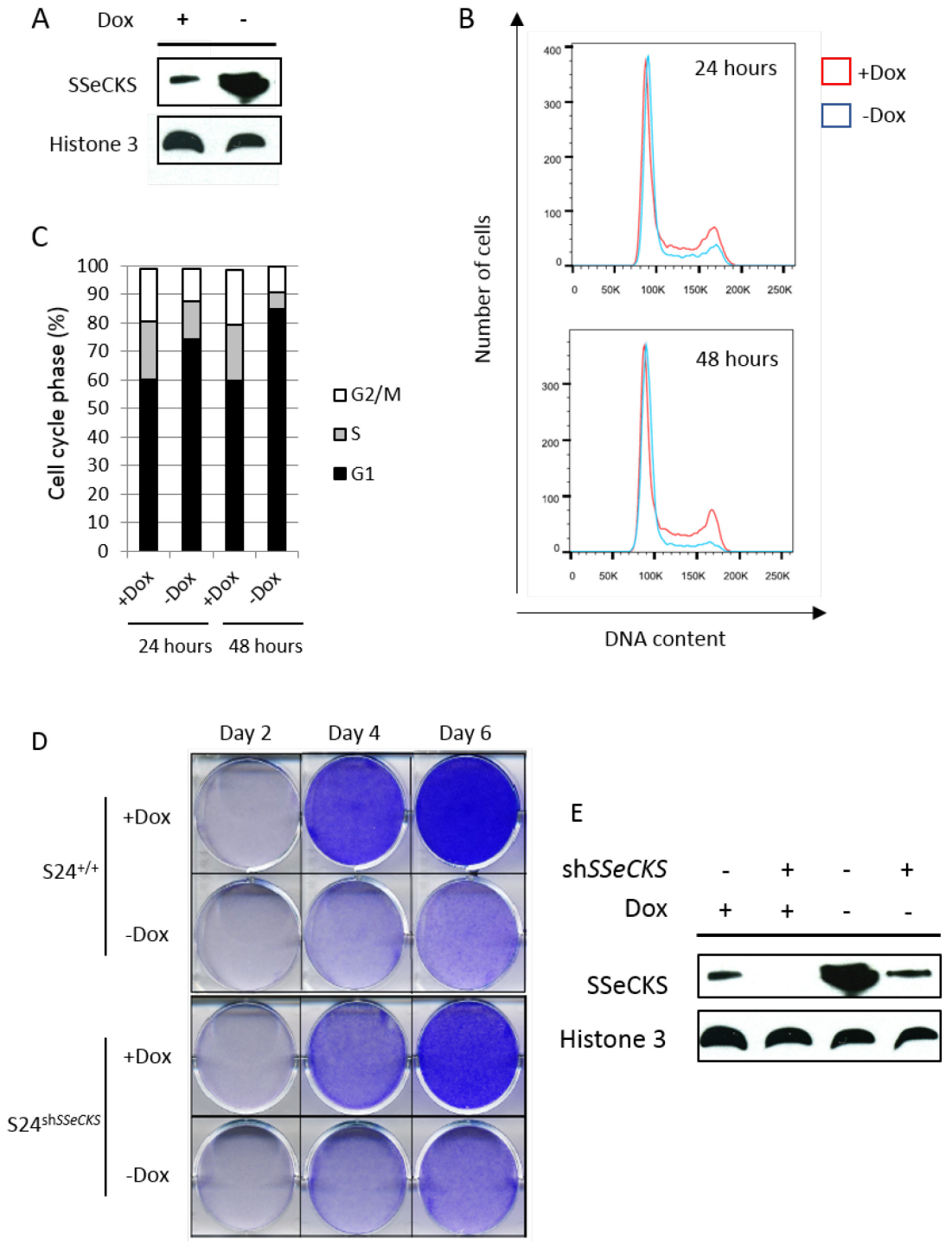

Figure 5.6 – *SSeCKS* overexpression induces G1 arrest in fibroblasts. (A) Western blot showing SSeCKS protein expression in S24 cells grown for 48 hours in the presence (+) or absence (-) of doxycycline (Dox). Histone 3 was used as a loading control. (B) PI staining of S24 cells grown in the presence (red lines) or absence (blue lines) of doxycycline for 24 and 48 hours. (C) Quantification of the cell cycle phases outlined in (B). (D) Colony formation assay of S24 cells grown for up to 6 days in the presence (+) or absence (-) of doxycycline, before staining with crystal violet. The top panel displays the confluency of wild type S24 cells, the bottom panel displays cells transfected with an shRNA targeting *SSeCKS*. (E) Western blot showing SSeCKS protein expression in S24 cells grown for 48 hours in the presence (+) or absence (-) of doxycycline (bottom panel) in wild type (-) or sh*SSeCKS* (+) transduced cells (top panel).

Having demonstrated that SSeCKS regulated the cell cycle, I proceeded to investigate the gene expression changes induced by *SSeCKS* overexpression. S24 cells were plated for 24 hours in the presence or absence of doxycycline and mRNA expression was measured by qPCR (figure 5.7A). *SSeCKS* overexpression instigated gene expression changes that were reminiscent of Ikaros overexpression. The transcription of *Myc* was significantly repressed following *SSeCKS* induction by doxycycline removal. The metabolic genes *Hk2* and *Ldha* were also significantly repressed, consistent with the downregulation of *Myc*. Interestingly *SSeCKS* overexpression upregulated the integrins *Itga5* and *Itgb1*. This is in contrast to the downregulation of these genes observed upon Ikaros induction in fibroblasts (figure 3.5A). The increase in integrin expression is consistent with SSeCKS-induced integrin β1 clustering observed in prostate cancer cells (Su *et al.,* 2013). *SSeCKS* expression results in enhanced adhesion in these cells and is hypothesised to be important in the suppression of metastasis (Su *et al.,* 2013).

I next looked at the protein levels of several cell cycle regulators following *SSeCKS* overexpression (figure 5.7B). In accordance with the reduction in *Myc* transcript, *SSeCKS* overexpression resulted in the depletion of Myc protein from these cells. Unexpectedly there appeared to be an increase in the amount of cyclin D2 protein expressed following doxycycline withdrawal. This is contrary to the reduction of cyclin D2 we would expect to observe in cells that are withdrawing from the cell cycle. A possible explanation for this result may be that SSeCKS is directly binding cyclin D2 and sequestering it in the cytoplasm. This may have the effect of stabilising cyclin D2 protein but preventing its nuclear localisation.

These results show that *SSeCKS* overexpression is sufficient to induce cell cycle withdrawal in fibroblasts independently of Ikaros. SSeCKS induces a similar, yet distinct gene expression signature to that of Ikaros. Interestingly SSeCKS and Ikaros both regulate the expression of *Myc*, further implicating this gene as a predominant target in the regulation of the cell cycle by Ikaros.

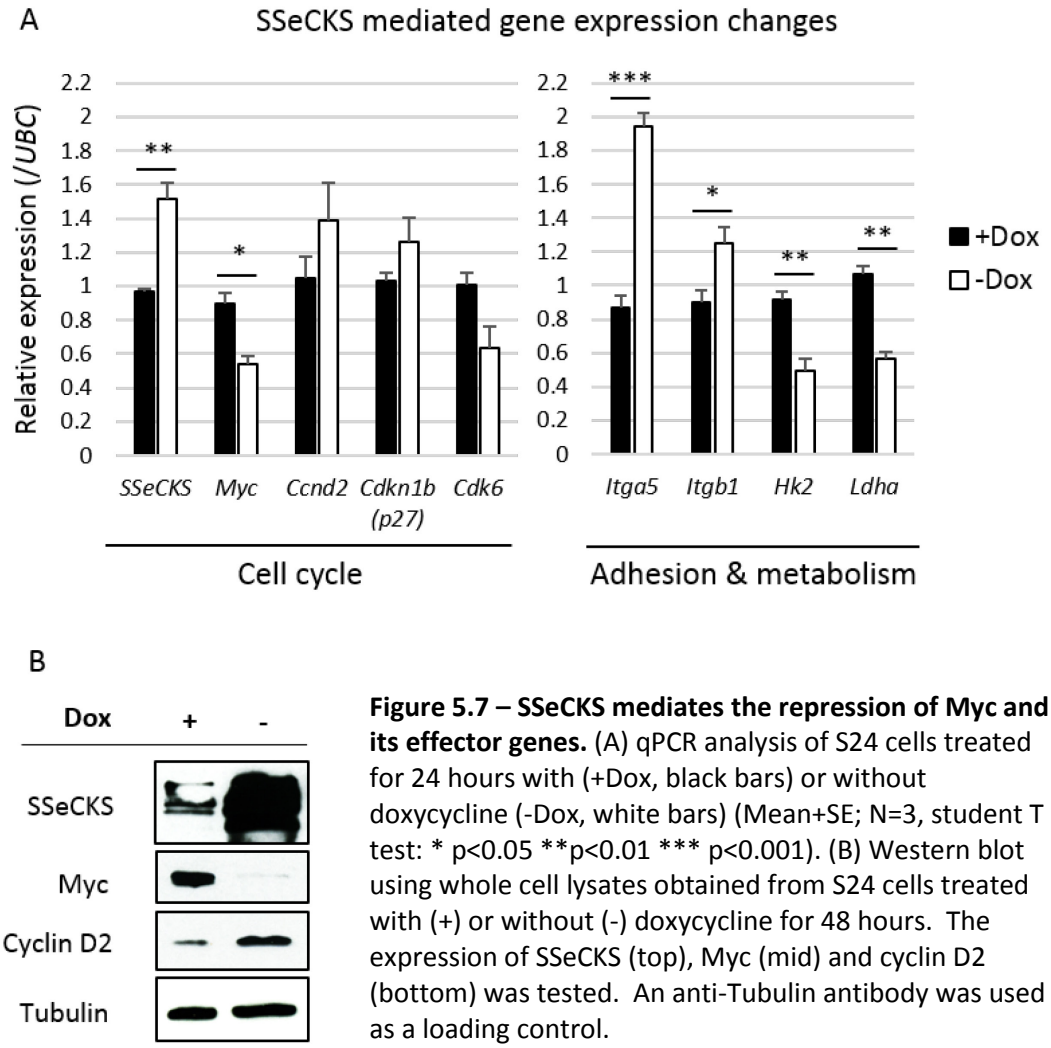

Figure 5.7 – SSeCKS mediates the repression of Myc and its effector genes. (A) qPCR analysis of S24 cells treated for 24 hours with (+Dox, black bars) or without doxycycline (-Dox, white bars) (Mean+SE; N=3, student T test: * $p<0.05$ ** $p<0.01$ *** $p<0.001$). (B) Western blot using whole cell lysates obtained from S24 cells treated with (+) or without (-) doxycycline for 48 hours. The expression of SSeCKS (top), Myc (mid) and cyclin D2 (bottom) was tested. An anti-Tubulin antibody was used as a loading control.

5.5 Ikaros and SSeCKS synergistically arrest the cell cycle

The previous results indicate that both Ikaros and SSeCKS can enforce G1 arrest partly through the repression of *Myc.* I was interested whether Ikaros and SSeCKS could synergistically arrest the cell cycle by converging at the level of *Myc* regulation. To this end I transduced S24 cells with the inducible Ikaros-ERt2 construct and treated with a combination of doxycycline and 4-OHT. The control treatment of doxycycline plus EtOH (+Dox +EtOH) would result in no overexpression of *SSeCKS* or Ikaros nuclear translocation, and consequently the cells would display wild type proliferation. Treatment with doxycycline plus 4-OHT (+Dox +4-OHT) would induce Ikaros translocation but not *SSeCKS*

expression. Treatment without doxycycline plus EtOH (-Dox +EtOH) would induce *SSeCKS* overexpression only. Treatment without doxycycline plus 4-OHT (-Dox +4-OHT) would both induce Ikaros translocation and *SSeCKS* overexpression in the same cells (figure 5.8A). I hypothesised that Ikaros and *SSeCKS* overexpression together would result in a greater arrest of the cell cycle than either condition alone. S24 cells expressing the inducible Ikaros-ERt2 construct were treated with the 4 conditions for 24 hours and the cell cycle profiles were determined by PI staining and flow cytometry (figure 5.8B,C). Control treated cells (+Dox +EtOH) proliferated normally as 60% of cells exhibited DNA content indicative of G1 phase. The induction of Ikaros or *SSeCKS* alone resulted in cell cycle arrest, as 75% and 70% of cells were in G1 phase respectively. When Ikaros and *SSeCKS* were induced together there was an even greater arrest, as >80% of cells were in G1 phase. This was significantly different from either condition alone. In conclusion Ikaros and SSeCKS can cooperate to synergistically arrest the fibroblast cell cycle.

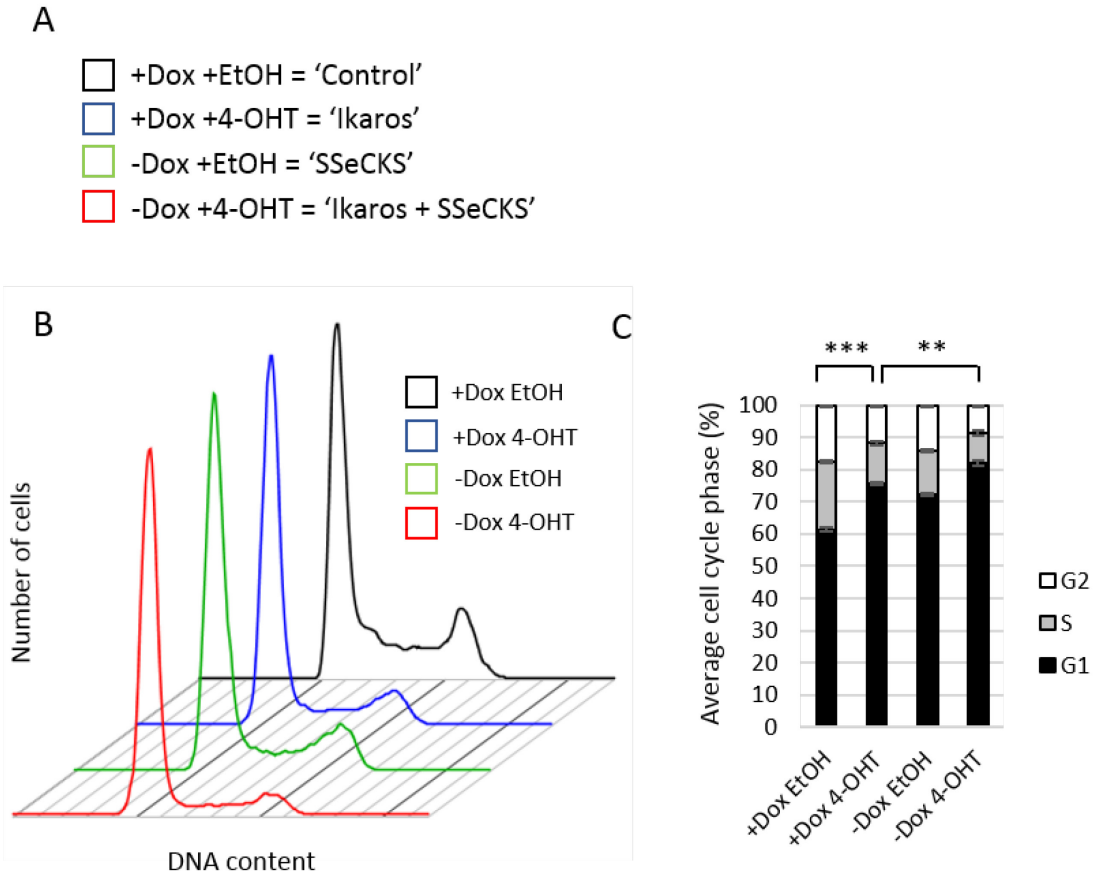

Figure 5.8 – Ikaros and SSeCKS cooperate to enforce G1 arrest. (A) Schematic outlining the 4 treatment conditions. Withdrawal of doxycycline induces *SSeCKS* expression and addition of 4-OHT induces Ikaros-ERt2 translocation into the nucleus. (B) Flow cytometry plots of cells stained with PI after 24 hours of each treatment condition. The cell cycle profiles of control (black), Ikaros (blue), *SSeCKS* (green) and Ikaros + *SSeCKS* (red) treatments are displayed. (C) Quantification of the cell cycle profiles displayed in (B) from 3 technical replicates. (Mean+SE; N=3, student T test: **p<0.01 *** p<0.001)

I examined the gene expression changes that occurred after treatment with the 4 conditions for 24 hours (figure 5.9A). Ikaros (+Dox +4-OHT, blue bars) upregulated the expression of *SSeCKS* and the cell cycle inhibitor *Cdkn1b*, and repressed the transcription of *Myc, Hk2* and *Ldha*. SSeCKS (-Dox +EtOH, green bars) repressed primary and mature Myc transcripts, though to a lesser extent than Ikaros. SSeCKS had no effect on *Cdkn1b* expression, indicating that this is an Ikaros-specific target gene. SSeCKS appeared to downregulate *Cdk6* expression independently of Ikaros. Thus it seems that Ikaros and SSeCKS have distinct and overlapping target genes that are coordinated to regulate G1 arrest. Looking at metabolic gene expression, the extent of *Hk2* and *Ldha* repression by SSeCKS correlated with the reduction in *Myc* transcript (around 50% reduction in all cases). This suggested that SSeCKS regulates the expression of these two genes through *Myc*. SSeCKS did not significantly upregulate the expression of *Itga5*. This is in contrast to the significant upregulation of *Itga5* observed in figure 5.7A. A possible explanation for this discrepancy may be that the Ikaros-ERt2 system is slightly 'leaky', meaning some Ikaros nuclear translocation may occur in the absence of 4-OHT. If this is the case then Ikaros could antagonise the SSeCKS-induced upregulation of *Itga5*. I can test this hypothesis by visualising Ikaros localisation in these cells by immunofluorescence under the 4 treatment conditions.

Unexpectedly I observed no upregulation in SSeCKS transcript following the removal of Doxycyline, despite a large and significant upregulation in SSeCKS protein (seen in figure 5.6A). It is possible that the primer set used to detect *SSeCKS* expression is complementary to the endogenous transcript present in these cells, and not the overexpressed transgene. It is unlikely that I am detecting specific isoforms of *SSeCKS* as the primers anneal to the 3' of the transcript, which is present in all isoforms. It may be necessary to design primers that specifically anneal to the overexpressed transgene to rectify this issue.

I next looked at the effect of Ikaros and *SSeCKS* induction together (Figure 5.9A -Dox +4-OHT, red bars). The combined effect of Ikaros and SSeCKS resulted in a highly significant repression of *Myc* transcript that was consistent with the synergistic cell cycle arrest observed in figure 5.8B. *Myc* transcription was significantly more repressed by this combined treatment than by Ikaros or SSeCKS alone. Thus Ikaros and SSeCKS both regulate the cell cycle and converge at the level of *Myc* transcription. Looking at other cell cycle genes, Ikaros and SSeCKS together downregulated the expression of *Ccnd2* to a small extent. There was no observed synergy in the expression of *Cdkn1b* or *Cdk6*, indicating that these genes were independently regulated by Ikaros and SSeCKS respectively. There was a small synergy observed in the expression of *Hk2* and *Ldha* as these genes were slightly more downregulated by Ikaros and SSeCKS together than either condition alone, possibly reflecting the level of *Myc* expression under these conditions. This did not reach statistical significance however. There also appeared to be no significant changes in integrin expression when Ikaros and *SSeCKS* were induced together, potentially reflecting the opposing transcriptional regulation that Ikaros and SSeCKS exert on these genes.

I performed western blot analysis on S24 cells to investigate the protein expression of SSeCKS, Myc and cyclin D2 after treatment with the 4 conditions for 24 hours (figure 5.9B). Ikaros induction (+Dox +4-OHT, lane 2) resulted in a small upregulation in SSeCKS protein expression and a large reduction in the level of Myc and cyclin D2 compared with the control treatment (+Dox +EtOH, lane 1). *SSeCKS* induction (-Dox +EtOH, lane 3) also depleted Myc protein, though not to the same extent as Ikaros. This reflected the gene expression pattern observed in figure 5.9A. When *SSeCKS* and Ikaros were induced together (-Dox +4-OHT, lane 4) there was a synergistic depletion of both Myc and cyclin D2 protein, rendering both bands barely detectable. This corroborates the gene expression data and confirms that both *Ikzf1* and *SSeCKS* regulate the expression of *Myc,* providing a common mechanism that both genes can exploit to regulate the progression past the G1 checkpoint.

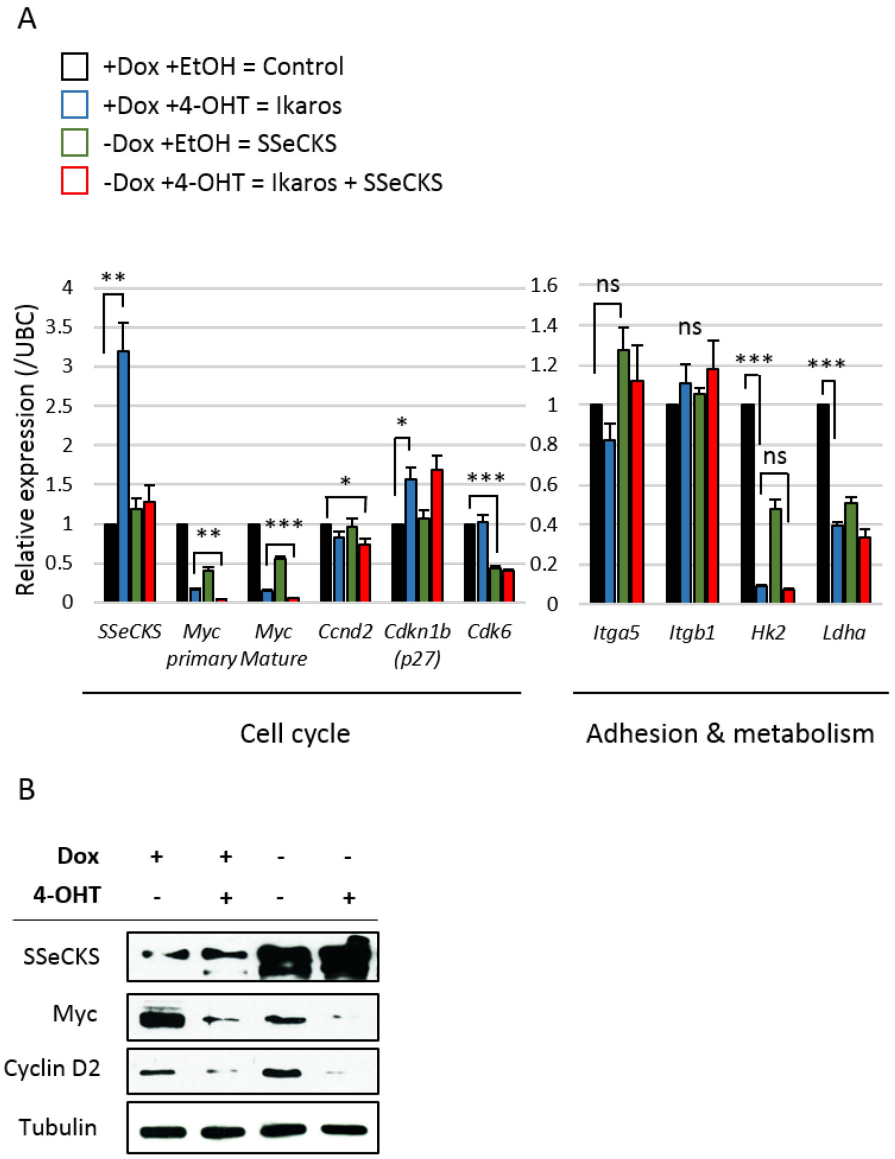

Figure 5.9 – Dissection of Ikaros and SSeCKS mediated gene expression changes. (A) qPCR analysis of S24 cells grown for 24 hours in the presence of control (+Dox +EtOH, black), Ikaros (+Dox +4-OHT, blue), *SSeCKS* (-Dox +EtOH, green) and Ikaros + *SSeCKS* (-Dox +4-OHT, red) treatments. Values were normalised to the housekeeping gene *Ubc*. (Mean+SE; N=3, student T test: * p<0.05 **p<0.01 *** p<0.001). (B) Western blot of S24 cells grown for 24 hours in the presence (+) or absence (-) of doxycycline (top panel) and treatment with EtOH (-) or 4-OHT (+) (bottom panel). The expression of SSeCKS, Myc and cyclin D2 was tested. An anti-tubulin antibody was used as a loading control.

5.6 Enforced *Myc* expression overrides SSeCKS-mediated cell cycle arrest

In the previous experiments I identified *Myc* as an important nexus in the regulation of the cell cycle by Ikaros and SSeCKS and demonstrated that enforced *Myc* expression was sufficient to override Ikaros-mediated cell cycle arrest (figure 3.6A). As SSeCKS appeared to regulate the cell cycle through *Myc*, I reasoned that enforced *Myc* expression would similarly override SSeCKS-mediated cell cycle arrest. To test this idea I infected S24 cells with an inducible Myc-ERt2 construct and treated them with a combination of doxycycline and 4-OHT. I then stained the cells with PI and checked the cell cycle profile by flow cytometry (figure 5.10A,B). Myc-ERt2 nuclear translocation increased the proportion of cells in S phase and decreased the proportion of cells in G1 as expected (+Dox +4-OHT, blue line). *SSeCKS* overexpression (-Dox +EtOH) resulted in an increase in the proportion of cells undergoing G1 arrest. When Myc-ERt2 and *SSeCKS* were induced together (-Dox +4-OHT) an increased proportion of cells were in S phase. This confirmed that enforced Myc expression was sufficient to override SSeCKS-mediated cell cycle arrest.

I went on to investigate the gene expression changes in these cells (figure 5.10C). The induction of Myc-ERt2 translocation (+Dox +4-OHT, blue bars) repressed the transcription of *SSeCKS* and endogenous *Myc.* This latter finding is expected as Myc negatively autoregulates its own expression (Penn *et al.,* 1990). Myc-ERt2 induction upregulated the expression of *Ccnd2* and the metabolic genes *Hk2* and *Ldha*. *SSeCKS* overexpression (-Dox +EtOH, green bar) was sufficient to repress the transcription of endogenous *Myc*. However *SSeCKS* overexpression was unable to reverse the upregulation of *Ccnd2, Hk2* and *Ldha* in the presence of enforced *Myc* expression, as there was no change in the expression of these genes when *SSeCKS* and Myc were induced in the same cells (-Dox +4-OHT, red bars). In conclusion, enforced *Myc* expression was sufficient to induce hyperproliferation and a corresponding increase in metabolic gene expression. SSeCKS was unable to enforce proliferative arrest when *Myc* expression was sustained in these cells.

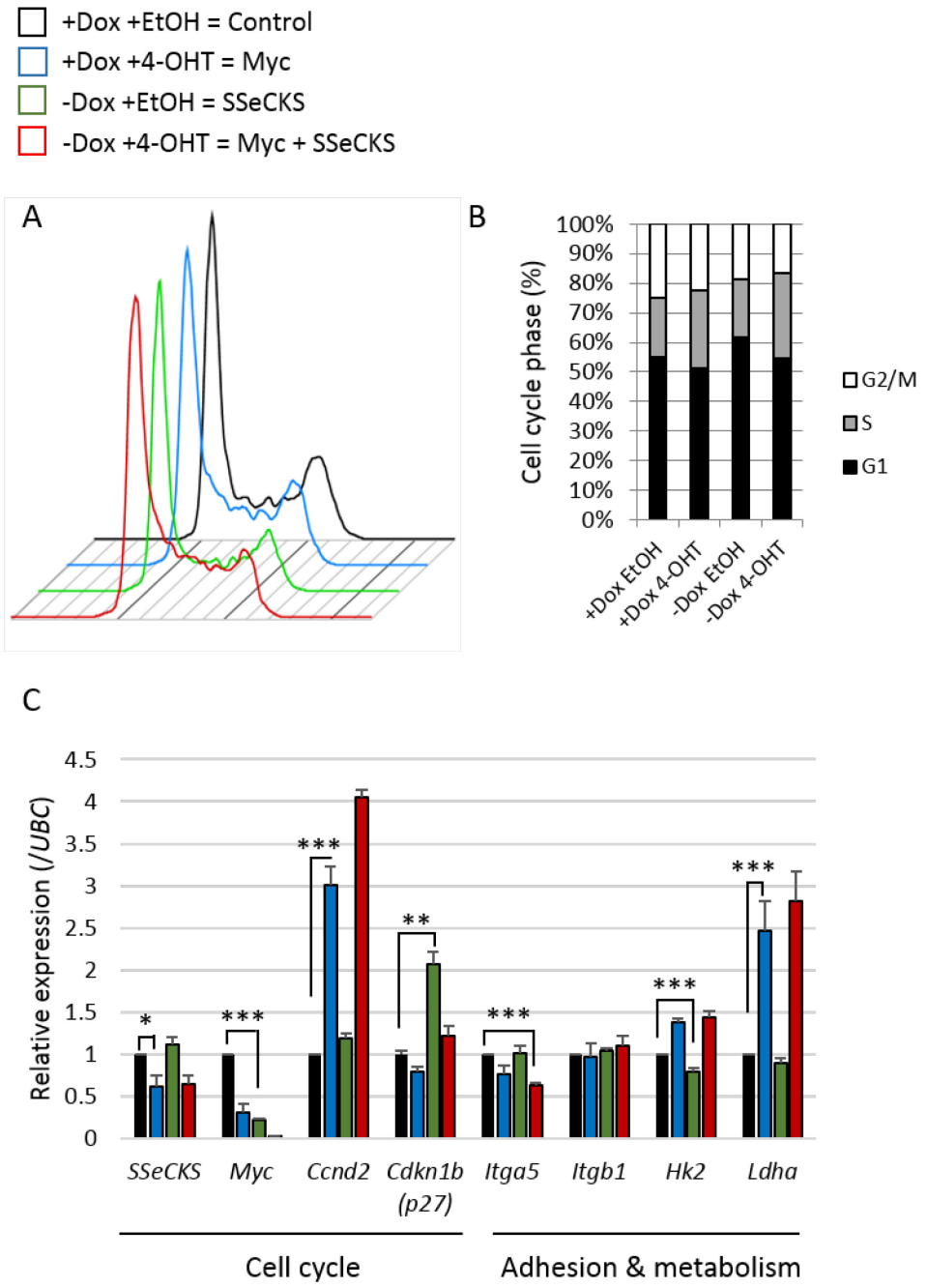

Figure 5.10 – Myc overrides *SSeCKS*-mediated cell cycle arrest. (A) PI profiles of S24 cells grown for 24 hours in the presence of control (+Dox +4-OHT, black), Myc (+Dox +4-OHT, blue), *SSeCKS* (-Dox +EtOH, green) and Myc + *SSeCKS* (-Dox +4-OHT, red) treatments. (B) Quantification of the cell cycle profiles displayed in (A). (C) qPCR analysis of S24 cells grown for 24 hours in the presence of control (black), Myc (blue), *SSeCKS* (green) and Myc + *SSeCKS* (red) treatments. Values were normalised to the housekeeping gene *Ubc*. (Mean+SE; N=3, student T test: * p<0.05 **p<0.01 *** p<0.001).

5.7 Global gene expression profiling of cells overexpressing *Ikzf1* and *SSeCKS*

In figure 5.9A I began to explore the relationship between Ikaros and SSeCKS in the regulation of the cell cycle. Looking at a small subset of genes by qPCR I made a number of interesting observations. Some genes, such as Myc, were cooperatively regulated by Ikaros and SSeCKS. Other genes were independently regulated by either Ikaros or SSeCKS alone (Cdkn1b and Cdk6 respectively). Antagonism may also exist between Ikaros and SSeCKS in the regulation of integrin-mediated adhesion. It would be interesting to observe the direction (up or down regulation) and extent of gene expression that is regulated by Ikaros and SSeCKS. It would also be interesting to examine the nature of these regulated genes; whether Ikaros and SSeCKS always cooperatively regulate the expression of cell cycle genes but oppose each other in the regulation of adhesion molecules for example.

To obtain a global view of Ikaros and SSeCKS-mediated gene expression changes I performed RNAseq analysis on S24 cells expressing the inducible Ikaros-ERt2 construct. I treated the cells for 24 hours with a combination of doxycycline and 4-OHT before extracting RNA and performing NGS library preparation. Three independent biological replicates were performed with the 4 combinatorial treatments of doxycycline and 4-OHT outlined in figure 5.9A. These samples were pooled and run in 2 lanes of the Illumina HiSeq flow cell. Sufficient read counts were generated so that each sample was represented by a sequencing depth of >38x106 reads, of which >90% mapped to the mouse genome. The RNA library preparation of one biological replicate was performed separately from the other two replicates and was subject to batch correction. Principal component analysis (PCA) of the 3 replicates is displayed in figure 5.11. The analysis shows tight clusters of data with little variance between biological replicates. The first principal component (PC1) accounts for the highest proportion of variance in the data (61%) and separates the groups based on the induction of Ikaros nuclear translocation by 4-OHT treatment. The second principal component (PC2) accounts for 20% of the variance and separates the groups based on SSeCKS upregulation in response to the withdrawal of doxycycline.

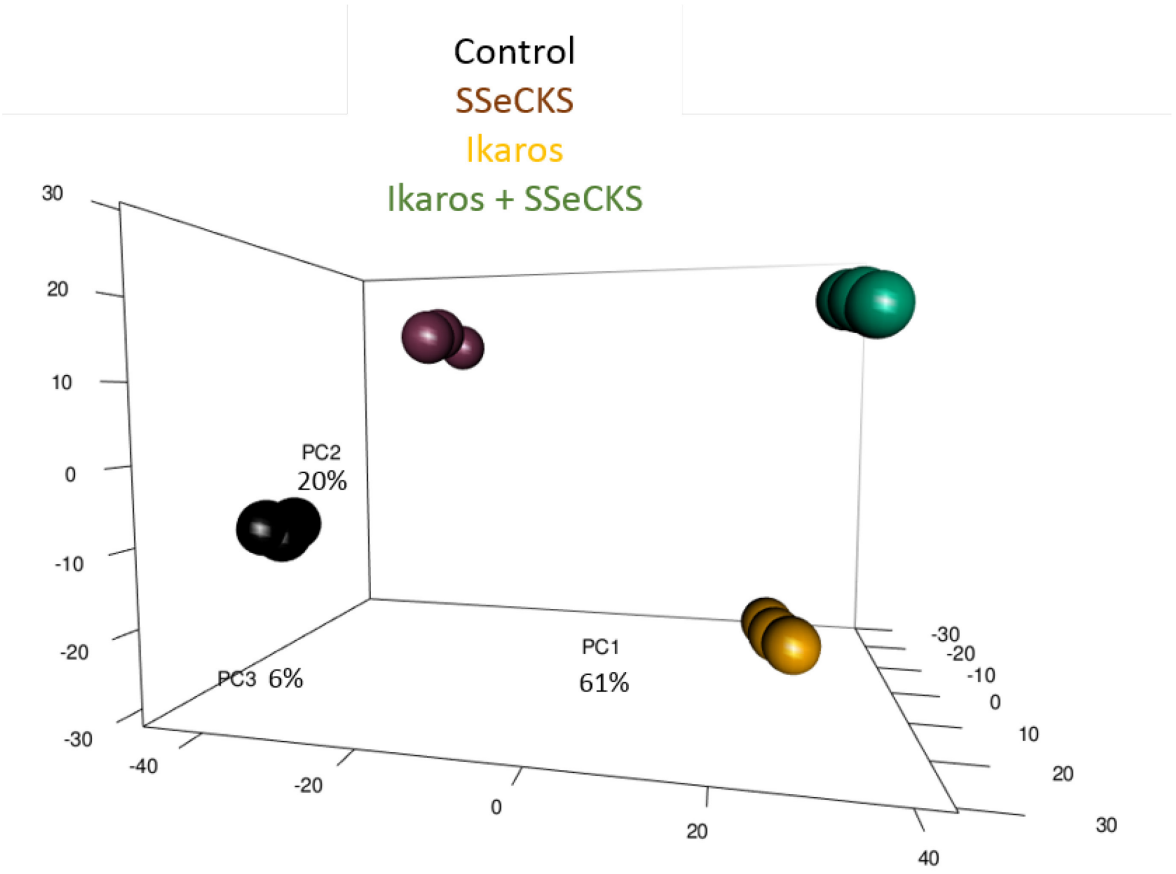

Figure 5.11- Principal component analysis. PCA plot describing the distribution of variance across the data. Biological replicates from 'Control' (+Dox +EtOH, black) '*SSeCKS*' (-Dox +EtOH, red), 'Ikaros' (+Dox +4-OHT, yellow) and 'Ikaros + *SSeCKS*' (-Dox +4-OHT, green) conditions cluster separately.

Following alignment, the differential expression of genes from each condition relative to the control treatment was calculated using the EdgeR package. To characterise the nature of the differentially expressed genes I segregated the most highly up- and downregulated genes for each treatment. I defined the top upregulated genes as having a false discovery rate of ≤0.01 and a log2 fold change of ≥1. I defined the top downregulated genes as having a false discovery rate of ≤0.01 and a log2 fold change of ≤-1. I discovered that this stringent threshold was lowering the number of differentially expressed genes in the '*SSeCKS*' (-Dox, EtOH) sample, so I relaxed the log2 fold change criteria for this treatment only to +/-0.5 for up and downregulated genes respectively. I then plotted the overlap of up- and downregulated genes separately for each treatment using the Venny online tool (bioinfogp.cnb.csic.es/tools/venny).

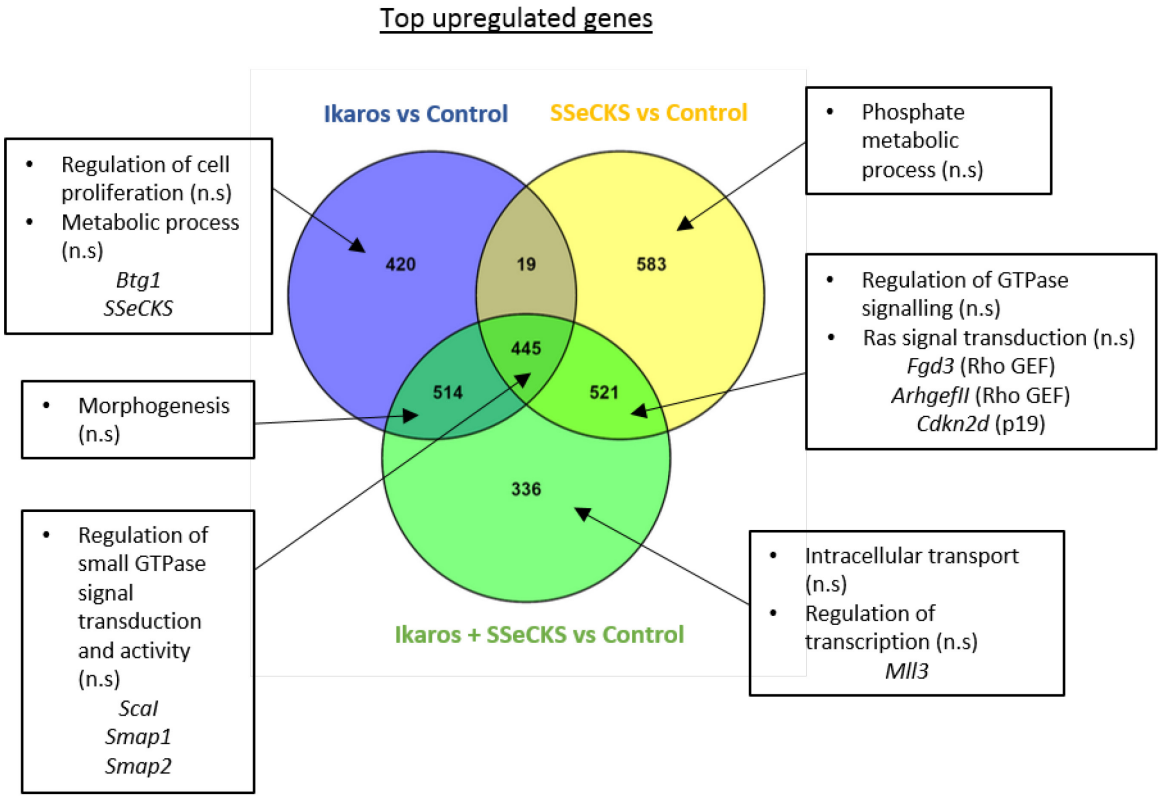

Figure 5.12 – Top upregulated genes. Venn diagram displaying the overlap of genes significantly upregulated between 'Ikaros' (+Dox +4-OHT, blue), '*SSeCKS*' (-Dox +EtOH, yellow) and 'Ikaros + *SSeCKS*' (-Dox +4-OHT, green) conditions relative to control. The numbers in each segment indicate the number of genes overlapping each condition. The boxes indicate the GO terms associated with each gene set.

Figure 5.12 shows the overlap between the top significantly upregulated genes for each treatment relative to control. The boxes display the top GO terms associated with each gene set with example genes shown in italics. The gene sets lacked statistical power so the GO terms were not significant (n.s). There were 445 genes that overlapped between all three conditions ('Ikaros', '*SSeCKS*' and 'Ikaros + *SSeCKS*') that were associated with the GO terms 'regulation of GTPase signal transduction' and 'GTPase activity'. One of these upregulated genes was *Scai* (suppressor of cancer cell invasion), a nuclear cofactor for MAL (megakaryocytic acute leukaemia) and serum response factor (SRF). This complex acts in a pathway downstream of Rho GTPase-mediated actin remodelling (Brandt et al., 2009). The expression of *Scai* is downregulated in an array of cancers and the depletion of *Scai* in a breast cancer cell line increased invasiveness, coinciding with an increase in the expression of the integrin *Itgb1* (Brandt *et al*., 2009). Therefore *Scai* upregulation may contribute to

Ikaros-mediated integrin repression. Interestingly ScaI is reported to associate with the SWI/SNF chromatin remodelling complex, and this association may be required for ScaI-mediated regulation of gene expression (Kressner *et al*., 2013).

Two guanine nucleotide exchange factors (GEFs) that activate members of the Rho GTPase family were upregulated in the overlapping '*SSeCKS'* and 'Ikaros + *SSeCKS'* gene sets. This further implies that actin dynamics and motility are regulated in response to Ikaros and *SSeCKS* induction. This upregulation was a surprising observation, as SSeCKS has previously been shown to suppress chemotaxis in fibroblasts by antagonising Cdc42 GTPase function at leading edge filopodia (Ko *et al.,* 2014). *Cdkn2d*, which encodes the cyclin-dependent kinase inhibitor p19, also appeared in this list. This gene was previously identified as an SSeCKS regulated gene by microarray analysis in S24 cells (Liu *et al.,* 2006).

Upregulated genes in the 'Ikaros + *SSeCKS'* condition displayed GO terms involved in the regulation of transcription. The histone H3K4 methyltransferase *Mll3* was upregulated in this gene set. Haploinsufficiency of *Mll3* can cooperate with other oncogenic events to promote acute myeloid leukaemia in mice (Chen *et al.,* 2014) and *Mll3* expression is upregulated at the transition from the large cycling (FrC') to resting (FrD) pre-B cell stage (Immgen.org). This potentially outlines a role for this chromatin modifier in pre-B cell development. There was a small but not significant increase in the expression of *Mll3* in B3 cells 48 hours after the introduction of Ikaros (Ferreiros-Vidal *et al.,* 2013). Of note, the integrin *Itga5* was included in the list of significantly upregulated genes in the '*SSeCKS'* only condition. This is consistent with the upregulation of this gene observed by qPCR in figure 5.7.

The GO terms associated with 'Ikaros' upregulated genes included the regulation of cell proliferation and metabolic processes. Of particular interest was the upregulated gene *Btg1*. B cell translocation gene (*Btg1*) is a member of an anti-proliferative family of proteins that includes *Tob2*, a gene I identified as a potential mediator of Ikaros growth arrest in the previous shRNA screen. *BTG1* was identified as a translocation partner of *MYC* in chronic

lymphocytic leukaemia (Rimokh *et al.,* 1991). *BTG1* expression is reportedly downregulated in breast cancer cell lines and is deleted in 9% of B-cell precursor ALL patients (Zhu *et al.,* 2013; Waanders *et al.,* 2012). The expression of *Btg1* is highest in quiescent lymphocytes and is downregulated upon mitogenic stimulation and S phase entry (Rouault *et al.,* 1992). The expression of *Btg1* is anti-correlated with *Myc*, and *BTG1* overexpression was sufficient to induce cell cycle arrest in 3T3 fibroblasts and breast cancer cell lines (Rouault *et al.,* 1992, Zhu *et al.,* 2013). I checked the expression of *Btg1* in B cell progenitors using the Immgen database. There was a large and striking increase in *Btg1* expression at the transition from the large cycling (FrC') to resting (FrD) pre-B cell stage (figure 5.13). ChIP-seq data confirmed that Ikaros binds to the promoter of *Btg1* in B3 cells and *Btg1* expression was significantly upregulated 48 hours after the introduction of Ikaros into these cells (Ferreiros-Vidal *et al.,* 2013). Further investigation of this gene may be warranted to better understand its role in the regulation of the cell cycle in pre-B cell development.

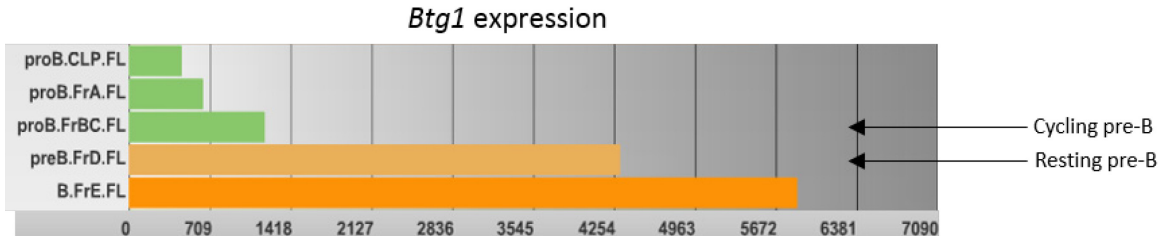

Figure 5.13 – *Btg1* expression in pre-B cell development. Graph showing the expression of *Btg1* in different stages of pre-B cell development based on microarray data available from immgen.org. The cycling (frC') and resting (FrD) pre-B cell stages are highlighted by arrows.

Figure 5.14 shows the overlap between the significantly downregulated genes for each condition relative to control. The GO terms associated with gene sets overlapping the 'Ikaros' and 'Ikaros + *SSeCKS*' conditions related to adhesion and migration. The integrin *Itgae* was found in this dataset, consistent with the suppression of integrin expression and signalling by Ikaros in pre-B cells (Joshi *et al.,* 2014). Genes downregulated in the '*SSeCKS*' and 'Ikaros + *SSeCKS*' conditions displayed highly significant GO terms associated with cell cycle regulation, division and transcriptional regulation. The mitogen activated protein kinase *Mapk7* (ERK5) was downregulated upon *SSeCKS* overexpression. The ERK5 signalling

cascade can upregulate the expression of *Ccnd1* (Mulloy *et al.,* 2003). Consistent with this observation, *Ccnd1* was also included in the '*SSeCKS*' and 'Ikaros + *SSeCKS*' downregulated datasets. Thus SSeCKS may be able to control the expression of *Ccnd1* via multiple ERK pathways and regulate the subcellular localisation of cyclin D1 protein by direct binding (Lin *et al.,* 2000).

The cyclin-dependent kinases *Cdk4, Cdk6* and *Cdk2* were all significantly repressed in the '*SSeCKS*' and 'Ikaros + *SSeCKS*' datasets, consistent with the cell cycle arrest observed in Ikaros and *SSeCKS* overexpressing cells. There appeared to be a downregulation of multiple members of the E2F family of transcription factors. *E2f2* and *E2f3* encode pro-proliferative transcriptional activators, required for progression into S phase. *E2f4, E2f7* and *E2f8* encode repressive members of the E2F family that antagonise E2F1 target gene transcription and cell cycle progression (DeGregori and Johnson, 2006). A global downregulation of *E2f* genes was also observed in B3 cells in response to Ikaros induction (Ferreiros-Vidal *et al.,* 2013). It would be interesting to see whether this transcriptional profile is represented in the protein expression of these family members. Western blot analysis of Ikaros-arrested murine leukaemic T cells failed to observe down regulation of E2F1 protein (Kathrein *et al.,* 2005), though there may be differences detected in other members of the E2F family.

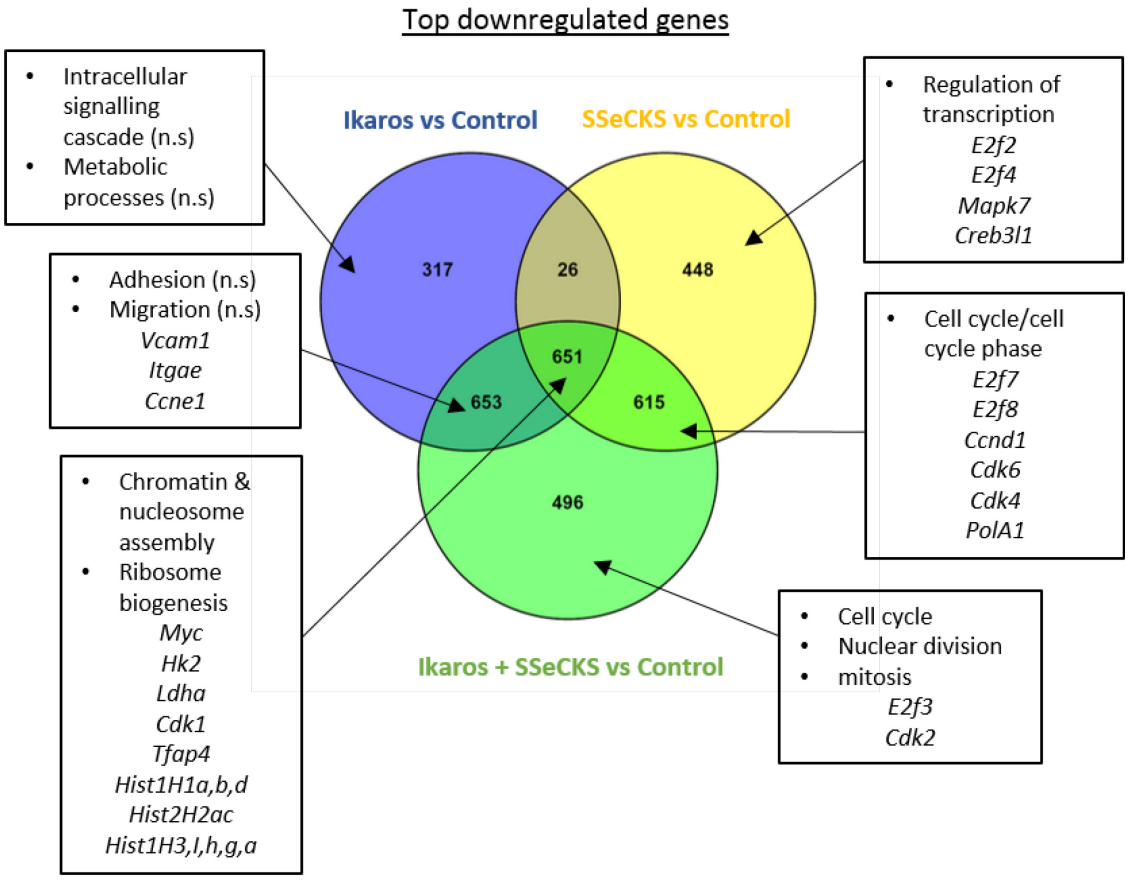

Figure 5.14 – Top downregulated genes. Venn diagram displaying the overlap of genes significantly downregulated between 'Ikaros' (+Dox +4-OHT, blue), '*SSeCKS*' (-Dox +EtOH, yellow) and 'Ikaros + *SSeCKS*' (-Dox +4-OHT, green) conditions relative to control. The numbers in each segment indicate the number of genes overlapping each condition. The boxes indicate the GO terms associated with each gene set.

There were 651 repressed genes that overlapped between all 3 conditions. These were associated with the GO terms 'Chromatin & nucleosome assembly' and 'ribosome biogenesis'. The genes downregulated in this dataset included *Myc*, and the metabolic genes *Hk2* and *Ldha* that were previously identified as Ikaros and SSeCKS regulated genes by qPCR (figure 5.9A). There was a striking downregulation of many histones in this dataset. This is likely because the majority of histones are transcribed during S phase and the cells in this experiment are arrested in G1 (Gunjan *et al.,* 2005). The ribosome biogenesis GO term is likely explained by the strong repression of *Myc* transcription by Ikaros and SSeCKS. Myc is a regulator of multiple steps in the biogenesis of ribosomes and can globally influence protein translation in the cell (Riggelen *et al.,* 2010).

One gene that stood out as particularly interesting was the transcription factor AP4 (*Tfap4*). *Tfap4* was strongly repressed by both Ikaros and SSeCKS displaying a log2 fold repression of -3 and -2.5 respectively. AP4 is a pro-proliferative transcription factor that is directly upregulated by Myc in an array of different cell types (Jung and Hermeking, 2009). AP4 directly represses the transcription of *Cdkn1a*, and knockdown of *Tfap4* in MCF-7 breast cancer cells partially ablated Myc-mediated S phase progression (Jung *et al.,* 2008). Ectopic expression of AP4 in these cells was sufficient to override p53-mediated cell cycle arrest in response to DNA damage (Jung *et al.,* 2008). Furthermore, ectopic expression of AP4 in the U-937 myelomonoblastic cell line prevented cell cycle withdrawal and differentiation in response to TPA treatment (Jung *et al.,* 2008). Serum deprived AP4-deficient MEFs display delayed entry into the cell cycle and defective *Cdk2* induction when stimulated by serum (Jackstadt and Hermeking, 2014). Ectopic *Myc* expression failed to rescue this phenotype, suggesting that AP4 was required for Myc-mediated cell cycle progression in response to serum stimulation (Jackstadt and Hermeking, 2014). Reintroduction of AP4 into *Tfap4* knockout MEFs directly upregulated *Cdk2* expression and enhanced DNA synthesis (Jackstadt and Hermeking, 2014). This observation is consistent with my RNA-seq analysis showing that both *Tfap4* and *Cdk2* were repressed in G1 arrested S24 fibroblasts in response to the induction of Ikaros and *SSeCKS*.

In lymphocytes *Tfap4* expression is highest in proliferating double-negative (DN) thymocytes and lowest in resting double-positive (DP) cells (Egawa and Littman, 2011). During thymocyte development, AP4 is required to silence CD4 expression in DN and CD8+ T cells (Egawa and Littman, 2011). AP4 is required for the maintenance of $CD8^+$ T cell proliferation in response to antigen stimulation and the maintenance of the metabolic gene program instilled by *Myc* (Chou *et al.,* 2014). This shows that AP4 can maintain expansion even after the depletion of Myc. In pre-B cells there is a large decrease in *Tfap4* expression at the transition from the large cycling (FrC') to resting (FrD) pre-B cells stages (figure 5.15). The promoter of *Tfap4* is bound by Ikaros in B3 cells, and microarray data shows that the expression of *Tfap4* was significantly downregulated after 6 hours of Ikaros induction in these cells (Ferreiros-Vidal *et al.,* 2013). Therefore *Tfap4* may be an important regulatory

target of Ikaros that must be repressed to terminate the pro-proliferative *Myc* transcriptional program required for pre-B cell differentiation.

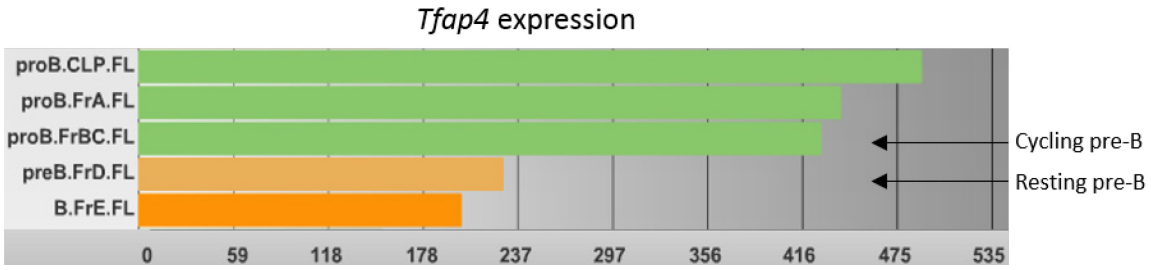

Figure 5.15 – *Tfap4* expression in pre-B cell development. Graph showing the expression of *Tfap4* in different stages of pre-B cell development based on microarray data available from immgen.org. The cycling and resting pre-B cell stages are highlighted by arrows.

5.8 Ikaros and SSeCKS synergistically regulate gene expression

I next investigated possible synergistic interactions in the regulation of gene expression by Ikaros and SSeCKS. I first segregated genes that were significantly up or downregulated (FDR ≤0.01). I defined up and downregulated genes as displaying a log2 fold change (log2FC) of ≥0 and ≤0 respectively in both the 'Ikaros' and 'Ikaros + *SSeCKS*' conditions relative to control. To detect synergistic upregulation I selected for genes that displayed a sum log2 fold change of ≥0.5 when I subtracted the log2 fold change of 'Ikaros' upregulated genes from 'Ikaros + *SSeCKS*' regulated genes. This is displayed in the following formula:

Synergistically upregulated genes = Log2FC≥0.5 (log2FC 'Ikaros + *SSeCKS*' vs control) – (log2FC 'Ikaros vs control').

These genes were upregulated to a greater extent when 'Ikaros and *SSeCKS*' were induced together than when 'Ikaros' was induced alone, resulting in a sum positive log2 fold change. This filter yielded 723 genes that were synergistically upregulated by Ikaros and SSeCKS.

Synergistically upregulated genes – GO terms

Term	Count	%	P-Value	Benjamini
regulation of small GTPase mediated signal transduction	25	3.7	7.9E-8	1.3E-4
regulation of Ras protein signal transduction	20	2.9	1.9E-6	1.5E-3
cellular macromolecule catabolic process	39	5.7	1.3E-5	7.0E-3
macromolecule catabolic process	40	5.8	2.7E-5	1.1E-2
modification-dependent macromolecule catabolic process	33	4.8	5.2E-5	1.7E-2
modification-dependent protein catabolic process	33	4.8	5.2E-5	1.7E-2

Figure 5.16 – Go terms associated with genes that were synergistically upregulated by Ikaros and SSeCKS. The GO terms associated with synergistically upregulated genes are listed, alongside the associated Benjamini Hochberg adjusted significance values (right column). The terms were generated by querying the DAVID functional annotation bioinformatic tool (https://david.ncifcrf.gov/) with the list of 723 synergistically upregulated genes.

The significant GO terms associated with this gene set were enriched for GTPase signalling and the regulation of Ras signal transduction (figure 5.16). Included in this set was *ScaI*, an inhibitor of serum response factor (SRF) gene regulation. SRF is positively regulated by the Ras/Raf/Mek/ERK and Rho GTPase pathways in response to serum (Juliano, 2009). Rho-stimulated actin stress fibre polymerisation facilitates the nuclear translocation of MAL and the activation of SRF transcriptional activity (Juliano, 2009). SCAI associates with the MAL/SRF complex and inhibits the activation of gene expression by this complex, including the target gene *Itgb1* (Brandt *et al.,* 2009; Juliano, 2009). Figure 5.17 displays the sequencing tracks mapped to the *ScaI* gene under each condition. There was a moderate increase in *ScaI* transcript abundance in the 'Ikaros' and '*SSeCKS*' conditions. *ScaI* transcript was further increased in the 'Ikaros + *SSeCKS*' condition, suggesting a synergistic upregulation of this gene.

Interestingly *Btg1* was not included in the list of synergistically upregulated genes. On further inspection it appeared that Ikaros and SSeCKS were exerting opposing effects on the transcription of this gene. *Btg1* was significantly upregulated by Ikaros but repressed by SSeCKS. When Ikaros and SSeCKS were induced together there was no significant change in *Btg1* expression. The consequence of this antagonism is unknown at this time.

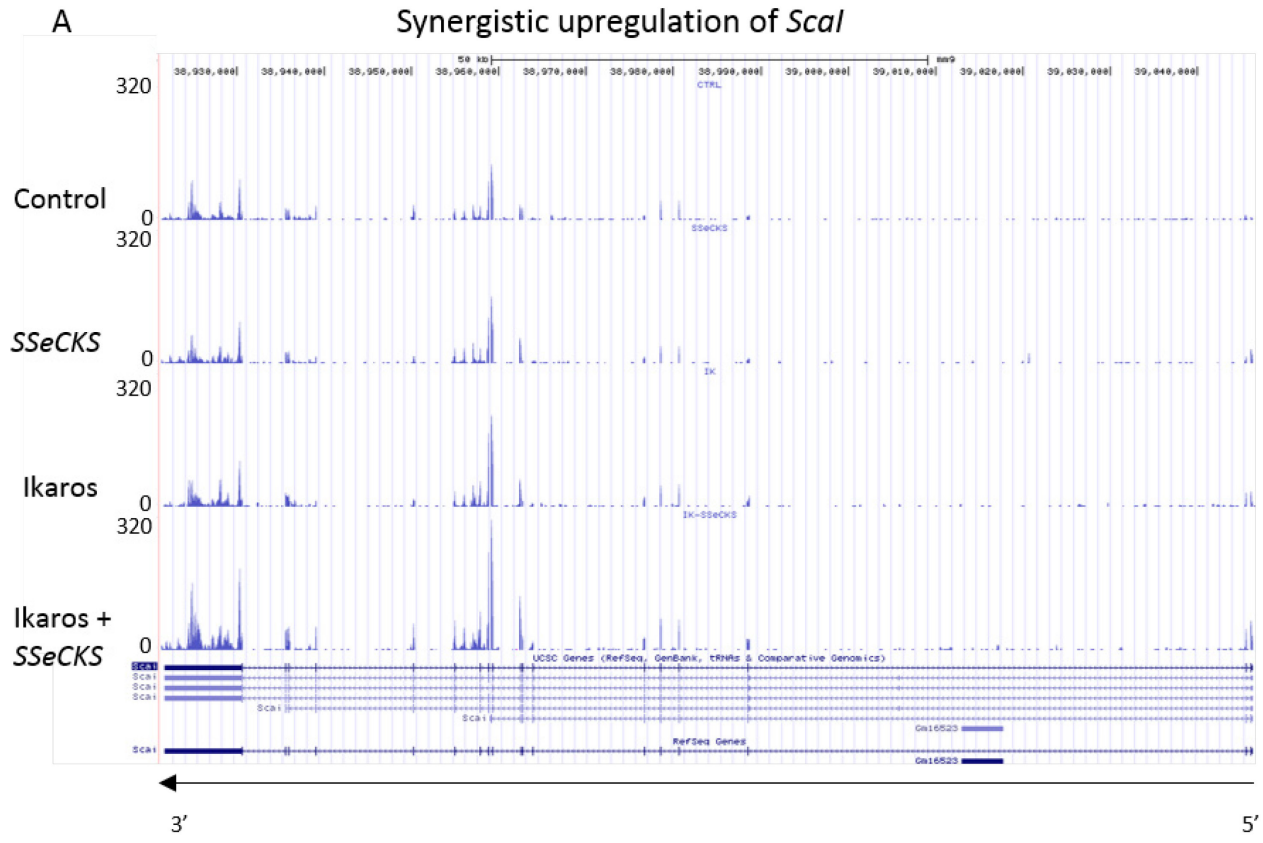

Figure 5.17 – *ScaI* is synergistically upregulated by Ikaros and SSeCKS. Figure displaying the sequence reads mapped to the *ScaI* gene in the UCSC genome browser (https://genome.ucsc.edu/). The peaks display the density of reads mapping to each exon of the *ScaI* gene in each of the 4 experimental conditions. Larger peaks indicate an increased expression. The scale on the Y axis is set to the same value to aid in the comparison between the conditions. The Refseq gene transcript is illustrated below the custom tracks (exons are indicated by blue shaded boxes) and the 5'-3' orientation of transcription is illustrated by the arrow.

I followed the same logic to detect synergistically repressed genes using the following formula:

Synergistically repressed genes = Log2FC≤ -0.5 (log2FC 'Ikaros + *SSeCKS*' vs control) – (log2FC 'Ikaros vs control').

These genes were more repressed when 'Ikaros and *SSeCKS*' were induced together than

when 'Ikaros' was induced alone, resulting in a sum negative log2 fold change. This filter yielded 1108 genes that were synergistically repressed by Ikaros and SSeCKS.

Synergistically downregulated genes – GO terms

	Count	%	P-Value	Benjamini
cell cycle	150	15.6	4.8E-63	1.1E-59
cell cycle process	112	11.6	2.2E-53	2.5E-50
cell cycle phase	102	10.6	2.2E-52	1.7E-49
M phase	94	9.8	5.8E-51	3.3E-48
mitotic cell cycle	84	8.7	8.6E-47	3.9E-44
mitosis	74	7.7	1.9E-45	7.2E-43
nuclear division	74	7.7	1.9E-45	7.2E-43
M phase of mitotic cell cycle	74	7.7	1.1E-44	3.5E-42
cell division	87	9.0	2.7E-44	7.6E-42
organelle fission	74	7.7	3.7E-44	9.4E-42
DNA metabolic process	93	9.7	2.9E-34	6.6E-32

Figure 5.18 – Go terms associated with genes synergistically downregulated by Ikaros and SSeCKS. The GO terms associated with synergistically repressed genes are listed, alongside the associated Benjamini Hochberg adjusted significance values (right column). The terms were generated by querying the DAVID functional annotation bioinformatic tool with the list of 1108 synergistically downregulated genes.

The GO terms associated with this gene set were extremely significant and related to the cell cycle and cell division (figure 5.18). Importantly this set of genes included *Myc*, validating the synergistic downregulation of this gene I observed by qPCR and western blot in figure 5.9. The log2 fold change in *Myc* expression relative to control was -2.6 in the 'Ikaros' condition and -4.1 in the 'Ikaros + *SSeCKS*' condition. *Tfap4* was also synergistically repressed, displaying a log2 fold change of -3 in the 'Ikaros' dataset and -5.6 in the 'Ikaros + *SSeCKS*' set. Consistent with the repression of *Tfap4* expression, *Cdk2* and *Cdk4* were also synergistically downregulated. The metabolic genes *Hk2* and *Ldha* do not appear in the list of synergistically repressed genes. This is consistent with qPCR analysis showing that there was no synergistic repression of these genes by Ikaros and SSeCKS (figure 5.9). The RNA-Seq tracks for the downregulated genes *Myc* and *Tfap4* are shown in figure 5.19. There is a progressive and striking decrease in the reads mapping to these loci upon the introduction of SSeCKS and Ikaros into the cells. The repression is most strongly observed in the 'Ikaros + *SSeCKS*' condition, where the peaks are barely detectable compared to the control

condition. In conclusion, Ikaros and SSeCKS cooperate to silence the expression of *Myc* in fibroblasts, and synergistically regulate the differential expression of hundreds of genes involved in processes such as cell cycle, adhesion and migration.

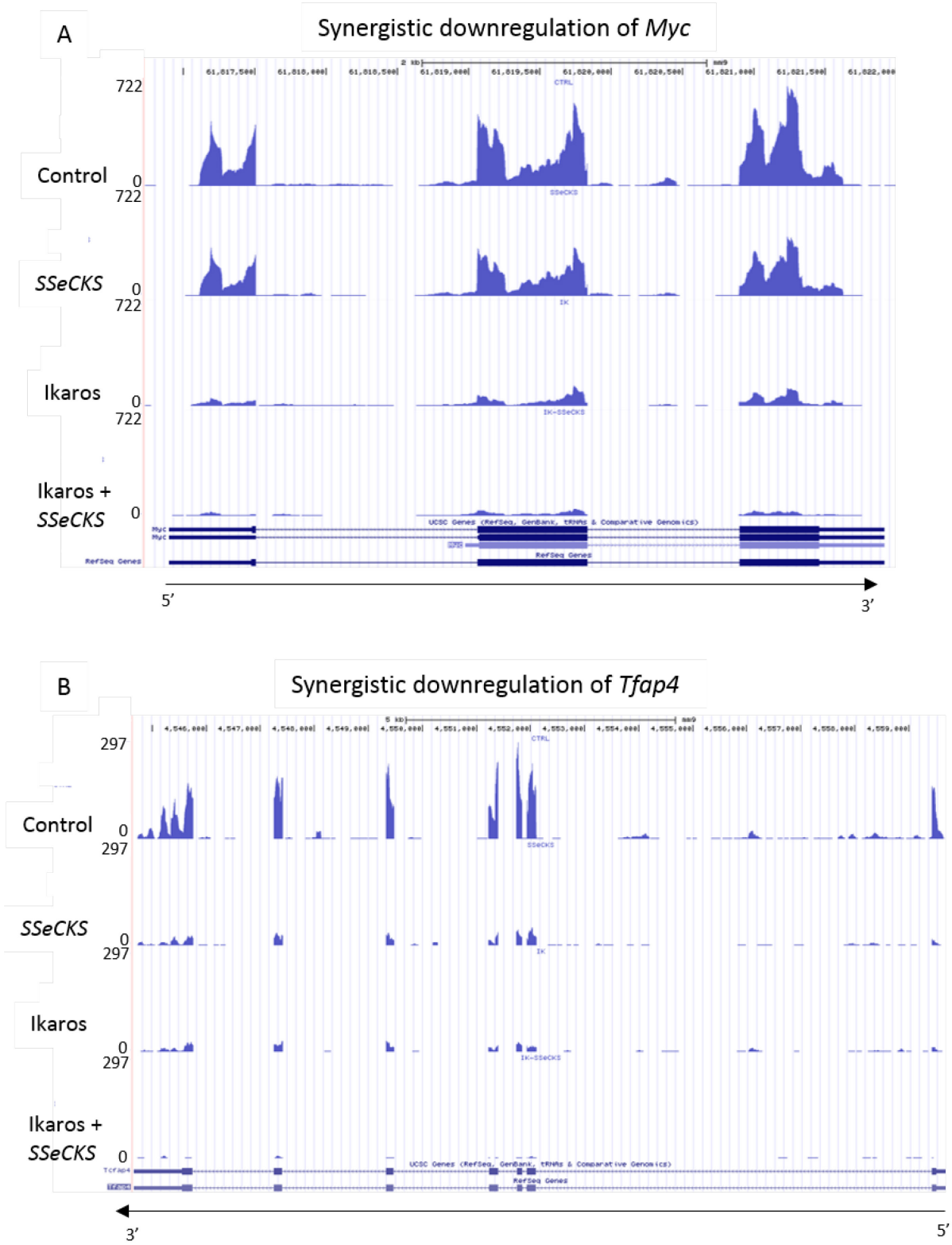

Figure 5.19 – Synergistic downregulation of *Myc* and *Tfap4*. Figure displaying the sequence reads mapped to the *Myc* (**A**) and *Tfap4* (**B**) genes in the UCSC genome browser. The peaks display the density of reads mapping to each exon of the genes under the 4 treatment conditions. Smaller peaks indicate a reduced expression. The scales on the Y axis of each gene are set to the same value to aid in the comparison between conditions. The Refseq gene transcripts are illustrated below the custom tracks (exons are indicated by blue shaded boxes) and the 5'-3' orientation of transcription is illustrated by the arrows.

5.9 Discussion

5.9.1 Transcriptional regulation of *SSeCKS*

SSeCKS is a putative tumour suppressor whose expression appears to be inversely correlated with cellular proliferation and transformation. *SSeCKS* was first characterised as a repressed gene in *Src* transformed 3T3 fibroblasts (Lin *et al*., 1995). *SSeCKS* expression is upregulated in contact inhibited fibroblasts and suppressed in serum-induced S phase progression (Nelson and Gelman, 1997). Distinct promoters induce the expression of two widely expressed SSeCKS protein isoforms, alpha and beta, that differ in the N-terminal myristoylation domain (Streb *et al.,* 2004). The alpha promoter is found at the 5' position of exon 1 and the beta promoter is 5' of exon 3 (Streb *et al.,* 2004). The expression of these isoforms can be induced by dexamethasone and retinoic acid respectively, which facilitate cell cycle withdrawal in glioma and vascular smooth muscle cells (Liu *et al.,* 2009; Streb *et al.,* 2011). Hypoxia in human vascular endothelial cells can induce *AKAP12/GRAVIN* expression in a HIF-dependent mechanism (Weissmuller *et al.,* 2014). AKAP12 is believed to prevent angiogenesis in these cells (Weissmuller *et al.,* 2014). Thus multiple stimuli can induce or suppress *SSeCKS* expression in a wide range of cell types influencing the balance between proliferation and quiescence.

Here I showed that Ikaros could bind directly to the promoter of *SSeCKS* to increase its transcription in pre-B cells and fibroblasts. Based on the location of the Ikaros peaks upstream of the first coding exon (figure 5.3A), it is likely that Ikaros binds to the alpha promoter of *SSeCKS*. The upregulation in transcription induced by Ikaros led to increased SSeCKS protein expression that correlated with cell cycle withdraw at 16 and 24 hours post 4-OHT treatment (figure 5.1 B). Ikaros appeared to induce both the alpha and beta isoforms of SSeCKS, as determined by the intensities of the upper and lower bands by western blot (figure 5.1b). The alpha isoform of SSeCKS encodes the N-terminal myristoylation motif that is lacking in the beta isoform. Myristoylation may facilitate the subcellular localisation of SSeCKS to the plasma membrane and endoplasmic reticulum derived vesicles (Streb *et al.,*

2004). It has been previously shown that the chromatin structure of the alpha promoter can influence the transcriptional state of the beta isoform. Sp1/Sp3 transcription factors can recruit the histone deacetylase 1 (HDAC1) complex to a GC-box in the alpha promoter of *SSeCKS,* repressing the expression of both *SSeCKS* isoforms in *Src* transformed 3T3 cells (Bu and Gelman, 2007). Treatment of these cells with the HDAC inhibitor TSA fully restored beta-*SSeCKS* expression, though histone acetylation was only increased at the alpha promoter (Bu and Gelman, 2007). Ikaros may similarly increase the expression of both isoforms of *SSeCKS* by altering the chromatin environment at the alpha promoter to a context more permissive for transcription. In support of this idea, Ikaros is able to suppress position effect variegation of a CD8 transgene in mouse thymocytes by binding to upstream regulatory elements (Harker *et al.,* 2002).

The upregulation of *SSeCKS* by Ikaros appears to coincide with the repression of *Myc* transcription. Furthermore, I showed that enforced *Myc* expression was sufficient to prevent the upregulation of *SSeCKS* by Ikaros, and override both Ikaros and SSeCKS-induced cell cycle arrest. Thus it seems that Myc depletion is a prerequisite for the induction of *SSeCKS* transcription and cell cycle withdrawal. Consistent with these findings is the observation that *SSeCKS* transcription is repressed in *Myc* transformed fibroblasts (Lin *et al.,* 1995). The requirement for Myc depletion appears at odds with the apparent lack of Myc binding at the *SSeCKS* promoter. The alpha promoter of *SSeCKS* contains an E-box sequence that is bound by USF1 and is required for *Src*-mediated repression of *SSeCKS* transcription (Bu and Gelman, 2007). Myc can also bind to E-box sequences, but gel shift assays failed to detect Myc binding at this site (Bu and Gelman, 2007). The repression of *SSeCKS* may therefore be a downstream consequence of Myc transcriptional activity, rather than a direct effect of Myc binding.

The expression of *AKAP12* is downregulated in a number of myeloid malignancies as a result of aberrant promoter hypermethylation (Boultwood *et al.,* 2004; Flotho *et al.,* 2007). Treatment of Kasumi-1 acute myeloid leukaemia cells with DNA methyltransferase and histone deacetylase inhibitors can reverse this methylation and restore *AKAP12* expression

(Flotho *et al.,* 2007). It would be interesting to test the cell cycle profile of Kasumi-1 cells with and without *AKAP12* expression, and see if Ikaros can arrest proliferation in the absence of *AKAP12*.

5.9.2 Mechanisms of SSeCKS-mediated cell cycle arrest

In fibroblasts SSeCKS has been shown to induce proliferative arrest by directly sequestering cyclin D1 in the cytoplasm (Lin et al., 2000; Lin and Gelman, 2002). I attempted to detect an association between SSeCKS and cyclin D proteins in pre-B cells following the upregulation of SSeCKS protein by Ikaros (figure 5.4A). No cyclin D2 or cyclin D3 protein was detected after immunoprecipitation with an anti-SSeCKS antibody. The cause of this negative result is unknown. One explanation may be that the interaction between SSeCKS and cyclins is weak and that optimisation of the lysis buffer may yield a positive result. Another potential issue is the fact that Ikaros downregulates cyclin D protein expression, thereby reducing the pool that can be sequestered by SSeCKS (figure 3.5B&C). To circumvent the weak interaction by pulldown, and depletion of cyclin D protein by Ikaros, I attempted to visualise cytoplasmic cyclin D localisation by cellular fractionation before cell cycle arrest (figure 5.4B). Cyclin D3 was undetected in the cytoplasm in the control condition, and this was unaffected by the induction of Ikaros. Another explanation for these negative results may be that SSeCKS-cyclin interactions are cell type specific, and that SSeCKS does not associate with cyclins in pre-B cells. I performed a pulldown in 3T3 fibroblasts using an anti-SSeCKS antibody to test this hypothesis. No cyclin D1 protein was detected after immunoprecipitation however (data not shown).

It is possible that the extent of SSeCKS protein upregulation by Ikaros is not sufficiently large to detect an association between cyclin D and SSeCKS. Previous studies outlining interactions between SSeCKS and cyclin D1 have utilised S24 cells that highly overexpress *SSeCKS* (Lin *et al.,* 2000; Lin and Gelman, 2002). Repeating the pulldown experiment in S24 cells may yield a positive result. Evidence supporting this idea came from the surprising

result that *SSeCKS* overexpression in S24 cells resulted in an increase in cyclin D2 protein (figure 5.7B). This is possibly due to the stabilisation of cyclin D2 by its association with SSeCKS. There are reports that posttranslational modifications are also important in the regulation of SSeCKS function. Serine phosphorylation by protein kinase C (PKC) antagonises the binding between SSeCKS and cyclin D1 and facilitates cyclin D1 nuclear translocation (Lin *et al.,* 2000). SSeCKS is phosphorylated on serine residues during serum induced G1/S progression (Nelson and Gelman, 1997) and is hyperphosphorylated and degraded in *Ras* transformed rat fibroblasts (Lin *et al.,* 1996). PKC phosphorylation also regulates the subcellular localisation of SSeCKS, potentially influencing downstream signalling (Lin *et al.,* 1996; Lin *et al.,* 2000). This raises the possibility that posttranslational modifications may play an important role in the regulation of the cell cycle by SSeCKS.

It has been previously shown that Ikaros can inhibit pre-B cell proliferation through the transcriptional regulation of *Myc* (Ma *et al.,* 2010). In the data presented here I have demonstrated that Ikaros can bind to the promoter of *SSeCKS* to upregulate its expression, and that *SSeCKS* overexpression was sufficient to induce cell cycle withdrawal. I have outlined a novel function for SSeCKS by cooperating with Ikaros to silence the expression of *Myc* in fibroblasts. The evidence for the synergistic regulation of *Myc* by Ikaros and SSeCKS comes from the observation that the overexpression of these two factors together resulted in a more severe depletion of Myc mRNA and protein than either factor alone, and caused an enhanced arrest of the cell cycle. From the RNAseq data it appears that Max, the binding partner of Myc, is also downregulated by Ikaros but only by a small log2 fold change of -0.37. Therefore *Myc* itself, rather than its binding partner is the main target of repression in response to Ikaros overexpression.

The analysis of synergistically downregulated genes by RNA-seq unearthed a shared target of Ikaros and SSeCKS that related to Myc function. The transcription factor AP4 is required for the maintenance of the Myc gene expression program in activated CD8+ T cells (Chou *et al.,* 2014). ChIP-Seq analysis revealed that more than 50% of AP4 and Myc peaks overlapped in these cells (Chou *et al.,* 2014). AP4 was required for the upregulation of

glycolytic enzymes needed to sustain a prolonged metabolically active and proliferative state upon T cell activation (Chou *et al.,* 2014). This suggests that AP4 may be partially required for the metabolic reprogramming controlled by Myc in activated lymphocytes (Wang *et al.,* 2011; Karmaus and Chi, 2014). Evidence in our lab suggests that Ikaros reprograms cellular metabolism to a quiescent state. This is partially mediated through the repression of *Myc* transcription (Ferreiros-Vidal, personal communication). The repression of *Tfap4* by Ikaros may contribute to the long-term maintenance of this quiescent state.

The observed downregulation of *Tfap4* may be due to direct transcriptional repression by Ikaros, by a reduction in the *Tfap4* positive regulator Myc, or both. As sustained *Myc* expression is sufficient to override Ikaros-mediated cell cycle arrest (figure 3.6), it would be interesting to test the contribution of AP4 to cell cycle progression. Enforcing *Tfap4* expression using an overexpression vector could test this idea. I could induce Ikaros-ERt2 nuclear translocation in the presence and absence of enforced *Tfap4* expression and look at the resultant cell cycle profiles. It is possible that the downregulation of *Tfap4* is required for differentiation to the small resting pre-B cell stage. Interestingly AP4 can bind to two sites in the promoter of *Ikzf3* (Aiolos). Mutation of these sites reduced luciferase reporter construct activity (Ghadiri *et al.,* 2007). This raises the intriguing possibility that AP4 can contribute to the upregulation of Ikaros family members, which in turn regulate *Tfap4* and *Myc* expression in a negative feedback loop. Thus *Tfap4* may offer another layer of regulation in the interplay between Ikaros and Myc in relation to metabolism, cell cycle and differentiation.

Given the observation that the enforced expression of *Myc* can override the transcriptional upregulation of *SSeCKS* and antagonise cell cycle arrest, we can begin to understand the temporal order of events that occur as the cells prepare to exit the cell cycle in response to Ikaros activity. The direct repression of *Myc* expression by Ikaros is an early event in cell cycle withdrawal, occurring less than two hours after the induction of Ikaros activity by 4-OHT treatment (Ferreiros-Vidal *et al.,* 2013). Following the depletion of *Myc,* Ikaros can upregulate the expression of *SSeCKS*. In turn SSeCKS reinforces cell cycle arrest by

cooperating with Ikaros to deplete Myc mRNA and protein in a feedback loop. In this model, the removal of SSeCKS would result in a less efficient (or less sustained) repression of *Myc* and allow the cells to slowly re-enter the cell cycle and proliferate. I could test this model by tracking the kinetics of *Myc* reexpression in *SSeCKS* knockdown fibroblasts in a time course experiment following the induction of Ikaros-ERt2 activity by 4-OHT.

The mechanism by which SSeCKS represses the transcription of *Myc* is unclear at this time. SSeCKS is unable to enforce transcriptional changes directly, and must indirectly influence nuclear signalling through its scaffolding functions. Integrin binding to the extracellular matrix can upregulate *Myc* expression through the Src/Mek/Erk pathway (Benaud and Dickson, 2001). The expression of *Myc* is also upregulated in *Rho* transformed cells (Berenjeno *et al.,* 2007). SSeCKS can inhibit the activity of RhoA in *Src* transformed fibroblasts (Gelman and Gao, 2006). SSeCKS can also scaffold Src away from focal adhesion complexes, preventing adherence-induced ERK activation (Su *et al.,* 2013). These may provide possible explanations for the repression of *Myc* transcription in response to *SSeCKS* overexpression.

Chapter 6

Discussion

In this report I have given an account of the regulation of the cell cycle by Ikaros. Ikaros coordinates the expression of hundreds of genes in multiple pathways encompassing the cell cycle, metabolism and integrin-mediated adhesion to enforce proliferative arrest and a quiescence-like state in cycling pre-B cells and fibroblasts. Ikaros is a tumour suppressor in mice and humans that is able to antagonise the hyperproliferative phenotype of cancer cells (Kathrein *et al.,* 2005; Trageser *et al.,* 2009; Ferreiros-Vidal *et al.,* 2013; Song *et al.,* 2015). Dysregulated intracellular signalling networks, reprogrammed energy metabolism and aberrant proliferation are hallmarks of cancer (Hanahan and Weinberg, 2000; Hanahan and Weinberg, 2011). Genomic instability results in the deletion of *IKZF1* in over 80% of Ph+ patients and correlates with poor prognosis (Mullighan *et al.,* 2008; Mullighan *et al.,* 2009). The tumour suppressive function of Ikaros may be linked to its role in cell cycle regulation so it is important to investigate this further.

I showed that Ikaros is able to repress the expression of *Myc* in fibroblasts, which is a key Ikaros target gene in pre-B cells (Ma *et al.,* 2010; Ferreiros-Vidal *et al.,* 2013). I demonstrated that enforced *Myc* expression was sufficient to override Ikaros-mediated cell cycle arrest. This indicates that Myc is a major focal point in the regulation of the cell cycle by Ikaros and that *Myc* downregulation is required for proliferative arrest. This result was consistent with the ability of Myc to override Aiolos-mediated arrest in pre-B cells (Ma *et al.,* 2010). Insensitivity to growth-arresting signals is a phenotype commonly observed in *Myc* transformed cells. DNA damage stabilises the tumour suppressor p53, which arrests cells in G1 by upregulating the cell cycle inhibitor p21. Sustained *Myc* expression is able to induce inappropriate S phase progression in the presence of DNA damage by upregulating cyclin expression and promoting the hyperphosphorylation of RB (Sheen and Dickson, 2002). Activation of an inducible MycER construct in early G1 is sufficient to

override the growth inhibitory signalling of TGF-beta (Alexandrow *et al.,* 1995). The expression of *Myc* is tightly regulated and is induced by mitogenic signalling (Waters *et al.,* 1991). *Myc* overexpression mimics pro-proliferative signalling and commits cells to inappropriate division by bypassing the serum-dependent restriction point in G1 phase (Eilers *et al.,* 1991). In lymphocyte development, the silencing of *Myc* by Ikaros and Aiolos contributes to proliferative arrest in large cycling pre-B cells (Ma *et al.,* 2010). Cell cycle arrest is required for the fidelity of immunoglobulin receptor rearrangement by Rag proteins (Zhang *et al.,* 2011). Failure to arrest may result in a developmental block at a stage of virtually unlimited proliferative potential with a high degree of genomic instability. Thus the regulation of the cell cycle by Ikaros, mediated partly through the repression of *Myc* transcription, is essential for the orderly differentiation of B cell precursors. This may go some way to explaining the high incidence of *IKZF1* deletions observed in leukaemia.

Although much progress has been made in elucidating the role of Ikaros in the regulation of the cell cycle, our understanding remains incomplete. Ikaros is able to bind key cell cycle regulatory genes to directly control their expression (Ferreiros-Vidal *et al.,* 2013). It is unclear if Ikaros acts alone to regulate cell cycle gene expression. Perhaps Ikaros requires cofactors and epigenetic remodelers, or it competes for binding with other transcription factors. The decision to remain quiescent or proliferate is a balance between a range of multiple competing signals that must be coordinated and integrated to ensure an appropriate and coherent response. It is of great interest to understand how Ikaros is able to coordinate these signals to enforce proliferative arrest. I performed a large-scale shRNA screen to find factors that are required for Ikaros-mediated cell cycle arrest in fibroblasts. Amongst some interesting candidates I identified the scaffolding protein SSeCKS. I demonstrated that *SSeCKS* is a direct transcriptional target of Ikaros in pre-B cells and fibroblasts and that knockdown of *SSeCKS* by RNAi was sufficient to alleviate Ikaros-enforced proliferative arrest. SSeCKS is not a transcription factor so cannot directly regulate the cell cycle machinery. Instead it acts as a molecular scaffold to

physically tether signalling molecules together in time and space. Scaffolding proteins are involved in diverse cellular processes and can positively or negatively regulate signalling pathways (Good *et al.,* 2011; Shaw and Filbert, 2009). Scaffolds can facilitate cross talk between molecules, potentially integrating multiple signals to produce a desired outcome (proliferation or quiescence for example). Despite lacking intrinsic enzymatic activity, scaffolds regulate the activity of other molecules to influence the relay of information from the membrane to the nucleus (Good *et al.,* 2011). Depletion of these proteins can cause a dysregulation of intracellular signalling and result in inappropriate proliferation. Thus the study of scaffolding proteins may have relevance to our understanding of the processes underlying quiescence and malignancy. One example of a scaffolding protein with an important role in the regulation of the cell cycle is BRCA1. Following exposure to ionising radiation, the DNA damage sensor ATM phosphorylates the BRCA1 tumour suppressor. BRCA1 can then serve as a scaffold by binding to p53 and facilitating its phosphorylation by ATM (Fabbro *et al.,* 2004). siRNA knockdown of BRCA1 prevents p53-dependent upregulation of p21, resulting in inappropriate cell cycle progression (Fabbro *et al.,* 2004). Talin is an example of another scaffolding protein that links integrin adhesion complexes to cell cycle progression. Talin depletion results in the failure to tether FAK to adhesion complexes and compromises integrin-mediated proliferation (Wang *et al.,* 2011). SSeCKS scaffolds Src away from FAK complexes in lipid rafts, disengaging Src and FAK complexes from activation of the ERK pathway (Su *et al.,* 2013). This presumably accounts for the depletion of *Ccnd1* observed upon SSeCKS expression in fibroblasts (Lin *et al.,* 2000). These examples illustrate the essential requirement for scaffolding proteins in the regulation of cellular proliferation and quiescence.

When considering the role of Ikaros in proliferative arrest it may be useful to differentiate between quiescence, a reversible non-proliferative state of cells that have exited the cell cycle, and G1 checkpoint arrest. Although quiescent cells have the same 2*n* DNA content as G1 cells, they do not immediately re-enter the cell cycle

upon mitogenic stimulation. This was demonstrated by recording the time it took for each division in 3T3 fibroblasts following a period of serum starvation (Zetterberg and Larsson, 1985). Cells in early G1 (less than 3 hours after mitosis) required an additional 8 hours to progress through G1 phase following the re-addition of serum than cells in late G1. This time lag was attributed to a reversible exit of the cell cycle to the G0 state (Zetterberg and Larsson, 1985). Quiescence is not a passive state characterised by an absence of proliferation, instead it is actively maintained and transcriptionally distinct from proliferating G1 cells (Coller *et al.,* 2006). The Rb-E2F pathway is suggested to act as a bistable switch governing the quiescence-proliferation transition (Yao *et al.,* 2008). A minimal module governing this transition consists of a mutual inhibition loop between Rb and E2F and a feedforward input from Myc (Yao, 2014). This module converts graded and transient serum signalling into a binary all-or-nothing commitment to the cell cycle (Yao, 2014). The RNAseq data I obtained showed that Ikaros and SSeCKS could control the expression of *Myc* and *E2f* members that comprise this module. They can also downregulate the expression of cyclins and cyclin-dependent kinases that function as positive inputs into the E2F switch (Yao, 2014).

The delayed entry into the cell cycle displayed by quiescent cells is explained in part by the requirement to reform pre-replication complexes (pre-RC) at origins of replication (Coller, 2007). Origins are licensed for replication in G1 phase by the sequential assembly of CDC6 and CDT1 to the origin recognition complex (ORC), followed by loading of the replicative helicase MCM2-7 (Coller, 2007). Members of the pre-RC are downregulated in quiescent cells and are no longer bound to chromatin (Kingsbury *et al.,* 2005). Following serum stimulation the formation of the pre-RC precedes cell cycle entry and the reacquisition of proliferative capacity (Kingsbury *et al.,* 2005). *Cdc6*, *Cdt1, Mcm2-5* and *Mcm7* all appear in the list of genes synergistically downregulated by Ikaros and SSeCKS in the RNAseq data, suggesting that Ikaros can antagonise DNA synthesis. Ikaros also colocalises with the replication machinery at sites of late replicating heterochromatin in activated T cells

(Avitahl *et al.,* 1999). In this capacity Ikaros may regulate the accessibility of DNA to the replication machinery. These observations suggest the idea that Ikaros does not simply 'slow down' G1 progression through checkpoint arrest but instead induces a 'deeper' G0 state of quiescence that increases the threshold required to re-enter proliferation (Yao, 2014). This idea could be explored further by looking at the chromatin bound fraction of pre-RC members in pre-B cells and fibroblasts following Ikaros and SSeCKS induced cell cycle arrest.

In the data presented here I have shown that SSeCKS can negatively regulate cell cycle progression by repressing the expression of *Myc*. This provides an additional mechanism for the repression of *Myc* by Ikaros. Ikaros can upregulate the expression of *SSeCKS* to synergistically silence the expression of *Myc.* A potential model for the regulation of the cell cycle in pre-B cells is outlined in figure 6.1. This hypothetical model is based partly on the experimental data I have provided and inferences gleaned from the literature. My data shows that in addition to *Myc*, Ikaros and SSeCKS can synergistically regulate the expression of hundreds of other genes to enforce a quiescence-like state. Whilst the downregulation of *Myc* is important, it is unlikely to be the only requirement for cell cycle withdrawal. AP4 (*Tfap4*) is required to maintain the clonal expansion of activated lymphocytes after the initial transient peak in *Myc* expression has subsided (Chou *et al.,* 2014). By RNAseq analysis I showed that *Tfap4* is also synergistically repressed by Ikaros and SSeCKS. It is likely that Ikaros can regulate many parallel pathways through Myc-dependent and independent mechanisms. Removal of Ikaros or SSeCKS may result in a loss of growth suppression and cause aberrant proliferation (figure 6.1B). In the context of pre-B cell development this could cause a block in differentiation at the large cycling pre-B cell stage. It is therefore important to study the role of SSeCKS in the development of pre-B cells to better understand the nature of Ikaros as a suppressor of leukaemia.

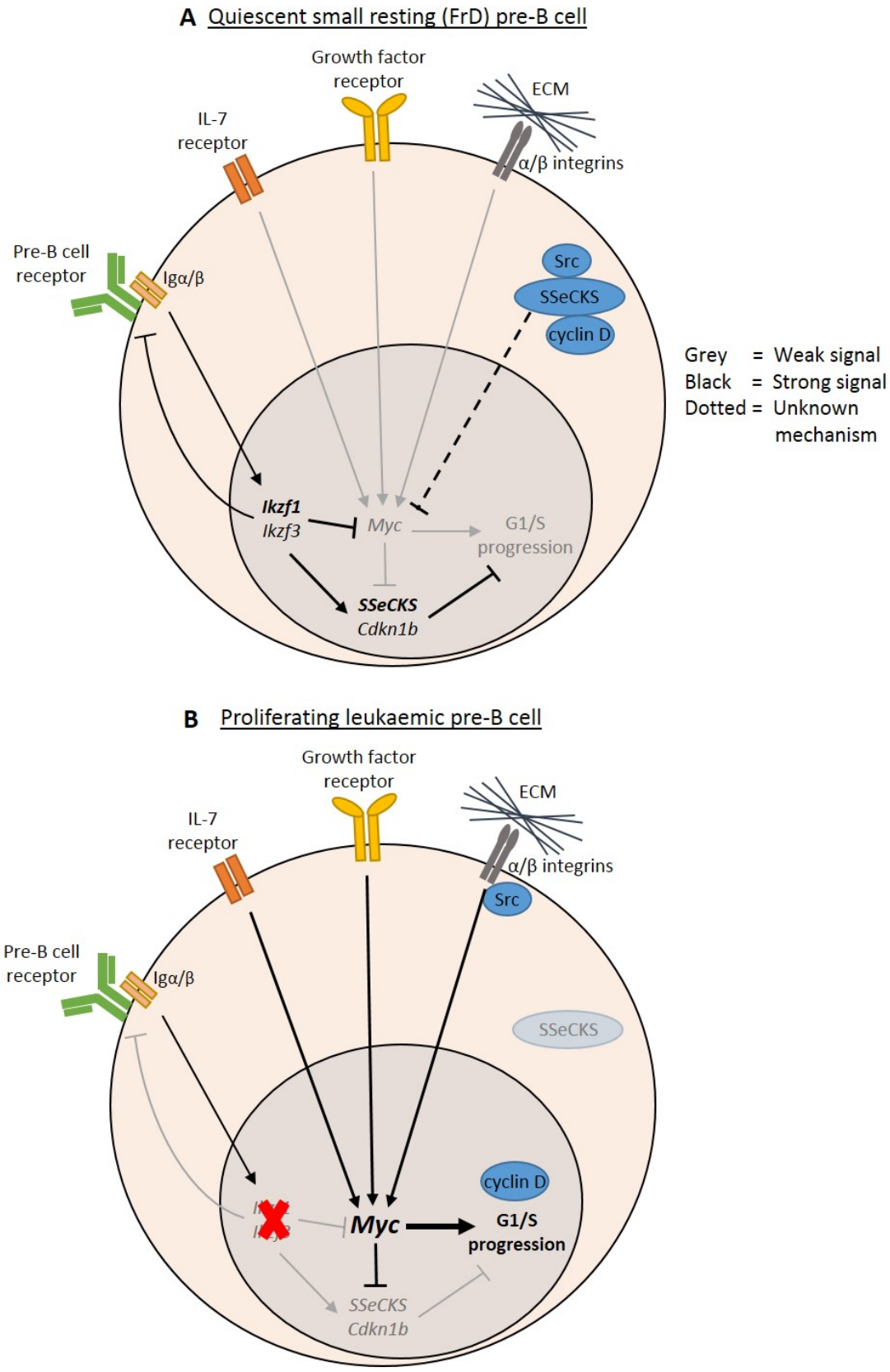
A Quiescent small resting (FrD) pre-B cell
Growth factor receptor
ECM
IL-7 receptor
α/β integrins
Pre-B cell receptor
Igα/β
Src
SSeCKS
cyclin D
Grey = Weak signal
Black = Strong signal
Dotted = Unknown mechanism
Ikzf1
Ikzf3
Myc
G1/S progression
SSeCKS
Cdkn1b
B Proliferating leukaemic pre-B cell
Growth factor receptor
ECM
IL-7 receptor
α/β integrins
Src
Pre-B cell receptor
Igα/β
SSeCKS
cyclin D
Myc
G1/S progression
SSeCKS
Cdkn1b

Figure 6.1 - **A balance between pro- and anti-proliferative signals determines the decision to cycle or remain quiescent**. (**A**) As the cells enter into the resting pre-B cell stage (FrD) pre-BCR signalling upregulates the expression of Ikaros family members which in turn downregulate pre-BCR signalling in a feedback loop. Ikaros is able to repress the expression of *Myc* and cyclin-dependent kinases and upregulate the expression of *Cdkn1b* and *SSeCKS*. SSeCKS cooperates with Ikaros to synergistically arrest the cell cycle. SSeCKS can potentially scaffold cyclin D in the cytoplasm and silence the expression of *Myc* through unknown mechanisms (dotted arrow). SSeCKS may disengage the activation of ERK by scaffolding Src away from adhesion junctions. Decreased ERK activity may partially compromise signalling downstream of cytokine, growth factor and integrin receptors (gray arrows), resulting in the depletion of Myc and entrance into a quiescent state. (**B**) *Ikzf1* deletions could alter the balance in favour of proliferation. The induction of negative regulators of the cell cycle could be compromised and pro-proliferative signals could be enhanced (Illustrated by thicker arrows). The dysregulation of Myc could promote inappropriate cell cycle progression, increasing the likelihood of further genomic instability and leukaemogenesis. *Ikzf1*=Ikaros, *Ikzf3*=Aiolos, *Cdkn1b*=p27, ECM= extracellular matrix.

6.1 Reflections and future directions

I performed an RNAi screen to probe Ikaros function in the regulation of the cell cycle. Advances in RNAi technology and next generation sequencing placed the possibility of performing large-scale loss of function screening within reach of the individual researcher. The pooled format of the screen allowed the simultaneous interrogation of thousands of genes that may contribute towards cell cycle arrest. By comparing the relative enrichment of each shRNA it was possible to identify genes that were required to cooperate with Ikaros to enforce cell cycle arrest. More recent technological advancements in genome editing technology have opened up new avenues of research by performing loss of function screens using clustered, regularly interspaced, short palindromic repeats coupled with Cas9 nuclease (CRISPR-Cas9). In this system a single-guide RNA (sgRNA) directs Cas9 double strand cleavage at homologous target loci. Indel mutations can arise from non-homologous end joining (NHEJ) repair of the double strand breaks. An array of sgRNA libraries have been developed that can systematically screen thousands of genes in positive

and negative selection loss of function screens (Sander and Joung, 2014). Such screens have been employed to enrich for factors that confer resistance to etoposide treatment in human leukaemic cell lines (Wang *et al.,* 2014) and resistance to a BRAF protein kinase inhibitor in melanoma (Shalem *et al.,* 2014). One advantage of CRISPR-Cas9 over RNAi is that it can result in gene knockout, as opposed to partial gene knockdown. This can ensure a complete loss of gene function. CRISPR-Cas9 can also be targeted to elements across the genome such as promoters, enhancers and introns. In other developments, catalytically inactive Cas9 can be fused to repressive chromatin modifying domains to silence gene transcription without deleting the gene (Gilbert *et al.,* 2013). Modifications to the sgRNA structure can facilitate the recruitment of an RNA binding protein, which in turn is fused to the transcription activation domains of different mammalian transcription factors (Konermann *et al.,* 2015). This can allow a systematic gain of function screen by activating the expression of a library of genes and non-coding RNAs (Konermann *et al.,* 2015). The creation of Cas9 transgenic mice has also opened up the possibility of performing *in vivo* sgRNA screens (Platt *et al.,* 2014). CRISPR-Cas9 does suffer from a similar potential for off-target effects as RNAi (Fu *et al.,* 2013). Mismatches outside of the essential 'seed region' of the sgRNA can lead to off-target activity (Jiang *et al.,* 2013). Modified Cas9 'nickases' have been developed that produce single strand nicks and can substantially reduce off target effects (Ran *et al.,* 2013). This is because double strand breaks require simultaneous cleavage by two closely spaced Cas9 enzymes. Individual off target nicks are efficiently repaired by base excision repair (Ran *et al.,* 2013). The ease and versatility of CRISPR-Cas9 technology means that it is becoming the tool of choice for performing genetic screens. For these reasons I would likely use this technology to perform future loss of function screens.

The analyses I have presented here have shone some light onto the complex mechanisms governing Ikaros-enforced cell cycle arrest. There are some areas however that could be given further consideration. The most obvious limitation of my study is that most of the experiments were performed in a reductionist system in

which Ikaros is not endogenously expressed. Ikaros regulates *SSeCKS* in pre-B cells and its expression is increased at the transition to the resting pre-B cell stage (FrD) (Immgen.org). This suggests that SSeCKS cooperates with Ikaros to enforce cell cycle arrest at this stage of pre-B cell development. In future work, I would like to demonstrate that SSeCKS is necessary and sufficient for Ikaros-mediated cell cycle arrest in pre-B cells. Non-adherent cell types are not suited to colony formation assays so I could detect proliferation rates more directly by PI staining or EdU incorporation. I could deplete SSeCKS in these cells using shRNA knockdown or CRISPR-Cas9 deletion to show the necessity of SSeCKS function in cell cycle arrest. To show that SSeCKS is sufficient to induce cell cycle arrest in pre-B cells I could use an *SSeCKS* overexpression construct similar to the TET regulated system in S24 cells. I could also potentially use the modified transactivating Cas9 to induce *SSeCKS* expression in pre-B cells (Konermann *et al.,* 2015). I would like to dissect the possible pathways that SSeCKS can use to enforce cell cycle arrest. SSeCKS may downregulate Myc expression through the attenuation of serum-induced ERK activation (Lin *et al.,* 2000). This could be tested by performing western blot with an antibody that recognizes active phosphorylated ERK using lysates obtained from cells arrested by Ikaros or SSeCKS. The use of MEK inhibitors could simulate SSeCKS overexpression by downregulating the expression of Myc and preventing entry into S phase (Cheng *et al.,* 1999; Marampon *et al.,* 2006). I showed that enforced expression of *Myc* was sufficient to override the cell cycle arrest induced by either Ikaros or SSeCKS. It would be interesting to test whether the combined action of Ikaros and SSeCKS together is sufficient to induce cell cycle arrest in the presence of enforced *Myc* expression. This could be achieved by transducing S24 cells with the inducible Myc-ERt2 and Ikaros-ERt2 expression constructs followed by cell cycle analysis. Focusing on the shRNA data, it would be useful to conduct a secondary screen in a manner outlined in 4.6.2 to identify further candidates required for Ikaros-induced cell cycle arrest. Finally a more nuanced analysis of the RNAseq data could be implemented. It would be interesting to compare the lists of differentially expressed genes in Ikaros and SSeCKS arrested cells with other publicly available

datasets analysing the transition from quiescence to proliferation in fibroblasts and haematopoetic cells. It may be possible to deduce an Ikaros and SSeCKS signature in the gene expression data that regulates this transition.

Bibliography

Adolfsson, J., Mansson, R., Buza-Vidas, N., Hultquist, A., Liuba, K., Jensen, C.T., Bryder, D., Yang, L., Borge, O.J., Thoren, L.A.*, et al.* (2005). Identification of Flt3+ lympho-myeloid stem cells lacking erythro-megakaryocytic potential a revised road map for adult blood lineage commitment. Cell *121*, 295-306.
Akakura, S., and Gelman, I.H. (2012). Pivotal Role of AKAP12 in the Regulation of Cellular Adhesion Dynamics: Control of Cytoskeletal Architecture, Cell Migration, and Mitogenic Signaling. Journal of signal transduction *2012*, 529179.
Akakura, S., Huang, C.H., Nelson, P.J., Foster, B., and Gelman, I.H. (2008). Loss of the ssecks/gravin/akap12 gene results in prostatic hyperplasia. Cancer Research *68*, 5096-5103.
Alcorta, D.A., Xiong, Y., Phelps, D., Hannon, G., Beach, D., and Barrett, J.C. (1996). Involvement of the cyclin-dependent kinase inhibitor p16 (INK4a) in replicative senescence of normal human fibroblasts. Proc Natl Acad Sci U S A *93*, 13742-13747.
Alexandrow, M.G., Kawabata, M., Aakre, M., and Moses, H.L. (1995). Overexpression of the C-Myc Oncoprotein Blocks the Growth-Inhibitory Response but Is Required for the Mitogenic Effects of Transforming Growth-Factor-Beta-1. P Natl Acad Sci USA *92*, 3239-3243.
Alkhatib, A., Werner, M., Hug, E., Herzog, S., Eschbach, C., Faraidun, H., Kohler, F., Wossning, T., and Jumaa, H. (2012). FoxO1 induces Ikaros splicing to promote immunoglobulin gene recombination. J Exp Med *209*, 395-406.
Anders, S., and Huber, W. (2010). Differential expression analysis for sequence count data. Genome biology *11*.
Avitahl, N., Winandy, S., Friedrich, C., Jones, B., Ge, Y., and Georgopoulos, K. (1999). Ikaros sets thresholds for T cell activation and regulates chromosome propagation. Immunity *10*, 333-343.
Ayer, D.E., Kretzner, L., and Eisenman, R.N. (1993). Mad: a heterodimeric partner for Max that antagonizes Myc transcriptional activity. Cell *72*, 211-222.
Bassermann, F., Eichner, R., and Pagano, M. (2014). The ubiquitin proteasome system - Implications for cell cycle control and the targeted treatment of cancer. Bba-Mol Cell Res *1843*, 150-162.
Bassik, M.C., Lebbink, R.J., Churchman, L.S., Ingolia, N.T., Patena, W., LeProust, E.M., Schuldiner, M., Weissman, J.S., and McManus, M.T. (2009). Rapid creation and quantitative monitoring of high coverage shRNA libraries. Nat Methods *6*, 443-U462.
Baudino, T.A., and Cleveland, J.L. (2001). The Max network gone mad. Mol Cell Biol *21*, 691-702.
Benaud, C.M., and Dickson, R.B. (2001). Regulation of the expression of c-Myc by beta1 integrins in epithelial cells. Oncogene *20*, 759-768.
Berberich, S., Hyde-DeRuyscher, N., Espenshade, P., and Cole, M. (1992). max encodes a sequence-specific DNA-binding protein and is not regulated by serum growth factors. Oncogene *7*, 775-779.

Berenjeno, I.M., Nunez, F., and Bustelo, X.R. (2007). Transcriptomal profiling of the cellular transformation induced by Rho subfamily GTPases. Oncogene *26*, 4295-4305.
Bernards, R., Brummelkamp, T.R., and Beijersbergen, R.L. (2006). shRNA libraries and their use in cancer genetics. Nat Methods *3*, 701-706.
Berns, K., Hijmans, E.M., Mullenders, J., Brummelkamp, T.R., Velds, A., Heimerikx, M., Kerkhoven, R.M., Madiredjo, M., Nijkamp, W., Weigelt, B.*, et al.* (2004). A large-scale RNAi screen in human cells identifies new components of the p53 pathway. Nature *428*, 431-437.
Bernstein, E., Caudy, A.A., Hammond, S.M., and Hannon, G.J. (2001). Role for a bidentate ribonuclease in the initiation step of RNA interference. Nature *409*, 363-366.
Beronja, S., Janki, P., Heller, E., Lien, W.H., Keyes, B.E., Oshimori, N., and Fuchs, E. (2013). RNAi screens in mice identify physiological regulators of oncogenic growth. Nature *501*, 185-+.
Blackwood, E.M., and Eisenman, R.N. (1991). Max: a helix-loop-helix zipper protein that forms a sequence-specific DNA-binding complex with Myc. Science *251*, 1211-1217.
Blomberg, I., and Hoffmann, I. (1999). Ectopic expression of Cdc25A accelerates the G(1)/S transition and leads to premature activation of cyclin E- and cyclin A-dependent kinases. Mol Cell Biol *19*, 6183-6194.
Botz, J., Zerfass-Thome, K., Spitkovsky, D., Delius, H., Vogt, B., Eilers, M., Hatzigeorgiou, A., and Jansen-Durr, P. (1996). Cell cycle regulation of the murine cyclin E gene depends on an E2F binding site in the promoter. Mol Cell Biol *16*, 3401-3409.
Boultwood, J., Pellagatti, A., Watkins, F., Campbell, L.J., Esoof, N., Cross, N.C.P., Eagleton, H., Littlewood, T.J., Fidler, C., and Wainscoat, J.S. (2004). Low expression of the putative tumour suppressor gene gravin in chronic myeloid leukaemia, myelodysplastic syndromes and acute myeloid leukaemia. Brit J Haematol *126*, 508-511.
Brandt, D., Baarlink, C., Kitzing, T., Kremmer, E., Ivaska, J., Nollau, P., and Grosse, R. (2009). SCAI acts as a suppressor of cancer cell invasion through the transcriptional control of beta 1-integrin. European journal of cell biology *88*, 25-25.
Bretones, G., Delgado, M.D., and Leon, J. (2015). Myc and cell cycle control. Biochim Biophys Acta *1849*, 506-516.
Brown, K.E., Baxter, J., Graf, D., Merkenschlager, M., and Fisher, A.G. (1999). Dynamic repositioning of genes in the nucleus of lymphocytes preparing for cell division. Mol Cell *3*, 207-217.
Brown, K.E., Guest, S.S., Smale, S.T., Hahm, K., Merkenschlager, M., and Fisher, A.G. (1997). Association of transcriptionally silent genes with Ikaros complexes at centromeric heterochromatin. Cell *91*, 845-854.
Bu, Y., and Gelman, I.H. (2007). v-Src-mediated down-regulation of SSeCKS metastasis suppressor gene promoter by the recruitment of HDAC1 into a USF1-Sp1-Sp3 complex. J Biol Chem *282*, 26725-26739.
Burrows, A.E., Smogorzewska, A., and Elledge, S.J. (2010). Polybromo-associated BRG1-associated factor components BRD7 and BAF180 are critical regulators of p53

required for induction of replicative senescence. P Natl Acad Sci USA *107*, 14280-14285.
Busslinger, M. (2004). Transcriptional control of early B cell development. Annu Rev Immunol *22*, 55-79.
Campeau, E., and Gobeil, S. (2011). RNA interference in mammals: behind the screen. Brief Funct Genomics *10*, 215-226.
Camus, A., Mesbah, K., Rallu, M., Babinet, C., and Barra, J. (2001). Gene trap insertion reveals two open reading frames in the mouse SSeCKS gene: the form predominantly detected in the nervous system is suppressed by the insertion while the other, specific of the testis, remains expressed. Mechanisms of development *105*, 79-91.
Cedar, H., and Bergman, Y. (2011). Epigenetics of haematopoietic cell development. Nat Rev Immunol *11*, 478-488.
Chellappan, S.P., Hiebert, S., Mudryj, M., Horowitz, J.M., and Nevins, J.R. (1991). The E2F transcription factor is a cellular target for the RB protein. Cell *65*, 1053-1061.
Chen, C., Liu, Y., Rappaport, A.R., Kitzing, T., Schultz, N., Zhao, Z., Shroff, A.S., Dickins, R.A., Vakoc, C.R., Bradner, J.E*., et al.* (2014). MLL3 Is a Haploinsufficient 7q Tumor Suppressor in Acute Myeloid Leukemia. Cancer Cell *25*, 652-665.
Chen, X., Esplin, B.L., Garrett, K.P., Welner, R.S., Webb, C.F., and Kincade, P.W. (2008). Retinoids accelerate B lineage lymphoid differentiation. J Immunol *180*, 138-145.
Cheng, M., Wang, D., and Roussel, M.F. (1999). Expression of c-Myc in response to colony-stimulating factor-1 requires mitogen-activated protein kinase kinase-1. J Biol Chem *274*, 6553-6558.
Chou, C., Pinto, A.K., Curtis, J.D., Persaud, S.P., Cella, M., Lin, C.C., Edelson, B.T., Allen, P.M., Colonna, M., Pearce, E.L*., et al.* (2014). c-Myc-induced transcription factor AP4 is required for host protection mediated by CD8(+) T cells. Nature Immunology *15*, 884-893.
Clark, M.R., Mandal, M., Ochiai, K., and Singh, H. (2014). Orchestrating B cell lymphopoiesis through interplay of IL-7 receptor and pre-B cell receptor signalling. Nat Rev Immunol *14*, 69-80.
Cobb, B.S., Morales-Alcelay, S., Kleiger, G., Brown, K.E., Fisher, A.G., and Smale, S.T. (2000). Targeting of Ikaros to pericentromeric heterochromatin by direct DNA binding. Genes Dev *14*, 2146-2160.
Coffin, J.M., Hughes, S.H., Varmus, H.E. (1997). Retroviruses. Cold Spring Harbor (NY): Cold Spring Harbor Laboratory Press; 1997. ISBN-10: 0-87969-571-4.
Coller, H.A. (2007). What's taking so long? S-phase entry from quiescence versus proliferation. Nat Rev Mol Cell Bio *8*, 667-670.
Coller, H.A., Grandori, C., Tamayo, P., Colbert, T., Lander, E.S., Eisenman, R.N., and Golub, T.R. (2000). Expression analysis with oligonucleotide microarrays reveals that MYC regulates genes involved in growth, cell cycle, signaling, and adhesion. Proc Natl Acad Sci U S A *97*, 3260-3265.
Coller, H.A., Sang, L.Y., and Roberts, J.M. (2006). A new description of cellular quiescence. Plos Biology *4*, 329-349.

Cooper, A.B., Sawai, C.M., Sicinska, E., Powers, S.E., Sicinski, P., Clark, M.R., and Aifantis, I. (2006). A unique function for cyclin D3 in early B cell development. Nat Immunol *7*, 489-497.
Corfe, S.A., and Paige, C.J. (2012). The many roles of IL-7 in B cell development; mediator of survival, proliferation and differentiation. Seminars in immunology *24*, 198-208.
Cowling, V.H., and Cole, M.D. (2007). The Myc transactivation domain promotes global phosphorylation of the RNA polymerase II carboxy-terminal domain independently of direct DNA binding. Mol Cell Biol *27*, 2059-2073.
Dalla-Favera, R., Bregni, M., Erikson, J., Patterson, D., Gallo, R.C., and Croce, C.M. (1982). Human c-myc onc gene is located on the region of chromosome 8 that is translocated in Burkitt lymphoma cells. Proc Natl Acad Sci U S A *79*, 7824-7827.
Dang, C.V. (1999). c-myc target genes involved in cell growth, apoptosis, and metabolism. Molecular and Cellular Biology *19*, 1-11.
Dang, C.V. (2012). MYC on the path to cancer. Cell *149*, 22-35.
Dang, C.V., Le, A., and Gao, P. (2009). MYC-Induced Cancer Cell Energy Metabolism and Therapeutic Opportunities. Clinical Cancer Research *15*, 6479-6483.
Dean, M., Levine, R.A., Ran, W., Kindy, M.S., Sonenshein, G.E., and Campisi, J. (1986). Regulation of c-myc transcription and mRNA abundance by serum growth factors and cell contact. J Biol Chem *261*, 9161-9166.
Dege, C., and Hagman, J. (2014). Mi-2/NuRD chromatin remodeling complexes regulate B and T-lymphocyte development and function. Immunological reviews *261*, 126-140.
DeGregori, J., and Johnson, D.G. (2006). Distinct and overlapping roles for E2F family members in transcription, proliferation and apoptosis. Curr Mol Med *6*, 739-748.
Desai, D., Gu, Y., and Morgan, D.O. (1992). Activation of human cyclin-dependent kinases in vitro. Molecular biology of the cell *3*, 571-582.
Dyson, N. (1998). The regulation of E2F by pRB-family proteins. Genes Dev *12*, 2245-2262.
Egawa, T., and Littman, D.R. (2011). Transcription factor AP4 modulates reversible and epigenetic silencing of the Cd4 gene. P Natl Acad Sci USA *108*, 14873-14878.
Eilers, M., Picard, D., Yamamoto, K.R., and Bishop, J.M. (1989). Chimaeras of myc oncoprotein and steroid receptors cause hormone-dependent transformation of cells. Nature *340*, 66-68.
Eilers, M., Schirm, S., and Bishop, J.M. (1991). The MYC protein activates transcription of the alpha-prothymosin gene. EMBO J *10*, 133-141.
Elbashir, S.M., Harborth, J., Lendeckel, W., Yalcin, A., Weber, K., and Tuschl, T. (2001). Duplexes of 21-nucleotide RNAs mediate RNA interference in cultured mammalian cells. Nature *411*, 494-498.
Evans, T., Rosenthal, E.T., Youngblom, J., Distel, D., and Hunt, T. (1983). Cyclin: a protein specified by maternal mRNA in sea urchin eggs that is destroyed at each cleavage division. Cell *33*, 389-396.
Fabbro, M., Savage, K., Hobson, K., Deans, A.J., Powell, S.N., McArthur, G.A., and Khanna, K.K. (2004). BRCA1-BARD1 complexes are required for p53(Ser-15)

phosphorylation and a G(1)/S arrest following ionizing radiation-induced DNA damage. Journal of Biological Chemistry *279*, 31251-31258.
Ferreiros-Vidal, I., Carroll, T., Taylor, B., Terry, A., Liang, Z., Bruno, L., Dharmalingam, G., Khadayate, S., Cobb, B.S., Smale, S.T*., et al.* (2013). Genome-wide identification of Ikaros targets elucidates its contribution to mouse B-cell lineage specification and pre-B-cell differentiation. Blood *121*, 1769-1782.
Fire, A., Xu, S.Q., Montgomery, M.K., Kostas, S.A., Driver, S.E., and Mello, C.C. (1998). Potent and specific genetic interference by double-stranded RNA in Caenorhabditis elegans. Nature *391*, 806-811.
Fisher, A.G., Burdet, C., Bunce, C., Merkenschlager, M., and Ceredig, R. (1995). Lymphoproliferative Disorders in Il-7 Transgenic Mice - Expansion of Immature B-Cells Which Retain Macrophage Potential. International immunology *7*, 415-423.
Flaberg, E., Markasz, L., Petranyi, G., Stuber, G., Dicso, F., Alchihabi, N., Olah, E., Csizy, I., Jozsa, T., Andren, O*., et al.* (2011). High-throughput live-cell imaging reveals differential inhibition of tumor cell proliferation by human fibroblasts. International Journal of Cancer *128*, 2793-2802.
Flemming, A., Brummer, T., Reth, M., and Jumaa, H. (2003). The adaptor protein SLP-65 acts as a tumor suppressor that limits pre-B cell expansion. Nat Immunol *4*, 38-43.
Flotho, C., Paulun, A., Batz, C., and Niemeyer, C.M. (2007). AKAP12, a gene with tumour suppressor properties, is a target of promoter DNA methylation in childhood myeloid malignancies. Brit J Haematol *138*, 644-650.
Fu, C., Turck, C.W., Kurosaki, T., and Chan, A.C. (1998). BLNK: a central linker protein in B cell activation. Immunity *9*, 93-103.
Fu, Y., Foden, J.A., Khayter, C., Maeder, M.L., Reyon, D., Joung, J.K., and Sander, J.D. (2013). High-frequency off-target mutagenesis induced by CRISPR-Cas nucleases in human cells. Nat Biotechnol *31*, 822-826.
Gartel, A.L., and Shchors, K. (2003). Mechanisms of c-myc-mediated transcriptional repression of growth arrest genes. Exp Cell Res *283*, 17-21.
Gelman, I.H. (2010). Emerging Roles for SSeCKS/Gravin/AKAP12 in the Control of Cell Proliferation, Cancer Malignancy, and Barriergenesis. Genes & cancer *1*, 1147-1156.
Gelman, I.H. (2012). Suppression of tumor and metastasis progression through the scaffolding functions of SSeCKS/Gravin/AKAP12. Cancer Metast Rev *31*, 493-500.
Gelman, I.H., and Gao, L.Q. (2006). SSeCKS/Gravin/AKAP12 metastasis suppressor inhibits podosome formation via RhoA- and Cdc42-dependent pathways. Molecular Cancer Research *4*, 151-158.
Georgopoulos, K., Bigby, M., Wang, J.H., Molnar, A., Wu, P., Winandy, S., and Sharpe, A. (1994). The Ikaros gene is required for the development of all lymphoid lineages. Cell *79*, 143-156.
Georgopoulos, K., Moore, D.D., and Derfler, B. (1992). Ikaros, an early lymphoid-specific transcription factor and a putative mediator for T cell commitment. Science *258*, 808-812.
Ghadiri, A., Duhamel, M., Fleischer, A., Reimann, A., Dessauge, F., and Rebollo, A. (2007). Critical function of Ikaros in controlling Aiolos gene expression. Febs Letters *581*, 1605-1616.

Gilbert, L.A., Larson, M.H., Morsut, L., Liu, Z.R., Brar, G.A., Torres, S.E., Stern-Ginossar, N., Brandman, O., Whitehead, E.H., Doudna, J.A., *et al.* (2013). CRISPR-Mediated Modular RNA-Guided Regulation of Transcription in Eukaryotes. Cell *154*, 442-451.
Goetz, C.A., Harmon, I.R., O'Neil, J.J., Burchill, M.A., and Farrar, M.A. (2004). STAT5 activation underlies IL7 receptor-dependent B cell development. J Immunol *172*, 4770-4778.
Gomez-del Arco, P., Maki, K., and Georgopoulos, K. (2004). Phosphorylation controls Ikaros's ability to negatively regulate the G(1)-S transition. Molecular and Cellular Biology *24*, 2797-2807.
Good, M.C., Zalatan, J.G., and Lim, W.A. (2011). Scaffold proteins: hubs for controlling the flow of cellular information. Science *332*, 680-686.
Gunjan, A., Paik, J., and Verreault, A. (2005). Regulation of histone synthesis and nucleosome assembly. Biochimie *87*, 625-635.
Gurel, Z., Ronni, T., Ho, S., Kuchar, J., Payne, K.J., Turk, C.W., and Dovat, S. (2008). Recruitment of ikaros to pericentromeric heterochromatin is regulated by phosphorylation. J Biol Chem *283*, 8291-8300.
Hahm, K., Cobb, B.S., McCarty, A.S., Brown, K.E., Klug, C.A., Lee, R., Akashi, K., Weissman, I.L., Fisher, A.G., and Smale, S.T. (1998). Helios, a T cell-restricted Ikaros family member that quantitatively associates with Ikaros at centromeric heterochromatin. Genes Dev *12*, 782-796.
Hahm, K., Ernst, P., Lo, K., Kim, G.S., Turck, C., and Smale, S.T. (1994). The lymphoid transcription factor LyF-1 is encoded by specific, alternatively spliced mRNAs derived from the Ikaros gene. Mol Cell Biol *14*, 7111-7123.
Hammond, S.M., Bernstein, E., Beach, D., and Hannon, G.J. (2000). An RNA-directed nuclease mediates post-transcriptional gene silencing in Drosophila cells. Nature *404*, 293-296.
Han, B., Poppinga, W.J., and Schmidt, M. (2015). Scaffolding during the cell cycle by A-kinase anchoring proteins. Pflugers Archiv : European journal of physiology.
Hanahan, D., and Weinberg, R.A. (2000). The hallmarks of cancer. Cell *100*, 57-70.
Hanahan, D., and Weinberg, R.A. (2011). Hallmarks of cancer: the next generation. Cell *144*, 646-674.
Hardy, R.R., Carmack, C.E., Shinton, S.A., Kemp, J.D., and Hayakawa, K. (1991). Resolution and characterization of pro-B and pre-pro-B cell stages in normal mouse bone marrow. J Exp Med *173*, 1213-1225.
Harker, N., Naito, T., Cortes, M., Hostert, A., Hirschberg, S., Tolaini, M., Roderick, K., Georgopoulos, K., and Kioussis, D. (2002). The CD8 alpha gene locus is regulated by the Ikaros family of proteins. Molecular Cell *10*, 1403-1415.
Hartwell, L.H., Culotti, J., Pringle, J.R., and Reid, B.J. (1974). Genetic control of the cell division cycle in yeast. Science *183*, 46-51.
Heiden, M.G.V., Cantley, L.C., and Thompson, C.B. (2009). Understanding the Warburg Effect: The Metabolic Requirements of Cell Proliferation. Science *324*, 1029-1033.
Heizmann, B., Kastner, P., and Chan, S. (2013). Ikaros is absolutely required for pre-B cell differentiation by attenuating IL-7 signals. J Exp Med *210*, 2823-2832.

Hendriks, R.W., and Middendorp, S. (2004). The pre-BCR checkpoint as a cell-autonomous proliferation switch. Trends Immunol *25*, 249-256.
Heng, T.S., Painter, M.W., and Immunological Genome Project, C. (2008). The Immunological Genome Project: networks of gene expression in immune cells. Nat Immunol *9*, 1091-1094.
Herzog, S., Reth, M., and Jumaa, H. (2009). Regulation of B-cell proliferation and differentiation by pre-B-cell receptor signalling. Nat Rev Immunol *9*, 195-205.
Hess, J., Werner, A., Wirth, T., Melchers, F., Jack, H.M., and Winkler, T.H. (2001). Induction of pre-B cell proliferation after de novo synthesis of the pre-B cell receptor. Proc Natl Acad Sci U S A *98*, 1745-1750.
Hiebert, S.W., Chellappan, S.P., Horowitz, J.M., and Nevins, J.R. (1992). The interaction of RB with E2F coincides with an inhibition of the transcriptional activity of E2F. Genes Dev *6*, 177-185.
Honma, Y., Kiyosawa, H., Mori, T., Oguri, A., Nikaido, T., Kanazawa, K., Tojo, M., Takeda, J., Tanno, Y., Yokoya, S.*, et al.* (1999). Eos: a novel member of the Ikaros gene family expressed predominantly in the developing nervous system. FEBS Lett *447*, 76-80.
Huang, D.W., Sherman, B.T., and Lempicki, R.A. (2009). Systematic and integrative analysis of large gene lists using DAVID bioinformatics resources. Nat Protoc *4*, 44-57.
Iguchi, T., Aoki, K., Ikawa, T., Taoka, M., Taya, C., Yoshitani, H., Toma-Hirano, M., Koiwai, O., Isobe, T., Kawamoto, H.*, et al.* (2015). BTB-ZF Protein Znf131 Regulates Cell Growth of Developing and Mature T Cells. J Immunol *195*, 982-993.
Ikematsu, N., Yoshida, Y., Kawamura-Tsuzuku, J., Ohsugi, M., Onda, M., Hirai, M., Fujimoto, J., and Yamamoto, T. (1999). Tob2, a novel anti-proliferative Tob/BTG1 family member, associates with a component of the CCR4 transcriptional regulatory complex capable of binding cyclin-dependent kinases. Oncogene *18*, 7432-7441.
Iusuf, D., Teunissen, S.F., Wagenaar, E., Rosing, H., Beijnen, J.H., and Schinkel, A.H. (2011). P-Glycoprotein (ABCB1) Transports the Primary Active Tamoxifen Metabolites Endoxifen and 4-Hydroxytamoxifen and Restricts Their Brain Penetration. J Pharmacol Exp Ther *337*, 710-717.
Jackstadt, R., and Hermeking, H. (2014). AP4 is required for mitogen- and c-MYC-induced cell cycle progression. Oncotarget *5*, 7316-7327.
Jiang, W.Y., Bikard, D., Cox, D., Zhang, F., and Marraffini, L.A. (2013). RNA-guided editing of bacterial genomes using CRISPR-Cas systems. Nature Biotechnology *31*, 233-239.
Johnson, D.G., Schwarz, J.K., Cress, W.D., and Nevins, J.R. (1993). Expression of transcription factor E2F1 induces quiescent cells to enter S phase. Nature *365*, 349-352.
Joshi, I., Yoshida, T., Jena, N., Qi, X., Zhang, J., Van Etten, R.A., and Georgopoulos, K. (2014). Loss of Ikaros DNA-binding function confers integrin-dependent survival on pre-B cells and progression to acute lymphoblastic leukemia. Nat Immunol *15*, 294-304.
Juliano, R. (2009). SCAI blocks MAL-evolent effects on cancer cell invasion. Nature Cell Biology *11*, 540-542.

Jung, P., and Hermeking, H. (2009). The c-MYC-AP4-p21 cascade. Cell Cycle *8*, 982-989.

Jung, P., Menssen, A., Mayr, D., and Hermeking, H. (2008). AP4 encodes a c-MYC-inducible repressor of p21. Proc Natl Acad Sci U S A *105*, 15046-15051.
Jung, Y.S., Qian, Y.J., and Chen, X.B. (2010). Examination of the expanding pathways for the regulation of p21 expression and activity. Cellular signalling *22*, 1003-1012.
Karmaus, P.W.F., and Chi, H.B. (2014). c-Myc and AP4: a relay team for metabolic reprogramming of CD8(+) T cells. Nature Immunology *15*, 828-829.
Kathrein, K.L., Lorenz, R., Innes, A.M., Griffiths, E., and Winandy, S. (2005). Ikaros induces quiescence and T-cell differentiation in a leukemia cell line. Mol Cell Biol *25*, 1645-1654.
Kato, J., Matsushime, H., Hiebert, S.W., Ewen, M.E., and Sherr, C.J. (1993). Direct binding of cyclin D to the retinoblastoma gene product (pRb) and pRb phosphorylation by the cyclin D-dependent kinase CDK4. Genes Dev *7*, 331-342.
Kerkhoff, E., Houben, R., Loffler, S., Troppmair, J., Lee, J.E., and Rapp, U.R. (1998). Regulation of c-myc expression by Ras/Raf signalling. Oncogene *16*, 211-216.
Kikuchi, K., Lai, A.Y., Hsu, C.L., and Kondo, M. (2005). IL-7 receptor signaling is necessary for stage transition in adult B cell development through up-regulation of EBF. J Exp Med *201*, 1197-1203.
Kim, J., Sif, S., Jones, B., Jackson, A., Koipally, J., Heller, E., Winandy, S., Viel, A., Sawyer, A., Ikeda, T.*, et al.* (1999). Ikaros DNA-binding proteins direct formation of chromatin remodeling complexes in lymphocytes. Immunity *10*, 345-355.
Kingsbury, S.R., Loddo, M., Fanshawe, T., Obermann, E.C., Prevost, A.T., Stoeber, K., and Williams, G.H. (2005). Repression of DNA replication licensing in quiescence is independent of geminin and may define the cell cycle state of progenitor cells. Experimental Cell Research *309*, 56-67.
Kirstetter, P., Thomas, M., Dierich, A., Kastner, P., and Chan, S. (2002). Ikaros is critical for B cell differentiation and function. Eur J Immunol *32*, 720-730.
Klein, F., Feldhahn, N., Herzog, S., Sprangers, M., Mooster, J.L., Jumaa, H., and Muschen, M. (2006). BCR-ABL1 induces aberrant splicing of IKAROS and lineage infidelity in pre-B lymphoblastic leukemia cells. Oncogene *25*, 1118-1124.
Knoepfler, P.S., Zhang, X.Y., Cheng, P.F., Gafken, P.R., McMahon, S.B., and Eisenman, R.N. (2006). Myc influences global chromatin structure. EMBO J *25*, 2723-2734.
Ko, H.K., Guo, L.W., Su, B., Gao, L.Q., and Gelman, I.H. (2014). Suppression of Chemotaxis by SSeCKS via Scaffolding of Phosphoinositol Phosphates and the Recruitment of the Cdc42 GEF, Frabin, to the Leading Edge. Plos One *9*.
Koff, A., Giordano, A., Desai, D., Yamashita, K., Harper, J.W., Elledge, S., Nishimoto, T., Morgan, D.O., Franza, B.R., and Roberts, J.M. (1992). Formation and activation of a cyclin E-cdk2 complex during the G1 phase of the human cell cycle. Science *257*, 1689-1694.
Koipally, J., and Georgopoulos, K. (2000). Ikaros interactions with CtBP reveal a repression mechanism that is independent of histone deacetylase activity. J Biol Chem *275*, 19594-19602.
Koipally, J., Kim, J., Jones, B., Jackson, A., Avitahl, N., Winandy, S., Trevisan, M., Nichogiannopoulou, A., Kelley, C., and Georgopoulos, K. (1999). Ikaros chromatin

remodeling complexes in the control of differentiation of the hemo-lymphoid system. Cold Spring Harb Symp Quant Biol *64*, 79-86.
Kolfschoten, I.G.M., van Leeuwen, B., Berns, K., Mullenders, J., Beijersbergen, R.L., Bernards, R., Voorhoeve, P.M., and Agami, R. (2005). A genetic screen identifies PITX1 as a suppressor of RAS activity and tumorigenicity. Cell *121*, 849-858.
Konermann, S., Brigham, M.D., Trevino, A.E., Joung, J., Abudayyeh, O.O., Barcena, C., Hsu, P.D., Habib, N., Gootenberg, J.S., Nishimasu, H.*, et al.* (2015). Genome-scale transcriptional activation by an engineered CRISPR-Cas9 complex. Nature *517*, 583-U332.
Kozar, K., Ciemerych, M.A., Rebel, V.I., Shigematsu, H., Zagozdzon, A., Sicinska, E., Geng, Y., Yu, Q., Bhattacharya, S., Bronson, R.T.*, et al.* (2004). Mouse development and cell proliferation in the absence of D-cyclins. Cell *118*, 477-491.
Kressner, C., Nollau, P., Grosse, R., and Brandt, D.T. (2013). Functional Interaction of SCAI with the SWI/SNF Complex for Transcription and Tumor Cell Invasion. Plos One *8*.
Land, H., Parada, L.F., and Weinberg, R.A. (1983). Tumorigenic conversion of primary embryo fibroblasts requires at least two cooperating oncogenes. Nature *304*, 596-602.
Langdon, W.Y., Harris, A.W., Cory, S., and Adams, J.M. (1986). The c-myc oncogene perturbs B lymphocyte development in E-mu-myc transgenic mice. Cell *47*, 11-18.
Lee, I.H., and Finkel, T. (2013). Metabolic regulation of the cell cycle. Current opinion in cell biology *25*, 724-729.
Li, Z., Song, C., Ouyang, H., Lai, L., Payne, K.J., and Dovat, S. (2012). Cell cycle-specific function of Ikaros in human leukemia. Pediatr Blood Cancer *59*, 69-76.
Lin, X., and Gelman, I.H. (2002). Calmodulin and cyclin D anchoring sites on the Src-suppressed C kinase substrate, SSeCKS. Biochem Biophys Res Commun *290*, 1368-1375.
Lin, X., Nelson, P., and Gelman, I.H. (2000). SSeCKS, a major protein kinase C substrate with tumor suppressor activity, regulates G(1)-->S progression by controlling the expression and cellular compartmentalization of cyclin D. Mol Cell Biol *20*, 7259-7272.
Lin, X., Nelson, P.J., Frankfort, B., Tombler, E., Johnson, R., and Gelman, I.H. (1995). Isolation and characterization of a novel mitogenic regulatory gene, 322, which is transcriptionally suppressed in cells transformed by src and ras. Mol Cell Biol *15*, 2754-2762.
Lin, X.Y., and Gelman, I.H. (1997). Reexpression of the major protein kinase C substrate, SSeCKS, suppresses v-src-induced morphological transformation and tumorigenesis. Cancer Research *57*, 2304-2312.
Lin, X.Y., Tombler, E., Nelson, P.J., Ross, M., and Gelman, I.H. (1996). A novel src- and ras-suppressed protein kinase c substrate associated with cytoskeletal architecture. Journal of Biological Chemistry *271*, 28430-28438.
Liu, H.O., Huang, X.D., Wang, H.M., Shen, A.G., and Cheng, C. (2009). Dexamethasone inhibits proliferation and stimulates SSeCKS expression in C6 rat glioma cell line. Brain research *1265*, 1-12.

Liu, J.D., Carmell, M.A., Rivas, F.V., Marsden, C.G., Thomson, J.M., Song, J.J., Hammond, S.M., Joshua-Tor, L., and Hannon, G.J. (2004). Argonaute2 is the catalytic engine of mammalian RNAi. Science *305*, 1437-1441.
Liu, Y., Gao, L., and Gelman, I.H. (2006a). SSeCKS/Gravin/AKAP12 attenuates expression of proliferative and angiogenic genes during suppression of v-Src-induced oncogenesis. BMC cancer *6*, 105.
Liu, Y.Z., Gao, L.Q., and Gelman, I.H. (2006b). SSeCKS/Gravin/AKAP12 attenuates expression of proliferative and angiogenic genes during suppression of v-Src-induced oncogenesis. BMC cancer *6*.
Lizardi, P.M., Forloni, M., and Wajapeyee, N. (2011). Genome-wide approaches for cancer gene discovery. Trends in biotechnology *29*, 558-568.
Lo, K., Landau, N.R., and Smale, S.T. (1991). LyF-1, a transcriptional regulator that interacts with a novel class of promoters for lymphocyte-specific genes. Mol Cell Biol *11*, 5229-5243.
Ludlow, J.W., Shon, J., Pipas, J.M., Livingston, D.M., and DeCaprio, J.A. (1990). The retinoblastoma susceptibility gene product undergoes cell cycle-dependent dephosphorylation and binding to and release from SV40 large T. Cell *60*, 387-396.
Ma, S., Pathak, S., Mandal, M., Trinh, L., Clark, M.R., and Lu, R. (2010). Ikaros and Aiolos inhibit pre-B-cell proliferation by directly suppressing c-Myc expression. Mol Cell Biol *30*, 4149-4158.
Ma, S., Pathak, S., Trinh, L., and Lu, R. (2008). Interferon regulatory factors 4 and 8 induce the expression of Ikaros and Aiolos to down-regulate pre-B-cell receptor and promote cell-cycle withdrawal in pre-B-cell development. Blood *111*, 1396-1403.
Mackarehtschian, K., Hardin, J.D., Moore, K.A., Boast, S., Goff, S.P., and Lemischka, I.R. (1995). Targeted disruption of the flk2/flt3 gene leads to deficiencies in primitive hematopoietic progenitors. Immunity *3*, 147-161.
Malumbres, M., Sotillo, R., Santamaria, D., Galan, J., Cerezo, A., Ortega, S., Dubus, P., and Barbacid, M. (2004). Mammalian cells cycle without the D-type cyclin-dependent kinases Cdk4 and Cdk6. Cell *118*, 493-504.
Mandel, E.M., and Grosschedl, R. (2010). Transcription control of early B cell differentiation. Curr Opin Immunol *22*, 161-167.
Marampon, F., Ciccarelli, C., and Zani, B.M. (2006). Down-regulation of c-Myc following MEK/ERK inhibition halts the expression of malignant phenotype in rhabdomyosarcoma and in non muscle-derived human tumors. Molecular cancer *5*, 31.
Matranga, C., Tomari, Y., Shin, C., Bartel, D.P., and Zamore, P.D. (2005). Passenger-strand cleavage facilitates assembly of siRNA into Ago2-containing RNAi enzyme complexes. Cell *123*, 607-620.
Matsushime, H., Ewen, M.E., Strom, D.K., Kato, J.Y., Hanks, S.K., Roussel, M.F., and Sherr, C.J. (1992). Identification and properties of an atypical catalytic subunit (p34PSK-J3/cdk4) for mammalian D type G1 cyclins. Cell *71*, 323-334.
Matsushime, H., Quelle, D.E., Shurtleff, S.A., Shibuya, M., Sherr, C.J., and Kato, J.Y. (1994). D-type cyclin-dependent kinase activity in mammalian cells. Mol Cell Biol *14*, 2066-2076.

Matsushime, H., Roussel, M.F., Ashmun, R.A., and Sherr, C.J. (1991). Colony-stimulating factor 1 regulates novel cyclins during the G1 phase of the cell cycle. Cell *65*, 701-713.
Meyer, N., and Penn, L.Z. (2008). Reflecting on 25 years with MYC. Nat Rev Cancer *8*, 976-990.
Meyerson, M., and Harlow, E. (1994). Identification of G1 kinase activity for cdk6, a novel cyclin D partner. Mol Cell Biol *14*, 2077-2086.
Miller, J.P., Izon, D., DeMuth, W., Gerstein, R., Bhandoola, A., and Allman, D. (2002). The earliest step in B lineage differentiation from common lymphoid progenitors is critically dependent upon interleukin 7. J Exp Med *196*, 705-711.
Mohr, S.E., Smith, J.A., Shamu, C.E., Neumuller, R.A., and Perrimon, N. (2014). RNAi screening comes of age: improved techniques and complementary approaches. Nat Rev Mol Cell Bio *15*, 591-600.
Molnar, A., and Georgopoulos, K. (1994). The Ikaros gene encodes a family of functionally diverse zinc finger DNA-binding proteins. Mol Cell Biol *14*, 8292-8303.
Molnar, A., Wu, P., Largespada, D.A., Vortkamp, A., Scherer, S., Copeland, N.G., Jenkins, N.A., Bruns, G., and Georgopoulos, K. (1996). The Ikaros gene encodes a family of lymphocyte-restricted zinc finger DNA binding proteins, highly conserved in human and mouse. J Immunol *156*, 585-592.
Moreno-Layseca, P., and Streuli, C.H. (2014). Signalling pathways linking integrins with cell cycle progression. Matrix Biology *34*, 144-153.
Morgan, B., Sun, L., Avitahl, N., Andrikopoulos, K., Ikeda, T., Gonzales, E., Wu, P., Neben, S., and Georgopoulos, K. (1997). Aiolos, a lymphoid restricted transcription factor that interacts with Ikaros to regulate lymphocyte differentiation. EMBO J *16*, 2004-2013.
Morrison, S.J., and Weissman, I.L. (1994). The long-term repopulating subset of hematopoietic stem cells is deterministic and isolatable by phenotype. Immunity *1*, 661-673.
Morrow, M.A., Lee, G., Gillis, S., Yancopoulos, G.D., and Alt, F.W. (1992). Interleukin-7 induces N-myc and c-myc expression in normal precursor B lymphocytes. Genes Dev *6*, 61-70.
Muchardt, C., and Yaniv, M. (2001). When the SWI/SNF complex remodels ... the cell cycle. Oncogene *20*, 3067-3075.
Mullighan, C.G., Miller, C.B., Radtke, I., Phillips, L.A., Dalton, J., Ma, J., White, D., Hughes, T.P., Le Beau, M.M., Pui, C.H.*, et al.* (2008). BCR-ABL1 lymphoblastic leukaemia is characterized by the deletion of Ikaros. Nature *453*, 110-114.
Mullighan, C.G., Su, X., Zhang, J., Radtke, I., Phillips, L.A., Miller, C.B., Ma, J., Liu, W., Cheng, C., Schulman, B.A.*, et al.* (2009). Deletion of IKZF1 and prognosis in acute lymphoblastic leukemia. N Engl J Med *360*, 470-480.
Mulloy, R., Salinas, S., Philips, A., and Hipskind, R.A. (2003). Activation of cyclin D1 expression by the ERK5 cascade. Oncogene *22*, 5387-5398.
Naito, T., Gomez-Del Arco, P., Williams, C.J., and Georgopoulos, K. (2007). Antagonistic interactions between Ikaros and the chromatin remodeler Mi-2beta determine silencer activity and Cd4 gene expression. Immunity *27*, 723-734.

Nakase, K., Ishimaru, F., Avitahl, N., Dansako, H., Matsuo, K., Fujii, K., Sezaki, N., Nakayama, H., Yano, T., Fukuda, S.*, et al.* (2000). Dominant negative isoform of the Ikaros gene in patients with adult B-cell acute lymphoblastic leukemia. Cancer Res *60*, 4062-4065.
Nakayama, J., Yamamoto, M., Hayashi, K., Satoh, H., Bundo, K., Kubo, M., Goitsuka, R., Farrar, M.A., and Kitamura, D. (2009). BLNK suppresses pre-B-cell leukemogenesis through inhibition of JAK3. Blood *113*, 1483-1492.
Napoli, C., Lemieux, C., and Jorgensen, R. (1990). Introduction of a Chimeric Chalcone Synthase Gene into Petunia Results in Reversible Co-Suppression of Homologous Genes in Trans. Plant Cell *2*, 279-289.
Nelson, P.J., and Gelman, I.H. (1997). Cell-cycle regulated expression and serine phosphorylation of the myristylated protein kinase C substrate, SSeCKS: Correlation with culture confluency, cell cycle phase and serum response. Molecular and Cellular Biochemistry *175*, 233-241.
Neumann, B., Held, M., Liebel, U., Erfle, H., Rogers, P., Pepperkok, R., and Ellenberg, J. (2006). High-throughput RNAi screening by time-lapse imaging of live human cells. Nat Methods *3*, 385-390.
Ng, S.Y., Yoshida, T., Zhang, J., and Georgopoulos, K. (2009). Genome-wide lineage-specific transcriptional networks underscore Ikaros-dependent lymphoid priming in hematopoietic stem cells. Immunity *30*, 493-507.
Nichogiannopoulou, A., Trevisan, M., Neben, S., Friedrich, C., and Georgopoulos, K. (1999). Defects in hemopoietic stem cell activity in Ikaros mutant mice. J Exp Med *190*, 1201-1214.
Nie, Z., Hu, G., Wei, G., Cui, K., Yamane, A., Resch, W., Wang, R., Green, D.R., Tessarollo, L., Casellas, R.*, et al.* (2012). c-Myc is a universal amplifier of expressed genes in lymphocytes and embryonic stem cells. Cell *151*, 68-79.
Nishimoto, N., Kubagawa, H., Ohno, T., Gartland, G.L., Stankovic, A.K., and Cooper, M.D. (1991). Normal pre-B cells express a receptor complex of mu heavy chains and surrogate light-chain proteins. Proc Natl Acad Sci U S A *88*, 6284-6288.
Nurse, P., and Bissett, Y. (1981). Gene required in G1 for commitment to cell cycle and in G2 for control of mitosis in fission yeast. Nature *292*, 558-560.
O'Keefe, E.P. (2013). siRNA and shRNA: Tools for protein knockdown by gene silencing. Mater Methods 3:197.
O'Neill, D.W., Schoetz, S.S., Lopez, R.A., Castle, M., Rabinowitz, L., Shor, E., Krawchuk, D., Goll, M.G., Renz, M., Seelig, H.P.*, et al.* (2000). An ikaros-containing chromatin-remodeling complex in adult-type erythroid cells. Mol Cell Biol *20*, 7572-7582.
Ochiai, K., Maienschein-Cline, M., Mandal, M., Triggs, J.R., Bertolino, E., Sciammas, R., Dinner, A.R., Clark, M.R., and Singh, H. (2012). A self-reinforcing regulatory network triggered by limiting IL-7 activates pre-BCR signaling and differentiation. Nat Immunol *13*, 300-307.
Oettinger, M.A., Schatz, D.G., Gorka, C., and Baltimore, D. (1990). RAG-1 and RAG-2, adjacent genes that synergistically activate V(D)J recombination. Science *248*, 1517-1523.

Orlofsky, A., and Stanley, E.R. (1987). CSF-1-induced gene expression in macrophages: dissociation from the mitogenic response. EMBO J *6*, 2947-2952.
Paddison, P.J., Caudy, A.A., Bernstein, E., Hannon, G.J., and Conklin, D.S. (2002). Short hairpin RNAs (shRNAs) induce sequence-specific silencing in mammalian cells. Gene Dev *16*, 948-958.
Pardee, A.B. (1974). A restriction point for control of normal animal cell proliferation. Proc Natl Acad Sci U S A *71*, 1286-1290.
Pavletich, N.P. (1999). Mechanisms of cyclin-dependent kinase regulation: structures of Cdks, their cyclin activators, and Cip and INK4 inhibitors. J Mol Biol *287*, 821-828.
Penn, L.J.Z., Brooks, M.W., Laufer, E.M., and Land, H. (1990). Negative Autoregulation of C-Myc Transcription. Embo Journal *9*, 1113-1121.
Perdomo, J., Holmes, M., Chong, B., and Crossley, M. (2000). Eos and pegasus, two members of the Ikaros family of proteins with distinct DNA binding activities. J Biol Chem *275*, 38347-38354.
Perez-Roger, I., Kim, S.H., Griffiths, B., Sewing, A., and Land, H. (1999). Cyclins D1 and D2 mediate myc-induced proliferation via sequestration of p27(Kip1) and p21(Cip1). EMBO J *18*, 5310-5320.
Perna, D., Faga, G., Verrecchia, A., Gorski, M.M., Barozzi, I., Narang, V., Khng, J., Lim, K.C., Sung, W.K., Sanges, R.*, et al.* (2012). Genome-wide mapping of Myc binding and gene regulation in serum-stimulated fibroblasts. Oncogene *31*, 1695-1709.
Peukert, K., Staller, P., Schneider, A., Carmichael, G., Hanel, F., and Eilers, M. (1997). An alternative pathway for gene regulation by Myc. EMBO J *16*, 5672-5686.
Platt, R.J., Chen, S., Zhou, Y., Yim, M.J., Swiech, L., Kempton, H.R., Dahlman, J.E., Parnas, O., Eisenhaure, T.M., Jovanovic, M.*, et al.* (2014). CRISPR-Cas9 knockin mice for genome editing and cancer modeling. Cell *159*, 440-455.
Polyak, K., Kato, J.Y., Solomon, M.J., Sherr, C.J., Massague, J., Roberts, J.M., and Koff, A. (1994). p27Kip1, a cyclin-Cdk inhibitor, links transforming growth factor-beta and contact inhibition to cell cycle arrest. Genes Dev *8*, 9-22.
Popescu, M., Gurel, Z., Ronni, T., Song, C., Hung, K.Y., Payne, K.J., and Dovat, S. (2009). Ikaros stability and pericentromeric localization are regulated by protein phosphatase 1. J Biol Chem *284*, 13869-13880.
Pulte, D., Lopez, R.A., Baker, S.T., Ward, M., Ritchie, E., Richardson, C.A., O'Neill, D.W., and Bank, A. (2006). Ikaros increases normal apoptosis in adult erythroid cells. American Journal of Hematology *81*, 12-18.
Quelle, D.E., Ashmun, R.A., Shurtleff, S.A., Kato, J.Y., Bar-Sagi, D., Roussel, M.F., and Sherr, C.J. (1993). Overexpression of mouse D-type cyclins accelerates G1 phase in rodent fibroblasts. Genes Dev *7*, 1559-1571.
Rahl, P.B., Lin, C.Y., Seila, A.C., Flynn, R.A., McCuine, S., Burge, C.B., Sharp, P.A., and Young, R.A. (2010). c-Myc regulates transcriptional pause release. Cell *141*, 432-445.
Ran, F.A., Hsu, P.D., Lin, C.Y., Gootenberg, J.S., Konermann, S., Trevino, A.E., Scott, D.A., Inoue, A., Matoba, S., Zhang, Y.*, et al.* (2013). Double nicking by RNA-guided CRISPR Cas9 for enhanced genome editing specificity. Cell *154*, 1380-1389.
Rao, D.D., Vorhies, J.S., Senzer, N., and Nemunaitis, J. (2009). siRNA vs. shRNA: Similarities and differences. Adv Drug Deliver Rev *61*, 746-759.

Rebollo, A., Ayllon, V., Fleischer, A., Martinez, C.A., and Zaballos, A. (2001). The association of Aiolos transcription factor and Bcl-xL is involved in the control of apoptosis. J Immunol *167*, 6366-6373.
Reed, S.I., Hadwiger, J.A., and Lorincz, A.T. (1985). Protein kinase activity associated with the product of the yeast cell division cycle gene CDC28. Proc Natl Acad Sci U S A *82*, 4055-4059.
Reth, M., Petrac, E., Wiese, P., Lobel, L., and Alt, F.W. (1987). Activation of V kappa gene rearrangement in pre-B cells follows the expression of membrane-bound immunoglobulin heavy chains. EMBO J *6*, 3299-3305.
Reynaud, D., Demarco, I.A., Reddy, K.L., Schjerven, H., Bertolino, E., Chen, Z., Smale, S.T., Winandy, S., and Singh, H. (2008). Regulation of B cell fate commitment and immunoglobulin heavy-chain gene rearrangements by Ikaros. Nat Immunol *9*, 927-936.
Rimokh, R., Rouault, J.P., Wahbi, K., Gadoux, M., Lafage, M., Archimbaud, E., Charrin, C., Gentilhomme, O., Germain, D., Samarut, J.*, et al.* (1991). A Chromosome 12 Coding Region Is Juxtaposed to the Myc Protooncogene Locus in a T(8,12)(Q24,Q22) Translocation in a Case of B-Cell Chronic Lymphocytic-Leukemia. Gene Chromosome Canc *3*, 24-36.
Romano, N., and Macino, G. (1992). Quelling - Transient Inactivation of Gene-Expression in Neurospora-Crassa by Transformation with Homologous Sequences. Molecular microbiology *6*, 3343-3353.
Rouault, J.P., Rimokh, R., Tessa, C., Paranhos, G., Ffrench, M., Duret, L., Garoccio, M., Germain, D., Samarut, J., and Magaud, J.P. (1992). Btg1, a Member of a New Family of Antiproliferative Genes. Embo Journal *11*, 1663-1670.
Ruijtenberg, S., and van den Heuvel, S. (2015). G1/S Inhibitors and the SWI/SNF Complex Control Cell-Cycle Exit during Muscle Differentiation. Cell *162*, 300-313.
Rutz, S., and Scheffold, A. (2004). Towards in vivo application of RNA interference - new toys, old problems. Arthritis Res Ther *6*, 78-85.
Sabbattini, P., Lundgren, M., Georgiou, A., Chow, C., Warnes, G., and Dillon, N. (2001). Binding of Ikaros to the lambda5 promoter silences transcription through a mechanism that does not require heterochromatin formation. EMBO J *20*, 2812-2822.
Salesse, S., and Verfaillie, C.M. (2002). BCR/ABL: from molecular mechanisms of leukemia induction to treatment of chronic myelogenous leukemia. Oncogene *21*, 8547-8559.
Sander, J.D., and Joung, J.K. (2014). CRISPR-Cas systems for editing, regulating and targeting genomes. Nat Biotechnol *32*, 347-355.
Schafer, K.A. (1998). The cell cycle: a review. Veterinary pathology *35*, 461-478.
Schjerven, H., McLaughlin, J., Arenzana, T.L., Frietze, S., Cheng, D., Wadsworth, S.E., Lawson, G.W., Bensinger, S.J., Farnham, P.J., Witte, O.N.*, et al.* (2013). Selective regulation of lymphopoiesis and leukemogenesis by individual zinc fingers of Ikaros. Nat Immunol *14*, 1073-1083.
Schlabach, M.R., Luo, J., Solimini, N.L., Hu, G., Xu, Q.K., Li, M.Z., Zhao, Z.M., Smogorzewska, A., Sowa, M.E., Ang, X.L.L.*, et al.* (2008). Cancer proliferation gene discovery through functional Genomics. Science *319*, 620-624.

Schlosser, I., Holzel, M., Hoffmann, R., Burtscher, H., Kohlhuber, F., Schuhmacher, M., Chapman, R., Weidle, U.H., and Eick, D. (2005). Dissection of transcriptional programmes in response to serum and c-Myc in a human B-cell line. Oncogene *24*, 520-524.
Schmidt, E.E., Pelz, O., Buhlmann, S., Kerr, G., Horn, T., and Boutros, M. (2013). GenomeRNAi: a database for cell-based and in vivo RNAi phenotypes, 2013 update. Nucleic Acids Research *41*, D1021-D1026.
Schwickert, T.A., Tagoh, H., Gultekin, S., Dakic, A., Axelsson, E., Minnich, M., Ebert, A., Werner, B., Roth, M., Cimmino, L.*, et al.* (2014). Stage-specific control of early B cell development by the transcription factor Ikaros. Nat Immunol *15*, 283-293.
Sears, R., Nuckolls, F., Haura, E., Taya, Y., Tamai, K., and Nevins, J.R. (2000). Multiple Ras-dependent phosphorylation pathways regulate Myc protein stability. Genes Dev *14*, 2501-2514.
Semenova, E., Jore, M.M., Datsenko, K.A., Semenova, A., Westra, E.R., Wanner, B., van der Oost, J., Brouns, S.J., and Severinov, K. (2011). Interference by clustered regularly interspaced short palindromic repeat (CRISPR) RNA is governed by a seed sequence. Proc Natl Acad Sci U S A *108*, 10098-10103.
Sen, G.L., and Blau, H.M. (2006). A brief history of RNAi: the silence of the genes. Faseb J *20*, 1293-1299.
Shalem, O., Sanjana, N.E., Hartenian, E., Shi, X., Scott, D.A., Mikkelsen, T.S., Heckl, D., Ebert, B.L., Root, D.E., Doench, J.G.*, et al.* (2014). Genome-Scale CRISPR-Cas9 Knockout Screening in Human Cells. Science *343*, 84-87.
Shan, B., and Lee, W.H. (1994). Deregulated expression of E2F-1 induces S-phase entry and leads to apoptosis. Mol Cell Biol *14*, 8166-8173.
Sharma, S., and Rao, A. (2009). RNAi screening: tips and techniques. Nature Immunology *10*, 799-804.
Shaw, A.S., and Filbert, E.L. (2009). Scaffold proteins and immune-cell signalling. Nat Rev Immunol *9*, 47-56.
Sheen, J.H., and Dickson, R.B. (2002). Overexpression of c-Myc alters G(1)/S arrest following ionizing radiation. Molecular and Cellular Biology *22*, 1819-1833.
Sherr, C.J., and Roberts, J.M. (1999). CDK inhibitors: positive and negative regulators of G1-phase progression. Genes Dev *13*, 1501-1512.
Shichiri, M., Hanson, K.D., and Sedivy, J.M. (1993). Effects of c-myc expression on proliferation, quiescence, and the G0 to G1 transition in nontransformed cells. Cell Growth Differ *4*, 93-104.
Silva, J.M., Marran, K., Parker, J.S., Silva, J., Golding, M., Schlabach, M.R., Elledge, S.J., Hannon, G.J., and Chang, K. (2008). Profiling essential genes in human mammary cells by multiplex RNAi screening. Science *319*, 617-620.
Sims, D., Mendes-Pereira, A.M., Frankum, J., Burgess, D., Cerone, M.A., Lombardelli, C., Mitsopoulos, C., Hakas, J., Murugaesu, N., Isacke, C.M.*, et al.* (2011). High-throughput RNA interference screening using pooled shRNA libraries and next generation sequencing. Genome biology *12*.
Singh, H., Medina, K.L., and Pongubala, J.M. (2005). Contingent gene regulatory networks and B cell fate specification. Proc Natl Acad Sci U S A *102*, 4949-4953.

Sitnicka, E., Bryder, D., Theilgaard-Monch, K., Buza-Vidas, N., Adolfsson, J., and Jacobsen, S.E. (2002). Key role of flt3 ligand in regulation of the common lymphoid progenitor but not in maintenance of the hematopoietic stem cell pool. Immunity *17*, 463-472.
Song, C., Gowda, C., Pan, X., Ding, Y., Tong, Y., Tan, B.H., Wang, H., Muthusami, S., Ge, Z., Sachdev, M.*, et al.* (2015). Targeting casein kinase II restores Ikaros tumor suppressor activity and demonstrates therapeutic efficacy in high-risk leukemia. Blood.
Streb, J.W., Kitchen, C.M., Gelman, I.H., and Miano, J.M. (2004). Multiple promoters direct expression of three AKAP12 isoforms with distinct subcellular and tissue distribution profiles. J Biol Chem *279*, 56014-56023.
Streb, J.W., Long, X., Lee, T.H., Sun, Q., Kitchen, C.M., Georger, M.A., Slivano, O.J., Blaner, W.S., Carr, D.W., Gelman, I.H.*, et al.* (2011). Retinoid-induced expression and activity of an immediate early tumor suppressor gene in vascular smooth muscle cells. Plos One *6*, e18538.
Su, B., Gao, L., Meng, F., Guo, L.W., Rothschild, J., and Gelman, I.H. (2013). Adhesion-mediated cytoskeletal remodeling is controlled by the direct scaffolding of Src from FAK complexes to lipid rafts by SSeCKS/AKAP12. Oncogene *32*, 2016-2026.
Sudbery, P.E., Goodey, A.R., and Carter, B.L. (1980). Genes which control cell proliferation in the yeast Saccharomyces cerevisiae. Nature *288*, 401-404.
Sun, L., Liu, A., and Georgopoulos, K. (1996). Zinc finger-mediated protein interactions modulate Ikaros activity, a molecular control of lymphocyte development. EMBO J *15*, 5358-5369.
Thompson, E.C., Cobb, B.S., Sabbattini, P., Meixlsperger, S., Parelho, V., Liberg, D., Taylor, B., Dillon, N., Georgopoulos, K., Jumaa, H.*, et al.* (2007). Ikaros DNA-binding proteins as integral components of B cell developmental-stage-specific regulatory circuits. Immunity *26*, 335-344.
Tomlinson, M.G., Lin, J., and Weiss, A. (2000). Lymphocytes with a complex: adapter proteins in antigen receptor signaling. Immunology today *21*, 584-591.
Trageser, D., Iacobucci, I., Nahar, R., Duy, C., von Levetzow, G., Klemm, L., Park, E., Schuh, W., Gruber, T., Herzog, S.*, et al.* (2009). Pre-B cell receptor-mediated cell cycle arrest in Philadelphia chromosome-positive acute lymphoblastic leukemia requires IKAROS function. J Exp Med *206*, 1739-1753.
Trinh, L.A., Ferrini, R., Cobb, B.S., Weinmann, A.S., Hahm, K., Ernst, P., Garraway, I.P., Merkenschlager, M., and Smale, S.T. (2001). Down-regulation of TDT transcription in CD4(+)CD8(+) thymocytes by Ikaros proteins in direct competition with an Ets activator. Genes Dev *15*, 1817-1832.
Uckun, F.M., Ma, H., Zhang, J., Ozer, Z., Dovat, S., Mao, C., Ishkhanian, R., Goodman, P., and Qazi, S. (2012). Serine phosphorylation by SYK is critical for nuclear localization and transcription factor function of Ikaros. Proc Natl Acad Sci U S A.
van Riggelen, J., Yetil, A., and Felsher, D.W. (2010). MYC as a regulator of ribosome biogenesis and protein synthesis. Nat Rev Cancer *10*, 301-309.
Vennstrom, B., Sheiness, D., Zabielski, J., and Bishop, J.M. (1982). Isolation and characterization of c-myc, a cellular homolog of the oncogene (v-myc) of avian myelocytomatosis virus strain 29. J Virol *42*, 773-779.

Vlach, J., Hennecke, S., Alevizopoulos, K., Conti, D., and Amati, B. (1996). Growth arrest by the cyclin-dependent kinase inhibitor p27Kip1 is abrogated by c-Myc. EMBO J *15*, 6595-6604.
Waanders, E., Scheijen, B., van der Meer, L.T., van Reijmersdal, S.V., van Emst, L., Kroeze, Y., Sonneveld, E., Hoogerbrugge, P.M., van Kessel, A.G., van Leeuwen, F.N.*, et al.* (2012). The Origin and Nature of Tightly Clustered BTG1 Deletions in Precursor B-Cell Acute Lymphoblastic Leukemia Support a Model of Multiclonal Evolution. Plos Genetics *8*.
Wang, H., Mannava, S., Grachtchouk, V., Zhuang, D., Soengas, M.S., Gudkov, A.V., Prochownik, E.V., and Nikiforov, M.A. (2008). c-Myc depletion inhibits proliferation of human tumor cells at various stages of the cell cycle. Oncogene *27*, 1905-1915.
Wang, J.H., Avitahl, N., Cariappa, A., Friedrich, C., Ikeda, T., Renold, A., Andrikopoulos, K., Liang, L., Pillai, S., Morgan, B.A.*, et al.* (1998). Aiolos regulates B cell activation and maturation to effector state. Immunity *9*, 543-553.
Wang, J.H., Nichogiannopoulou, A., Wu, L., Sun, L., Sharpe, A.H., Bigby, M., and Georgopoulos, K. (1996). Selective defects in the development of the fetal and adult lymphoid system in mice with an Ikaros null mutation. Immunity *5*, 537-549.
Wang, P.B., Ballestrem, C., and Streuli, C.H. (2011a). The C terminus of talin links integrins to cell cycle progression. Journal of Cell Biology *195*, 499-513.
Wang, R.N., Dillon, C.P., Shi, L.Z., Milasta, S., Carter, R., Finkelstein, D., McCormick, L.L., Fitzgerald, P., Chi, H.B., Munger, J.*, et al.* (2011b). The Transcription Factor Myc Controls Metabolic Reprogramming upon T Lymphocyte Activation. Immunity *35*, 871-882.
Wang, T., Wei, J.J., Sabatini, D.M., and Lander, E.S. (2014). Genetic Screens in Human Cells Using the CRISPR-Cas9 System. Science *343*, 80-84.
Waters, C.M., Littlewood, T.D., Hancock, D.C., Moore, J.P., and Evan, G.I. (1991). C-Myc Protein Expression in Untransformed Fibroblasts. Oncogene *6*, 797-805.
Weissmuller, T., Glover, L.E., Fennimore, B., Curtis, V.F., MacManus, C.F., Ehrentraut, S.F., Campbell, E.L., Scully, M., Grove, B.D., and Colgan, S.P. (2014). HIF-dependent regulation of AKAP12 (gravin) in the control of human vascular endothelial function. Faseb J *28*, 256-264.
Westbrook, T.F., Martin, E.S., Schlabach, M.R., Leng, Y.M., Liang, A.C., Feng, B., Zhao, J.J., Roberts, T.M., Mandel, G., Hannon, G.J.*, et al.* (2005). A genetic screen for candidate tumor suppressors identifies REST. Cell *121*, 837-848.
Winandy, S., Wu, P., and Georgopoulos, K. (1995). A dominant mutation in the Ikaros gene leads to rapid development of leukemia and lymphoma. Cell *83*, 289-299.
Yang, W., Shen, J., Wu, M., Arsura, M., FitzGerald, M., Suldan, Z., Kim, D.W., Hofmann, C.S., Pianetti, S., Romieu-Mourez, R.*, et al.* (2001). Repression of transcription of the p27(Kip1) cyclin-dependent kinase inhibitor gene by c-Myc. Oncogene *20*, 1688-1702.
Yao, G. (2014). Modelling mammalian cellular quiescence. Interface Focus *4*.
Yao, G., Lee, T.J., Mori, S., Nevins, J.R., and You, L.C. (2008). A bistable Rb-E2F switch underlies the restriction point. Nature Cell Biology *10*, 476-U255.

Yasuda, T., Sanjo, H., Pages, G., Kawano, Y., Karasuyama, H., Pouyssegur, J., Ogata, M., and Kurosaki, T. (2008). Erk kinases link pre-B cell receptor signaling to transcriptional events required for early B cell expansion. Immunity *28*, 499-508.
Yoshida, T., Ng, S.Y., Zuniga-Pflucker, J.C., and Georgopoulos, K. (2006). Early hematopoietic lineage restrictions directed by Ikaros. Nat Immunol *7*, 382-391.
Zeller, K.I., Zhao, X., Lee, C.W., Chiu, K.P., Yao, F., Yustein, J.T., Ooi, H.S., Orlov, Y.L., Shahab, A., Yong, H.C*., et al.* (2006). Global mapping of c-Myc binding sites and target gene networks in human B cells. Proc Natl Acad Sci U S A *103*, 17834-17839.
Zetterberg, A., and Larsson, O. (1985). Kinetic-Analysis of Regulatory Events in G1 Leading to Proliferation or Quiescence of Swiss 3t3 Cells. P Natl Acad Sci USA *82*, 5365-5369.
Zhang, J., Jackson, A.F., Naito, T., Dose, M., Seavitt, J., Liu, F., Heller, E.J., Kashiwagi, M., Yoshida, T., Gounari, F*., et al.* (2012). Harnessing of the nucleosome-remodeling-deacetylase complex controls lymphocyte development and prevents leukemogenesis. Nat Immunol *13*, 86-94.
Zhang, L., Reynolds, T.L., Shan, X., and Desiderio, S. (2011). Coupling of V(D)J recombination to the cell cycle suppresses genomic instability and lymphoid tumorigenesis. Immunity *34*, 163-174.
Zhang, W., Sloan-Lancaster, J., Kitchen, J., Trible, R.P., and Samelson, L.E. (1998). LAT: the ZAP-70 tyrosine kinase substrate that links T cell receptor to cellular activation. Cell *92*, 83-92.
Zhu, R., Zou, S.T., Wan, J.M., Li, W., Li, X.L., and Zhu, W. (2013). BTG1 inhibits breast cancer cell growth through induction of cell cycle arrest and apoptosis. Oncology Reports *30*, 2137-2144.
Zuber, J., McJunkin, K., Fellmann, C., Dow, L.E., Taylor, M.J., Hannon, G.J., and Lowe, S.W. (2011). Toolkit for evaluating genes required for proliferation and survival using tetracycline-regulated RNAi. Nature Biotechnology *29*, 79-+.

Supplementary materials

Go terms for shRNA enriched in 4-OHT treated samples relative to EtOH treated samples

Sublist	Category	Term	RT	Genes	Count	%	P-Value	Benjamini
	GOTERM_BP_FAT	regulation of cell death	RT		112	8.2	5.8E-16	2.1E-12
	GOTERM_BP_FAT	regulation of programmed cell death	RT		111	8.1	9.8E-16	1.9E-12
	GOTERM_BP_FAT	regulation of apoptosis	RT		110	8.1	1.1E-15	1.4E-12
	GOTERM_BP_FAT	response to wounding	RT		78	5.7	3.6E-14	3.5E-11
	GOTERM_BP_FAT	phosphorylation	RT		126	9.2	1.3E-13	1.0E-10
	GOTERM_BP_FAT	phosphate metabolic process	RT		142	10.4	7.0E-13	4.4E-10

Figure S.1 GO terms for enriched hits from the ERt2 system.

A Enriched hits (bound by Ikaros)

Term	RT	Genes	Count	%	P-Value	Benjamini
regulation of cell cycle	RT		17	9.1	9.1E-9	1.6E-5
regulation of apoptosis	RT		26	13.9	1.8E-8	1.6E-5
regulation of programmed cell death	RT		26	13.9	2.4E-8	1.4E-5
regulation of cell death	RT		26	13.9	2.6E-8	1.2E-5
positive regulation of apoptosis	RT		16	8.6	4.4E-7	1.6E-4
positive regulation of programmed cell death	RT		16	8.6	4.9E-7	1.4E-4
hemopoiesis	RT		16	8.6	5.1E-7	1.3E-4

B Enriched hits (not bound by Ikaros)

Term	RT	Genes	Count	%	P-Value	Benjamini
cell-cell signaling	RT		20	9.0	4.3E-8	7.5E-5
behavior	RT		20	9.0	6.8E-6	5.9E-3
negative regulation of cell death	RT		14	6.3	5.9E-5	1.3E-2
prostate gland morphogenesis	RT		6	2.7	3.8E-5	1.3E-2
negative regulation of apoptosis	RT		14	6.3	4.6E-5	1.3E-2
prostate gland epithelium morphogenesis	RT		6	2.7	3.1E-5	1.3E-2

Figure S.2 GO terms for enriched hits using the MSCV-*Ikzf1* expression system. The DAVID tool was queried using the top enriched hits that were bound by Ikaros (A) or not bound by Ikaros (B).

All depleted hits

Term	RT	Genes	Count	%	P-Value	Benjamini
cell morphogenesis	RT		13	8.0	8.4E-5	1.2E-1
cellular component morphogenesis	RT		13	8.0	2.8E-4	1.9E-1
positive regulation of immune system process	RT		10	6.2	2.8E-4	1.3E-1
regulation of lymphocyte differentiation	RT		6	3.7	3.2E-4	1.1E-1
cell morphogenesis involved in differentiation	RT		10	6.2	3.5E-4	9.9E-2
positive regulation of lymphocyte differentiation	RT		5	3.1	3.9E-4	9.4E-2

Figure S.3 GO terms for depleted hits using the MSCV-*Ikzf1* expression system.

A Kegg pathway all enriched hits

Category	Term	RT	Genes	Count	%	P-Value	Benjamini
KEGG_PATHWAY	Pathways in cancer	RT		33	8.0	6.4E-6	1.0E-3
KEGG_PATHWAY	Prostate cancer	RT		15	3.7	2.5E-5	2.1E-3
KEGG_PATHWAY	Glioma	RT		10	2.4	1.5E-3	8.0E-2
KEGG_PATHWAY	Pancreatic cancer	RT		10	2.4	3.5E-3	1.3E-1
KEGG_PATHWAY	Colorectal cancer	RT		11	2.7	3.6E-3	1.1E-1
KEGG_PATHWAY	TGF-beta signaling pathway	RT		11	2.7	3.9E-3	1.0E-1
KEGG_PATHWAY	Focal adhesion	RT		18	4.4	4.8E-3	1.1E-1
KEGG_PATHWAY	Chronic myeloid leukemia	RT		10	2.4	5.0E-3	9.8E-2
KEGG_PATHWAY	Endometrial cancer	RT		8	2.0	6.4E-3	1.1E-1
KEGG_PATHWAY	Hedgehog signaling pathway	RT		8	2.0	7.9E-3	1.2E-1
KEGG_PATHWAY	Cell cycle	RT		13	3.2	8.7E-3	1.2E-1

B Kegg pathway Ikaros bound hits

Category	Term	RT	Genes	Count	%	P-Value	Benjam
KEGG_PATHWAY	Cell cycle	RT		11	5.9	1.5E-4	2.1E-2
KEGG_PATHWAY	Prostate cancer	RT		9	4.8	3.0E-4	2.0E-2
KEGG_PATHWAY	Endometrial cancer	RT		6	3.2	3.0E-3	1.3E-1
KEGG_PATHWAY	Chronic myeloid leukemia	RT		7	3.7	3.2E-3	1.0E-1
KEGG_PATHWAY	Pathways in cancer	RT		15	8.0	3.2E-3	8.5E-2
KEGG_PATHWAY	Acute myeloid leukemia	RT		6	3.2	4.5E-3	9.7E-2

Figure S.4 Kegg pathway terms for Ikaros bound hits

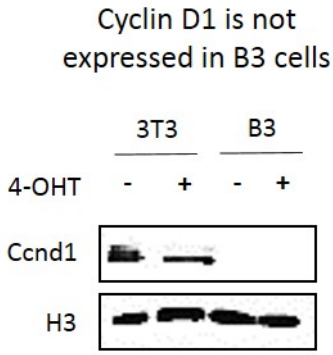

Figure S.5 Western blot for cyclin D1 expression in 3T3 cells and B3 cells

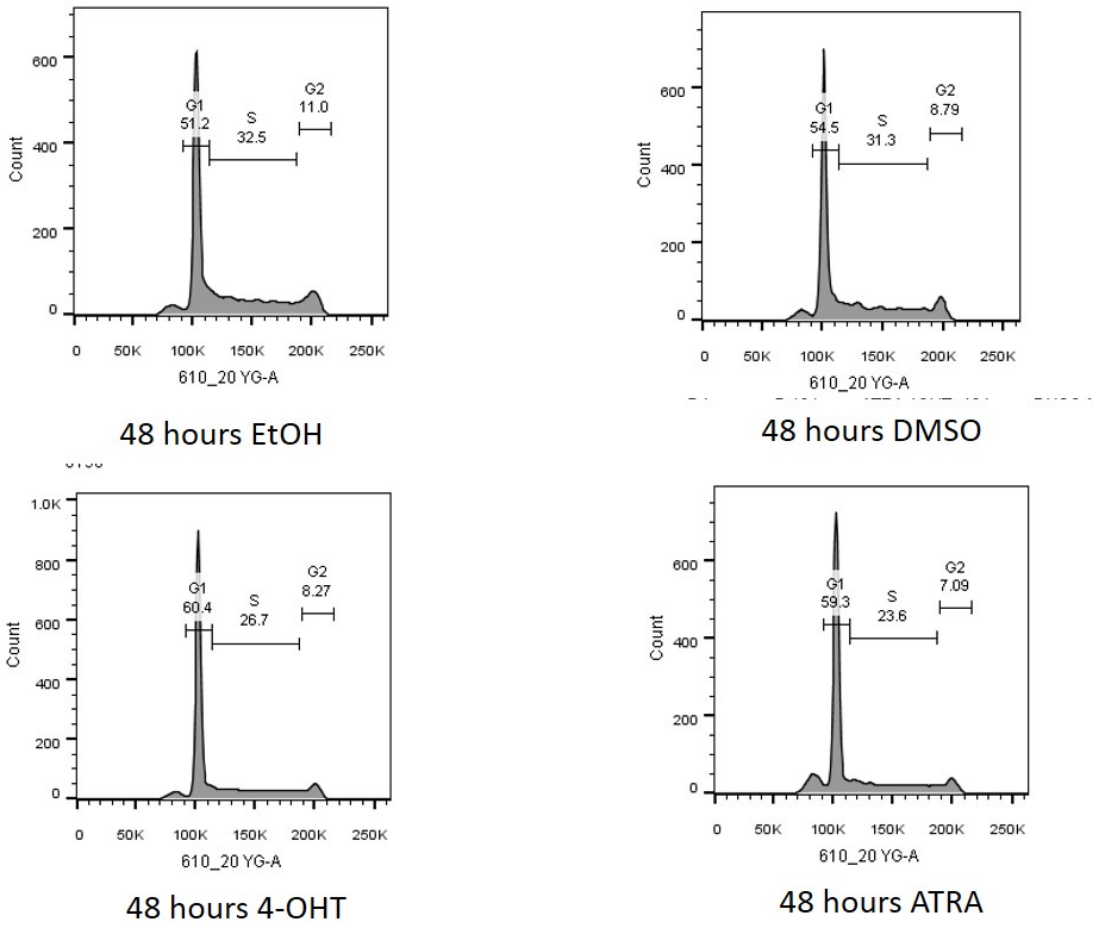

Figure S.6 PI profiles of primary pre-B cells treated for 48 hours with EtOH, 4-OHT, DMSO or ATRA.